Ghent University

Faculty of Sciences

Department of Plant Biotechnology and Genetics

Arabidopsis leaf mutants reveal conserved and unique proteins involved in auxin and light signaling

Steven De Groeve

Thesis submitted to obtain the degree of Doctor (Ph.D.) in Sciences: Biotechnology

Academic year 2010-2011

Promotor: Prof. Dr. Dirk Inzé
Co-Promotor: Dr. Mieke Van Lijsebettens

Jury Members

Promotor	Prof. Dr. Inzé (secretary) Department of Plant Systems Biology (PSB) Flanders Institute for Biotechnology (VIB) Faculty of Science Department of Molecular Genetics
Co-Promoter	Dr. Mieke Van Lijsebettens Department of Plant Systems Biology (PSB) Flanders Institute for Biotechnology (VIB) Faculty of Science Department of Molecular Genetics
Promotion Commission	Prof. Dr. Marcelle Holsters (chair) Department of Plant Systems Biology (PSB) Flanders Institute for Biotechnology (VIB) Faculty of Science Department of Molecular Genetics
	Prof. Dr. Patrik Verstreken Department of Molecular and Developmental Genetics Flanders Insitute for Biotechnology (VIB) KULeuven, Center for Human Genetics
	Dr. Michael Metzlaff Senior Group Leader Technology Licensing & Research Liaison Management Bayer BioScience N.V.
	Prof. Dr. Lieven De Veylder Department of Plant Systems Biology (PSB) Flanders Institute for Biotechnology (VIB) Faculty of Science Department of Molecular Genetics
	Prof. Dr. Frank Van Breusegem Department of Plant Systems Biology (PSB) Flanders Institute for Biotechnology (VIB) Faculty of Science Department of Molecular Genetics
	Prof. Dr. Geert De Jaeger Department of Plant Systems Biology (PSB) Flanders Institute for Biotechnology (VIB) Faculty of Science Department of Molecular Genetics
	Prof. Dr. Domique Van Der Straeten Department of Physiology, Ghent University Laboratory of Functional Plant Biology
	Dr. Hilde Nelissen Department of Plant Systems Biology (PSB) Flanders Institute for Biotechnology (VIB) Faculty of Science Department of Molecular Genetics

Table Of Contents

Abbreviations

6-AU	6-azauracil
AG	AGAMOUS
ATP	Adenosine Triphosphate
BinGO	Biological Networks Gene Ontology
CAF1	Chromatin Assembly Factor 1
cDNA	Complementary DNA
ChIP	Chromatin Immunoprecipitation
COMPASS	Complex Proteins Associated with Set1
CTD	C-Terminal Domain
DAG	Days After Germination
DAPI	4’,6-Diamidino-2-Phenylindole
DAS	Days After Sowing
DE	Differentially Expressed
DIC	Differential Interference Contrast
DMSO	Dimethylsulfoxide
DNA	Deoxyribonucleic acid
DRL1	DEFORMED ROOTS AND LEAVES1
ELO	Elongata
ELP	Elongator protein
EMS	Ethyl methanesulfonate
FACT	Facilitates Chromatin Transcription
FLC	Flower Locus C
GCN5	GENERAL CONTROL NONDEREPRESSED-5
GFP	Green Fluorescent Protein
GO	Gene ontology
GTF	General Transcription Factors
GNAT	GCN5-RELATED N-ACETYL TRANSFERASE
GUS	β-Glucoronidase
H3K14Ac	Histone H3 Lysine 14 acetylation
HAT	Histone Acetyltransferase

HB	homeobox
HD2	histone deacetylase 2
HDAC	Histone Deacetylase
HMT	Histone Methyltransferase
HUB1	Histone Monoubiquitination 1
IKAP	IKAPPAB KINASE COMPLEX-ASSOCIATED PROTEIN
IKI	INSENSITIVE TO KILLER
KNOX	Knotted Like Homeobox
KTI	K. LACTIS TOXIN INSENSITIVE
KYP	KRYPTONITE
LD	Long Day
LFY	LEAFY
LUG	LEUNIG
MADS	MCM1 AGAMOUS DEFICIENS SRF
MALDI-TOF	Matrix-Assisted Laser Desorption/Ionization-Time-of-Flight MS
mRNA	messenger Ribonucleic Acid
MSMO	Murashige Skoog Medium with Minimal Organics
NAM	NO APICAL MERISTEM
NLS	Nuclear Localization Signal
OE	Overexpression
Paf1c	Polymerase II Associated Factor 1 Complex
PcG	Polycomb Group
PCR	Polymerase Chain Reaction
PID	PINOID
PIN1	PIN-FORMED1
QPCR	Quantitative PCR
RAM	Root apical meristem
RNA	Ribonucleic Acid
RNAPII	RNA Polymerase II
SAGA	Spt-Ada-Gcn5-acetyltransferase
SAM	shoot apical meristem

SD	Short Day
STAT3	SIGNAL TRANSDUCER AND ACTIVATOR OF TRANSCRIPTION3
StIP1	STAT3 INTERACTING PROTEIN
STM	SHOOTMERISTEMLESS
SWI/SNF	SWItch/Sucrose NonFermentable
TAF	TBP-ASSOCIATED PROTEIN
TAP	Tandem Affinity Purification
TBP	TATA Binding Protein
T-DNA	Transfer DNA
TOT	Toxin target
TrxG	Trithorax Group
WUS	WUSHEL
Y2H	Yeast-2-Hybrid

Objectives

Growth and development in plants is steered by the meristems which are established on both poles of the embryo and become active after germination. The activity of the shoot apical meristem (SAM) leads to the formation of lateral organs such as leaves which are responsible for photosynthesis. At flowering time the SAM is transformed to the inflorescence meristem which produces flowers as lateral organs. The root apical meristem is responsible for the growth of the primary root and is important in water- and mineral-uptake. Within the research group "Chromatin and Growth Control" several genes are being cloned of which the mutant phenotype shows a defect in leaf growth. This way the genes coding for components of the Elongator complex were identified. In yeast Elongator was defined as a histone acetyltransferase (HAT) complex associated with RNA polymerase II to facilitate transcription elongation. In this thesis the loci of two other leaf mutants *ang3* and *ron3* belonging to the *angusta* and *rotunda* class respectively were cloned. By transcript profiling of the leaf mutants using micro-array data we try to pinpoint in which biological process the gene is involved. Localization studies and tandem affinity purification of the respective protein helps to identify which molecular pathways are likely to be affected. With detailed phenotypical analysis of the mutants we are often able to link the affected processes to observed phenotypes. Depending on the obtained results we perform specific experiments (ChIP, hormone measurements,…) to verify the true function of the protein. This work aimed at investigating the role of the Elongator complex in plants and several objectives were put forward

1. To prove the role of Elongator in transcription
2. To identify target genes of Elongator using chromatin-immuno-precipitation

Besides the functional characterization of the Elongator complex, two other leaf mutants *ang3* and *ron3* belonging to the *angusta* and *rotunda* class respectively were cloned and functionally characterized. The genes were cloned by fine-mapping combined with sequence analysis of candidate genes in the genetic interval around the locus of interest. Molecular analysis of the genes was combined with morphological and cellular analyses of the corresponding mutants to determine the cellular basis of the observed growth defects and to gain deeper insight into the function of the genes.

LITERATURE

Chapter 1

Transcription and Chromatin Modifications

I. Introduction

DNA contains the complete genetic information that defines the structure of an organism and the eukaryotic cell has developed a strategy to compact the DNA within the constraints of the nucleus: DNA is packaged into a nucleoprotein complex, known as chromatin.

Early on it has been proposed that chromatin structure is based on a repeating unit of eight histone molecules and about 200 DNA base pairs (Kornberg, 1974) and later the structure of this repeating unit , the nucleosoom, has been been solved (Arents *et al*., 1991; Luger *et al*., 1977). The nucleosome core particle contains two copies of each histone protein (H2A, H2B, H3 and H4) and 146 basepairs (bp) of superhelical DNA wrapped around this histone octamer. The DNA between two core particles, connecting one nucleosome to the next in chromatin, is referred to as "linker" DNA and is wrapped around histone H1 , which is involved in the further DNA packaging that leads to the final chromatin structure (Fig. 1). Chromatin is found in two varieties: euchromatin and heterochromatin (Elgin, 1996). Originally, the two forms were distinguished cytologically by how intensely they stained – euchromatin is less intense, while heterochromatin stains intensely, indicating tighter packing. Heterochromatin mainly consists of genetically inactive satellite sequences and many genes are repressed to various extents whereas in euchromatic regions genes are actively transcribed.

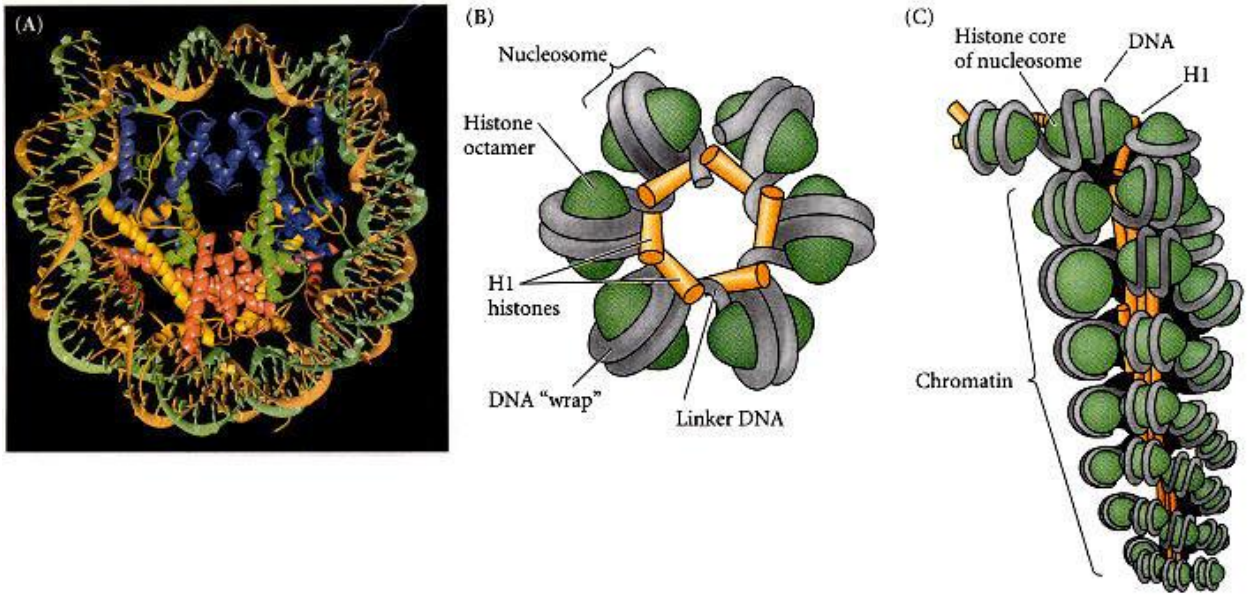

Fig. 1. Nucleosome and chromatin structure. (A) Model of nucleosome structure as seen by X-ray crystallography at a resolution of 2.8 Å. Histones H2A and H2B are yellow and red, respectively; H3 is purple, and H4 is green. The DNA helix is wound about the protein core. The histone tails

extend from the core and are the sites for modification, which may disrupt the formation of nucleosome assemblages. (B) Histone H1 can draw nucleosomes together into compact forms. About 140 base pairs of DNA encircle each histone octamer, and about 60 base pairs of DNA link the nucleosomes together. (C) Model for the arrangement of nucleosomes in the highly compacted solenoidal chromatin structure. (A from Luger *et al*. 1997, photograph courtesy of the authors; B, C after Wolfe 1993.)

The functions of chromatin are to package DNA into a smaller volume to fit in the cell, to strengthen the DNA to allow mitosis and meiosis, and to serve as a mechanism to control expression and DNA replication. Here we will focus on the impact of histone modifications on the chromatin status as a mechanism to control gene expression during transcription. Modifications of the histone tails may promote or disrupt contact with the DNA and/or between adjacent histones, controlling fiber formation, and thereby modulating the accessibility of chromatin for transcription (Tse, 1998).

II. The process of transcription

The synthesis of a messenger RNA in the nucleus of a eukaryotic cell is an immensely complex undertaking. Each step in the pathway requires an enormous number of protein factors and identifying them and figuring out how they work has been a major goal of molecular biologists for the last two decades. During transcription a sequence of RNA is synthesized from a complementary template strand of DNA which is read from the 3' → 5' direction but synthesized in the 5' → 3'. This process takes place in the nucleus of the cell in eukaryotes and the cytoplasm or nucleoid (if present) in prokaryotes. Three different RNA polymerases are identified in eukaryotic organisms and are responsible for the synthesis of ribosomal RNA (RNAPI), pre-messenger RNA (RNAPII) and small RNAs including transfer RNA (RNAPIII) (Cramer, 2002). In addition plant genomes contain RNAPIV for synthesis of small interfering RNA (siRNA) (Herr *et al*., 2005). Although all three eukaryotic RNA polymerases are very similar in structure and subunit configuration, RNA Polymerase II uniquely possesses an extra C-terminal domain (CTD) on its largest subunit, Rpb1. The main function of the CTD would serve as a binding platform for other proteins involved in transcription, mRNA processing and histone modifications. RNAPII is responsible for the production of mRNA during transcription and the process of transcription can be divided into 3 stages: *initiation*, *elongation* and *termination*.

A. Transcription initiation

During initiation transcription factors bind to promoter regions consisting of DNA sequences upstream of the start site of transcription. The most common type of promoter is a short DNA sequence called the TATA box, found -30 base pairs from the start site of transcription. This sequence is recognized by the TATA binding protein (TBP) which is a subunit of the general transcription factor (GTF) TFIID. TATA binding protein (TBP) or the TBP containing complex TFIID binds to the TATA box in an association that is greatly stabilized by the subsequent binding of TFIIB, which contacts both TBP and the DNA. The presence of TFIIB allows the recruitment of a TFIIF-RNA polymerase II complex and then of TFIIE and TFIIH. Another GTF, TFIIA, can join the initiation complex at any stage of assembly. Like TFIIB, TFIIA greatly stabilizes the association of TBP with the TATA box. The role of the various transcription factors in directing transcription initiation is the subject of intense studies. While TBP and TFIIB play central roles in the nucleation of the transcription initiation complex, TFIIF, TFIIE, and TFIIH play roles at later steps. TFIIF interacts directly with RNA polymerase II and TFIIB and is required for stable assembly of RNA polymerase II with the TATA-TBP-TFIIB complex. It also inhibits nonspecific binding of RNA polymerase II to nonpromoter sequences and stimulates the rate of transcription elongation. TFIIE incorporation into the TATA-TBP-TFIIB-RNA polymerase II-TFIIF complex is required for subsequent assembly of TFIIH. TFIIE and TFIIH are involved in promoter melting and promoter clearance. TFIIE regulates the activities of TFIIH, which possesses both ATP-dependent helicase activities and a kinase activity capable of phosphorylating the C-terminal domain of RNA polymerase II. The helicase activity is thought to be involved in promoter melting. The C-terminal domain kinase activity may be involved in promoter clearance and transcription elongation. In addition, TFIIE plays a direct role in promoter melting, perhaps by binding to the single-stranded region and thereby stabilizing the melted region of the promoter, and has been shown to help recruit TBP and TFIIA to the TATA box. The different GTFs together with the RNA polymerase II complex form the pre-initiation complex (PIC) (Fig. 2). In these initial phases Mediator, a complex composed of more than 20 subunits, connects the GTFs with RNAPII. Mediator is a large, multisubunit complex that is essential for transcription of mRNA by RNA Pol II in eukaryotes and is believed to bridge transcriptional activators and the general transcription machinery (Kornberg *et al*.,2005).

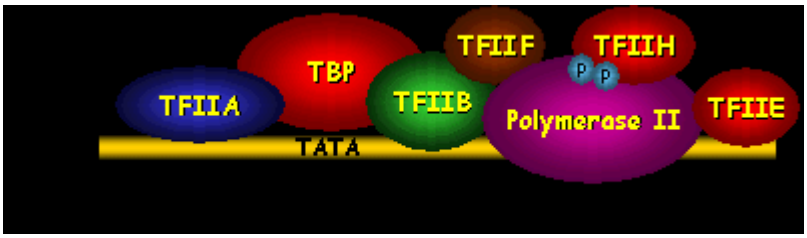

Fig. 2. Schematic overview of the pre-initiation complex (PIC). The general transcription factors are assembled around a TATA-box promoter. Phosphorylation of a subunit of RNA Polymerase II is thought to be critical in the onset to transcriptional elongation (Dahmus, M.E.(1996) J Biol Chem 271, 19009-12).

B. Transcription elongation

After assembly of the PIC at the promoter, RNA polymerase II traverses the template strand and uses base pairing complementarity with the DNA template to create an RNA copy in a process called transcription elongation. At the start of transcription elongation the Mediator complex stimulates the TFIIH kinase , which phosphorylates the CTD of RNAPII on Ser5 and Ser7. CTD phosphorylation then triggers Mediator dissociation (Max *et al*., 2007). Therefore, once Mediator has completed its mission of helping to deliver polymerase to the promoter, it triggers its own release from the CTD. While polymerase proceeds to elongation, Mediator may remain associated with the promoter as part of the scaffold complex to facilitate subsequent rounds of polymerase recruitment and reinitiation (Yudkovsky *et al*., 2000). Transcription elongation is highly regulated both by protein factors that bind to a DNA template, the RNA transcript or the transcription complex as it moves along the template. Important components which bind with RNA polymerase II during elongation consist of SAGA, FACT, Paf1c, TFIIS, RAD6/Bre1, COMPASS, Elongator and others which will be discussed in the following chapters (Fig. 3). Most of these complexes play a function in relaxing the chromatin state to allow RNAPII passage during transcription but recently another level of transcriptional regulation has been identified during elongation. Many developmental and inducible Drosophila and mammalian genes already contain RNAPII in their promoter proximal regions in a so-called “stalled” state. The activation of this stalled RNAPII would be responsible for the expression of these genes (Saunders *et al*., 2006). By chromatin immuno precipitation it was shown that the promoter of the heat shock inducible gene Hsp70 in Drosophila already contains RNAPII when the gene was not induced. Moreover, transcription already initiated RNA synthesis of 20-50 nucleotides of RNA but is stalled afterwards. Upon induction RNAPII is able to escape from the Hsp70 promoter-proximal

region and transcribe the full length RNA. Further chip-chip experiments in both human and Drosophila using tiling oligonucleotide microarrays have demonstrated that RNAPII stalling is a genome-wide phenomenon (ENCODE project, Nature 2007). Whether this extra level of transcriptional regulation also exists in plants is still under investigation.

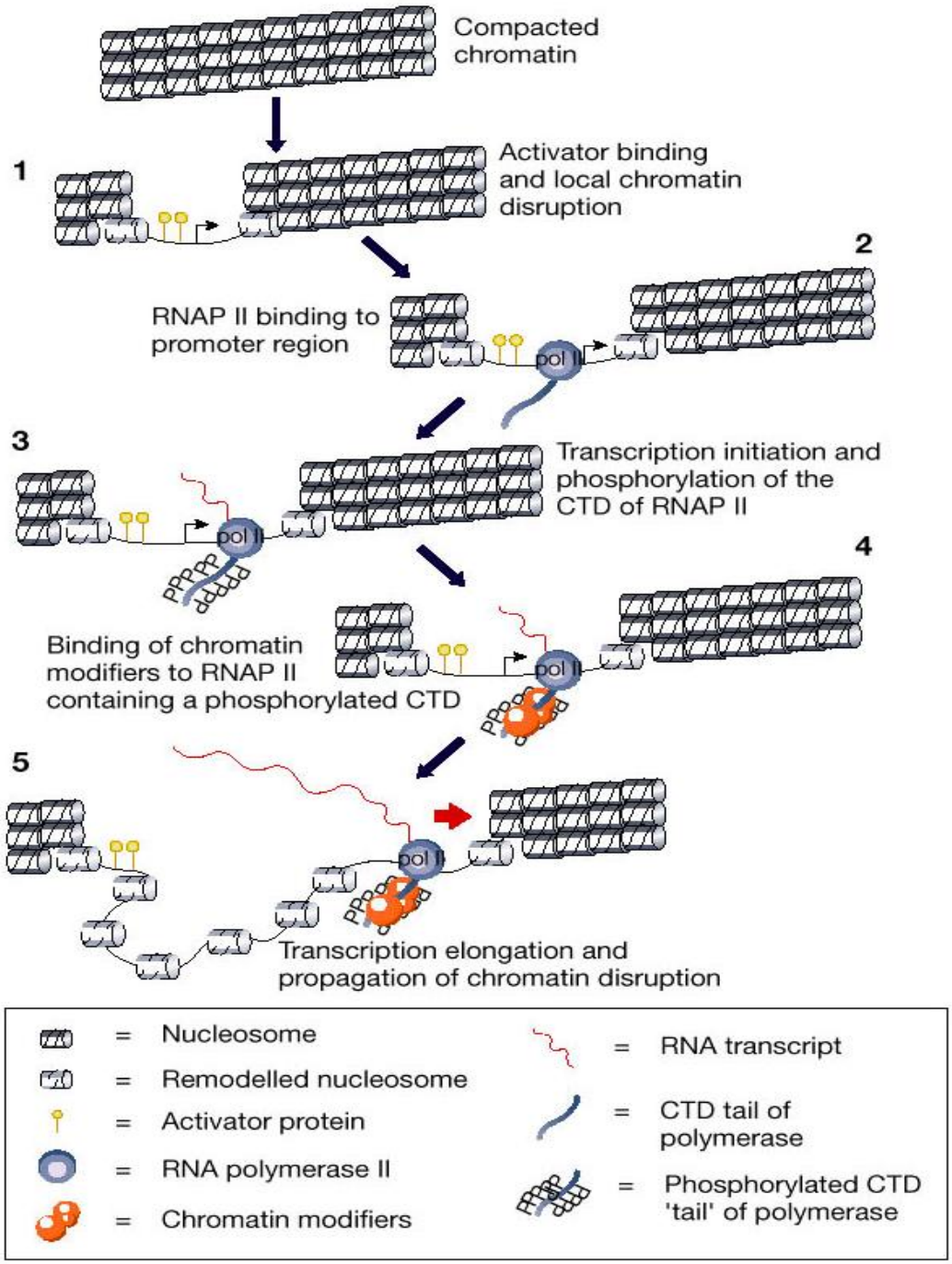

Fig. 3. Binding of activator proteins to the promoter results in recruitment of chromatin-modifying activities and local chromatin disruption (1). With the assistance of the general transcription factors, RNAP II then binds to the promoter region (2). Shortly after the initiation of

transcription, the C-terminal domain (CTD) of RNAP II is hyperphosphorylated (3). RNAP II with a hyperphosphorylated CTD is recognized and bound by chromatin-modifying factors such as PCAF and/or elongator (4). The chromatin-modifying activities then travel with elongating RNAP II, leading to the propagation of chromatin disruption (5) (Reinberg *et al*., 2006).

C. Transcription termination

Termination of transcription by RNAP II is an essential step in the production of pre-mRNAs. The intrinsic termination signal in the DNA template contains a GC-rich element followed by an oligo(T) sequence. Termination however may not occur until the polymerase has transcribed a significant distance downstream of the poly(A) site. Termination dissociates the 3′ cleavage product and the polymerase from the DNA template and prevents transcriptional interference of downstream genes. The mechanism of termination is poorly understood but it appears to require recognition of the poly(A) site and transcriptional pausing. The nascent RNA forms a stable 3' hairpin followed by 7-9 uridine residues. Upon hairpin formation, the RNA stemloop invades into the upstream region of the RNA-DNA hybrid and disrupts those contacts triggering termination of transcription.

III. Chromatin modifications during transcription initiation and elongation

The DNA of eukaryotic cells is tightly packed in the form of chromatin and since the transcription process requires binding and traveling of large protein complexes through the DNA, the loosening of the chromatin structure is necessary.

Nucleosomes exhibit dynamic properties and are mobilized to alternative positions along the DNA, or at times are ejected, by remodellers to provide regulated access to DNA sequences. Nucleosome repositioning and ejection are important for many chromatin functions: to space nucleosomes properly during chromatin assembly, to enable the ordered access of transcription factors to specific genes during transcriptional regulation and to regulate the access of DNA-repair factors to DNA lesions in chromatin (Owen-Hughes, 2003). In addition, nucleosomes can be covalently modified on lysine residues that reside in their amino-terminal tails, which extend from the core histones. It has been proposed that distinct histone modifications, on one or more tails, act sequentially or in combination to form a 'histone code' that is, read by other proteins to bring about distinct downstream events (Strahl., 2000). These two dynamic processes (modification and repositioning) work in concert to establish or alter the regional properties of

chromatin, although the relative importance and order of these processes vary when individual loci are examined.

A. Chromatin remodelers

As well as the formation of the pre-initiation complex at promoter regions as the passage of RNAPII during elongation requires the de-condensation of the chromatin and this is done by chromatin remodeling complexes. In many cases, the chromatin remodeling machines function as transcriptional co-activators by facilitating access of transcription factors to DNA packaged in nucleosomes. However, some remodeling complexes exert a negative effect on transcription or are dedicated to other processes such as chromatin assembly (Verbsky and Richards, 2001), indeed, sealing back the chromatin after the passage of RNAPII is as important as opening it to avoid cryptic transcription start sites that would lead to wrong mRNA molecules synthesis.

ATP-dependent chromatin remodeling complexes use the energy of ATP to modify the structure of chromatin. Four main families of remodelers have been identified: SWI/SNF, ISWI, CHD and INO80/SWR. These modelers play a role in modifying the chromatin structure at the promoter of genes and in RNAPII transcript elongation. They act by catalyzing the fluidity in the position and conformation of nucleosomes (Lusser and Kadonaga, 2003). They are thought to do this by catalyzing the interconversion between various chromatin states via an activated intermediate consisting of the remodeling factor and a nucleosome with weakened histone-DNA contacts. For example the activity of RSC, a SWI-SNF modeler, was enhanced by histone acetylation which may increase the affinity of RSC for the nucleosome (Kasten *et al*., 2003).

The Arabidopsis genome encodes more than 40 different proteins belonging to ATP-dependent chromatin remodeling complexes, which can be grouped into three major types, namely SWI2/SNF2, ISWI and CHD based on the presence of other protein motifs in addition to the ATPase domain. Among them, only AtBRM, SPLAYED (SYD), PICKLE (PKL), DECREASE IN DNA METHYLATION (DDM1), MORPEUS MOLECULE (MOM), DRD1 and PHOTOPERIOD INDEPENDENT EARLY FLOWERING1 (PIE1) have been functionally characterized (Hsieh and Fischer, 2005). The existence of these SWI/SNF-type proteins however is only based on homology studies and so far no complete plant chromatin remodeling complexes have been isolated and characterized (Jerzmanowski, 2007). Mutation in one of these, SPLAYED (SYD), cause severe developmental defects. SYD is required for the maintenance of the shoot apical meristem, for the repression of floral transition, for proper floral homeotic gene expression

and for ovule development. *Syd* mutations enhance the floral phenotype of weak *leafy* (*lfy*) alleles, suggesting that SYD is a coactivator of LFY. However, SYD also acts as a LFY-dependent repressor of the transition from inflorescence to flower meristem (Wagner and Meyerowitz, 2002). AtBRM is a SNF2 family protein homolog of Brahma, the ATPase of the Drosophila SWI/SNF complex involved in chromatin remodeling during transcription. In contrast to its Drosophila counterpart, BRM is not an essential gene. Homozygous BRM loss of function mutants are viable but exhibit numerous defects including dwarfism, altered leaf and root development and several reproduction defects (Hurtado *et al*., 2006). Flowers of brm loss-of-function mutants have several developmental abnormalities, including homeotic transformations in the second and third floral whorls and brm mutants present reduced levels of APETALA2, APETALA3, PISTILLATA and NAC-LIKE, ACTIVATED BY AP3/PI. Loss of PICKLE (PKL), another member of the Arabidopsis SNF2-like proteins, affect root development and repression of LEAFY COTELYDON1 (LEC1), which controls embryonic identity (Ogas, 1999). Many of these SWI/SNF homologues are part of multisubunit complexes, for example BRM interacts with AtSWI3C and AtSWI3B, suggesting that a plant SWI/SNF-like complex is functional in plants as in the case of the mammalian SWI/SNF complexes.

B. Histone chaperones

Histone chaperones are histone-binding proteins involved in intracellular histone dynamics, as well as histone storage and replication-associated chromatin assembly. However, much recent evidence has revealed a role for these factors in regulating elongation-coupled changes to chromatin. FACT (facilitates chromatin transcription) was one of the first histone chaperones to be identified as having a role in transcript elongation (Orphanides *et al*., 1998; 1999). FACT has intrinsic histone chaperone activity and appears to facilitate elongation at least partly by destabilizing nucleosome structure so that one histone H2A-H2B is removed during RNAPII passage (Reinberg *et al*., 2006). Although the mechanisms of chaperone mediated nucleosome disassembly and reassembly are not fully known yet, three possibilities have been proposed (Svejstrup, 2010). First, as in the case of FACT, these factors may directly alter nucleosome stability. Interestingly, this effect appears to be enhanced by histone acetylation (Swaminathan *et al*, 2005; Ito *et al*., 2000). Second, they may act as a sink for histones released during elongation and a source of histones during post-elongation chromatin reassembly. Finally, histone

chaperones may act in combination with ATP-dependent chromatin remodeling machines to directly mediate nucleosome disassembly.

In Arabidopsis, a FACT complex consisting of SSRP1 and SPT16 has been identified that associates over the entire transcribed region of RNAPII-transcribed genes, indicating a role in transcript elongation. Moreover, the presence of Arabidopsis FACT in the euchromatin of meristematic cells and developing tissues, and its absence from terminally differentiated cells, suggests that it plays a role in differentiation and development processes (Duroux *et al*., 2004). FACT localizes to inducible genes only after induction of transcription, and the association of the complex with the genes correlates with the level of transcription. Plants with reduced levels of FACT subunits are affected in vegetative and reproductive development (Lolas *et al*., 2010). The FACT mutants *spt16-1, spt16-2 and ssrp1-2* have a reduced leaf size due to a lower cell number suggesting that cell division is affected. In addition the ssrp1-2, spt16-1 and spt16-2 are early flowering and have a 'bushy' architecture due to increased number of primary and secondary inflorescenses showing that FACT plays an important role in plant development. Interestingly mutation in the genes encoding the histone H2B mono-ubiquitinases HUB1/2 share phenotypical characteristics with mutations in the FACT complex and recently a genetical interaction between these two complexes was discovered which suggests that HUB and FACT regulate common target genes but can also act independently in the regulation of others (Lolas *et al*., 2010).

Recently other histone chaperones in plants have been identified with a direct role in transcriptional regulation. AtFKBP53, possesses histone chaperone activity and is required for repressing ribosomal gene expression in Arabidopsis. The AtFKBP53 protein is a multidomain protein with a typical peptidylprolyl isomerase (PPIase) domain and several highly charged domains. AtFKBP53 has histone chaperone activity and the charged acidic domains are sufficient for the activity. AtFKBP53 interacts with histone H3 through the acidic domains, whereas the PPIase domain is dispensable for histone chaperone activity or histone binding. Ribosomal RNA gene (18S rDNA) is overexpressed when AtFKBP53 activity is reduced or eliminated in Arabidopsis plants. Chromatin immunoprecipitation assay showed that AtFKBP53 is associated with the 18S rDNA gene chromatin, implicating that AtFKBP53 represses rRNA genes at the chromatin level (Li and Huan, 2010). Other histone chaperones don't play a role in transcriptional regulation but possess a nucleosome assembly function. For example, Chromatin assembly factor 1 (CAF1) has a conserved chaperone activity for chromatin assembly at the DNA

replication fork during S phase. CAF1 targets acetylated histone H3-H4 dimers to newly synthesized DNA, thus allowing nucleosome assembly (Polo and Almouzni, 2006).

C. Covalent histone modifications

In this chapter we will focus on the role of covalent histone modifications in the regulation of gene expression in euchromatin. These modifications can activate or repress transcription by affecting internucleosomal contacts or changing electrostatic charge generating more 'open' or 'closed' chromatin configurations. Secondly, the covalently attached moieties can act as a binding surface for elongation-associated effector complexes. Within a histone, the amino acid modified, the type of modification and the degree of modification (eg. monomethylation, dimethylation or trimethylation) all affect whether a given modification is activating or repressive (Berger, 2007).

1. Histone acetylation

The best studied histone modification is the acetylation of the amino-terminal tails of the histones. Animal and yeast histone acetyltransferases (HAT) interact with transcription activators, indicating a positive role in transcription for this posttranslational modification (Roth *et al*., 2001). Histone deacetyltranferases (HDACs) in turn interact with transcriptional repressors, suggesting that deacetylation is involved in repression and silencing (Courey and Jia, 2001). The interplay between HATs and HDACs results in a dynamic equilibrium between acetylation and deacetylation at promoters and regulatory regions that affect chromatin structure and transcription. Transcriptional activity is typically correlated with dramatic histone hyperacetylation in the promoter of genes (Workman *et al*., 1998; Pokholok *et al*., 2005). Interestingly, active transcription also correlates with histone acetylation in the coding region of genes, but here the observed increases are often surprisingly modest (Kouskouti *et al*., 2005). This might argue that histone acetylation does not play an important role in RNAPII transcript elongation through chromatin. However, HATs and HDACs are enriched in the coding region of genes (Govind *et al*., 2007) indicating substantial turnover of acetylation. Moreover, the research performed in this thesis shows that by mutation of Elongator the level of histone acetylation in chromatin is reduced in the coding region of genes (chapter 4). The best studied HAT, Gcn5, is another candidate for coupling RNAPII movement to histone acetylation. Gcn5 is a member of

the SAGA (Spt-Ada-Gcn5-acetyltransferase) coactivator complex, whose members have been shown to interact physicially and genetically with TFIIS and other elongation factors (Wery *et al*., 2004; Milgrom *et al*., 2005). The deletion of Gcn5 in yeast reduces H3 acetylation levels within coding regions of genes resulting in defects in nucleosome eviction and elongation (Krisjuhan *et al*., 2002). Histone acetylation is reversed by the action of HDACs in a process that also play an important role during transcript elongation. Cotranscriptional H3K36 methylation by the RNAPII-associated Set2 complex recruits the Rp3dSHDACcomplex, resulting in histone deacetylation in the wake of RNAPII passage. This pathway is crucial for reestablishing the chromatin structure that is perturbed by the movement of RNAPII through the gene. Thus, prevention of cryptic transcription initiation from within coding units in the wake of elongating RNAPII is achieved via two mechanisms: H3K36me-directed histone deacetylation and histone chaperone-mediated nucleosome reassembly (Carrozza *et al*., 2005, Keogh *et al*., 2005, Joshi *et al*., 2005).

Sequence and domain analyses of the Arabidopsis genome have revealed four families of HATs, and three families of HDAC, consisting of 12 genes and 18 genes respectively (Pandey *et al*., 2002) (Table 1). The HAT group is divided into four types based on primary homology with yeast and mammalian HATs: GNAT, MYST, p300/CBP, and TAF1. The GNAT (GCN5-related N-acetyltransferase) family is generally considered to comprise three subfamilies, designated GCN5 (General Control Nonderepressible protein5), ELP3 (a transcriptional Elongator complex Protein), and HAT1 in higher eukaryotes. In the *Arabidopsis* genome, a single homolog of each of the GCN5, ELP3, and HAT1 subfamilies (HAG1/AtGCN5, HAG3, and HAG2, respectively) has been identified (Pandey *et al*., 2002). The *Arabidopsis* genome contains two MYST (for 'MOZ, Ybf2/Sas2 and Tip60') family genes (*HAG4* and *HAG5*), five p300/CBP (CREB-binding protein)-type HAT domain genes (*HAC1*, *HAC2*, *HAC4*, *HAC5*, and *HAC12*), and two TAF1 (for 'TATA-binding protein (TBP)-associated factor') genes (*HAF1* and *HAF2*). The HDACs group in plants is divided into 3 families: RPD3/HDA1 (histone deacetylase 1 protein), SIR2 (silent information regulator protein 2) and a plant specific family of HDACs , HD2 which was discovered in maize. The N-terminal lysine residues of histone H3 (K9, K14, K18, K23, and K27) and H4 (K5, K8, K12, K16, and K20) are found to be acetylation/deacetylation targets in *Arabidopsis* (Zhang *et al*., 2007; Earley *et al*., 2007). As reviewed (Chen and Tian, 2007) histone acetylation in plants affects a variety of biological processes in response to internal and external

signals, such as cell differentiation, growth, development, light, temperature, and abiotic and biotic stresses. The reversible changes in histone acetylation also contribute to cell cycle regulation and epigenetic silencing of rDNA and redundant genes in response to interspecific hybridization and polyploidy.

Table 1. Genes encoding HAT and HDAC homologs in *Arabidopsis* (modified from Pandey *et al*., 2002)

HDAC gene family	Arabidopsis gene name	Gene code
RPD3/HDA1	HDA2	At5g26040
	HDA5	At5g61060
	HDA6	At5g63110
	HDA7	At5g35600
	HDA8	At1g08460
	HDA9	At3g44680
	HDA10	At3g44660
	HDA14	At4g33470
	HDA15	At3g18520
	HDA17	At3g44490
	HDA18	At5g61070
	HDA19	At4g38130
HD2	HDT1	At3g44750
	HDT2	At5g22650
	HDT3	At5g03740
	HDT4	At2g27840
SIR2	SRT1	At5g55760
	SRT2	At5g09230
HAT gene family	**Arabidopsis gene name**	**Gene code**
GNAT	HAG1/GCN5	At3g54610
	HAG2	At5g56740
	HAG3/ELO3	At5g50320
MYST	HAG4	At5g64610
	HAG5	At5g09740
CBP	HAC1	At1g79000
	HAC2	At1g67220
	HAC4	At1g55970
	HAC5	At3g12980
	HAC12	At1g16710
TAFII250	HAF1	At1g32750
	HAF2	At3g19040

Although the identification of these Arabidopsis HAT and HDAC families was performed by sequence similarity, differences were found with respect to sizes of gene families and multi-

domain protein structures compared to the animal and fungi kingdoms (Table 2). The most notable difference is the existence of the HDAC family, HD2, found only in plants. Four HD2 proteins are identified in Arabidopsis and they all contain a conserved N-terminus with the HD2-type HDAC domain, a central acidic domain and variant C-terminal domain. The silencing of one of these HD2 proteins, HDT1, results in aborted seed development (Wu *et al*., 2000). On the other hand plants only posses two SIR2 family proteins (SRT1 and SRT2) which is less then animals (4) and fungi (3). It is possible that the HD2 family has taken over some of the functions of the SIR2 family. The GNAT/MYST superfamily of HAT proteins is defined by the presence of a HAT domain which is comprised of four motifs, A-D, for the GNAT proteins while the MYST proteins only possess the A motif of the HAT domain. A single homologue is found in Arabidopsis for all subfamilies (GCN5, ELP3, HAT1, HAG4 and HAG5) of the GNAT/MYST superfamily. Also in the animal and fungi genomes a single representative of these subfamilies was identified suggesting that the plant proteins may form complexes similar to those formed in yeast and animals (Table 2). In contrast the CREB-binding protein (CBP) and $TAF_{II}250$ family of HAT proteins have major differences in domain architecture between plants and animals. The most notable difference is the absence of a bromodomain in the plant CBP-type HATs. The role of the bromodomain in the animal proteins is to bind acetylated histones. The lack of a bromodomain in the plant proteins suggests that these proteins utilize a different domain to perform this function or that another bromodomain protein acts as a bridge between acetylated histones and CBP-type HATs. In addition the CBP family in plants has been amplified to five genes as compared to a single representative in most animals and none in fungi. The diversity in these chromatin modifying enzymes among plants, animals and fungi reflects important differences in the manner in which chromatin controls gene expression and supports the suggestion that plants have developed mechanisms of global gene regulation related to their unique developmental pathways and environmental response.

Table 2. Summary of the HDAC and HAT homologs found in plants, fungi and animals. Organism abbrivations as follows: *Arabidopsis thaliana* (At), *Saccharomyces cerevisiae* (Sc), *Schizosaccharomyces pombe* (Sp), *Caenorhabditis elegans* (Ce), *Drosophila melangoster* (Dm). (Pandey *et al*., 2002)

Homology groups	Plants		Fungi		Animals
	At	Sc	Sp	Dm	Ce
HDAC homology groups					
RPD3/HDA1 family (*HDA* genes)					
Class I	4	3	2	2	3
Class II	3	1	1	2	4
Class III	1	0	0	0	1
Unclassified	2	1	0	0	0
HD2 family (*HDT* genes)	4	0	0	0	0
SIR2 family (*SRT* genes)					
Class I	0	5	3	1	1
Class II	1	0	0	1	2
Class IV	1	0	0	2	1
Total HDAC homologs	16	10	6	9	12
HAT homology groups					
GNAT-MYST superfamily (*HAG* genes)					
GNAT family					
GCN5	1	1	1	1	1
ELP3	1	1	1	1	1
HAT1	1	1	1	1	1
HPA2	0	2	1	0	0
MYST family	2	3	2	5	4
CBP family (*HAC* genes)	5	0	0	1	1
TAFII250 family (*HAF* genes)	2	1	1	1	1
Total HAT homologs	12	9	7	10	9

2. Histone methylation

Whereas the effects of histone acetylation on nucleosome behavior and stability are well documented, the role of histone methylation is less clear. Histones are methylated on their arginine or lysine residues. A feature of this modification is that arginines can be mono or dimethylated while the lysine residues can be mono, di or trimethylated. The different methylation states can have distinct function. The methylation marks are written on lysine or arginine by distinct enzymes, namely, histone lysine methyltransferases (HKMTs) or protein arginine methyltransferases (PRMTs). In contrast to histone acetylation, the methylation on

lysines does not affect the net charge of the modified residues, but it elevates the hydrophobicity and may alter intra- or intermolecular interactions or create new binding surfaces for regulatory proteins. Generally, histone H3K9 and H3K27 methylation are associated with silenced regions, whereas H3K4 and H3K36 methylation are associated with active genes (Berger, 2007). However the mono and dimethylation of histone H3K9 and H3K27 is typical for silenced chromatin but the trimethylation is enriched in euchromatin which shows the complexity of these modifications. Moreover, the methylation of H3K9 seems to be associated with DNA methylation and is critical for maintenance of genomewide transcriptional gene silencing and genome stability (Vaillant and Paszkowski, 2007). Histone H3K4 methylation is mediated by Trithorax group (TrxG) proteins, which act antagonistically to PcG proteins in regulating the homeotic gene (HOX gene) expression in animals. The functions of TrxG and PcG proteins are conserved in plants and animals, where PcG proteins are generally required for maintaining a repressive state and TrxG proteins are responsible for the maintenance of an active state (Pien and Grossniklaus, 2007). ARABIDOPSIS TRITHORAX 1 (ATX1) is an active histone methyltransferase specific for histone H3K4 (Alvarez-Venegas *et al*., 2003). Mutations in ATX1 lead to abnormal floral organ identity and slightly early flowering. ATX1 directly interacts with the promoter and first exon of FLC locus and catalyzes H3K4me3 modification. Histone H3K36 is specifically methylated by histone methyltransferase ASH1 in mammals and Drosophila, and H3K36me2/3 are linked to transcription elongation (Berger 2007, Li *et al*., 2007). The Arabidopsis genome encodes at least four ASH1 homologues and three ASH1-related proteins. Among them, the methyltransferase activities of SDG8, SDG26, and SDG4 have been identified in vivo and in vitro (Cartagena *et al*., 2008, Xu *et al*., 2008, Zhao *et al*., 2004). SDG8 is the major H3K36 methyltransferase in vivo. Mutation of SDG8 leads to early flowering phenotypes, increased shoot branching and altered carotenoid composition. SDG8 activates expression of FLC and MADS AFFECTING FLOWERING (MAF) genes while SDG23 has the opposite effect.

Arginine residues on histones are also methylated and the reaction is catalyzed by a small group of protein arginine methyltransferases (PRMTs). In Arabidopsis, nine PRMTs are present in the genome and methylation mainly occurs at Arg2, Arg8, Arg17, Arg26 of histone H3 and Arg3 of histone H4. AtPRMTs are involved in many processes such as transcription regulation, RNA

processing, nuclear transport, DNA-damage repair and signal transduction (Bedford and Richard, 2005).

3. Histone ubiquitylation

Ubiquitin is a small (76 AA) highly conserved protein which performs a wide range of functions upon conjugation to its target proteins. The addition of ubiquitin onto a protein often commits the labeled protein to degradation in the proteasome but ubiquitination is also involved in stress responses, signaling networks, intracellular trafficking, protein-protein interactions and transcription (Smalle and Vierstra, 2004; Welchman *et al*., 2005). Ubiquitination is carried out by a set of three enzymes, E1, the ubiquitin activating enzyme, E2, the ubiquitin-conjugating enzyme, and E3, the ubiquitin ligase. Ubiquitin is first activated by E1, before being transferred to its active site, the amino acid cystein. This transfer requires ATP, making the process energy-dependent. The ubiquitin molecule is then passed on to the second enzyme of the complex, E2 (ubiquitin-conjugating enzyme), before reaching the final enzyme, E3, the ubiquitin protein ligase, which recognises, binds the target substrate and labels it with the ubiquitin. Substrates can be mono-or polyubiquitinated; whereas polyubiquitination targets proteins for degradation via the 26S proteasome, monoubiquitination generally acts as a tag that marks the substrate protein to signal for a particular function. One well-characterized example of this process is the monoubiquitination of histones H2A and H2B. The outcome of these modifications is dependent on a lot of factors and is different for histone H2A and H2B but one common theme in H2A and H2B ubiquitination is the involvement of histone crosstalk, particularly Lys-4 H3 di-and trimethylation (reviewed in Osley, 2006). H2B ubiquitination is required for Lys-4 H3 methylation and appears to assist FACT in stimulating RNA polymerase II during transcription elongation whereas H2A ubiquitination inhibits Lys-4 H3 methylation and recruitment of FACT and transcription elongation.

Rad6, the E2 ubiquitin conjugase that catalyzes H2B monoubiquitination, was first identified in S. cerevisiae (Robzyk *et al*., 2000) and acts in conjunction with the E3 ubiquitin ligase Bre1 to monoubiquitinate H2B in vivo (Hwang *et al*., 2003). This ubiquitination has been associated with the transcriptional activation of various classes of genes and is mediated through association with the RNAPII-regulating complex (Xiao *et al*., 2005). Interestingly this ubiquitination is a prerequisite for the methylation of lysine 4 and lysine 79 of histone H3 (Dover *et al*., 2002; Weake and Workman, 2008) and this in turn induces gene expression (Roh *et al*., 2006). In yeast

the Lys-4 H3 methylation is catalyzed by Set1, which functions as part of the COMPASS complex. COMPASS associates with the elongating form of RNAP polymerase II and the PAF complex (reviewed in Shilatifard, 2006) illustrating the complex interactions between histone modifying complexes and RNAPII.

In the Arabidopsis genome, there are two BRE1 homologues (Histone Monoubiquitination HUB1 and HUB2) and three RAD6 homologues (Ubiquitin Carrier protein1 UBC1, UBC2 and UBC3). Mutations in HUB1 or HUB2 lead to defects in seed dormancy and bushy plants (Liu *et al*., 2007) and *hub1* or *hub2* plants are small with narrow leaf laminae and short primary roots (Fleury *et al*., 2007) and show an early flowering phenotype (Cao *et al*., 2008). These results are consistent with the observation that HUB1 and HUB2 form homodimers and heterodimers and act together in the same complex. Mutation of one of the RAD6 homologues (UBC1-3) in Arabidopsis does not lead to any phenotype but the *ubc1ubc2* double mutant exhibited a phenotype similar to that of hub1 or hub2 suggesting functional redundancy between UBC1 and UBC2. The functionality of the Arabidopsis Rad6/Bre1 is conserved i.e. H2B was monoubiquitinated in an in vitro assay (Fleury *et al*., 2007) and ubiquitination levels of H2B are down in the hub1 mutants (Liu *et al*., 2007). Whether the Rad6/Bre1 targets specific genes or acts as a general ubiquitination complex is unsure although it seems to be directly involved in the regulation of FLC (Cao *et al*., 2008).

D. DNA methylation and histone modifications

DNA methylation involves the addition of a methyl group to position 5 of the cytosine pyrimidine ring or the number 6 nitrogen of the adenine purine ring. DNA methylation might affect the transcription of genes in two ways. First, the methylation of DNA itself may physically impede the binding of transcriptional proteins to the gene, and second, methylated DNA may be bound by proteins knows as methyl-CpG-binding domain proteins (MBDs). MBD proteins then recruit additional proteins to the locus, such as histone deacetylases and other chromatin remodeling proteins that can modify histones, thereby forming compact, inactive chromatin (Bird 2002). DNA methylation in plants differ from that of mammals: while DNA methylation in mammals mainly occurs on the cytosine nucleotide in a CpG site, in plants the cytosine can be methylated at CpG, CpHpG and CpHpH sites, where H represents any nucleotide but guanine. Recently the relationship between DNA methylation, chromatin structure and gene silencing was well established (Fuks 2005). The *Arabidopsis thaliana* genome contains at least ten genes that

encode DNA methyltransferases that can be divided into three main families based on their function and/or sequence homology to mammalian DNA methyltransferases. *Arabidopsis* MET1 (homologue of the Dnmt1 responsible for maintenance of CG methylation in mammals) is the most extensively studied plant DNA methyltransferase. Shortly after its discovery, transgenic plants with reduced levels of DNA methylation due to the expression of *MET1* antisense RNA were generated (Tariq and Paszkowsk, 2004)**.** Abnormalities in these plants (delayed flowering and loss of gene silencing) pointed towards a complex role of MET1 in plant development. In Arabidopsis *kyp* (a well-known HMT) mutants not only methylation of histones was abolished but also DNA methylation which indicates that histone methylation directs DNA methylation (Jackson et al., 2002). Other reports show that histone methylation is a downstream event of DNA methylation (Gendrel et al., 2002). *met1* mutants with reduced levels of CG and CNG methylation provided evidence that the loss of DNA methylation affects H3K9 methylation. The order of these events is still under investigation. Nevertheless, the link between DNA methylation and other histone modifications is an interesting research field and will reveal a complex network between different epigenetic marks.

IV. Chromatin and environment

Epigenetic studies inherited changes in phenotype or gene expression caused by mechanisms other than changes in the DNA sequence. These changes include imprinting, gene silencing, X chromosome inactivation, maternal effects and regulation of histone modifications and heterochromatin.

The development of different organs, tissues and cell lineages are the consequence of differences in programmed gene expression. These different programs occur without changes to the sequence of the DNA indicating that development is epigenetic (Reik, 2007) but epigenetic changes can also be acquired throughout the life of an organism in response to environmental exposure. Studies in yeast have shown that upon heat shock the nucleosomes of the HSP82 (heat shock protein 82) promotor are hyperacetylated before they are temporarily sequestered (Zhao *et al*., 2005). Also in higher animals epigenetic changes occur upon environmental stimuli. Rats which were fed a protein-restricted diet during pregnancy resulted in persisting changes in DNA methylation and expression of the glucocorticoid receptor (GR) (Lillycrop *et al*., 2005) due to a 20% lower CpG methylation in the GR gene promoter of the offspring. The methylation of fetal

DNA that occurs *in utero* as a result of low dietary levels of folate, methionine, or selenium can change epigenetic programming that can persist into adulthood (Zaina *et al.*, 2005). Also chromatin-modifying enzymes are susceptible to environmental agents and metabolites and this is no different in plants. Plants are sessile and need to constantly regulate their developmental and physiological processes to respond to various internal and external stimuli. Environmental changes induce epigenetic changes in plants affecting development. The transition to flowering is a major developmental switch that integrates several signals from the environment, such as cold and day length. The key integrator in flowering time in Arabidopsis is FLC, a transcription factor that acts as a floral repressor. *FLC* prevents plants from flowering until winter has passed. The repression of *FLC* by prolonged cold (called vernalization) involves both an initial repression of *FLC* during the cold and subsequent maintenance of repression after a return to warm temperatures in *A. thaliana. VERNALIZATION INSENSITIVE 3* (*VIN3*) is one of the initial repressor of *FLC* during cold treatment. *VIN3* encodes a PHD domain chromatin remodelling protein and expression is induced after several weeks of cold treatment (Sung and Amasino, 2004). Activation of *VIN3* triggers chromatin remodeling and leads to an increase in the levels of repressive histone modifications at *FLC* chromatin, such as histone H3 lysine 27 di- and trimethylation (H3K27me2, H3K27me3), histone H3 lysine 9 dimethylation, and histone H4 arginine 3 dimethylation, as well as the loss of histone modifications associated with active transcription, such as histone H3 acetylation and histone H3 lysine 4 di- and trimethylation (H3K4me2, H3K4me3) (Bastow *et al*., 2004, Sung and Amasino, 2004, Sung *et al*., 2006 and Schmitz *et al*., 2008). This chromatin remodeling results in a repression of *FLC* and promotes flowering.

Another environmental cue which induces epigenetic changes in plants is light. Light is the single most important environmental parameter for plant development and Arabidopsis adapts its development to changes in different light parameters such as direction, duration, quantity and wavelength (Whitelam *et al*., 1998; Thomas, 2006). The effect of light on histone modifications has been established however the detailed mechanisms of light-regulated gene transcription remain obscure. For example, light-regulated expression of the pea (Pisum sativum) plastocyanin gene (PetE) was reported to specifically correlate with the acetylation of histones H3 and H4 (Chua *et al*., 2001, 2003). Mutation in the HAT GCN5 results in a long-hypocotyl phenotype and reduced light-inducible gene expression of the IAA3/SHY2 gene. This reduced expression is

correlated with reduced acetylation of histones H3 and H4 on the core promoter regions (Benhamed *et al*., 2006) whereas mutation of the histone deacetylase HD1 induced opposite effects. A recent study showed a direct connection between four histone modifications (H3K4me3, H3K9Ac, H3K9me2 and H3K27me3) and the expression level of six genes that showed distinct changes in their mRNA abundance in dark and white light-grown seedlings (Guo *et al*., 2008). When they compared expression levels of these genes with their histone state , five genes showed an increase in H3K4me3 or H3K9ac under white light or darkness in parallel to increased transcript levels in the same light environment. In contrast, H3K9me2 and H3K27me3 were enriched in darkness for four genes, while the transcript levels of the respective genes were up-regulated in white light. This shows that changes in histone modifications and gene expression are cooperatively regulated by light during Arabidopsis development. How the different histone modifying factors integrate these light signals remains unclear.

Interestingly plants do not only change their physiology upon stimuli from the the environment but also changes in their genome have been observed. For example, when plants are exposed to elevated UV-B radiation an increase in the frequency of somatic homologous DNA rearrangements are observed (Ries et al., 2000). Recently it was shown that plants from successive generations of the original stressed plants inherited the capacity for genomic change referred to as transgenerational stress memory (Molinier et al., 2006). Arabidopsis plants treated with short-wavelength radiation or flagellin show increased somatic homologous recombination of a transgenic reporter and these increased levels of homologous recombination persist in the subsequent, untreated generations. The authors conclude that environmental factors lead to increased genomic flexibility even in successive, untreated generations, and may increase the potential for adaptation. How these changes in genome flexibility are inherited is still under investigation.

Chapter 2

The Elongator Complex

I. Elongator in yeast

A. Introduction

As discussed in the previous chapter, the repressive context of chromatin puts severe constraints on the rate of elongation by RNAPII. This problem prompted researchers to look for factors binding to RNAPII facilitating transcription elongation through chromatin. As such the Elongator complex was identified in yeast by its association with the hyperphosphorylated form of RNAPII (Otero *et al*., 1999). The Elongator complex is an unstable six-subunit complex composed of two subcomplexes: core-Elongator, comprised of Elp1, Elp2 and Elp3 (Wittschieben *et al*., 1999) and a smaller three-subunit module composed of Elp4, Elp5 and Elp6 (Winkler *et al*., 2001). Elp1 is the largest subunit and is considered to serve as docking station for the other subunits. Elp2 is a WD40 protein which are thought to be involved in protein-protein interactions. Elp3 is a conserved member of the GNAT (Gcn5-related N-actetyltransferase) protein family (see Chapter1) and possesses a C-terminal histone acetyltransferase (HAT) domain and an N-terminal sequence that resembles an iron-sulfur (FeS) cluster motif. The HAT domain is well characterized, but the role of the FeS cluster is unclear however, a fully functional FeS cluster is required for Elongator integrity and for the association of the complex with its accessory factors KTI11 and KTI12 (see further) (Greenwood *et al*., 2009).

Mutation in any of the genes encoding the subunits of the Elongator complex causes a multitude of phenotypes in yeast with the most notable one its resistance to zymocin. Zymocin, a toxin secreted by the yeast *Kluyveromyces lactis*, is a heterotrimeric (αβγ) protein complex and the expression of its smallest subunit in *S. Cerevisiae* , the γ-toxin, is lethal while the α- and β-subunits are involved in zymocin docking and γ-toxin import (Jablonowski *et al*., 2001). The toxin causes sensitive budding yeast cells to arrest at the unbudded G1 stage of the cell cycle with an unreplicated DNA content. In a screen for zymocin resistant mutants TOT1 (γ-toxin target), TOT2, TOT3, TOT7, TOT5 and TOT6 were picked up and shown to be allelic to the genes coding for the subunits of the Elongator complex ELP1, ELP2, ELP3, ELP4, ELP5 and ELP6, respectively (Frohloff *et al*., 2001). In addition, other genes in *S. cerevisiae* were identified which confer resistance to zymocin upon mutation, KTI11, KTI12, KTI13 and KTI14 (Fichtner *et al*., 2002). KTI12 is unique in the sense that it also renders cells resistant to zymocin when maintained in multicopy or overexpressed from the GAL10 promoter. KTI12 physically interacts with Elongator, and cell fractionation demonstrates partial co-migration with RNAPII and

Elongator. The observations that multicopy KTI12 results in a mild Elongator phenotype but does not affect Elongator assembly, indicate that KTI12 may not be a subunit of Elongator but, rather, modulates/regulates Elongator function (Fichtner *et al*., 2002). KTI11 is a small, highly conserved CSL zinc finger-containing protein found in many eukaryotes that interacts with core-Elongator. KTI13 was shown to be allelic to α-TUBULIN SUPPRESSOR1 (ATS1), a protein with a potential role in regulatory interactions between microtubules and the cell cycle, as suggested by genetic and physical interactions with NUCLEOSOME ASSEMBLY PROTEIN1 (NAP1), and genetic interactions with α-tubulin1 (TUB1) (Zabel *et al*., 2008).

Besides the resistance to zymocin, Elongator mutants showed severe growth delay when the mutant strains were introduced to new growth conditions such as the change from glucose as carbon source to galactose. Once adapted, however, the mutant cells grew with a similar rate as the wild type (Otero *et al*., 1999). The slower adaptation is a consequence of decreased/delayed transcription of the GAL1-10 (galactose-inducible genes) transcripts as measured by Northern analysis. Transcription of the PHO5 gene (which is expressed when phosphate is limiting in the medium) or the INO1 gene (expressed when inositol levels are low) were also significantly delayed in the Elongator mutant. By contrast, the level of expression of genes that are constitutive such as TUB2 or ACT1 remained unaffected upon experimental conditions. Other phenotypes include thermosensitivity, sensitivity toward caffeine and the drug 6-azauracil (6-AU).

B. Elongator function in transcription

The Elongator complex was found tightly associated with the hyperphosphorylated form of the RNAPII CTD, indicating a role for this complex during transcription elongation. To test this hypothesis, yeast strains lacking the ELP1 subunit were grown in the presence of 6-AU (Otero *et al*., 1999). 6-AU inhibits enzymes in the nucleotide metabolism pathway and leads to depletion of UTP and GTP in yeast cells and thus affecting elongation efficiency of RNAPII. For example, the only phenotype of yeast strains lacking the gene PPR2/SII, which encodes RNAPII elongation factor TFIIS (see chapter1) is sensitivity to 6-AU. *elp1Δ* cells were only marginally sensitive to 50ug/ml 6-AU while *siiΔ* cells showed a moderate sensitivity at this concentration of 6-AU. In contrast, *elp1Δ siiΔ* double mutants were hypersensitive to 6-AU. The drug-induced, synthetic phenotype of *elp1Δ siiΔ* double mutants suggests a role for Elongator in transcription elongation in vivo. The ELP3 component of the Elongator complex is a HAT , whose sequence is

remarkably conserved in eukaryotes (Chapter 1). The HAT activity of core-Elongator (ELP1, ELP2 and ELP3) is directed to all four core histones, however holo-Elongator HAT activity targets specifically histone H3 (lysine-14) and histone H4 (lysine-8 and lysine-12) indicating a role for ELP4, ELP5 and ELP6 in substrate specificity (Wittschieben *et al*., 1999; Winkler *et al*., 2002). The function of the Elongator complex can thus be explained by facilitating the progress of the RNAPII through the nucleosomes by acetylating histones. To examine whether Elongator is important for gene expression in vivo microarray analyses were performed on strains with deletions of the Elongator genes *ELP1, ELP2, ELP4,* and *ELP6 (Krogan and Greenblat, 2001).* A subset of 52 genes had expression levels reduced at least 1.5-fold when Elongator deletion mutants were compared to the wild type. More importantly, the effects of the *elp4Δ* and *elp6Δ* mutations correlated almost perfectly with the effects of *elp1Δ* and *elp2Δ* mutations strongly indicating that the two subcomplexes of Elongator have similar effects on gene expression. The 52 downregulated genes did not show any clear relationship so it is not clear what processes are affected by the mutations. A subset of 44 genes had mRNA levels that were increased at least 1.5-fold when an Elongator gene was deleted. Many of these induced genes are involved in amino acid metabolism, and a similar subset of genes has previously been shown to be induced when *S. cerevisiae* cells were grown in the presence of carcinogenic alkylating agents, oxidizing agents, and ionizing radiation (Jelinsky *et al*., 2000). Therefore, it is likely that upon deletion of an Elongator gene, the up-regulation that occurs for a number of genes is an indirect consequence of the reduced expression of one or more genes that occurs when Elongator is missing.

All these data suggests that Elongator would function in transcription elongation but surprisingly Elongator could not be detected on yeast genes by chromatin immunoprecipitation (ChIP) (Pokholok *et al*., 2002). Moreover, in situ immunofluorescence of ELP1-ELP3 showed that Elongator is predominantly located in the cytoplasm and the authors suggest that Elongator may belong to a class of cytoplasmic, B-type histone acetyltransferases that are thought to catalyze acetylation events linked to transport of newly synthesized histone from the cytoplasm to the nucleus (Roth *et al*., 2001). However Elongator was found to coimmunoprecipitate nascent, unspliced pre-mRNA which strongly supports the idea that the complex is active in the nucleus during transcription (Gilbert *et al*., 2004). It remains to be explained why Elongator was found in the cytoplasm (Pokholok *et al* 2002) as later evidence showed that the ELP1 subunit contains a

NLS sequence essential for Elongator function and fusion of this NLS sequence to green fluorescent protein (GFP) co-localized the NLS-GFP with DAPI-stained nuclear compartments (Fichtner *et al*., 2003).

C. Elongator function in tRNA modification

The function of Elongator in transcription does not provide any straightforward explanation for the mechanism of resistance to zymocin upon Elongator mutation. Only recently the molecular basis behind this phenomenon has been uncovered. By analyzing modified nucleosides in individual tRNA species, it was found that the ELP1-ELP6 and KTI11-KTI13 genes are all required for an early step in the synthesis of 5-methoxycarbonylmethyl (mcm5) and 5-carbamoylmethyl (ncm5) groups present on uridines at the wobble position in tRNA. Immunoprecipitation of tRNA showed that the ELP1 and ELP3 proteins specifically coprecipitate a tRNA susceptible to formation of an mcm5 side chain, indicating a role of Elongator in tRNA modification. The presence of mcm5U, ncm5U, or derivates thereof at the wobble position is required for accurate and efficient translation, suggesting that the phenotypes of elp1-6 and kti11-13 mutants could be caused by a translation defect (Huang *et al*., 2005). A mcm5 side-chain can be found in $tRNA^{Glu}_{mcm^5s^2UUC}$, $tRNA^{Lys}_{mcm^5s^2UUU}$, $tRNA^{Gln}_{mcm^5s^2UUG}$, $tRNA^{Gly}_{mcm^5UCC,}$ and $tRNA^{Arg}_{mcm^5UCU}$ (Johansson and Byström 2002) but only a reduction of $tRNA^{Glu}_{mcm^5s^2UUC}$ was found upon treatment with zymocin. These findings led to the hypothesis that zymocin may be an RNAse that specifically cleaves certain modified, but not unmodified, tRNAs (Lu *et al*., 2005). In the absence of Elongator function, the tRNAs targeted by the toxin are no longer correctly modified and hence no longer degraded which leaves the cells unaffected by the toxin. This hypothesis doesn't rule out that Elongator might regulate the transcription of certain tRNA modifying enzymes and that the zymocin resistance is a secondary effect. However Esberg *et al*. looked for multi-copy suppressors of *elp* phenotypes and isolated two tRNA genes, $tRNA^{Lys}_{s2UUU}$ and $tRNA^{Gln}_{s2UUG}$. Overexpression of these two tRNA species suppressed all observed elongator phenotypes indicating that translation is the underlying mechanism regulated by Elongator (Esberg *et al*., 2006). The results suggest that lack of a wobble mcm5 or s2 group in $tRNA^{Lys}_{s2UUU}$ and $tRNA^{Gln}_{s2UUG}$ lead to a reduced ability to read the cognate A ending and/or the near-cognate G ending codons and that this defect can be suppressed by increasing the tRNA levels. This type of dosage compensation has been described previously where the phenotypes of

a tRNA modification mutant can be counteracted by increasing the levels of the hypomodified tRNA (Anderson *et al*., 1998; Astrom *et al*., 1999).

II. Elongator in Human and Drosophila

Soon after the identification of the Elongator complex in yeast, the human Elongator was purified and characterized (Hawkes *et al*., 2001). Human Elongator is a component of early elongation complexes formed in HeLa nuclear cell extracts and can directly interact with RNAPII in solution. The complex also consists of 6 subunits and homologues of the WD40 repeat protein, ELP2, the HAT, ELP3, and ELP1 and ELP4 are present. The holo-Elongator is capable of acetylating histone H3 and H4. Intriguingly, the closest homologue of ELP1 in human cells is encoded by the IKAP gene (Slaugenhaupt and Gusella, 2002), while the closest mouse homologue of ELP2 is StIP1. Mutations in the IKAP gene can result in the severe human hereditary disorder familial dysautonomia (FD) while StIP1 was identified through its interaction with the transcriptional activator signal transducer and activator of transcription 3 (STAT3). Familial dysautonomia is a developmental disorder of the sensory and autonomic nervous system. Recent studies have shown that two mutations in the IKAP gene are responsible for the disease. The major FD mutation is a splice mutation that results in aberrant tissue-specific mRNA splicing. To study the role of human Elongator in transcription , RNAi and fibroblasts from FD patients were used to identify Elongator target genes (Close *et al*., 2006). HeLa cells were transfected with RNAi oligos that target the IKAP/hELP1 transcript and total mRNA was then extracted and subjected to micro-array analysis. The expression of about 100 genes was significantly downregulated as a result of IKAP/hELP1 RNAi and a significant proportion of the downregulated genes encode proteins regulating cell motility. Although Elongator is recruited to both the target and non-target genes, only target genes show histone H3 hypoacetylation and progressively lower RNAPII density through the coding region in FD cells. By ChIP with IKAP/hELP1, the tubulin, gelsolin and beclin-1 genes were detected although only the gelsolin and beclin-1 gene showed lower expression and hypoacetylation in IKAP/hELP1 depleted fibroblasts. Taken together with the data from the yeast model, these results using human cells strongly point to a function for Elongator in histone acetylation during transcript elongation. The impaired cell motility observed in cells with decreased levels of IKAP/hELP1 protein might underlie FD as the actin cytoskeleton and cell motility play crucial roles in nerve cell growth, cone motility, axon outgrowth and guidance. Misregulation of ELP3 has also been implicated in

the motor neuron degenerative disorder amyotrophic lateral sclerosis (ALS). Two independent studies to identify genes important in neuronal function or survival showed that ELP3 is critical for axonal biology (Simpson *et al*., 2008). In the first, an association study of microsatellite markers in human populations showed that allelic variants of ELP3 were associated with ALS. In the second, a mutagenesis screen in Drosophila for genes important in neuronal communication and survival identified two different loss of function mutations, both in ELP3. The studies related to ALS and FD support a nuclear-based epigenetic role for Elongator components ELP1 and ELP3 in neuronal gene regulation. However, recent studies support a cytoplasm-based role for ELP3 in the acetylation of alfa-tubulin required for the migration and differentiation of projection neurons in cultured mouse cortical neurons (Gardiner *et al*., 2007; Creppe *et al*., 2009; Wynshaw-Boris 2009) and in motor neuron axonal branching and length in zebra fish (Simpson *et al*., 2009). Creppe and colleagues demonstrated that depletion of either the Elongator scaffold subunit ELP1 or the catalytic subunit ELP3 by short hairpin RNAs (shRNAs) reduced the migration speed of bipolar and multipolar cortical neurons in the mouse brain. The depletion of ELP1 or ELP3 also results in strong defects in the branching of differentiated projection neurons. Creppe *et al*. then demonstrated that cytoplasmic ELP1 and ELP3 colocalized and copurified with microtubules and histone deacetylase 6 (HDAC6) in cultured human cells. ELP1 and ELP3 also partially colocalized with acetylated α-tubulin in these cells, suggesting that Elongator may influence the acetylation of microtubules. Moreover, the expression in the mouse brain of a form of alfa tubulin that cannot be acetylated caused similar defects in neuronal migration and branching as the depletetion of ELP1 and ELP3.

Because of the need to further characterize the multiple nuclear and cytoplasm-based roles of ELP3 in the developing nervous system, Drosophila has been recently used as an in vivo multicellular model system. In Drosophila, the ELP3 homologue was picked up as an interactor of 14-3-3 proteins (Karam *et al*., 2010). 14-3-3 proteins are a family of conserved regulatory molecules expressed in all eukaryotic cells that have the ability to bind a multitude of functionally diverse signaling proteins, including kinases, phosphatases, and transmembrane receptors. 14-3-3 proteins also bind histone H3 but only when it is phosphorylated at Ser10 by the action of the JIL-1 kinase. 14-3-3 proteins localize to active genes in a JIL-1-dependent manner and interact with ELP3. JIL-1 and 14-3-3 are required for ELP3 binding to chromatin, and in the absence of either protein, levels of H3K9 acetylation are significantly reduced. These data

provide evidence that 14-3-3 mediates a novel histone crosstalk that promotes transcription elongation in Drosophila by its interaction with ELP3. The ubiquitous reduction of ELP3 in Drosophila resulted in lethality but no defects in development were observed until the late pupal stage, which is the stage at which the majority of lethality occurs (Singh *et al*., 2010). It demonstrates that ELP3 is essential for multicellular development and should provide researchers with a valuable in vivo model for the functional analysis of ELP3 during development. In Drosophila high levels of ELP3 during embryogenesis were detected in the nervous system of the fly and loss of ELP3 in the nervous system resulted in expansion of synaptic boutons in the larval fly neuromuscular junction.

The understanding of the molecular mechanism of ELP3 in the process of neuronal development could pave the way for the design of selective epigenetic-based therapeutics for treatment of diseases affecting synaptic plasticity and degeneration.

III. The Elongator complex in plants

A. Identification of the Elongator complex

In our research unit 'chromatin and growth control' genes important for leaf growth are being identified by mutational analysis. One of the first mutants, defective in lateral leaf growth, was the Ds-induced drl1-2 mutant (Nelissen *et al*., 2003). The drl1-2 mutant displayed a very narrow leaf lamina, reduced hypocotyl elongation and root growth and a delay in flowering. Also no clear transition between lamina and petiole was observed as compared to the wild type (Fig. 1A and B). A Ds insertion into the DEFORMED ROOTS AND LEAVES1 (DRL1) gene was responsible for the drl1-2 phenotype. The DRL1 protein is the plant homolog of the yeast TOT4/KTI12 protein which was identified as an interactor of the Elongator complex in yeast (see Chapter II.1). A BLAST search was used to find the Arabidopsis homologs of the yeast Elongator components and besides DRL1 (At1g13870), Arabidopsis homologs were identified: At5g13680 (ELP1), At1g49540 (ELP2), At5g50320 (ELP3), At3g11220 (ELP4), At2g18410 (ELP5) and At4g10090 (ELP6). This was the first proof of the existence of the Elongator complex in plants and an in silico analysis showed that the functional domains of the ELO2, ELO3 and ELO1 proteins were conserved between yeast and Arabidopsis (Nelissen *et al*., 2003; Nelissen *et al*., 2005). Around the same time a large-scale screening of EMS mutagenized Arabidopis was performed to identify genes that control leaf morphogenesis (Berna *et al*., 1999). The mutants were divided into different classes according to the shape and size of the leaves and

divided into 94 complementation groups. One of those classes, the *elongata* class, contained 4 members, *elo1-4*, with a reduced leaf lamina width (Fig. 1C). The striking similarity in phenotype between the drl1-2 mutant and members of the *elongata* class prompted researchers to identify the mutated genes in the *elongata* class and found that drl1-2 is actually allelic to elo4 and the other 3 mutants (*elo1, elo2* and *elo3*) are all mutated in genes coding for the structural components of the Elongator complex, ELP4, ELP1 and ELP3 respectively (Nelissen *et al*., 2005). The nomenclature of Elongator components in yeast and Arabidopsis is summarized in Table 1.

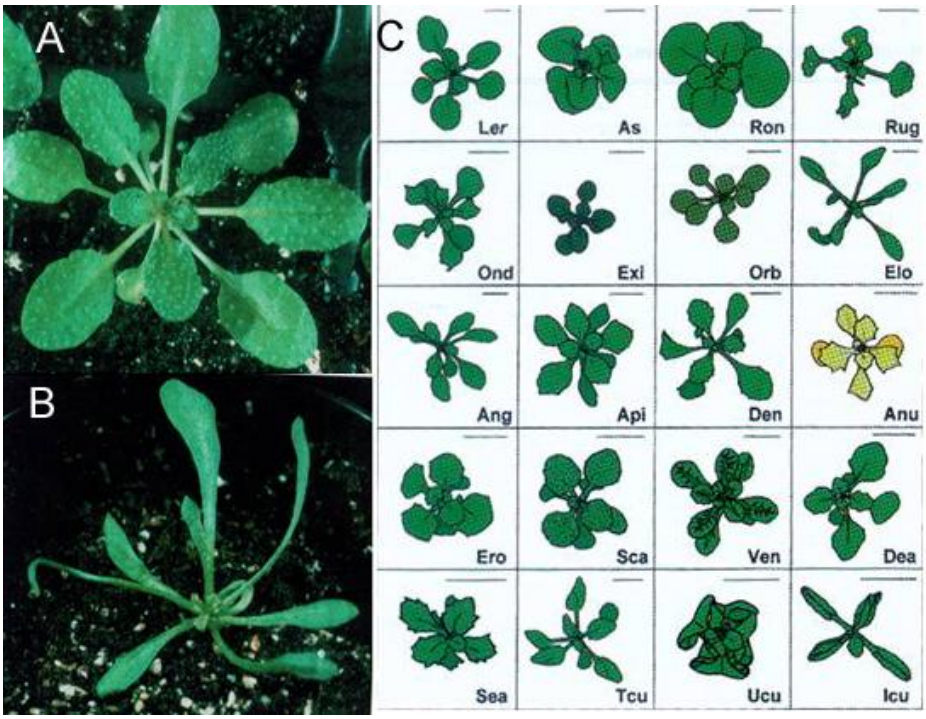

Fig. 1. A. and B. Fully grown rosette of wild type and *drl1-2* (Nelissen *et al*., 2003). C. Diagram showing representative individuals of the phenotypic classes with abnormal leaves in the EMS mutagenized collection (Berná *et al*., 1999). Note the similarity between *drl1-2* and the Elo class.

Table 1. Nomenclature of the Elongator components in yeast, human and Arabidopsis

Yeast	Arabidopsis	AGI	Human	protein type
TOT4/KTI12	DRL1/ELO4	At1g13870	AAH12173	Elongator associated protein
TOT1/ELP1	ELO2/ABO1/GNS1	At5g13680	IKAP	chaperone
TOT2/ELP2	ELP2	At1g49540	StIP1	WD-40 like
TOT3/ELP3	ELO3	At5g50320	hELP3	histon acetyltransferase
TOT7/ELP4	ELO1	At3g11220	hELP4	unknown protein
TOT5/ELP5	ELP5	At2g18410	hELP5	hypothetical protein
TOT6/ELP6	ELP6	At4g10090	hELP6	unknown protein

All *elo* mutants showed a reduction in the leaf lamina width due to a reduction in cell number and root growth was significantly inhibited due to a decrease in cell production (Figure 2). Unlike in yeast, measurements of ploidy levels by flow cytometry showed no differences between the *elo* mutants and the wild type. The phenotypic analysis of the elo mutants showed that the Elongator genes have a positive effect on lateral leaf and primary root growth and the similar phenotypes of the different *elo* mutants suggest that the Elongator genes might play a role in the same complex as is the case in yeast. Transmission electron microscopy on leaves of Ler and *elo1* revealed that the *elo1* mutant has fewer stacked granal thylakoids and plastoglobules (Falcone *et al*., 2007) To verify whether the different Elongator components in plants form a complex as in yeast, double mutant analysis was performed between different plant Elongator mutants (Nelissen *et al*., 2005). Since all the Elongator mutants show a very narrow leaf phenotype and the differences between the different *elo* and *drl* mutants are subtle, the growth of the primary root was used as this allowed a clear distinction between some *elo* and *drl* mutants (Fig. 2).

Fig.2. Comparison of the *elo* and *drl* mutants with Ler (22DAG; Nelissen *et al*., 2005)

The *elo3elo1, elo2elo1, elo2elo3, elo4elo1* and *elo2drl1-2* DMs had phenotypes similar to those of *elo1, elo1, elo2, elo4* and *drl1-2,* respectively. DRL1 is epistatic to ELO2 and ELO1 in accordance with the proposed role for DRL1 as a regulator of the holocomplex (Fichtner *et al*., 2002). ELO1 is epistatic over ELO2 and ELO3, indicating the importance of the accessory subcomplex for the function of the core subcomplex. ELO2 is epistatic to ELO3 and shows the

importance of the ELO2 protein (ELP1) in keeping the functionality of the catalytic subunit of the complex (see also human Elongator). The proposed model of the Elongator complex in yeast correlates with these epistatis data and suggests structural and functional conservance of the Elongator complex in plants (Fig. 3).

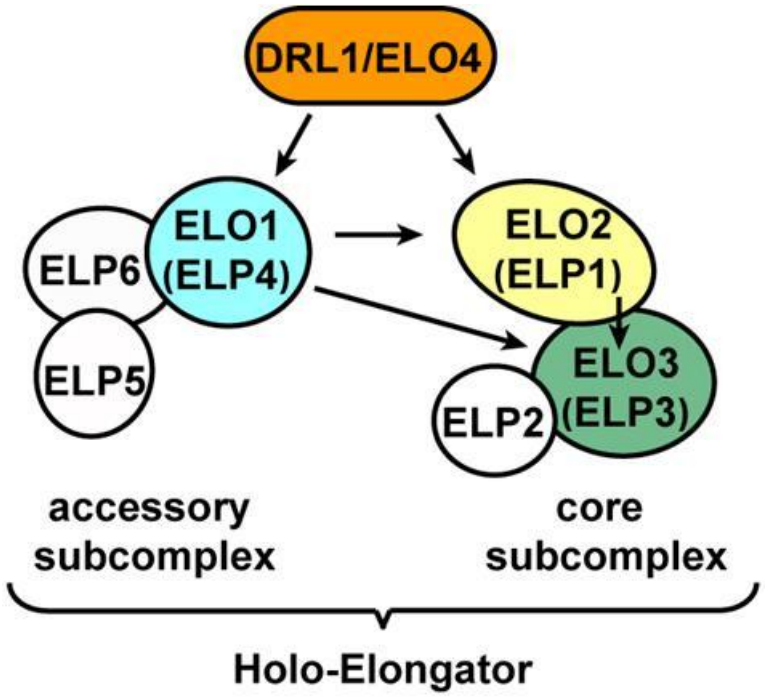

Fig. 3. The Elongator complex in yeast. The arrows show the genetic interactions between the various ELO genes in Arabidopsis (taken from Nelissen *et al*., 2005).

B. Function of Elongator in plants

In yeast, the Elongator complex is considered a histone acetyltransferase which binds to the elongating form of the RNAPII during transcription although recent evidence also suggests a cytoplasmatic role in tRNA modifications (see Chapter 2.I). To look into the function of Elongator in plants, a double mutant between *elo4/drl1-2* and the *struwwelpeter1* (*swp1*) mutant was generated. The SWP1 gene encodes a component of the Mediator complex that associates with the RNAPII transcription initiation complex. The double mutants showed a phenotype similar to that of the *swp1* mutants: no growth retardation, small serrations in the first leaves, and normal growth of the primary root and inflorescence indicating that SWP1 is epistatic to ELO4/DRL1. This observation positions Elongator more downstream in the RNAPII-mediated

transcription process than Mediator in the plant system, which is consistent with the role of the yeast Elongator complex in transcription elongation (Nelissen *et al*., 2005).

As discussed previously the overexpression of two tRNA species in yeast suppressed all of the Elongator phenotypes (Esberg *et al*., 2006) and the authors argue that the role of Elongator in tRNA modification/translation underlies the pleiotropic effects of *elp* mutations. Recently an identical function of Elongator in plants has been proposed as *Arabidopsis* mutants lacking the Elongator subunit ELP3/ELO3 have an identical defect in tRNA wobble uridine modification (Mehlgarten *et al*., 2010). RNA was isolated from *elo3* mutant and wild type plants, degraded to nucleosides and analysed by HPLC. The elution profiles were similar for both samples except for the 5-carbamoyl-methyluridine (ncm^5U) and mcm^5s^2U moieties eluted. Both modified uridine nucleosides were lacking in the *elo3* mutant sample. So the *elo3* mutation prevented the ncm^5- and mcm^5s^2-uridine modifications from being generated supporting the view that plant Elongator is involved in tRNA modification in a way similar to its yeast homologue. Furthermore, when AtELP3 and AtELP1 were introduced in a yeast elp1Δ elp3Δ double mutant , the complete plant-yeast chimeric Elongator complex could be precipitated and restored γ-toxin sensitivity indicating structural and functional conservation of the Elongator complex between yeast and plants. Interestingly, the expression of AtELP3 alone in a yeast elp3Δ did not complement the *Elongator* phenotype indicating that AtELP3 needs to interact with AtELP1 to generate a functional Elongator complex. Unfortunately the authors overlook the wealth of data on Elongator's role in transcription (see previous chapters) and do not provide any evidence that yeast components of the Elongator complex can substitute for the Elongator components in multicellular organisms such as plants and human. During this thesis we focused on the function of the Elongator complex in plants and while the components of the Elongator complex are conserved from yeast to Arabidopsis, the function of the Elongator complex might have evolved in multicellular organisms compared to the unicellular yeast.

The Elongator complex in plants has been identified in 2 different mutational screens indicating the complex biological networks in which Elongator is involved. In a screen for drought-resistant mutants, the abo1 mutation was isolated and abo1 mutants show ABA hypersensitivity in the inhibition of seedling growth and the promotion of stomatal closing. Furthermore, the abo1 mutant is more resistant to oxidative stress, which may be related to its ABA hypersensitivity and increased drought tolerance. Mutation in ABO1 also influence the development of guard cells,

resulting in a reduction of stomata compared to the wild type what might explain the increase in drought tolerance. *abo1* is allelic to *elo2* and thus mutated in the gene coding for the largest subunit of the Elongator complex, yELP1/hIKAP. The authors postulate that ABO1/ELO2 may not directly participate in controlling the growth and development of guard cells but rather influence the mRNA elongation process of genes that play a role in guard cell growth and development. The fact that *abo1/elo2* mutants are hypersensitive to ABA-induced stomatal closure suggests that some genes responsible for stomatal closure could also be involved in regulating guard cell growth. The expression of ABO1/ELO2 in the yeast tot1/elp1Δ Elongator mutant restored sensitivity towards growth inhibition by the zymocin γ-toxin and suggests functional Elongator conservation. However other phenotypes of the yeast tot1/elp1Δ Elongator mutant such as caffeine sensitivity seemed to be unaltered upon expression of ABO1/ELO2 (Chen *et al*., 2006). This might indicate that some Elongator functions are conserved from yeast to plants while others are not. In agreement with this hypothesis is the observation that the cell proliferation rate in *elo* mutants in plants is not due to a defect in the cell cycle core machinery (Nelissen *et al*., 2005) while in yeast the reduced cell divistion rate is a consequence of a G1 delay (Otero *et al*., 1999). In addition , the human ELP3 was only able to partially complement the functional defects of yeast elp3Δ cells (Huang *et al*., 2005) but this phenomenon could be the consequence of the absence of the human ELP1/IKAP and interaction with human ELP3 as is the case in plants (Mehlgarten *et al*., 2010). The link between Elongator and ABA prompted researchers to develop a genetic screen to identify Arabidopsis mutants in which root growth was hypersensitive to ABA (Zhou *et al*., 2009). Two new mutants (*elp2* and *elp6*) were identified and the genes coded for the ELP2 and ELP6 subunits of the Elongator complex. Following these findings, they analyzed ABA sensitivity in seed germination and seedling growth for the *abo1/elo2/elp1*, *elp2*, *elp6* and *elp4/elo1* mutants and found that all these mutants were hypersensitive when grown on medium containing ABA. ABA has an important role in stomatal movement and the *abo1/elo2/elp1* mutation enhanced ABA-induced stomatal closure and increased drought tolerance (Chen *et al*., 2006). This is also the case for the *elp2* mutant but not for the *elp6* and *elp4/elo1* mutant. Since ABO1/ELP1, ELP2 and ELP3 form the core subcomplex and ELP4/ELO1, ELP6 and ELP5 form the accessory subcomplex of the holo-Elongator, these results suggest that the two subcomplexes might have different functions in ABA-mediated stomatal movement. Micro-array analysis of genes affected by *elp1* or *elp4* and subsequent

analysis of specific genes in the four mutants showed that MYBL2 was downregulated and CAT3 was upregulated in the four mutants. MYBL2 is a single repeat MYB transcription factor with a suppressive role in the biosynthesis of anthocyanin (Dubos *et al*., 2008; Matsui *et al*., 2008). Each of the four mutants contained between six and seven times more anthocyanin than the wild type and indicated that Elongator mutations negatively regulate the expression of genes in the anthocyanin biosynthesis pathway, probably by directly controlling the expression of the MYBL2 gene during transcription elongation (Fig. 4). CAT3 (catalase 3) catalyzes the decomposition of hydrogen peroxide (H_2O_2) and its expression was upregulated in all four mutants. This may explain the methyl viologen-resistant phenotypes of the four mutants when growing in light as methyl viologen blocks electron transport during photosyntesis, and enhances H_2O_2 production in chloroplasts under light.

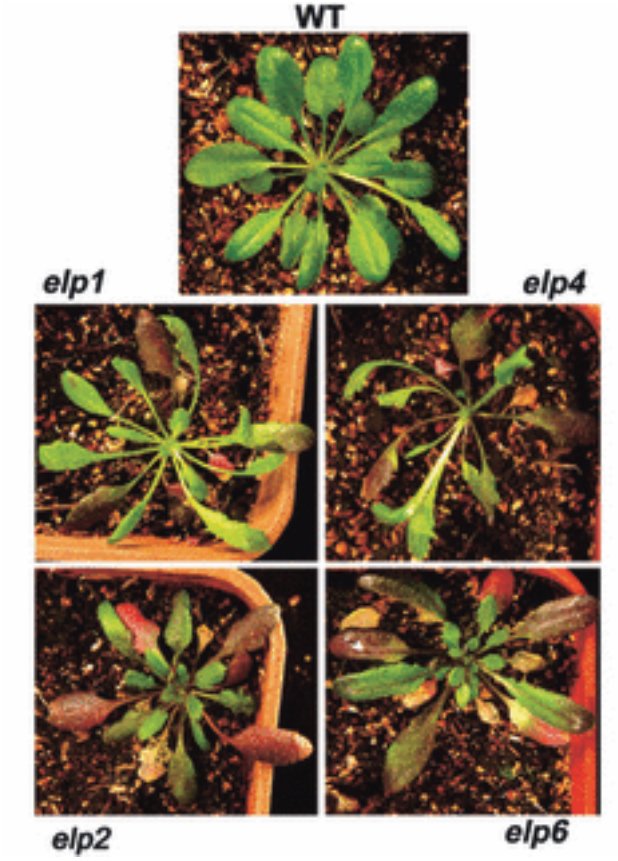

Fig. 4. Anthocyanin accumulation in Elongator mutants and in the wild type in strong light. Four-week-old seedlings were treated with strong light for 2 days before they were photographed (Zhou *et al*., 2009).

Besides the hypersensitivity to abscisic acid and resistance to oxidative stress upon Elongator mutation, loss-of-function mutants of the Arabidopsis Elongator subunit 2 (AtELP2) show that

Elongator in plants is also involved in plant immune responses (Defraia *et al*., 2010). Salicylic acid (SA) is an important component of defense-related signal transduction and is essential for activation of systemic acquired resistance (SAR). Elevated cellular SA levels induce transcriptional changes that are largely controlled by the transcription coactivator NPR1 (nonexpressor of pathogenesis-related (PR) genes). Mutations in the NPR1 gene significantly block SA-mediated transcription reprogramming, compromise basal immunity, and render the plant completely defective in SAR (Wang *et al*., 2006). During pathogen infection, *npr1* plants hyperaccumulate SA which results in cytotoxic effects and *npr1* plants fail to develop beyond the cotyledon stage when grown on medium containing high concentrations of SA. How NPR1 prevents both SA hyperaccumulation and SA toxicity is unknown. In an EMS-induced mutagenic screen of *npr1* plants, the *gns1* (green npr1 seedling on SA medium) mutation restored SA tolerance and suppressed SA hyperaccumulation. Mapping of the GNS1 locus led to the identification of the Elongator gene encoding subunit 2 (AtELP2). Upon overexpression of AtELP2 in the *npr1gns1* double mutant , sensitivity to SA toxicity and SA hyperaccumulation was restored. The *Atelp2* single mutant also exhibits pathogen susceptibility, indicating that AtELP2 contributes to basal immunity but SAR remains intact. Since transcriptional changes during basal immunity and SAR differ mostly in speed and scale (Maleck *et al*., 2000; Tao *et al*., 2003), it is likely that defense gene induction in AtELP2 is delayed and/or decreased. As mentioned before (see Chapter II.1) , the Elongator mutants in yeast also show a slower adaptation to environmental changes as a consequence of delayed gene induction (Otero *et al*., 1999). From these data the authors postulate that Elongator functions as an accelerator of transcriptional reprogramming in response to environmental stimuli and does this by facilitating RNAPII transcription through acetylation of histones in defense genes (Defraia *et al*., 2010).

Chapter 3

Relationship between Auxin, Growth and Light

I. Introduction

In plants, axis formation and patterning is not confined to embryogenesis but continues throughout the life cycle and are reiterated upon the initiation of new structures such as lateral organs. Above the ground, the primary shoot apical meristem produces lateral organs such as leaves and flowers that are arranged in a specific pattern, called phyllotaxis. Under the ground, the primary root apical meristem generates daughter cells that gradually acquire cell fate according to their position ultimately resulting in differentiated cell files with a specific function. The initiation of lateral root formation occurs in the differentiation zone and follows a rigid pattern. Recent work has suggested that the growth regulator auxin has a key role in both the initiation and formation of those lateral organs. A feature of auxin action is the existence of feedback loops through which auxin regulates its own transport and creates auxin gradients. The creation of auxin gradients requires the polar and active transport of this phytohormone to regions where it will exert its function. The best characterized auxin transport proteins are the influx carrier AUX1 and a family of efflux carriers called PIN-formed (PIN) consisting of eight members. These proteins are localized on the plasma membrane but remain mobile (ie regulating directional flux of auxin). Intracellular auxin is perceived by a receptor (transport inhibitor resistant 1 (TIR1)), triggering the auxin response through SKP1-CULLIN/cdc53-F-box $(SCF)^{TIR1}$ –mediated degradation of auxin/indole-3-acetic acid (AUX/IAA) proteins, which inhibit transcription factors named auxin response factors (ARFs). This way the ARFs can bind to their respective promoters of auxin-responsive genes and results in a transcription response. In turn, this response feeds back onto the regulation of the transport machinery and triggers other specific targets. Recently another level of regulating auxin response has been suggested by the observation that several auxin-related proteins such as PIN5 and the PIN phosphatase complex, PP2A, have a perinuclear and cytoplasmic localization and that auxin is transported across the ER membrane (Friml and Jones, 2010). This might point to a role in regulating auxin homeostasis in the cell by compartimentalization.

In this chapter we will focus on the role of auxin in determining leaf shape, primary and lateral root formation as defects in those features are observed in the plant mutants studied in this thesis.

II. Leaf initiation and shape

Leaf initials are specified at the flanks of the shoot apical meristem (SAM) and correspond to sites of elevated auxin activity resulting from convergence points of PIN1 polarity in the epidermal layer. At the same time, basal PIN1 polarity in subepidermal cells of the leaf initial internalizes auxin flow through the center of the leaf, defining the position of the future midvein (Reinhardt *et al*., 2003; Heisler *et al*., 2005). This suggests that factors which control PIN1 polarization play a critical role in both leaf and midvein formation. The elevated levels of auxins at the leaf initials deplete the auxin from their proximity which inhibits the initiation of neighbouring leaf primordia at the periphery of the SAM (Fig. 1B). After their initiation, leaf primordia start to produce auxin and this causes the reversal of PIN1 polarity so that auxin is transported back to the meristem to contribute to subsequent leaf initiation events (Heisler *et al*., 2005). These auxin distributions are responsible for the correct leaf initiation pattern termed phylotaxis.

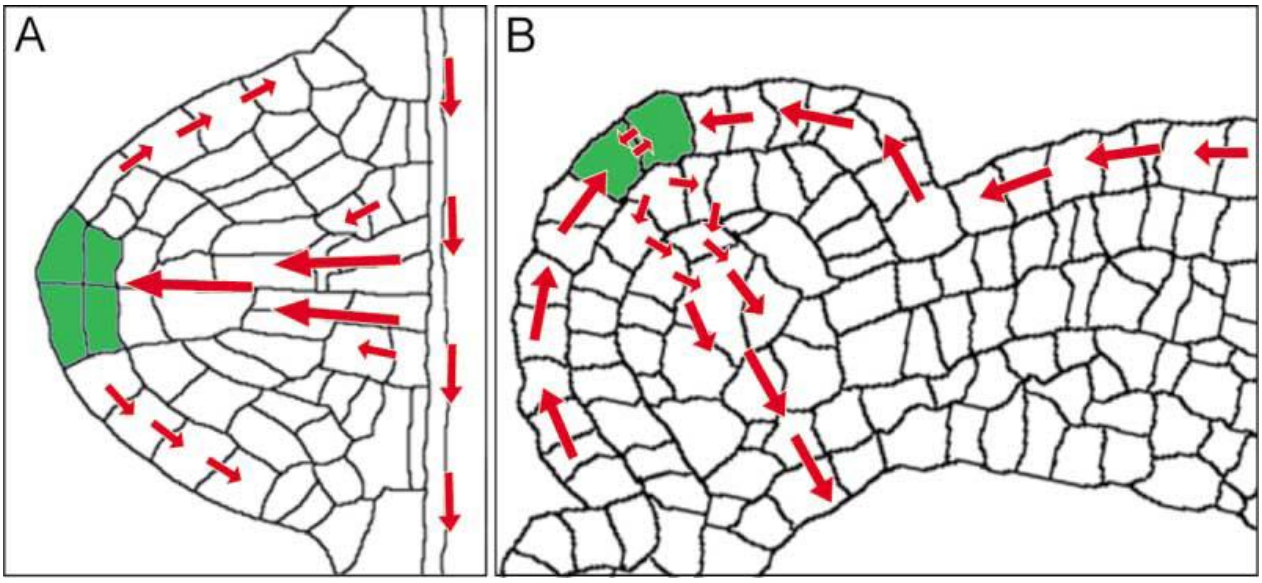

Fig. 1. Model for Auxin Transport and Distribution in Root- and Shoot-Derived Organ Primordia (Benkova *et al.*, 2003)
(A) Lateral root primordium: auxin is provided by PIN-dependent auxin transport through the primordium interior toward the tip, where it accumulates. From here, part of the auxin is retrieved by a PIN2-dependent auxin route through the outer layers.
(B) Aerial organ primordium: PIN1 is a major component for auxin distribution. Auxin is provided to the primordium tip through the outer layers. From the tip, auxin is drained through a gradually established transport route toward the vasculature. Places of auxin accumulation are depicted in green. Presumptive routes of auxin transport are depicted by red arrows.

Besides the local auxin activity in the leaf initiation process, the downregulation of class I KNOTTED1-like homeobox (KNOX) genes at leaf primordia in plants is another determant of the leaf initiation process. Members of the KNOX gene family are expressed within the SAM region of all plant species, where they promote SAM self regulation, but their expression is excluded from leaf initials. In Arabidopsis, KNOX expression in the leaf is repressed by the action of ASYMMETRIC LEAVES (AS1) and in the SAM AS1 activity is repressed by the SHOOTMERISTEMLESS KNOX protein. Interestingly, the complementary expression patterns of auxin activity reporters and KNOX during early organ specification at the SAM suggests that auxin may also contribute to KNOX repression in the leaves (Heisler *et al*., 2005).

Also leaf shape seems to be at least partly controlled by auxin distribution. The perturbation of auxin transport results in leaves that fail to initiate the characteristic marginal projections, called serrations (Hay *et al*., 2006). Similarly the ectopic expression of KNOX in leaves causes the presence of these serrations (Zgurski *et al*., 2005). As in leaf initials, the convergence of epidermal PIN1 at the tips of forming serrations or lobes defines local auxin activity maxima. Thus the auxin dependent mechanism that triggers leaf initiation at the flanks of the SAM may be later redeployed within leaves to elaborate leaf shape (Scarpella *et al*., 2010).

Primary leaf morphogenesis temporally coincides with the formation of major veins and a variety of substances such as cytokinins, brassinosteroids and auxin have been reported to promote vascular differentiation (Fukuda 2004). Auxin is unique in this process as it can trigger vascular cell differentiation and induce vascular strand formation. Plant vascular cells originate from procambial cells, which are vascular stem cells. Many aspects of venation patterning in plant leaves can be explained by the auxin canalization model (Sachs, 1991; Rolland-Lagan and Prusinkiewicz, 2005). This model suggests that auxin flow, starting initially by diffusion, induces the formation of the polar-auxin-transport-cell system. This in turn promotes auxin transport, leading to canalization of the auxin flow along a narrow column of cells. This continuous polar transport of auxin through cells finally results in the differentiation of procambial cells and thus vascular strands.

III. Primary root, gravitropism, lateral roots and root hairs

Auxin is synthesized in meristematic regions at the shoot apex and transported to the primary root tip. There it is redirected through the root cortical and epidermal tissues to generate a basipetal auxin concentration gradient (i.e. away from the organ apex).

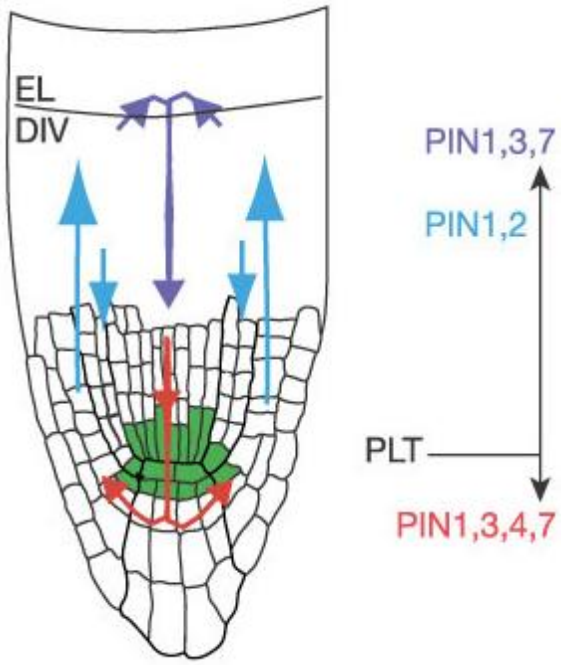

Fig. 2. In post-embryonic roots, PIN-mediated auxin transport stabilizes the stem cell region and regulates cell division in the meristem zone and cell expansion in the elongation zone. Members of the *PIN* gene family generate primordium-specific auxin distribution. PIN1 appears to be the primary mediator of IAA movement through the vascular tissues to the primary root tip, with PIN3, PIN4, and PIN7 contributing to this transport in adjacent tissues in the lower primary root. Once at the primary root tip, auxin is redistributed basipetally through cortical and epidermal cells in a PIN2-dependent transport stream. In the root elongation zone PIN3 and PIN7 mediate lateral re-direction of basipetally transported auxin into the PIN1-dependent auxin transport stream.

Multiple PIN proteins function together to regulate auxin transport, tropic growth and the maintenance of the root apical meristem. PIN1 appears to be the primary mediator of IAA movement through the vascular tissues to the primary root tip, with PIN3, PIN4, and PIN7 contributing to this transport in adjacent tissues in the lower primary root (Blilou *et al*., 2005 – Fig. 2). Once at the primary root tip, auxin is redistributed basipetally through cortical and epidermal cells in a PIN2-dependent transport stream. In the root elongation zone PIN3 and PIN7 mediate lateral re-direction of basipetally transported auxin into the PIN1-dependent auxin transport stream. Once re-directed, auxin reaches the root tip and the process is repeated, creating a 'reflux loop' (Fig. 2). So two different streams of auxin flow can be distinguished in the primary root: (1) the rootward auxin flow through the vasculature and central cylinder controlled by PIN1 and PIN4 and (2) the shootward auxin flow from the columella through the lateral root cap and epidermis controlled by PIN2. These two directional flows have a major role in the gravitropic response of the primary root as the bending of the root is driven by formation of a

differential auxin gradient between the upper and lower sides of the root upon gravistimulation and regulated by the polar transport of auxin. PIN proteins actively cycle between the plasma membrane and endosomes and any disruption of the polar targeting of the PIN proteins causes defects in this gravitropic response. Treatment with brefeldin, a fungal toxin that targets GNOM, a specific ARF-GEF required for PIN traffic, causes defects in gravitropic response (Rahman *et al*., 2010). The phosphorylation status of the PIN proteins also influences their targeting, with antagonistic effects on targeting being found for the PINOID protein kinase and type 2A protein phosphatase (PP2A). For example, the weak gravitropism of a mutant with aberrant PP2A activity, *pp2aa1*, is largely rescued by concomitant loss of PINOID kinase function (Sukumar *et al*., 2009). These data show that auxin flow in the root is important for optimal gravitropic response.

Lateral root (LR) initation in Arabidopsis starts from asymmetric, anticlinal cell division of two adjacent protoxylem pericycle cells of the same file, resulting in shorter and longer daughter cells (De Smet *et al*., 2006a; Fukaki *et al*., 2008). The shorter daughter cells expand radially over several rounds of cell division, and these cells divide periclinally to make outer and inner layer. A mature LR primordium is formed through several developmental stages with well-ordered cell divisions and cell differentiation. Eventually, a new meristem is formed, which is anatomically identical to the primary root meristem (Malamy and Benfey 1997). The sites of LR initiation are not predetermined but occur at regular temporal intervals and with regular spacing (Fig. 3).

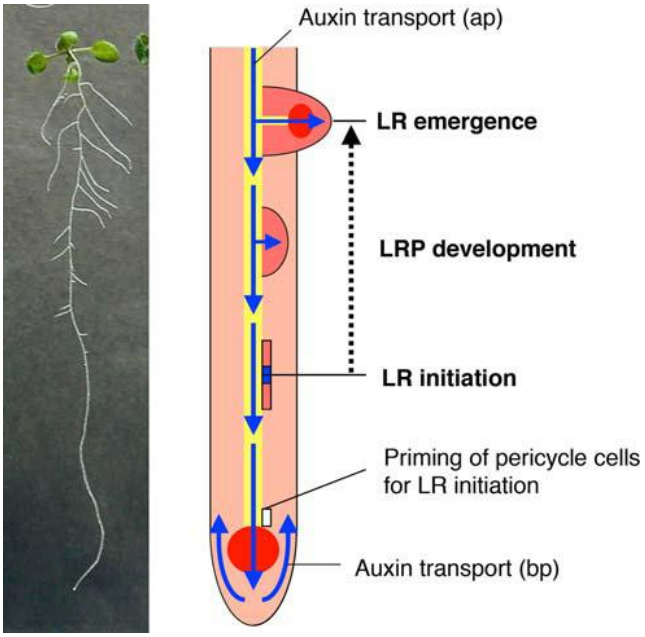

Fig. 3. Developmental events during LR formation. (Fukaki *et al*., 2009).

Recently it became clear that before any visible sign of division, particular protoxylem pericycle cells appear to receive an auxin trigger proximal to the root meristem. This auxin signal occurs at regular temporal intervals and seems to be the driving force behind the regular spacing of lateral roots (De Smet *et al*., 2007). Thus as in leaf primordia, auxin accumulates at the position of future root primordia and at later stages a shift in auxin flow mediated by repositioning of efflux carriers (Sauer *et al*., 2006) changes the growth axis of the newly initiated lateral root such that it is perpendicular to the growth axis of the main root. As a result, auxin will be transported through the interior of the primordium towards the new root tip, where it accumulates (Benkova *et al*., 2003). Subsequently, part of the auxin will be retrieved through the outer layers ('fountain model') (Fig. 1.A).

Auxin also plays a major role in growing root hairs. Root hairs are long, thin tubular outgrowths from epidermal cells that are produced in the differentiating zone of the root. They are not essential for plant growth and development but are useful to study plant cell growth and tip growth in particular. Root hair specific expression of PINOID (PID) and PIN3 suppressed root hair growth by promoting auxin efflux from the root hair cell. Also overexpression of PIN1-PIN4, PIN7 and PIN8 greatly inhibited root hair growth, suggesting that these PINs facilitate auxin efflux and decrease internal auxin levels in the hair cell. However, root-hair specific overexpression of the auxin influx carriers AUX1 enhanced root hair growth , most likely by increasing cellular auxin levels in root hair cells (Ganguly *et al*., 2010). Mutation in auxin response genes, AUX1, AXR1, AXR2 and AXR3 all affect root hair growth and the application of external auxin or auxin transport inhibitors increased root hair length in seedling (Okada and Shimura, 1994) while the number of root hairs remained unchanged. Although auxin is a positive regulator of root hair development and necessary for normal root hair elongation, it remains unclear how auxin concentrations in the root hair cells influence tip growth.

IV. Influence of light on auxin responses

Light is essential for plant growth and provides not only energy for photosynthesis but also information on seasonal timing and local habitat condtions. The major light receptors are the blue-light absorbing cryptochromes, phototropins, ZTL-like F-box proteins, the red and far-red light absorbing phytochromes and the recently discovered UV-B-receptor UVR8 (Rizzini et al.,

2011). These photoreceptors adjust plant development in response to changes in the light environment. The phytochromes are unique amongst photoreceptors and exist in two isomeric forms, an inactive Red light-absorbing form, Pr, and an active Far Red light-absorbing form, Pfr. Exposure to red light photo-converts a high proportion of Pr to the active Pfr form, which promotes "photomorphogenic" development. Far red light does the reverse, photo-converting Pfr to the inactive Pr, with a consequential shift in development to the "skotomorphogenic" state (Halliday *et al*., 2009). FR light conditions simulate dense vegetation and create a low Pfr /Pr ratio which allows plants to "detect" the presence of neighboring plants. Plants grown in these conditions are more elongated with increased apical dominance, paler and are early flowering, characteristics referred to as the "shade avoidance" syndrome (Franklin 2008). Because low R:FR light is perceived by the phytochromes and triggers dramatic changes in gene expression that, in seedlings, eventually result in an increased hypocotyl elongation to overgrow competitors, hypocotyl measurements in seedlings are often used to observe photomorphogenic response. Auxin has been specifically linked to this photomorphogenic response as hypocotyl elongation for seedlings grown on media containing NPA (an auxin transport inhibitor) was significantly reduced under different light conditions but not for dark-grown seedlings (Estelle *et al*., 1998) (Fig. 4).

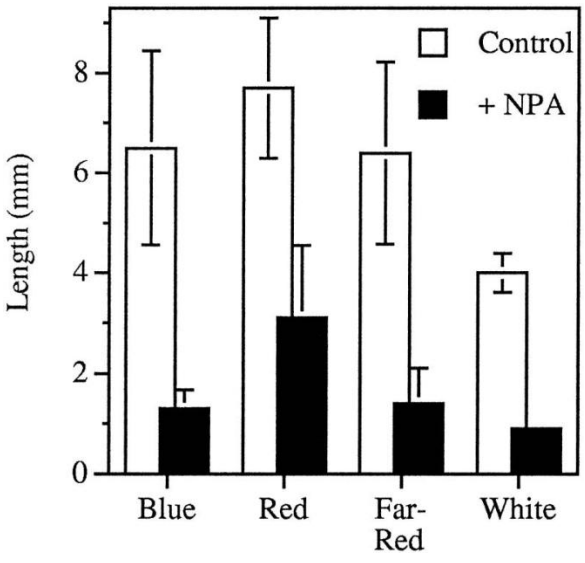

Fig. 4. The effect of light quality on hypocotyl elongation and on the inhibition of hypocotyl elongation by 1.0 μm NPA. Seedlings were grown under continuous white light, blue light, far-red light or red light for 7 d. Inhibition of hypocotyl elongation by NPA was absent in dark-grown seedlings. (Estelle *et al*., 1998).

Auxin controls numerous developmental processes such as organogenesis, tissue patterning, tropic responses, cell division and expansion and more links between light and auxin have been established. For example, under shade conditions auxin biosynthesis is rapidly induced in leaves in a process involving TRYPTOPHAN AMINOTRANSFERASE OF ARABIDOPSIS1 (TAA1),

an enhancer of IAA biosynthesis (Tao *et al*., 2008). Active phyB reduces IAA levels by repression of TAA1 transcript levels. Moreover, light signaling mutants and seedlings with deficiencies in auxin biosynthesis often show similar phenotypes and *taa1* mutants show short hypocotyls and expanded cotyledons which is typical for light signaling mutants. Light doesn't influence auxin responses solely by modulating IAA biosynthesis but also by regulating the expression of several Aux/IAA, SAUR and GH3 genes which are gene families whose transcription is rapidly activated by auxin. Transcriptome analysis has shown that members of these gene families are rapidly regulated by phytochrome during seedling de-etiolation and auxin-related genes are highly represented among the genes with altered expression under low R:FR-ratio light (Franklin and Whitelam 2007). Another mechanism in which light influences auxin responses is by modulating the polar auxin transport. As mentioned before, polar auxin transport is controlled by influx (AUX1) and efflux (PINs) carrier proteins. This polar auxin transport can by impeded by application of N-1-naphylphtalamic acid (NPA) and results in altered auxin distribution which modifies shoot and root development. This effect however is more pronounced in light-grown seedlings with little effect on dark-grown seedlings indicating a link between light and polar auxin transport (Jensen *et al*., 1998). Light also influences the cellular localization of PIN1 and PIN3 proteins. The cellular localization of PIN1 and PIN3 proteins in dark-grown seedlings changes from basal to lateral upon exposure to directional blue light. As a result, an auxin gradient is established to control differential cell expansion on the illuminated versus the nonilluminated side of the hypocotyl (Friml *et al*., 2002; Blakeslee *et al*., 2004). In a recent study it was shown that PIN3 relocalization plays an important role in the shade avoidance response. In low R:FR conditions hypocotyl elongation is induced and involves the accumulation of free IAA in the hypocotyl. This accumulation requires auxin transport regulation through PIN3, which is likely to allow for increased auxin transport to the cortex and epidermal cells. To establish this auxin gradient, low R:FR induces increased PIN3 gene expression and PIN3 protein abundance and induces a predominantly lateral cellular localization of PIN3 in the endodermis cells. The fitness of pin3 mutants was impaired by competing wild-type neighbors indicating that PIN3-mediated control of shade avoidance is of great importance in the shade avoidance response (Keuskamp *et al*., 2010).

Light is a potent regulator of growth and development and the coupling of light and auxin signaling allows development to be optimized for the local environment.

RESEARCH

Chapter 4

Plant Elongator regulates auxin-related genes during RNA polymerase II transcription elongation

Proc Natl Acad Sci USA (2010) 107: 1678-1683

Hilde Nelissen[1], Steven De Groeve[1] , Delphine Fleury, Pia Neyt, Leonardo Bruno , Beatrice Bitonti, Filip Vandenbussche, Dominique Van Der Straeten, Takahiro Yamaguchi, Hirokazu Tsukaya, Geert De Jaeger, Andreas Houben, and Mieke Van Lijsebettens

[1] These authors contributed equally to this work

Steven De Groeve wrote the subcellular localization and ChIP parts and performed all Q-PCRs, subcellular localization studies, ChIP experiments and auxin-induced gene expression assay

In eukaryotes, transcription of protein-encoding genes is strongly regulated by posttranslational modifications of histones that affect the accessibility of the DNA by RNA polymerase II (RNAPII). The Elongator complex was originally identified in yeast as a histone acetyltransferase (HAT) complex that activates RNAPII-mediated transcription. In *Arabidopsis thaliana*, the *elongator* mutants *elo1*, *elo2*, and *elo3* with decreased lateral leaf and primary root growth due to reduced cell proliferation, identified homologs of components of the yeast Elongator complex, Elp4, Elp1, and Elp3, respectively. Here we show that the Elongator complex purified from plant cell cultures as a six-component complex. The role of plant Elongator in transcription elongation was supported by colocalization of the HAT enzyme, ELO3, with euchromatin and the phosphorylated form of RNAPII, and reduced histone H3 lysine 14 acetylation at the coding region of the *SHORT HYPOCOTYL 2* auxin repressor and the *LAX2* auxin influx carrier gene with reduced expression levels in the *elo3* mutant. Additional auxin-related genes were downregulated in the transcriptome of *elo* mutants but not targeted by the Elongator HAT activity showing specificity in target gene selection. Biological relevance was apparent by auxin-related phenotypes and marker gene analysis. Ethylene and jasmonic acid signaling and abiotic stress responses were upregulated in the *elo* transcriptome and might contribute to the pleiotropic *elo* phenotype. Thus, although the structure of Elongator and its substrate are conserved, divergence in target gene selection has occurred and is specific in plants and shows that auxin signaling and influx are under chromatin control.

I. Introduction

In plants, growth and form are determined by the spatial and temporal regulation of cell division and cell expansion in which plant hormones play a crucial role. The plant hormone auxin is a major integrator of stimuli to steer cell expansion and, hence, growth. In addition, its polar distribution results in concentration gradients and maxima that are interpreted by specific cells through a nuclear signaling pathway, leading to transcriptional changes and the onset of specific developmental programs, such as primary root apical meristem maintenance and daughter cell specification, lateral root initiation and gravitropism, leaf vascular patterning, and leaf and flower initiation and positioning (Vanneste *et al*., 2009). Auxin enhances the affinity of TIR1 for AUX/IAAs (Kepinski *et al*., 2005, Dharmasiri *et al*., 2005) and this leads to their ubiquitination by the SCF^{TIR1} E3 ligase (dos Santos Maraschin *et al*., 2009), their subsequent degradation by the proteasome and complex transcriptional reprogramming through the AUXIN RESPONSE FACTOR (ARF) transcription factors. Mutants in signaling components, such as *bodenlos* (*bdl*, BDL/IAA12) and *short hypocotyl 2* (*shy2*, SHY2/IAA3), are defective in proximo-distal axis formation as visualized by a short primary root and reduced shoot apical dominance (Tian *et al*., 1999; Hamann *et al*., 2002). Components of the cellular auxin transport machinery are transmembrane influx (AUX1/LAX1) and efflux (PIN1 to PIN8) carriers in addition to P-glycoproteins (PGPs) of the ABCB transporter family (Vanneste *et al*., 2009). Crosstalk of auxin signaling with other hormone signaling pathways, such as ethylene, provides other levels of complexity to the plant for developmental programming upon environmental and endogenous stimuli. The integration of such developmental programs together with metabolic and physiological pathways contributes to the complex trait of growth in plants. Their transcriptional or translational control mechanisms are well-studied, but much less is known on their epigenetic regulation, i.e. the histone code and the genomic DNA methylation state also regulate gene expression and change in response to developmental and environmental cues (Nelissen *et al*., 2007).

We studied the genetic and epigenetic regulation of growth in the model plant *Arabidopsis thaliana* by using the leaf as experimental system. Leaf mutants with narrow and elongated lamina shape allowed the identification of the plant homologs of the yeast Elongator complex components (Nelissen *et al*., 2005). In yeast and human, Elongator consists of the core subcomplex consisting of

ELP1, ELP2, and ELP3 and the accessory subcomplex containing ELP4, ELP5, and ELP6 (Krogan *et al*., 2001, Hawkes *et al*., 2002). The copurification of the Elongator complex with the phosphorylated RNA polymerase II (RNAPII) (Otero *et al*., 1999) and the *in vivo* histone acetyl transferase (HAT) activity (Winkler *et al*., 2002) suggested a role for the complex in RNAPII transcription elongation in yeast (Otero *et al*., 1999, Winkler *et al*., 2002). The yeast Elongator complex was also reported to have a function in exocytosis, tubulin acetylation, and tRNA modification. In yeast, the Elongator mutants slowly adapt to changes in growth conditions, whereas in humans, they cause a neuronal disease, called familial dysautonomia (Svejstrup *et al*., 2007). In mammals, genes involved in cell motility and fibroblast and embryogenic development were found to be direct targets for acetylation by the Elongator complex during transcription elongation (Close *et al*., 2006; Chen *et al*., 2009), while in yeast no direct transcriptional targets of the complex were identified until now.

Here we show that the structure of the Elongator complex as well as its function in RNAPII transcription elongation is conserved in plants. Novel, auxin-related phenotypes were identified in the *elo* mutants that correlated with reduced acetylation of H3K14 in auxin biology-related genes, revealing a plant-specific target process and genes for Elongator.

II. Results and Discussion

A. Elongator complex purification in plant cell cultures

In *Arabidopsis*, the phenotypic resemblance of the different knockdown *elongator* (*elo*) mutants, the clustering of their transcriptome, and their epistatic interactions (Nelissen *et al*., 2005) suggested that the ELO proteins function in a complex. To verify the existence and composition of an Elongator complex in plants, a tandem affinity purification (TAP) was done on extracts of *Arabidopsis* cell suspension cultures, transformed with overexpression constructs for *ELO3* fused to a G protein and streptavidin-binding peptide (GS-TAP) tag. The wild-type phenotype was restored after transformation of the *elo3-1* mutant with the tagged *ELO3* construct and was functional. Two purifications with p35S-GStag-ELO3 were separated on polyacrylamide gels and stained with Coomassie Brilliant Blue (Fig. 1). Subsequently, the entire gel lanes were sliced in fragments and sequenced by mass spectrometry that revealed the presence of ELO2, AtELP2, ELO3, ELO1, AtELP5, and AtELP6 (Table 1 and Fig. 1), corresponding to the homologs of the six

Elongator components in yeast. All six components were purified in other TAPs with ELO1, ELO3, and AtELP5 as bait (Table 1 and Fig. 1).

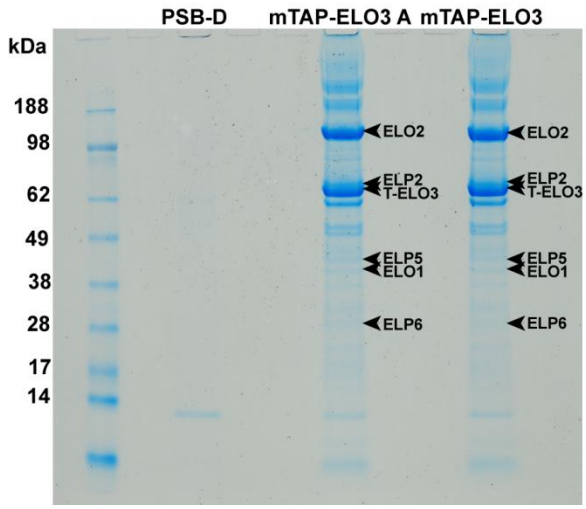

Fig. 1. TAP of the Elongator complex. NuPage gel containing two independent TAP eluates with GStag-ELO3 (referred to as mTAP-ELO3) as bait and a control TAP on the untransformed PSB-D cell culture. Elongator subunits ELO2, ELP2, ELO3, ELO1, ELP5, and ELP6 are indicated after their identification by mass spectrometry. The prefex ´T´ is for the tagged bait protein. kDa, kiloDalton.

Table 1. Copurified proteins identified by MS in TAP eluates of *Arabidopsis* cell cultures using ELO3, ELO1, AtELP5, and ELO2 as bait. AtELP1, AtELP3 and AtELP4 refer to the *Arabidopsis* homologs for the yeast ELP1, ELP3, and ELP4, respectively, and were renamed ELO2, ELO3, and ELO1 in *Arabidopsis* according to the names of the respective mutants (Tian *et al*., 1999).The number between parentheses corresponds to the number of experiments. The bait proteins were always identified in the respective TAP experiments (not indicated).

Gene code	Interactor	Number of experiments in which the interaction was identified			
		ELO3/AtELP3 (5)	ELO1/AtELP4 (4)	AtELP5 (3)	ELO2/AtELP1 (2)
At5g13680	ELO2/AtELP1	4	2	2	/
At1g49540	AtELP2	4	1	0	2
At5g50320	ELO3/AtELP3	/	2	1	2
At3g11220	ELO1/AtELP4	4	/	3	0
At2g18410	AtELP5	5	3	/	0
At4g10090	AtELP6	5	3	3	0

This showed that the plant homologs of the yeast Elongator as identified through mutational analysis and BLAST search interacted in vivo and that besides the previously described ELO proteins (Nelissen *et al*., 2005), the three components encoded by At1g49540, At2g18410 and

At4g10090 (Nelissen *et al*., 2003) could now be annotated as the Elongator components, *AtELP2*, *AtELP5*, and *AtELP6*, respectively. Stoichiometric concentrations of ELO1, AtELP5, and AtELP6 were found on gels with the tagged ELO1 or AtELP5 as bait when compared to the lower concentrations of ELO2, AtELP2, and ELO3 (Fig. 1); in contrast, with ELO2 as bait, only stoichiometric concentrations of AtELP2 and ELO3 could be detected (Fig. 1; Table 1). These data suggest that the plant Elongator complex also consists of two discrete subcomplexes as was put forward for yeast (Krogan *et al*., 2001). Pairwise yeast two-hybrid analysis revealed that ELO1 interacted with AtELP6, but not with AtELP5, while AtELP5 interacted with AtELP6, but not with ELO1 (Fig. 2). In summary, an Elongator complex is formed in plants with a structure similar to that in yeast and human.

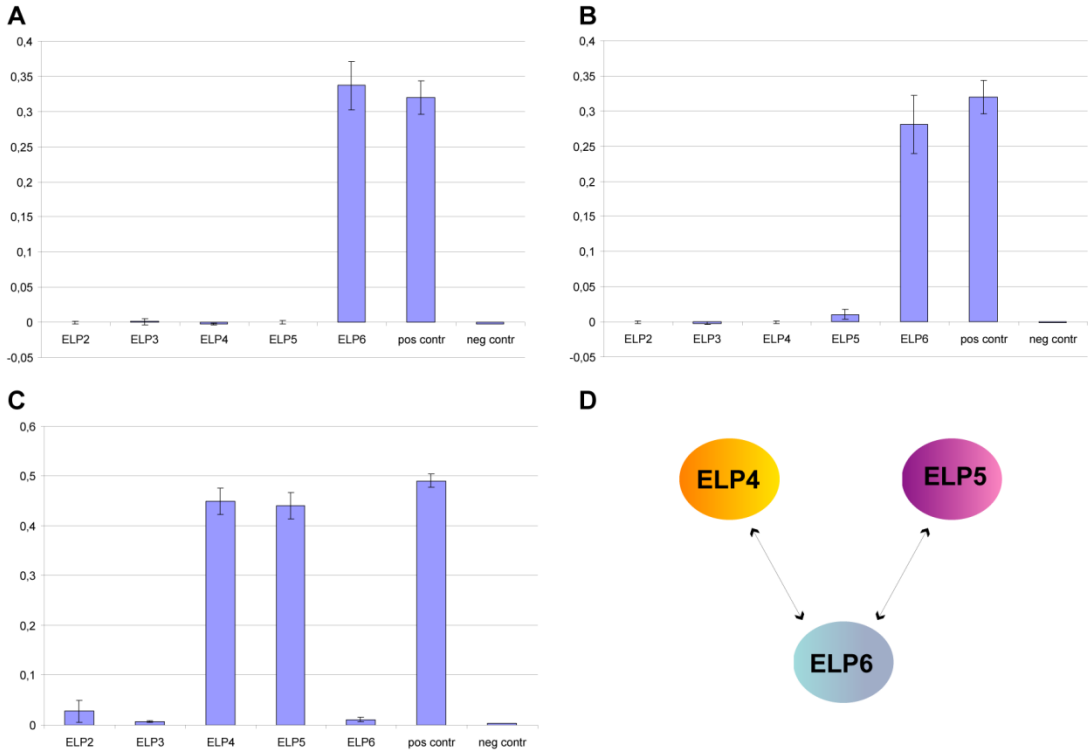

Fig. 2. Yeast two-hybrid interactions between ELO1, ELP5, and ELP6. The interaction between two proteins were quantified as the optical density (OD_{600}) of the yeast growth in synthetic drop-out medium (SD) without leucine, tryptophan, and histidine and supplemented with 10 mM 3-amino-1,2,4-triazole. The abscissa represents the proteins fused to the AD domain to which (*A*) BD-ELO1, (*B*) BD-AtELP5, and (*C*) BD-AtELP6 were hybridized. (*D*) Schematic overview of the interactions between ELO1, AtELP5, and AtELP6. For each interaction, three independent biological repeats and at least two technical repeats were carried out. The provided constructs within the ProQuest™ Two-HybridSystem with Gateway® Technology (Invitrogen) of the interacting proteins DmDP and DmE2F were used as reference; the negative controls consisted of a

yeast strain containing an empty GAL4-AD vector that was mated with the GAL4-BD fusion of the protein of interest.

B. GFP-ELO3 protein localization in euchromatic regions in interphase nuclei

As all Elongator components copurify with ELO3, it was used to investigate the subcellular localization of the complex in plants. ELO3 contained a GCN5-related *N*-acetyltransferase family domain with a very high homology (67% identity and 80% similarity) with its yeast counterpart, hinting at functional conservation. Linking of the Green Fluorescent Protein (GFP) to the N-terminus of ELO3 did not abolish its function, because the mutant phenotype in *elo3-1* and *elo3-6* was restored to the wild type upon transformation. Several independent T2 transgenic plants overexpressing the *GFP-ELO3* fusion gene were analyzed. The GFP-ELO3 fusion protein was localized predominantly in the nucleus and, to a lesser extent, in the cytoplasm (Fig. 3*A*). The red fluorescent dye *N*-(3-triethylammoniumpropyl)-4-(p-diethylaminophenylhexatrienyl)-pyridinium 2Br (FM4-64) facilitated the visualization of the tissue context and did not overlap with GFP fluorescence, indicating that ELO3 was not located in the plasma membrane. Deconvolution microscopy for superior optical resolution of globular structures was applied to nuclei in root tissues and revealed the nonhomogenous nuclear-localized GFP-ELO3 fluorescence. Big and small 'signal holes' that putatively represented the nucleolus and heterochromatic chromocenters, respectively (Fig. 3*B*), were analyzed by colocalization studies of GFP-ELO3 with immunodetection of dimethylated histone H3 labeling at lysine 4 (H3K4me2) (Fig. 3*C*), an atypical histone mark associated with euchromatin in *Arabidopsis* (Gendrel *et al*., 2005), of dimethylated histone H3 at lysine 9 (H3K9me2) antibody (Fig. 3*D*), a histone mark diagnostic for heterochromatin (Soppe *et al*., 2002), and of the labeled phosphorylated large subunit of eukaryotic RNAPII, which catalyzes transcription elongation of most eukaryotic genes into mRNA. The immunofluorescence pattern of GFP-ELO3 overlapped with that of H3K4me2 and the phosphorylated large subunit of eukaryotic RNAPII, while the brightly 4',6-diamidino-2-phenylindole (DAPI)-stained heterochromatic chromocenters remained unlabelled. In contrast, the GFP-ELO3 and H3K9me2 signals were almost mutually excluded. The signal pairs GFP-ELO3/H3K4me2 and GFP-ELO3/RNAPII overlapped and had a similar profile in contrast to the GFP-ELO3/H3K9me2 signals that did not match well (Fig. 4). The data indicate that the Elongator complex is involved in the process of RNAPII transcription elongation in plants

and, hence, its nuclear function in transcription is conserved between yeast (Otero *et al*., 1999), human (Winkler *et al*., 2002), and plants

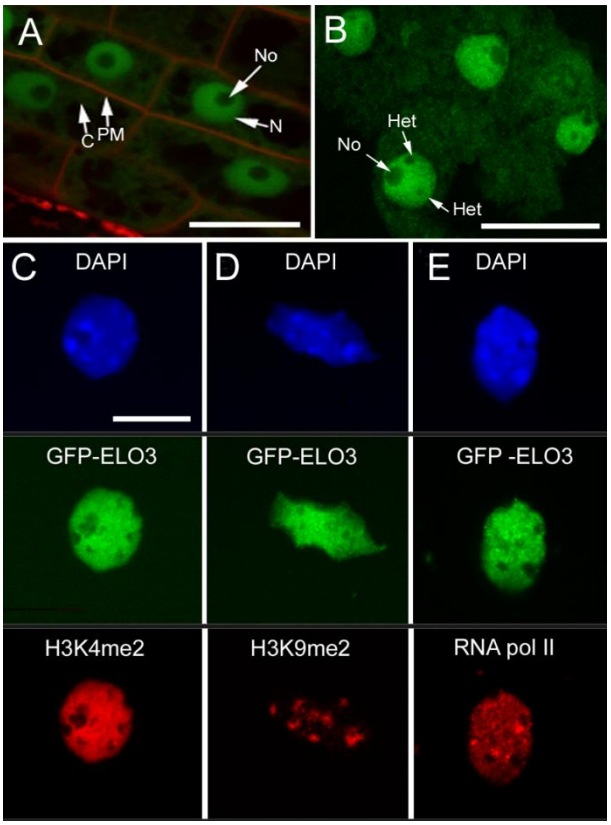

Fig. 3. Localization of the GFP-ELO3 fusion protein and euchromatin colocalization in 4C interphase nuclei of *Arabidopsis*.
(*A*, *B*) Transgenic primary root tissue of 4-day-old seedlings, visualized with confocal microscopy (*A*) and deconvolution microscopy (*B*). C, cytoplasm; Het, heterochromatin; N, nucleus; No, nucleolus; PM, plasma membrane. (Scale bars: 20 µm in *A* and *B*). (*C*) Anti-GFP and anti-histone H3K4me2 sera examination of the presence of ELO3 and transcriptionally potent chromatin on interphase by indirect immunofluorescence. (*D*) Heterochromatic regions detected with anti-histone H3K9me2, not overlapping with the loalization of GFP-ELO3. (*E*) Double-immunolabeling with anti-RNAPII and anti-GFP to reveal a potential link between gene transcription and localization of GFP-ELO3. Most of the brightly DAPI-stained heterochromatic regions revealed a reduced labeling of GFP-ELO3, anti-histone H3K4me2, and RNAPII. In all combinations, the genomic DNA was visualized by DAPI staining. DAPI fluorescence is blue, GFP antibody signal is green, and the other antibody signals are red (Scale bars: 5 µm in *C*, *D*, and *E*).

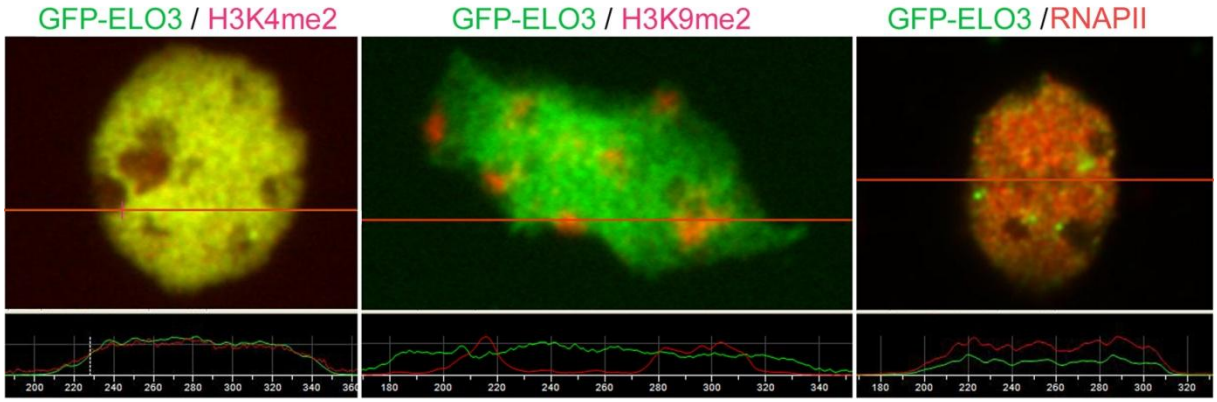

Fig. 4. Pseudo colored picture pairs of GFP-ELO3/H3K4me2, GFP-ELO3/H3K9me2 and GFP-ELO3/ RNAPII immunolabeled nuclei were merged and the fluorescence intensity value of line scans is shown below each corresponding figure. Fluorescence intensity value of line scans were calculated using NIS-Elements (Nikon). To quantify the overlapping of red and green signals the signal distribution of the matching immunostaining signals (red versus green) was measured and the Chi²-test (using the program SigmaStat) was employed to test whether the distribution of red

and green signals differs GFP-ELO3/H3K4me2: Chi^2=26.943, df =24, P=0.307: no significant difference between red and green signals;GFP-ELO3/H3K9me2: Chi^2=1389.571, df =43, P<0.001: a significant difference (***) between red and green signals; GFP- ELO3/RNAPII: Chi^2=37.572, df=26, P=0.066: no significant difference between red and green signals.

C. *ELO* genes are expressed in meristems

The spatial and temporal expression patterns of the *ELO1, ELO2*, and *ELO3* genes were identical and only shown for *ELO3* (Fig. 5). High transcript accumulation was observed in the shoot apical meristem, the emerging leaf primordia, and provascular strands of young seedlings (Fig. 5 *A* and *B*), at the adaxial side of leaf primordia (Fig. 5 *B*), in primary and lateral root meristems (Fig. 5 *D* and *E*), and throughout the young, developing floral bud, especially in the reproductive and vascular tissues. No transcripts were detected in the differentiated zones of primary and lateral roots (Fig. 5 *D* and *E*). In conclusion, *ELO* genes were expressed in meristematic tissues, such as shoot apices, root tips, and adaxial sides of leaf primordia that determine cell proliferation and growth. Hence, the reduced cell proliferation in *elo* mutants (Nelissen *et al*., 2005) can be explained by a depletion of the Elongator complex, specifically in meristematic and dividing tissues. Based on the conservation of the *ELO3* histone acetyltransferase (HAT) and its colocalization with euchromatin and phosphorylated RNAPII (Fig. 3), we conclude that Elongator is a putatively positive regulator of mRNA transcription in dividing tissues.

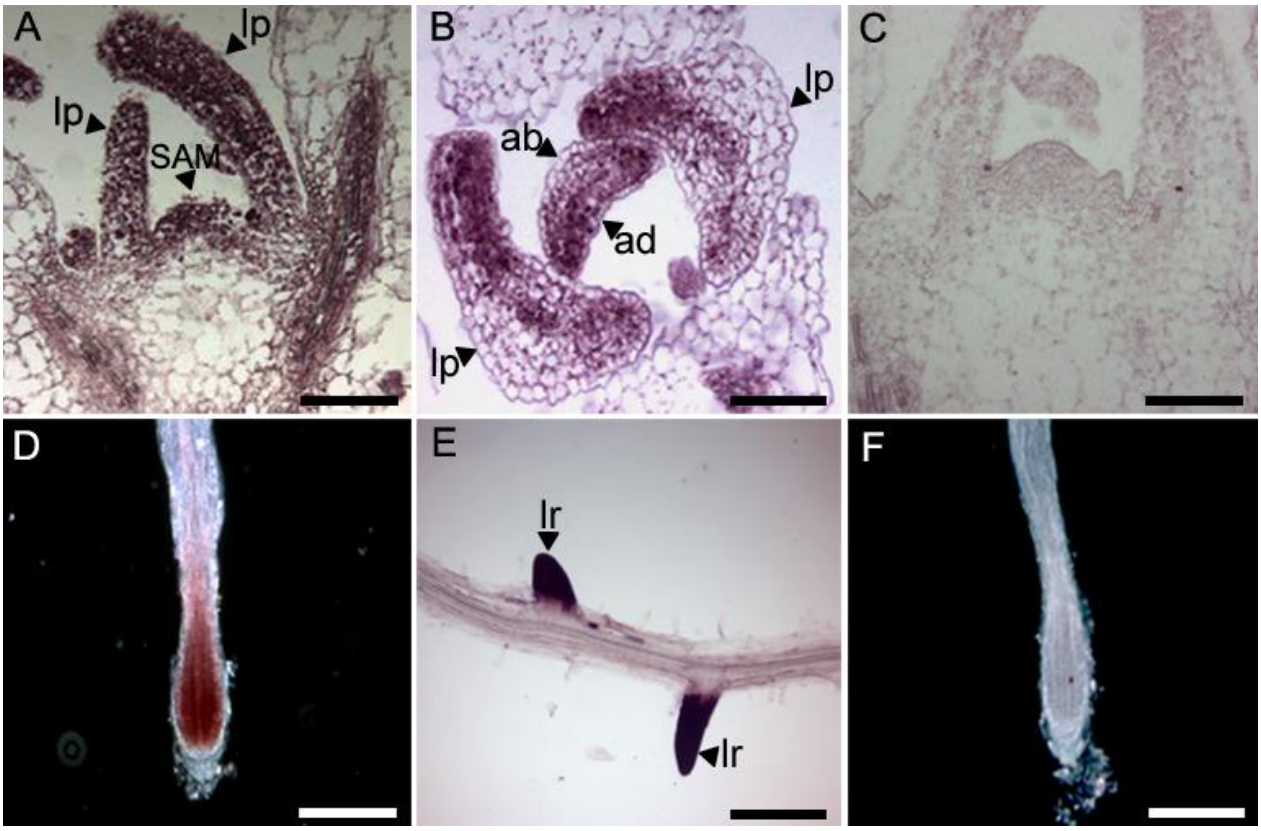

Fig. 5. In situ hybridization pattern of *ELO3* antisense probe.
(*A*) Longitudinal section of 14-day-old shoot apical meristem and early leaf primordia. (*B*) Cross section of 14-day-old leaf primordia. (*C*) Longitudinal section of 14-day-old shoot apical meristem and early leaf primordia hybridized with *ELO3* sense probe. (*D*) Whole-mount hybridization of 14-day-old primary root. (*E*) Whole-mount hybridization of 14-day-old lateral roots. (*F*) Whole-mount hybridization of 14-day-old primary root with *ELO3* sense probe. ab, abaxial surface; ad, adaxial surface; lp, leaf primordium; lr, lateral root; SAM, shoot apical meristem (Scale bars, 70 μm in *A-C*, 100 μm in *D*, *E*, and *F*).

D. Modulation of auxin-related gene expression in *elo* mutants

As histone acetylation positively affects the RNAPII transcription efficiency (Nelissen *et al*., 2007), we analyzed the gene classes downregulated in the *elo* mutants to identify plant-specific pathways targeted by Elongator that might explain the phenotypes of the *elo* mutants. Microarray analyses on shoot apices of *elo* and Landsberg *erecta* (L*er*) seedlings had previously indicated that the *elo* mutants clustered together in one group of differentially expressed genes (Nelissen *et al*., 2005). In the same data set, the overrepresented Gene Ontology (GO) categories of the genes specifically downregulated in the *elo* mutants were analyzed with BiNGO (Maere *et al*., 2005). A restricted number of significant classes ($P<0.001$) was obtained: chromatin assembly, pattern specification, vascular tissue development, and response to auxin stimulus. Most strikingly, a large number of

primary and secondary auxin response genes were present, i.e. two *SAUR*, *IAA14/SLR*, *IAA13*, *IAA11*, *ATHB8*, *IAA3/SHY2*, *IAA12/BDL*, *ARF10*, *ARF11*, *ARF18*, *ACL5*, in addition to auxin biosynthesis (*TAR2*), and auxin transport (*LAX2* and *PIN4*). The aldehyde oxidase 1, involved in auxin biosynthesis, auxin transporters (*PGP1* and *PGP4*) and auxin-responsive genes were upregulated (Table 2). The auxin metabolism, transport, perception, and signaling were severely affected in the *elo* mutants and could be responsible for the leaf and root growth phenotypes observed in the *elo* mutants (Nelissen *et al*., 2005).

Table 2. Fold change of down- and upregulated (differentially expressed, DE) genes putatively involved in hormonal regulated processes in the *elo* mutants compared to the wild type. The DE genes were identified at $P < 0.05$ with an empirical Bayes' *t* test and Holm's *P* correction. Hormone responsive genes were included when a differential expression was indicated by TAIR (www.arabidopsis.org) or Genevestigator (www.genevestigator.com). .

Hormone	GO class	Gene code	Gene name	*elo2-1*	*elo3-1*
Downregulated					
Auxin	Biosynthesis	At4g24670	*TAR2*	0.6	0.4
	Transport	At5g19530	*ACL5*	0.2	0.1
		At2g21050	*LAX2*	0.4	0.3
		At2g01420	*PIN4*	0.6	0.7
	IAA	At1g04240	*IAA3/SHY2*	0.3	0.3
		At4g14550	*IAA14/SLR*	0.3	0.4
		At2g33310	*IAA13*	0.5	0.5
		At4g28640	*IAA11*	0.7	0.5
		At1g04550	*IAA12/BDL*	0.6	0.5
	Auxin response	At1g29440	*SAUR*	0.1	0.1
		At1g29450	*SAUR*	0.2	0.2
		At2g37030	Auxin responsive	0.3	0.4
	ARF	At2g46530	*ARF11*	0.7	0.3
		At2g28350	*ARF10*	0.6	0.5
		At3g61830	*ARF18*	0.5	0.6
	TF	At4g32880	*ATHB8*	0.4	0.2
Cytokinin	Degradation	At3g63440	*CKX7*	0.3	0.3
		At4g29740	Cytokinin oxidase	0.6	0.6
	Perception	At2g01830	*WOL1*	1	0.5
		At5g35750	*AKH2*	0.7	0.7
	Signaling	At1g48270	*GCR1*	0.8	0.6
Upregulated					
Auxin	Biosynthesis	At5g20960	*AAO1*	2.5	3.8

	Transport	At1g77690	*LAX3*	1.2	1.4
		At2g36910	*PCP1*	1.7	2
		At2g47000	*PGP4*	6.8	7.6
	Protein degradation	At1g05180	*AXR1*	1.3	1.1
	IAA	At3g16500	*IAA26*	1.3	1.4
		At5g25890	*IAA28*	2.3	1.5
	Response	At5g20990	*CNX1*	1.2	1.2
		At5g65940	*CHY1*	1.7	1.8
	GH3	At5g13360	Auxin responsive	2.8	2.5
	Miscellaneous	At5g12330	*LRP1*	2.6	3.2
Cytokinin	Synthesis	At3g63110	*IPT3*	1.2	1.2
		At1g62360	*STM*	2.9	3.1
	Signaling	At1g03430	*AHP5*	1.2	1.3
		At1g70510	*KNAT2*	1.4	1.8
		At3g16360	*AHP4*	3.5	3.3
	Response	At1g61630	*CRF6*	10.9	18.8
Ethylene	Synthesis	At1g62380	ACO2	1.1	1.5
	Response	At1g44830	*ERF/AP2* family	1.9	2
		At5g13330	*ERF/AP2* family	2.5	10
		At4g17500	*ERF*	2.7	4.7
		At2g38210	Ethylene-responsive protein	3	3.4
		At1g06160	*ERF*	4.1	2.8
		At2g31730	Ethylene-responsive protein	1.3	2
		At2g42680	*MBF1A*	1.3	1.2
		At1g05710	Ethylene-responsive protein	5.3	4.8
		At3g04720	*PR-4*	27.7	16.1
Jasmonic acid	Synthesis	At4g16760	*ACX1*	1.6	1.5
		At5g42650	*AOS*	3.4	2.2
		At3g45140	*LOX2*	7.3	6.1
	Response	At5g24780	*VSP1*	7.1	10.7
		At1g19670	*CORI1*	3.1	3.1

E. Auxin biology-related phenotypes in *elo* mutants

Previously, the *elo* mutants had been described with narrow leaves and short primary root (Nelissen *et al*., 2005). To verify whether the reduced expression of auxin biology-related genes in the *elo*

mutants is biologically relevant, apical dominance, inflorescence phylotaxis, leaf venation patterning, and lateral root density were studied in the strong *elo1-1*, *elo2-1*, and *elo3-1* and the weak *elo1-10* and *elo3-10* alleles of L*er* and Columbia-0 (Col-0), respectively.

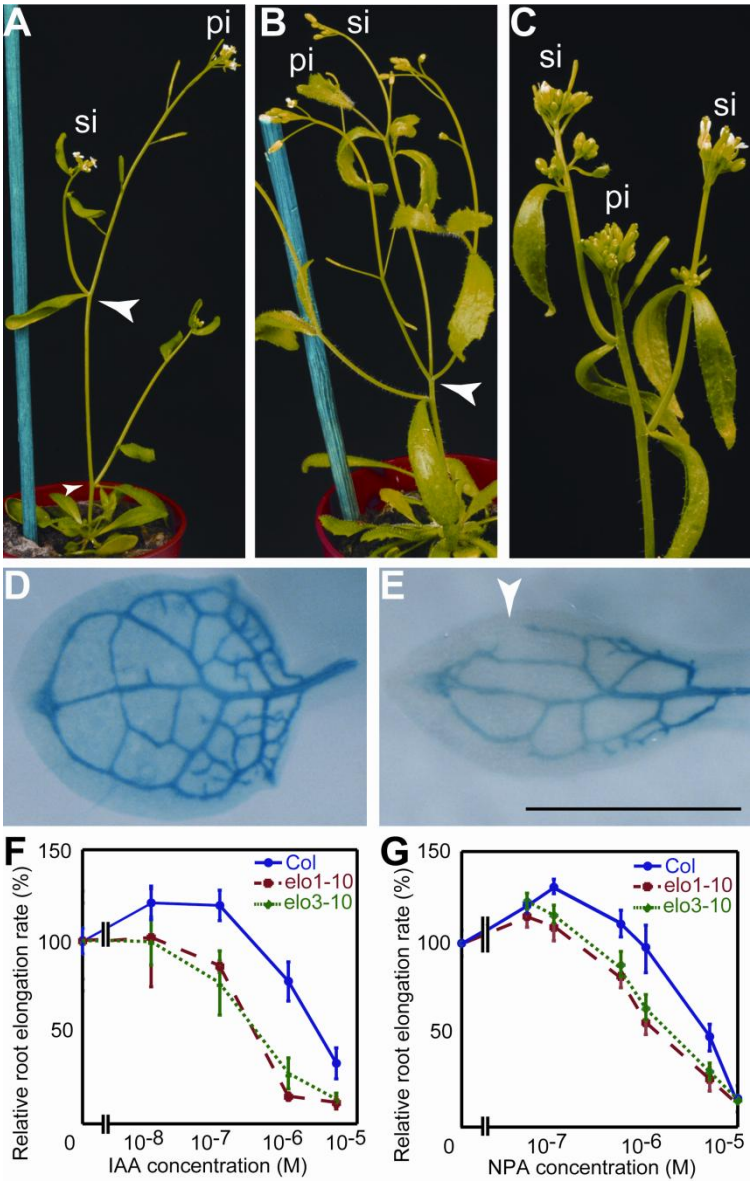

Fig. 6. Auxin-related phenotypes in *elo* alleles.
(*A*) Wild-type inflorescence. (*B*) *elo3-6* showing altered phylotaxis of the secondary inflorescence branches (arrowheads). (*C*) *elo1-1* showing reduced apical dominance. (*D)* venation pattern visualized by X-Gluc histochemical assay of wild type and (*E*) *elo3-1* mutant transformed with p*ATHB8-GUS* showing open venation (arrowhead). (*F*) Primary root length on increasing levels of exogenous applied IAA and (*G*) NPA. Pi, primary inflorescence; si, secondary inflorescence. (Scale bar: 1 mm).

In wild-type *Arabidopsis*, the modulation of auxin transport capacity in the main stem has been proposed to regulate bud outgrowth (Bennett *et al*., 2006). In the *elo* mutants, apical dominance was clearly reduced, resulting in a precocious growth stop of the primary inflorescence and an overgrowth of the secondary branches, relative to the primary inflorescence (Fig. 6 *A-C*, Fig. 7*A*).

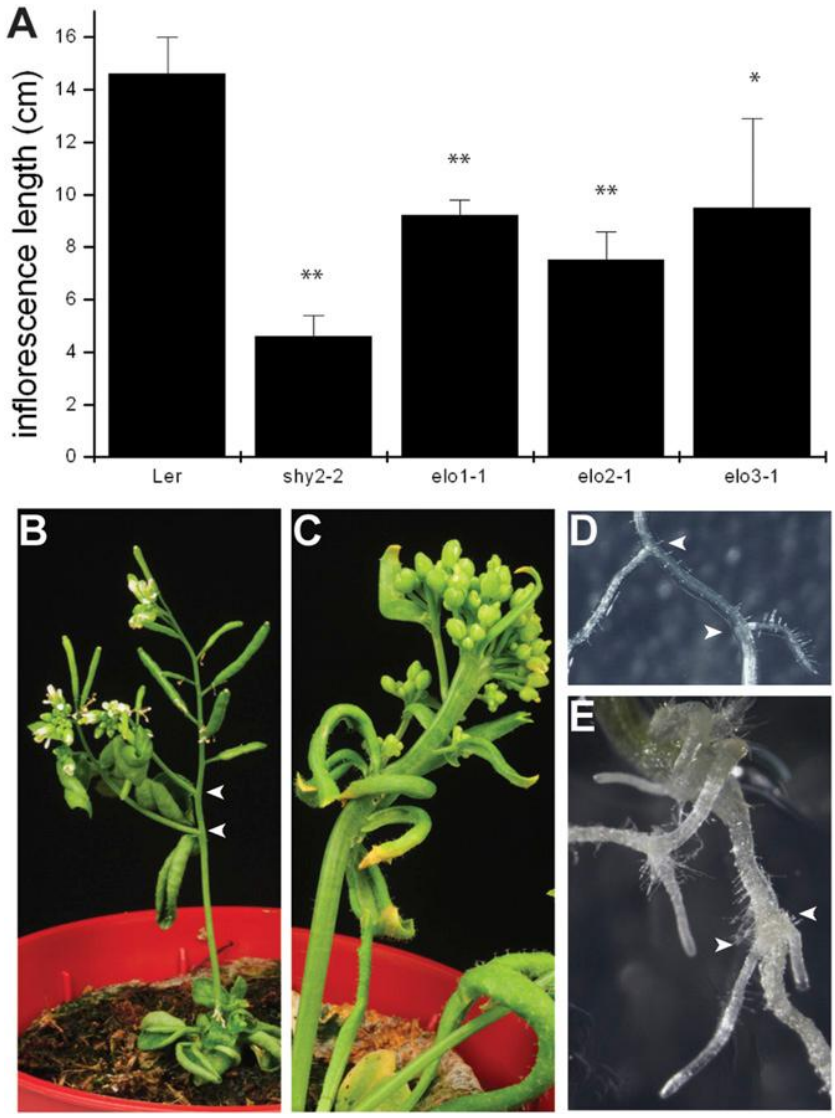

Fig. 7. Additional auxin-related phenotypes in the elo alleles. (A) Primary inflorescence length in elo and shy2-2 mutants in comparison with the Ler wild type (6 weeks after sowing). Error bars represent standard error. *P < 0.05 and **P < 0.001, respectively, according to Student's t test. (B) shy2-altered phyllotaxis (arrowheads). (B) Fasciated inflorescence of elo3-1. (C) Wild-type root with normal lateral root spacing (arrowheads). (D) elo2-1 root with oppositely emerging lateral roots (arrowhead).

This reduced apical dominance in the *elo* mutants supports a defective auxin biology. The position of lateral organs, the phylotaxis, is determined by auxin maxima at the shoot or inflorescence meristems and results in a spiral in *Arabidopsis* (Reinhardt *et al*., 2003). In the *elo* mutants, the phylotaxis is defective with secondary inflorescences originating at the same node or ectopically causing irregular internode length (Fig. 6 *A* and *B*) indicating that the auxin maxima were not properly established in the *elo* mutants and suggesting a role for Elongator in auxin distribution or signaling. Such defects also occurred in the *shy2-2* mutants (Fig. 7*B*). Secondary branches that are subtended by cauline leaves in wild-type *Arabidopsis* were often absent in the *elo* mutants (Fig. 6*B*). The putative ectopic auxin accumulation could be the consequence of a defect in the auxin transport and relate to the differentially expressed auxin-related genes in *elo* mutants (Table 2). The p*ATHB8-GUS* marker for provascular cell state revealed a defective venation patterning in the *elo* mutants, with disconnected primary loops and reduced secondary and tertiary veins, which is typical for an altered auxin distribution (Fig. 6 *D* and *E*) (Donner *et al*., 2009).

Auxin signaling affects primary and lateral root growth - mutants of the *AUX/IAA* auxin response-related genes have a very short primary root (Tian *et al*., 1999; Hamann *et al*., 2002). Similarly, in the *elo* mutants, primary roots were severely reduced (Nelissen *et al*., 2005) and often grew agravitropically, with a significantly reduced lateral root density (number of lateral roots/cm): 1.7 ± 0.9 in *elo1-1* and 1.4 ± 1.1 in *elo3-1* mutants versus 2.5 ± 0.6 in the L*er* control. In addition, ectopic lateral roots were observed in *elo2-1* (Fig. 7 *D* and *E*). Thus, the short primary root, the low lateral root density, and the ectopic lateral roots observed in the *elo* mutants argue also for a defect in auxin signaling or distribution.

The weak *elo1-10* and *elo3-10* alleles in which the primary root growth was not severely compromised, were used to investigate the effect of increasing levels of exogenously applied IAA and the auxin transport inhibitor *N*-1-naphthylphthalamic acid (NPA). Low concentrations of both supplied chemicals reduced growth in the *elo* mutants, suggesting that the endogenous level of auxin was higher in the *elo* mutants and that the auxin transport was compromised in the mutants (Fig. 6 *F* and *G*). Levels of free IAA were determined in shoot apices of 14-day-old seedlings that coincide with sites of auxin biosynthesis. The free IAA concentration was 3-fold higher in *elo2-1* than that in L*er* (Fig. 8*A*), possibly interfering with the autoregulation of the shoot apical meristem and the reason for the, sometimes, extremely fasciated inflorescence stems in the *elo* mutants (Fig. 7*C*).

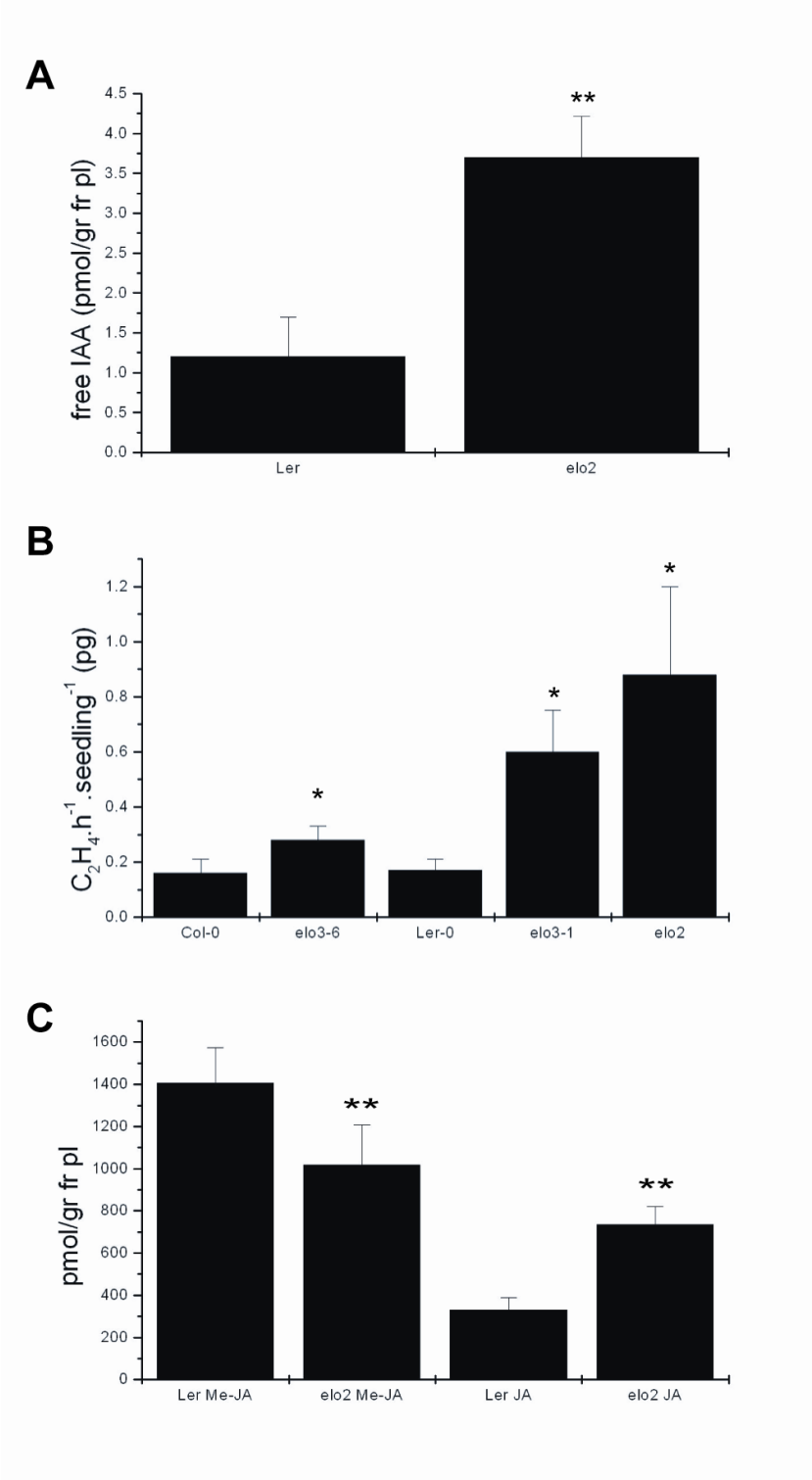

Fig. 8. Hormone measurements in the elo alleles. (A) Free indole-3-acetic acid (IAA) content in elo2-1 compared to the Ler wild-type free IAA purified by a combined solid-phase extraction, methylated, and analyzed by micro-LC-(ES+)MS/MS. The error bars represent standard deviation. Five replicates were performed. According to Student's t test, the difference between elo2 and Ler is highly significant for $P < 0.001$. (B) Ethylene (C2H4) content in the elo mutants compared to that of the respective Ler and Col wild type. Error bars represent standard deviation; *$P < 0.05$ in a Student's t test. Biologically independent replica experiments were done in duplicate. (C) Jasmonic acid (JA) content in elo2-1 compared to that of the Ler wild type. JA and methyl jasmonate (Me-JA) were separated by solid-phase extraction. After solid-phase extraction, JA was methylated with diazomethane before analysis by GC-MS with the electron impact mode (EI(+) GC-MS) and measured as Me-JA. The concentrations of JA and Me-JA were calculated per gram of fresh weight and the data analyzed statistically with SPSS by a t test with three replicates. Error bars represent standard deviation. According to the t test, the difference between elo2 and Ler is highly significant for $P < 0.01$ for JA-Me and for $P < 0.001$ for JA.

F. Hormonal misregulation might contribute to the pleiotropic phenotype of the *elo* mutants

In each of the *elo* mutants, the ethylene emanation had increased significantly (Fig. 8*B*) and the jasmonic acid (JA) content in the *elo2-1* mutant as well (Fig. 8*C*), which correlated with the transcriptional upregulation of ethylene-responsive genes (*AP2/ERF*), JA biosynthesis genes (*ACX1*, *AOS*, *LOX1*, and *LOX2*), and two major JA response genes (*VSP1* and *COR1*) in the *elo* mutants (Table 2). It is not clear whether the increased biosynthesis of ethylene and JA is the consequence of elevated auxin levels. However, increased JA might contribute to the short root phenotype of the *elo* mutants and the downregulation of histone genes in the GO category "chromatin assembly" of their transcriptome because exogenous addition of JA reduces replication, root growth, and histone gene expression (Swiatek *et al*., 2002; Lorenzo *et al*., 2005). The GO categories abiotic stress, defense to pathogen, and anthocyanin biosynthesis were significantly upregulated in the microarray data set, which might be the consequence of JA or ethylene overproduction in the *elo* mutants. This observation correlates with the previously identified *abo1/elo2* allele as abscisic acid (ABA)-hypersensitive with a drought-resistance phenotype (Chen *et al*., 2006) and resistance of *elo* mutants to oxidative stress produced by methyl viologen and increased anthocyanin biosynthesis (Zhou *et al*., 2009).

G. Elongator targets specific genes related to auxin biology

Based on the *elo* phenotypes and the transcriptome, we identified a number of genes with reduced expression levels (Table 2) as putative targets of Elongator, i.e. the *SHY2/IAA3* and *BDL/IAA12* repressors, the *ATHB8* auxin response gene (Donner *et al*., 2009), the *LAX2* influx carrier, the *PIN4* efflux carrier, and the *AP2/ERF* ethylene response gene. The downregulation of these genes in the *elo* mutant was verified with quantitative (q)PCR (Fig. 9 and 10). We investigated whether the reduced expression of the selected genes was related to reduced acetylation levels of histone H3 lysine-14 in their promoter and/or coding regions because H3K14 is the predominant substrate of the ELP3 HAT in yeast (Winkler *et al*., 2002). DNA of the *elo3-6* mutant and Col-0 wild type, immunoprecipitated with an antibody against acetylated H3K14 or histone H3 was normalized by using a primer pair specific for the 5' end of *ACTIN2/7*, a constitutively expressed gene (Table 2). qPCR after chromatin immunoprecipitation (ChIP) with antibodies against H3K14Ac was used as a measure for the amount of acetylated H3K14, but remained unchanged at the promoter and coding sequence of the *ACTIN2/7* gene between the *elo* mutant and the wild type (Fig. 10).

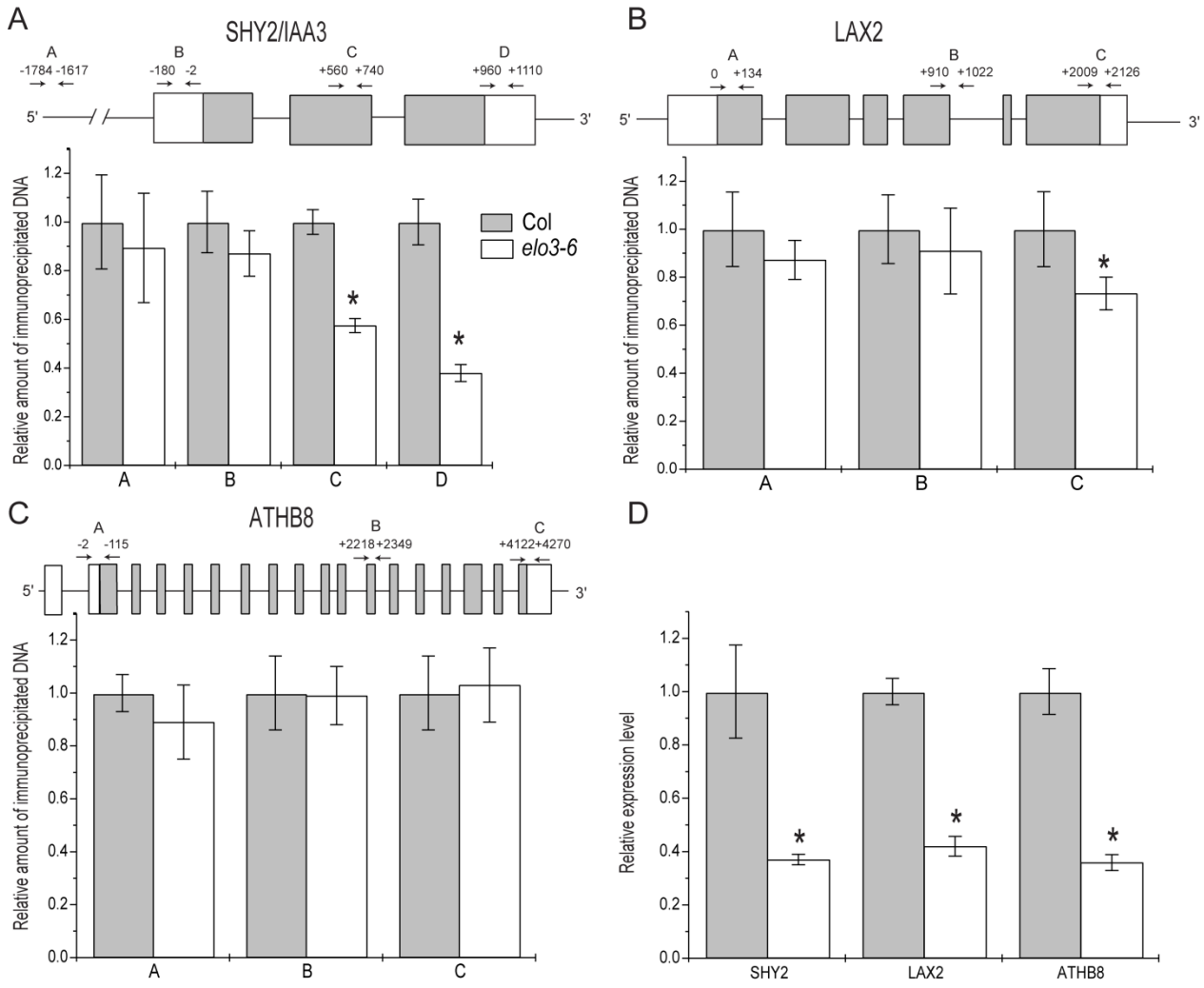

Fig. 9. ChIP analysis of H3K14 acetylation at *SHY2/IAA3* (*A*), *LAX2* (*B*) and *ATHB8* (*C*) genes and relative expression level in *elo3-6* (*D*).
Gene structure and position of primers relative to the initiation ATG codon are indicated. White and grey boxes are untranslated sequences and exons, respectively. Relative amount of immunoprecipitated chromatin fragments as determined by real-time PCR compared to the wild type (arbitrarily given as 1). Error bars represent SD values of at least three repetitions. *, significant differences between wild type and mutant according to a *t*-test ($p<0.05$).

qPCR after ChIP showed significantly reduced levels with primers corresponding to the coding and 3'-untranslated regions of the *SHY2/IAA3* gene in the *elo* mutant and normal levels with primers against the upstream and core promoter regions (Fig. 9*A*). Similarly, qPCR levels with primers in the 3'-untranslated region of the *LAX2* gene were significantly lower in the *elo* mutant (Fig. 9*B*), but did not differ with primer pairs for *ATHB8* (Fig. 9*C*), *PIN4*, *BDL/IAA12*, and *AP2/ERF* (Fig. 10), indicating that the decreased expression level was an indirect effect of the *elo* mutation. In summary, the reduced H3K14 acetylation levels at the coding and 3'-untranslated regions of the

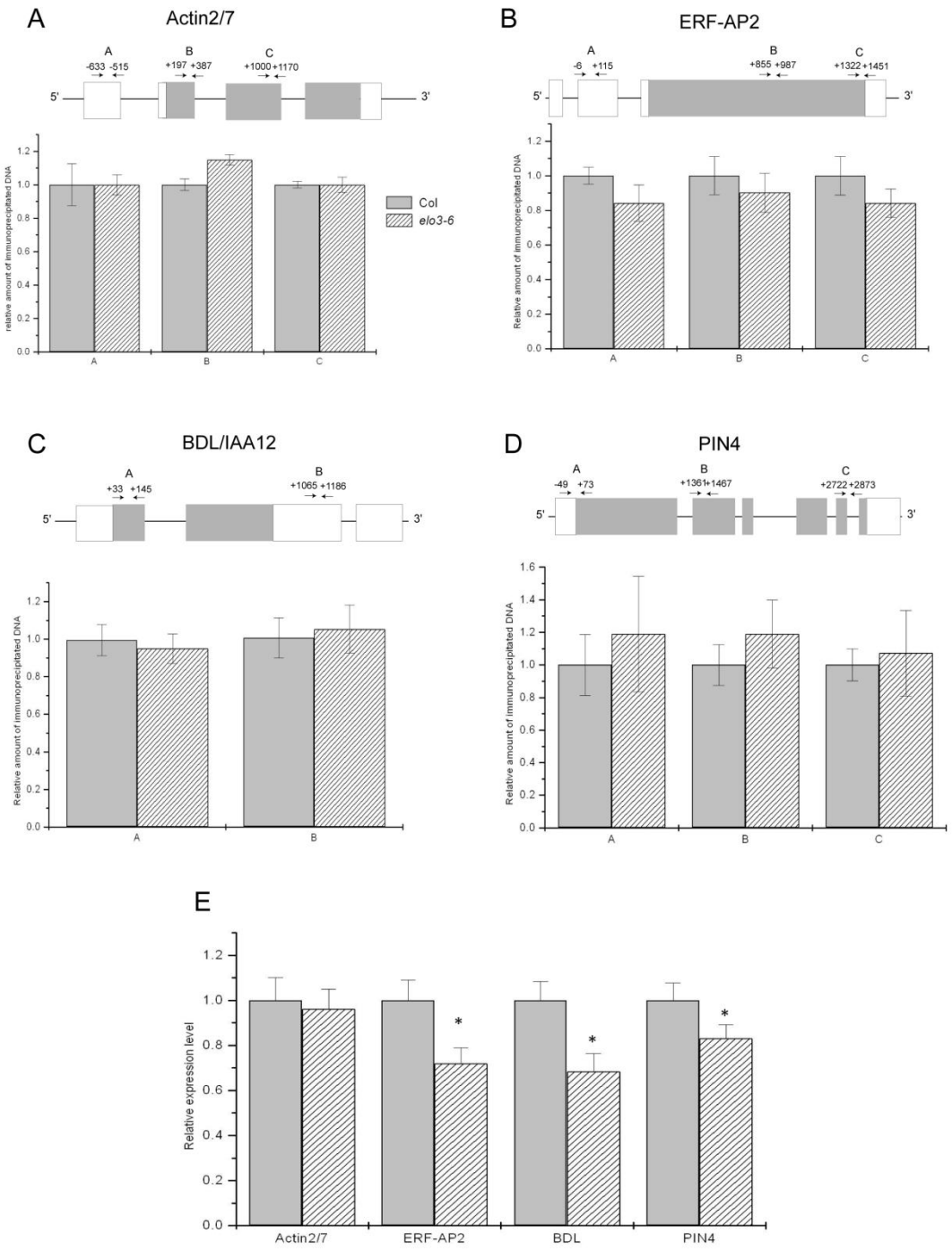

Fig. 10. ChIP analysis of ACTIN2/7 (*A*), ERF-AP2 (*B*), BDL (*C*), PIN4 (*D*) genes and relative expression level in *elo3-6* (*E*). Gene structures and position of primers relative to the initiation ATG codon are indicated. White and grey boxes are untranslated sequences and exons, respectively. Graphs: relative amount of immunoprecipitated chromatin fragments as determined by real-time PCR compared to the wild type (arbitrarily given as 1). Error bars represent SD values from at least three repetitions.

SHY2/IAA3 and *LAX2* genes in the *elo* mutants explained the lowered expression levels and identified these genes as direct targets for Elongator HAT activity, arguing for an Elongator HAT activity during RNAPII transcription elongation. Indeed, our analysis shows that the Elongator complex targets specific genes for acetylation and transcriptional regulation rather than affecting transcription generally, which adds important novel mechanistic information on the Elongator function in transcription.

To further assess whether Elongator is directly involved in the H3K14 acetylation at the *SHY2/IAA3* locus, we used the GFP-ELO3 line to perform ChIP analysis with antibody against GFP (Abcam). After immunoprecipitation we looked for enrichment of the SHY2/IAA3 locus compared to the input by Q-PCR using primer pair B (Fig 11 and 9A). As a control a free GFP line was used. The enrichment of the SHY2/IAA3 locus shows that Elongator is tightly associated with the SHY2/IAA3 locus while no enrichment was found in the control line.

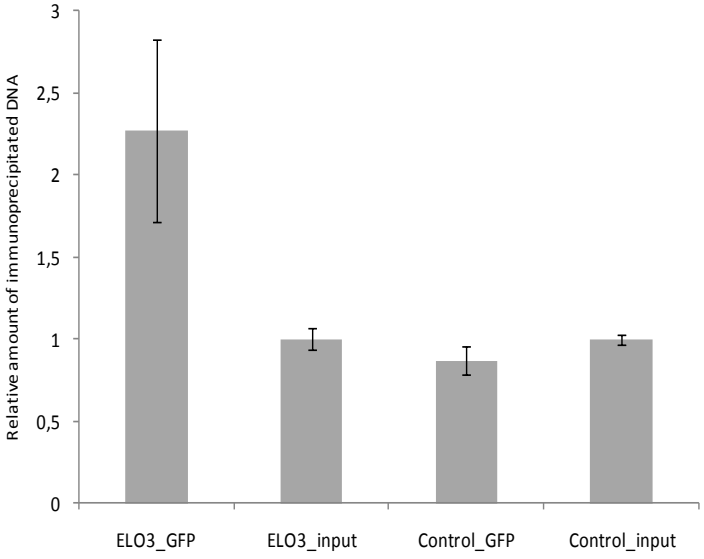

Fig. 11. ChIP analysis on the ELO3-GFP line. Immunoprecipitation of DNA using the GFP antibody was followed by Q-PCR analysis of the SHY2/IAA3 locus for ELO3-GFP and free GFP lines. Primerpair B: fwd 5'GAAAACAGTTTCTTCTCTCTCTACCA3' rev 5'TCTTCAAGAATTGCAGGAGAAG3'

H. Conclusion

We demonstrated that the protein structure of the Elongator complex is conserved from yeast and mammals to plants. Our data suggest a role of Elongator in RNAPII transcription elongation in plants through ELO3 (GCN5 HAT family) acetylation of H3K14 in coding and 3'-untranslated regions of specific genes, such as *SHY2/IAA3* and *LAX2*. These genes are part of auxin-related processes that are plant specific. Hence, the function of Elongator, although conserved in substrate selection, evolved in plants with respect to target preference. Besides the target of the ELO3 HAT,

the *SHY2/IAA3* gene is also the target of the GCN5 HAT that acetylates specifically its promoter (Benhamed *et al*., 2006), suggesting a complex chromatin-related control for this gene.

Several genes, which are induced by external stimuli that provoke cellular responses, are regulated at the level of transcription elongation (Muse *et al*., 2007). For these genes, the RNAPII initiation complex is stalled or paused in the proximity of the promoters in the absence of the appropriate stimulus. Upon stimulation, the C-terminal domain of the RNAPII gets phosphorylated and transcription elongation is resumed, allowing a fast response. In this manner, transcription elongation factors are thought to control the transcription rates of early response genes in a stimulus and gene-specific way (Fujita *et al*., 2009). Also in *Arabidopsis*, GCN5 acetylated gene subsets in a stimulus dependent manner, while the exact mechanism of gene specificity remained to be established (Benhamed *et al*., 2008). Our working hypothesis puts the Elongator complex forward as a factor that steers the transcription elongation of a subset of early response genes, regulated by signals from the environment. Auxin-induced expression of *SHY2/IAA3* was not affected in the *elo* mutants (Fig. 12), indicating that ARF-mediated gene activation of *SHY2/IAA3* acts independent of the Elongator pathway. The Elongator complex might not react to the auxin stimulus, be dose dependent, or only be responsible for basal transcription of this gene. A future challenge will be to prove this hypothesis and to identify the upstream regulation of the Elongator complex.

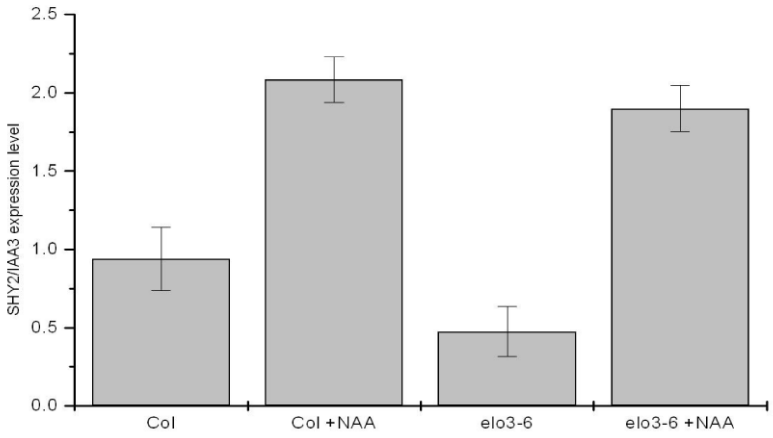

Fig. 12. *SHY2/IAA3* gene expression induction assay by external auxin. Wild type Col and *elo3-6* mutants were grown for 5 days under constant light conditions and transferred to liquid growth medium containing 1μM NAA. After 1 hour samples were immediately frozen in liquid nitrogen followed by RNA

isolation. Expression level of *SHY2/IAA3* was measured by RT-PCR. The error flags represent the standard deviation of 3 repeats.

The Elongator-dependent chromatin-mediated regulation of the auxin signaling gene *SHY2/IAA3* and the auxin influx carrier *LAX2* might, in part, explain the auxin-related phenotypes observed in the *elo* mutants: both gain-of-function and loss-of-function alleles of *shy2* display short primary roots, while only the gain-of-function mutation reduces lateral root formation (Tian *et al*., 1999). Thus, the decreased lateral root formation in the *elo* mutants cannot simply be explained by a downregulation of *SHY2/IAA3*. It was hypothesized that *shy2* mutations might alter the auxin transport (Tian *et al*., 1999); therefore, the combinatorial downregulation of both *SHY2/IAA3* and *LAX2* in the *elo* mutants might result in a severely aberrant auxin distribution. In the triple *lax* mutant, the auxin distribution is disturbed, with decreased angles of phylotaxis and narrow leaf shapes (Bainbridge *et al*., 2008), which are also typical phenotypes of the *elo* mutants. In addition, upregulation of JA, ethylene, and abiotic stress-related genes might contribute to other aspects of the *elo* phenotype, such as reduced DNA replication and, hence, lessened cell proliferation (Nelissen *et al*., 2005) and resistance to abiotic stress (Zhou *et al*., 2009). In analogy with the high number of target genes of the GCN5 HAT (Benhamed *et al*., 2008), it is expected that the majority of the direct targets of the Elongator complex has to be identified, which will allow to get the complete picture of the molecular mechanisms underlying the *elo* phenotypes.

III. Materials and Methods

Plant material and growth conditions. The mutants *elo1-1, elo2-1,* and *elo3-1* (Nelissen *et al*., 2005) were in L*er*, the *elo3-6* mutant in Col-0 (GABI-KAT collection code GABI555_H06), and the *elo1-10* and *elo3-10* in Col-0 were isolated from a X-ray-irradiated M2 population (line #111) and T-DNA-mutagenized T2 population (line #2018), respectively. In *elo1-10*, the genomic region was deleted, including the 5th exon to the 3' end of the *ELO1* gene and, in *elo3-10*, a single base deletion occurred at 2452A of the *ELO3* gene, resulting in a frame shift and a premature stop codon with 28 amino acid residues. The p*ATHB8-GUS* line (N296) was obtained from the Nottingham Arabidopsis Seed Stock Centre. The growth chamber conditions were: 16 h/8 h (day/night) with white light (neon tubes, cool white), 100 μmol$esm^{-2}s^{-1}$ light intensity, and 20°C.

***In situ* hybridization.** Short and specific (GSTs) fragments of *ELO1* (At3g11220), *ELO2* (At5g13680), and *ELO3* (At5g50320) genes were cloned in the pGEM-T-Easy vector (Promega). Digoxigenin (DIG)-labeled RNA sense and antisense probes were synthesized by T7 and SP6 polymerase-driven *in vitro* transcription, respectively (DIG-RNA labeling Kit protocol; Roche Diagnostic).

Root tips, shoot apices and leaves, and floral buds were excised from 7-, 12-, and 20-day-old L*er* seedlings, respectively, fixed, dehydrated, embedded in paraffin, cut into 8-µm sections, and hybridized (55°C) to a DIG-labeled antisense RNA probe as described (Canas *et al*., 1994). Transcript accumulation was visualized as a violet/brown staining.

Microarray analysis. Shoot apices consisting of the shoot apical meristem and first and second leaf primordia at the petioleless stage of seedlings between 11 and 18 days after germination *in vitro* were harvested. RNA was extracted with the TriZOL method (Invitrogen). ATH1 Affymetrix chips were used for hybridization (Nelissen *et al*., 2005) and the data are available on ArrayExpress (E-MEXP-300). The molecular processes affected specifically in the *elo* mutants were obtained by subtracting the differentially expressed transcripts also present in the *drl1-2* and *hub1-1* (Fleury *et al*., 2007) mutants, two narrow-leaf mutants of which the transcriptomics were analyzed simultaneously.

Tandem affinity purifications. The TAP tag was fused C-terminally (ELO1 and AtELP5) or N-terminally (AtELP2 and ELO3) to the various cDNA clones expressed from the 35S promoter and transformed in wild-type *Arabidopsis* cell suspension cultures (PSB-D). The TAP was carried out as described (Van Leene *et al*., 2007; 2008) with minor modifications: 300 mM NaCl in the extraction buffer and two subsequent centrifugation steps at 47,807g after extraction (omitting the ultracentrifugation step). Total protein extract (200 mg) was loaded on the IgG column. Eluted proteins were separated on 4-12% NuPAGE gels; the entire gel lanes were cut into fragments and analyzed by Maldi-TOF-TOF-MS. To increase the stringency of the data set, contaminating proteins due to experimental background were systematically subtracted from the copurified protein lists. Proteins with a probability-based identity of at least 95% and present in at least two independent TAP experiments were retained as interactors. Therefore, no other proteins represented by additional bands on gel could be assigned as Elongator components or interactors.

Localization of GFP-ELO3 in plant cells. Plants were grown vertically *in vitro* for 4 days and primary roots analyzed with a confocal microscope 100M with software package LSM 510 version 3.2 (Zeiss). GFP fluorescence was imaged at 488 nm excitation. Emission fluorescence was captured in the frame-scanning mode, alternating GFP fluorescence via a 500- to 550-nm bandpass emission filter. The FM4-64 dye (5 μg/ml) that intercalates into the plasma membrane was imaged at 511 nm excitation to visualize the tissue context.

Deconvolution microscopy was used for superior optical resolution of globular structures. Each photograph was collected as sequential image along the Z-axis with approximately 11 slices per specimen. All images were collected in grey scale and pseudocoloured with Adobe Photoshop. Projections (maximum intensity) were done with the program AnalySIS (Soft Imaging System).

Analysis of the nuclear proteins by indirect immunofluorescence. Replicated (4C) nuclei of young *Arabidopsis ELO3-GFP* leaf tissue were immunostained and analyzed as described previously (Soppe *et al*., 2002). Following primary antibodies were used: rabbit anti-RNA polymerase II CTD phospho Ser5 (ACTIVE MOTIF; diluted 1:100), mouse monoclonal anti-GFP (Roche; diluted 1:100), rabbit anti-histone H3K4me2 (Upstate; diluted 1:300), and rabbit anti-histone H3K9me2 (Upstate; diluted 1:300).

Chromatin immunoprecipitation (ChIP). ChIP was done as described previously with minor modifications (Bowler *et al*., 2004). Seeds of Col-0 and the *elo3-6* mutant were sown on Murashige and Skoog medium and grown in vitro under short-day conditions. Seedlings were harvested after 3 weeks and fixed in 1% formaldehyde for 10 min in a vacuum and neutralized by 0.125 M glycine for 5 min. Samples were ground in liquid nitrogen and nuclei were isolated and lysed in the presence of protease inhibitors. The isolated chromatin was sonicated 5 times for 30 s in a Branson sonifier water bath. The antibodies for immunoprecipitation were purchased from Upstate Biotechnology: anti-histone H3K14Ac (07-353) and anti-histone H3 (05-499). Immunoprecipitated DNA was purified with the Roche PCR Purification Kit and dissolved in 50 μl supplemented with RNase A and analyzed by real-time PCR (Biorad iCycler) with primers in the promoter and coding regions of the tested genes (Figs. 9 and 10).

Yeast two-hybrid analysis. For the yeast two-hybrid analysis, the ProQuest™ Two-HybridSystem with the Gateway Technology (Invitrogen) was used. None of the constructs was self-activated in a colony-lift filter assay with 5-bromo-4-chloro-3-indolyl-ß-D-galactopyranoside as substrate. The provided constructs of the interacting proteins DmDP and DmE2F were used as reference for the interactions; the negative controls consisted of a yeast strain containing an empty GAL4-AD vector that was mated with the GAL4-BD fusion of the protein of interest. For each interaction, three independent biological repeats and at least two technical repeats were carried out.

Hormone measurements. The free IAA, methyl-JA, and JA were extracted from 14-day-old shoots grown *in vitro* of L*er* and *elo2-1* seedlings and incubated overnight in 80% methanol at -20°C. Three and five replicates were taken for JA and IAA measurements, respectively. Free IAA was purified by a combined solid-phase extraction, methylated, and analyzed by micro-LC-(ES+)MS/MS (1). For JA measurements, O^{18}-JA and O^{18}-Me-JA (100 ng each) were added to the extracts. The 1'-O^{18}-JA was synthesized from H_2O^{18} (95%; Cambridge Isotope Laboratories), separated by solid-phase extraction and methylated with diazomethane before measurement by GC-MS (TRIO 2000; Waters-Micromass). Ethylene was measured as described (2), with some modifications. Seeds (300) were surface sterilized and sown in a 10-ml vial containing 5 ml of half-strength Murashige and Skoog medium with 1% sucrose and 0.8% plant tissue culture agar. The vial was placed for 2 days at 4°C in darkness, exposed to white light for 6 h at 21°C, and kept at 22°C for 2 days of growth in darkness. The vials were capped, left in darkness for 24 h, and subsequently flushed with hydrocarbon-free air. Ethylene in the headspace was detected with an ETD-300 photo-acoustic ethylene detector (Sensor Sense). Two biologically independent replica experiments were done with highly similar results.

Primers used for analyzing chromatine immuno precipitation. SHY2-A: fwd 5'CTTACGTTCCACTGACGGATT3' rev 5'CTTGACAGAACAGGTCATAAGTTTG3' SHY2-B: fwd 5'GAAAACAGTTTCTTCTCTCTCTACCA3' rev 5'TCTTCAAGAATTGCAGGAGAAG3' SHY2-C: fwd 5' TGGATGCTCATTGGTGATGT3' rev 5'GCCTAAACCTTTGGCTTCTG3' SHY2-D: fwd 5'GGTCTTAAGCATATGAAACTGGAAC3' rev 5'GATCAATGAGAACGCAAAACAG3' ACTIN2/7-A: fwd 5'CGTTTCGCTTTCCTTAGTGTTAGCT3' rev 5'AGCGAACGGATCTAGAGACTCACCTTG3' ACTIN2/7-B: fwd 5'GTCGTCCTAGGCACACTGGT3' rev 5'CAACACGAAGCTCGTTGTAGA3' ACTIN2/7-C: fwd 5'CCTGGAATCCATGAAACAACT3' rev 5'GGTGCAACCACCTTGATCTT3' BDL-A: fwd

5’GGAGAGTGAGCTGGAATTGG3’	rev	5’GCAGAGCGTTTAGACCCAAC3’	BDL-B:	fwd
5’GGATCATGGGAACCTCAGAA3’	rev	5’TCTGCTCTTGACGTCTTGGA3’	ERF-AP2-A:	fwd
5’CGGATTTATGTCGGCTGTGT3’	rev	5’AGCAGAAGCGAAGAGCGTTA3’	ERF-AP2-B:	fwd
5’GCACTGGCTTCTTCAGGTTC3’	rev	5’CAGAAGTAGGGGAACGCAAG3’	ERF-AP2-C:	fwd
5’ATCTGACAACACCGCCTCTC3’	rev	5’AGATCAGACCGCAAGGATCA3’	PIN4-A:	fwd
5’CCCTCAAATGCCACTGTCTT3’	rev	5’CCGTAGGCGAGAATCATAGC3’	PIN4-B:	fwd
5’GTGATGATATCGGCGGTCTT3’	rev	5’CCGTGGAATTAGACCCCATT3’	PIN4-C:	fwd
5’TGTGCATCCCACGATTCTAA3’	rev	5’CCAAATATGACCCTGCATCC3’	LAX2-A:	fwd
5’GGAGAACGGTGAGAAAGCAG3’	rev	5’ATTGGAAGCACAGCTGAACC3’	LAX2-B:	fwd
5’ACCATTGCCTCTATCCTCCA3’	rev	5’TTGGGTAAAGTGGTCCCAAA3’	LAX2-C:	fwd
5’GTTCGGTGGTTGGGCTAGTA3’	rev	5’AAATTCAAAGGCCGTGAGTG3’	ATHB8-A:	fwd
5’AGATGGGAGGAGGAAGCAAT3’	rev	5’CGCATAGAGCTCGGTTTAGG3’	ATHB8-B:	fwd
5’GTTCAGCGATGAAGGATGGT3’	rev	5’ATTGGCAAATGGGAGACTTG3’	ATHB8-C:	fwd
5’GCATGGGAAGAGCAGTAACG3’	rev	5’CCAGTTGAGGAACATGAAGC3’		

IV. Acknowledgements

The authors thank J. Fuchs for flow-sorting of nuclei and K. Kumke for technical assistance; G. Persiau, E. Van De Slijke, and D. Eeckhout for help with TAP and MS; E. Prinsen for IAA and JA measurements; and M. De Cock for help in preparing the manuscript. This work was supported by the European Research Training Network (contract no. HPRN-CT-2002-00267), the Institute for the Promotion of Innovation through Science and Technology in Flanders (“Generisch Basisonderzoek aan de Universiteiten,” grant 20193). H.N. and S.D.G. are indebted to the Institute for the Promotion of Innovation through Science and Technology in Flanders for a postdoctoral and a predoctoral fellowship, respectively. F.V. is a postdoctoral fellow of the Research Foundation-Flanders.

Chapter 5:

Elongator function related to light and Elongator conservation across species

Steven De Groeve wrote this chapter and performed all experiments

I. Introduction

Although Elongator structure and function in RNAPII transcription is conserved between yeast, plant and humans, the physiological processes affected upon complex disruption indicate distinct roles played by the complex in uni- and multicellular organisms. Both in yeast and in plants Elongator affects the cell division rate. Nevertheless, while in yeast, mutants are retarded in growth because of slow adaptation to changing environmental conditions; in plants and humans developmental processes are disturbed. In humans, mutations in Elongator components affect neuronal development and result in diseases such as familial dysautonomia and amyotrophic lateral sclerosis (Chapter 2). In the model plant, *Arabidopsis*, Elongator mutants are known for narrow leaves and short roots due to reduced cell proliferation, but germination, vegetative growth, and the reproductive developmental phases are also affected. According to Elongator's role in growth, in situ hybridization experiments indicated that the *ELO* genes were expressed exclusively in meristematic and dividing tissues (Chapter 4). The auxin-related phenotypes of *elo* mutants such as reduced apical dominance, altered auxin sensitivity and defective venation patterning are correlated with down-regulation of genes related to auxin signaling and reduced histone acetylation at the auxin response regulator, IAA3/SHY2 (Chapter 4). Consequently, the Elongator complex might have originated early in evolution but acquired more functions in multicellular organisms where it fulfills kingdom-specific roles. Interestingly, the IAA3/SHY2 is unique among the auxin response regulators in the sense that it's expression is dependent on light and follows a circadian pattern during the day. Three families of photoreceptors have been identified for light perception in higher plant tissues, the red/far-red (R/FR) light-absorbing phytochromes (PHY), the recently discovered UV-B receptor UVR8 (Rizzini et al., 2011) and the UV-A/blue light (B)-absorbing cryptochromes and phototropins. PHY regulate two adaptive features of light-grown plants. These are proximity perception, leading to shade avoidance responses, and photoperiodic perception, leading to floral induction in some species. Phytochromes exist as two photo-interconvertible forms, Pr (red light-absorbing phytochrome) and Pfr (far-red light-absorbing phytochrome), depending on the light conditions. On irradiation of the appropriate wavelength, the biologically active form of phytochrome interacts with the phytochrome kinase substrate (PKS1/PKS2) and translocates into the nucleus from the cytosol ultimately leading to the modulation of the transcriptome and changes in growth and

development in which phytochrome interacting factors (PIFs) play an important role (Fig. 1).

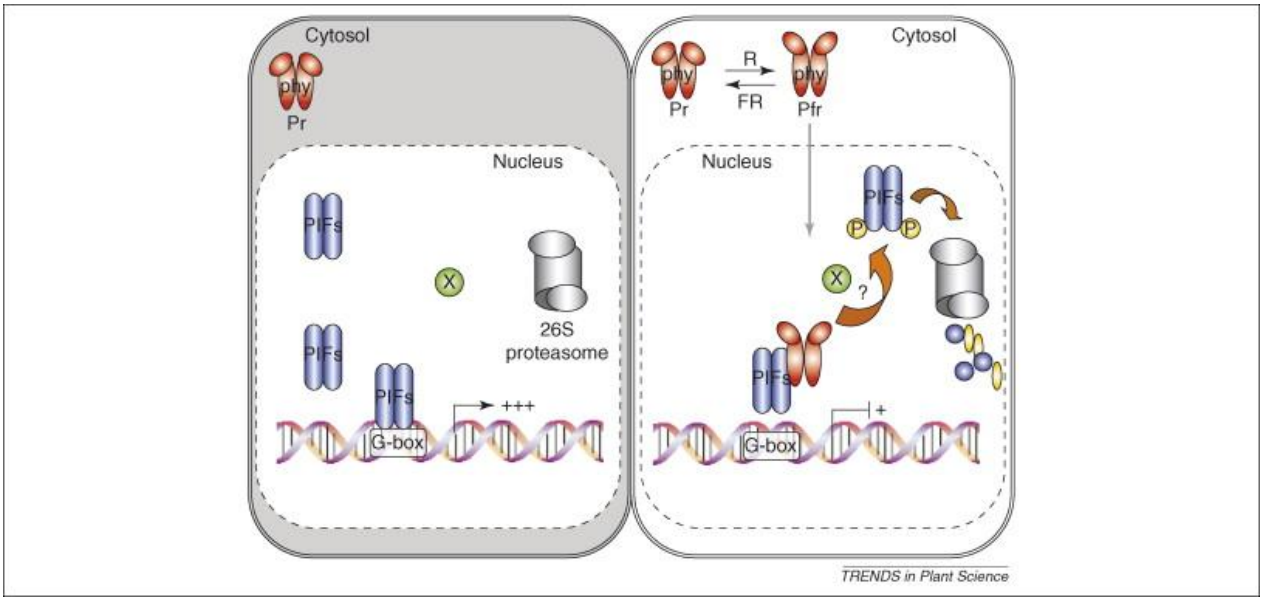

Fig 1. Model of PIF function in phytochrome signaling pathways. **(a)** In the dark, PIFs are constitutively localized to the nucleus, whereas phytochromes are localized to the cytosol. PIFs negatively regulate photomorphogenesis by activating gene expression. **(b)** Light signals induce photoconversion of phytochromes to the active Pfr forms before nuclear migration. In the nucleus, phytochromes physically interact with PIFs, which results in phosphorylation of PIF3 and possibly other PIFs either directly or indirectly. The phosphorylated forms of PIFs are recognized by an ubiquitin ligase and are subsequently degraded by the 26S proteasome. The light-induced proteolytic removal of PIFs results in relieving the negative regulation of photomorphogenesis. X, indicates an unknown factor that might be involved in the light-induced phosphorylation of PIFs. (Castillon *et al*., 2007).

Research has identified a complex and interconnecting signaling network downstream of these photoreceptors, together with a considerable number of signaling intermediates. These integrators, namely PHYTOCHROME-INTERACTING FACTOR 3 (PIF3), PIF4, PIF3-LIKE 5 (PIL5)/PIF1 and LONG HYPOCOTYL 5 (HY5), are key light signaling components and they link light signals to developmental programs such as the circadian clock, flowering time, phytohormone regulation and photomorphogenesis. According to recent reports, expression of light-dependent genes can also be regulated by protein complexes modulating chromatin activity through posttranslational modificiations including histone acetylation and represents another level of transcription regulation (Servet *et al*., 2010). We therefore looked into plant specific growth and developmental responses related to light in the elongata mutants.

II. Results

A. Altered photomorphogenesis in Elongator mutants

The typical leaf phenotype of the Elongator mutants (very narrow leaf lamina, increased petiole length and no clear transition between lamina and petiole) shows a high resemblance to the triple *phyBDE* and quadruple *phyABDE* phytochrome mutants (Fig 2). Especially the loss of phyA in the triple phyBDE mutant causes a severe decrease in lamina width and an increase in the elongation of the petioles (Franklin *et al*., 2003). Interestingly, the SHY2/IAA3 gene, which is a target gene of Elongator (Chapter 4), is a light-inducible gene . All together the data suggest that Elongator might play a role in "translating" the light signals perceived by the phytochromes.

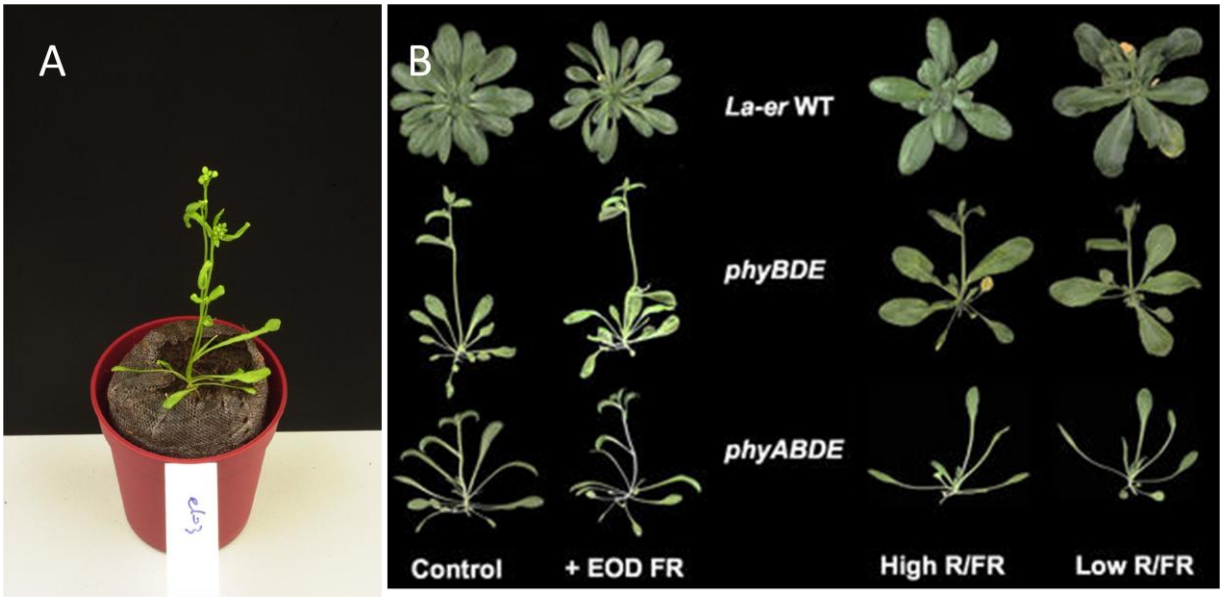

Fig. 2. Similarity between the *elo3-1* mutant and the triple *phyBDE* and quadruple *phyABDE* mutant. A. Narrow leaf phenotype of the *elo3-1* mutant (Ler background) grown in long day conditions (16hrs light/8hrs dark). B. Ler, *phyBDE*, and *phyABDE* mutants (Ler background) were grown for 36 d at 16°C under 8-h light and 16-h dark cycles (control), the same conditions with 15-min end of day (EOD) FR treatments (+EOD FR), and under continuous irradiation of high and low R:FR (Franklin *et al*., 2003).

To examine whether Elongator coding genes are involved in photomorphogenesis, a hypocotyl assay was done. Seeds of the wild type and the *elo3-6* mutant were germinated under different light conditions including complete darkness, white light, blue, far-red and red light. At day 7 after germination, hypocotyl lengths (a characteristic photomorphogenic trait) were measured and statistically analyzed to determine significant differences. In the dark and in blue light, hypocotyl lengths of the wild type and the *elo3-6* mutant were similar. In white light and red light conditions,

measuring predominantly phyB activity, hypocotyls of the *elo3-6* seedlings were significantly shorter than wild-type hypocotyls, showing an enhanced photomorphogenic phenotype (Fig 3). However in the far-red light condition, measuring predominantly phyA activity, elo3-6 seedlings showed a light-hyposensitive phenotype with significantly longer hypocotyls compared with those of the wild type. To confirm these observations, we analyzed other alleles of the Elongator mutants in their respective background (*elo3-1* (Ler) , *elo1-1* (Ler) and *elo3-2* (Ws)) and similar results were obtained for all mutants (Fig. 4). Hence, in Elongator mutants, phyA and phyB activity or signaling are affected.

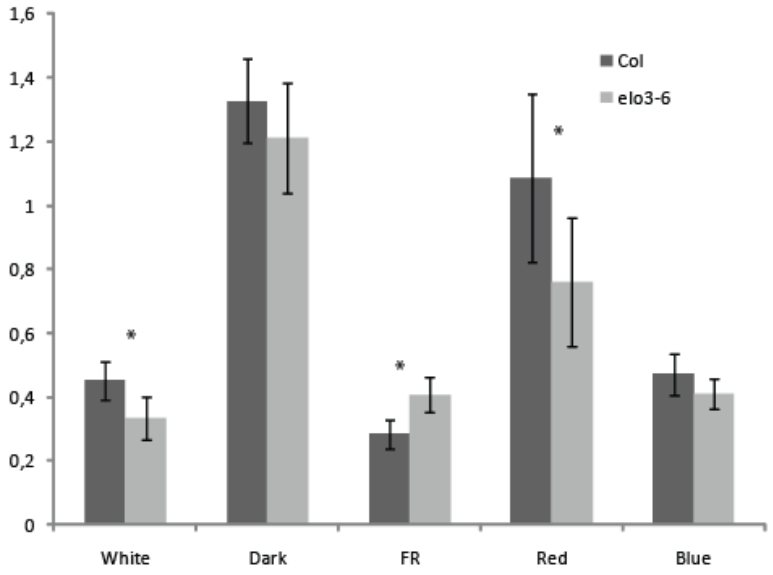

Fig. 3. Seven-day-old seedling hypocotyl lengths of wild type Col and *elo3-6* grown in darkness or under white light, red, far-red and blue light. The asterisks indicate a statistically significant difference between mutant and wild type (t-test, $P<0.05$). Error bars represent standard deviation of at least 20 seedlings.

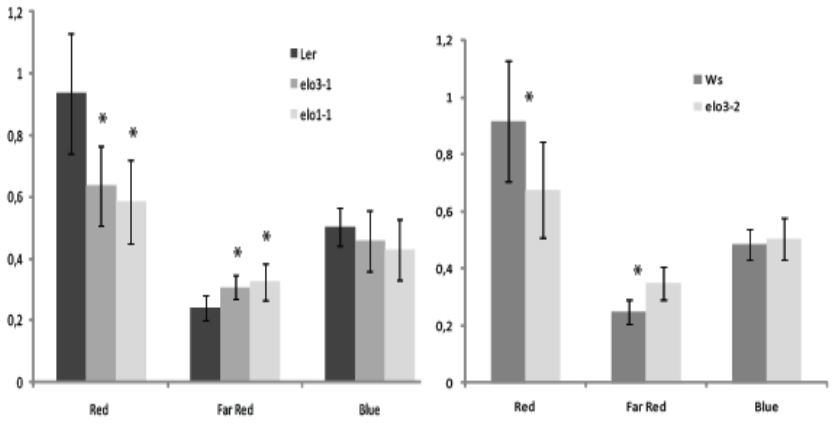

Fig. 4. Seven-day-old seedling hypocotyl lengths of wild type Ler and Ws and Elongator mutants *elo3-1*, *elo1-1* and *elo3-2* grown under red, far-red and blue light. The asterisks indicate a statistically significant difference between mutant and wild type (t-test, $P<0.05$)

B. Light and clock-related genes differentially expressed between *elo* mutants and wild type

Since mutation in Elongator subunits causes photomorphogenic defects we looked into the previously obtained micro-array dataset between *elo3* seedlings and wild type for differentially expressed genes with a role in light signaling (Nelissen *et al*., 2005 - accession no. E-MEXP-300, Table 1). Interestingly, both PIF3 and PIF4 are downregulated in the *elo* mutant and could explain why both phyA and phyB signaling is affected in the *elo* mutants since the phytochromes have these signaling components in common and thus might be direct targets of Elongator HAT activity.

Table 1. Light- and clock-related genes downregulated in *elo3* mutants.

Response to light stimulus	Fold change	Gene name
AT5G67385	2,33	phototropic-response protein
AT1G14280	2,00	PKS1
AT3G19850	4,03	NPH3 protein
AT5G20230	2,38	Blue-copper-binding protein
AT1G02340	3,03	HFR1
AT3G18780	2,14	ACT2
AT2G43010	2,04	PIF4
AT3G15850	2,53	FAD5
AT1G09530	2,14	PIF3
AT5G08790	2,01	NAM
AT4G32770	2,19	VTE1
AT5G02120	2,68	thylakoid protein
AT5G59920	2,06	UV-B insensitive
AT4G15480	3,14	unknown
AT1G42970	2,06	GAPB
AT2G30520	3,32	RPT2
AT4G03400	2,27	GH3-related
AT1G07600	2,23	Metallothionein1
AT4G31500	2,04	ATR4
AT5G04140	2,38	unknown
AT1G34000	2,64	OPH2
AT3G59220	3,76	unknown
AT2G47450	2,83	Chloroplast signal recogn.
AT2G46340	2,33	SPA
AT1G01060	2,50	LHY
AT2G46830	2,42	CCA1
AT5G02810	1,40	PPR7
AT2G46790	2,20	PPR9

Several clock-related genes such as LHY, CCA1, HFR1, PPR7 and PPR9 were significantly down regulated in the *elo* mutants (Table 1). Other genes in the same pathway were upregulated (Jumonji 2-fold and APRR3 2.5-fold) in the *elo* mutants and are probably the consequence of secondary effects. The micro-array data on these genes were confirmed by real-time PCR as shown in Fig 5.

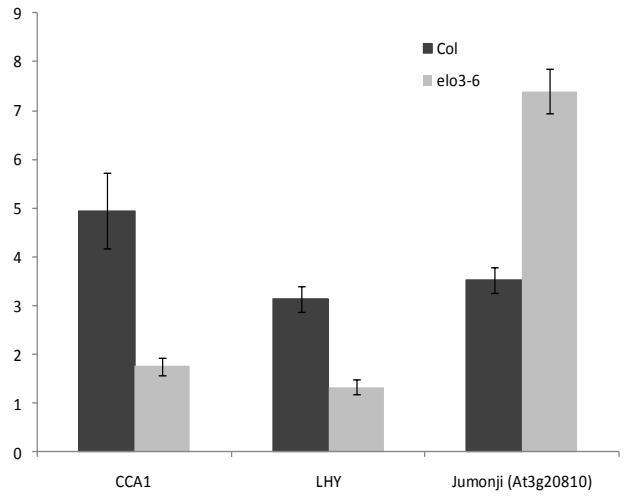

Fig. 5. Q-PCR on circadian clock genes. Error flags represent standard deviation of 3 repeats.

C. Circadian gene expression profile

To investigate whether this misregulation of circadian clock related genes was due to a phase shift in the clock or a mere consequence of underexpression in the *elo* mutants, a QPCR analysis was done on the *elo3-6* mutant and the wild type Columbia in a 48 hours time course experiment on plants grown for 12 days in short day conditions and after transfer to continuous light with sampling at 4 hrs time intervals (Fig. 6).

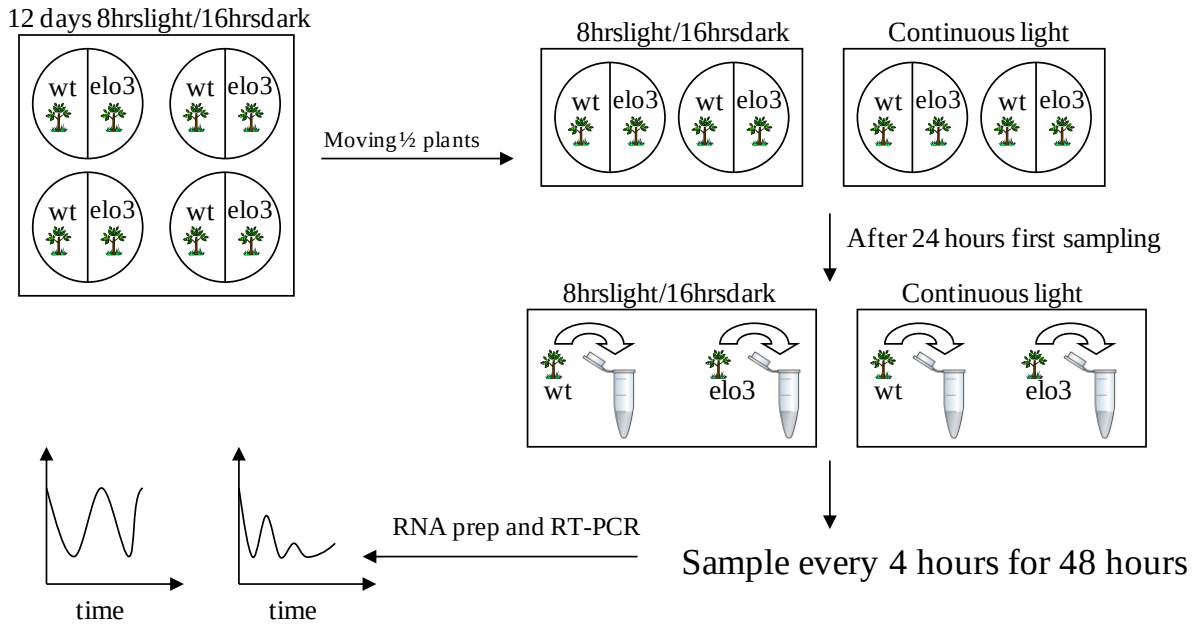

Fig. 6. Time-course experiment on the *elo3-6* mutant and Columbia wild type. Plants were grown for 12 days in short day conditions (8hrs light/16hrs dark) and afterwards half of them were moved

to continuous light and the other half stayed at the short day condition. After 24 hours samples were taken every 4 hours for a period of 48 hours. RNA was isolated and used for Q-PCR measurements.

The expression profiles of the circadian clock genes CCA1 and LHY showed the typical diurnal fluctuation in transcripts for the wild type and the *elo3-6* mutant but the amplitudes were severely reduced in the *elo3-6* mutant (Fig. 7.A and B) confirming the micro-array results (Table 1). The expression of the these central circadian clock genes was most severely reduced in the *elo3-6* mutant at early morning when their expression is normally maximal (CCA1 and LHY are so called early-morning genes). During the day , expression levels of CCA1 and LHY drop for both the elo3-6 mutant and wild type to similar levels. Seedling were also transferred to continuous light after growing for 10 days in short day conditions to analyze whether the 10 days entrainment period would be enough to sustain a "free-running" period in the *elo3-6* mutant. The expression profiles in the *elo3-6* mutants of CCA1 and LHY still shows the diurnal fluctuation in transcripts but has a general lower expression compared to the wild type (Fig 7.C and D.).

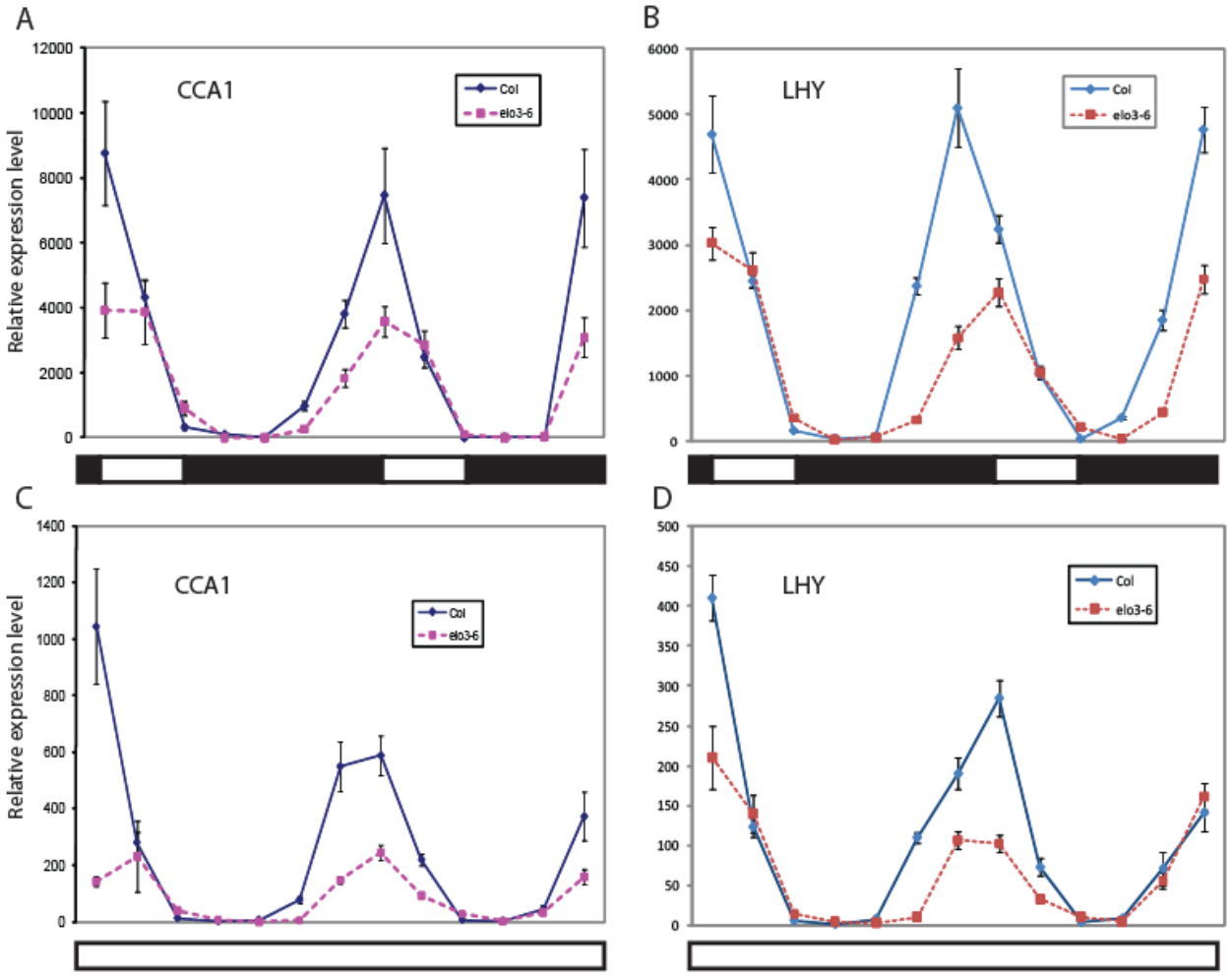

Fig. 7. Q-PCR data for CCA1 and LHY showing a circadian clock pattern in the Col wild type and the elo3-6 mutant. Seedlings used for harvesting were treated in time course of short day (A and B) to continuous light (C and D) conditions. Averages of three technical repeats are presented. White and black boxes at the bottom of the graph represent alternation of light and dark respectively.

To test whether the *LHY* gene is a direct target of Elongator activity, chromatin immunoprecipitation (ChIP) analysis was performed. For the *LHY* gene the levels of histone H3K14 acetylation were reduced in the *elo3-6* mutant for primercombinations B, C and D (Figure 8). Primercombination A in the upstream region of the LHY gene showed no reduction in histone H3K14 acetylation. The data indicate that LHY is a direct target of Elongator HAT activity at its coding region as is the case for SHY2/IAA3 (Chapter 4; Nelissen *et al*., 2010).

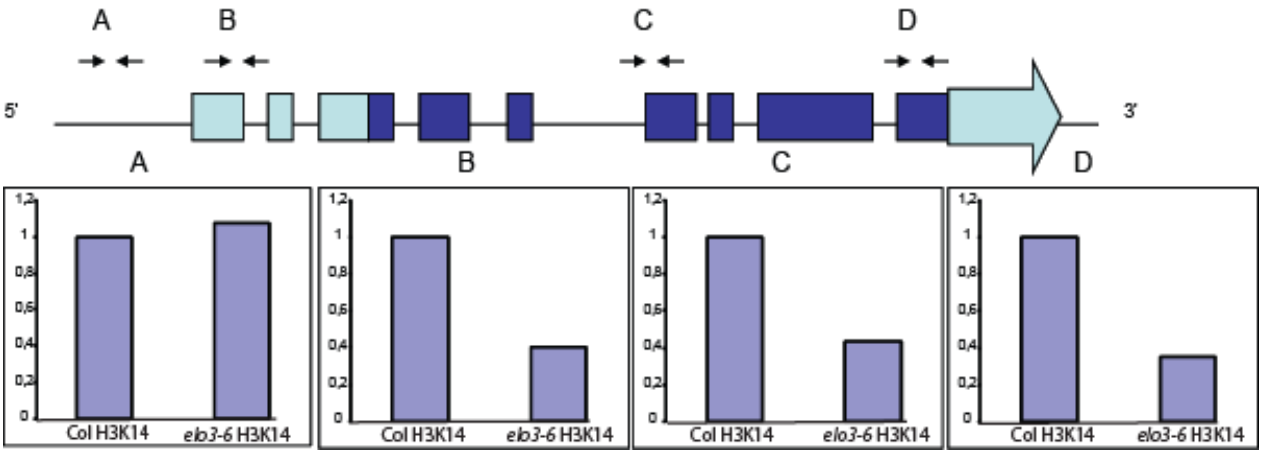

Fig. 8. ChIP PCR data on LHY. Primercombinations and gene structure of *LHY* is presented with dark blue boxes and light blue boxes for exons and UTR's respectively. The level of histone H3K14 acetylation in the *elo3-6* mutant is shown for each primercombination in comparison with WT levels (arbitrary chosen at 1). No error flags as experiment was only performed once.

D. Yeast, Drosophila and Human ELP3 in plants

Although the Elongator complex is conserved between yeast, plants and humans several roles have been conferred to the Elongator complex between the different kingdoms including histone acetylation, tubulin acetylation, exocytosis and tRNA modification (see Chapter 2 and 5). Moreover, the data presented here indicate that Elongator might fulfill kingdom-specific roles as the auxin and light signaling pathways are unique in plants. We investigated whether Elongator components from other species could complement the *elongata* phenotypes in Arabidopsis. We chose the ELO3 subunit for our complementation study as this subunit contains the catalytic activity of the Elongator complex within its histone acetyltransferase (HAT) domain and disruption of this subunit causes severe phenotypes in Arabidopsis. In addition to a HAT domain at the C terminus, these proteins have an N-terminal domain similar to the catalytic domain of S-adenosylmethionine (SAM) radical enzymes (Fig. 9). The function of this SAM domain is unclear but a role in histone demethylation has been suggested (Chinenov *et al*., 2002). We cloned the ELO3 coding sequence of Human, Drosophila and Saccharomyces in the pK7WGF2 Gateway vector (Karimi *et al*., 2002) containing the 35S promoter and GFP open reading frame. The protein sequence of the ELO3 subunit is highly conserved between these species as shown in Figure 10.

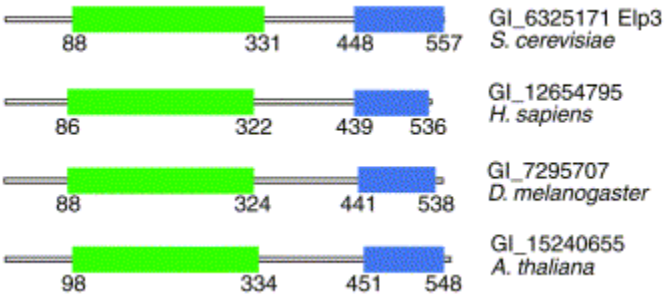

Fig. 9. Domain structure of ELP3-related proteins from Arabidopis, human, Drosophila and yeast. The SAM domain is shown in green and the HAT domain in blue. Numbers indicate amino acid portions in each protein.

The identity between the Arabidopsis ELP3 and human, Drosophila and yeast ELP3 is 75%, 73% and 70% respectively (NCBI Blast). The highest identities are found in the two catalytic domains of ELP3 suggesting that both enzymatic activities are functionally or mechanistically coupled and directed towards highly conserved substrates while the N terminus of the ELP3 subunit is highly divergent between the different species (Fig. 10).

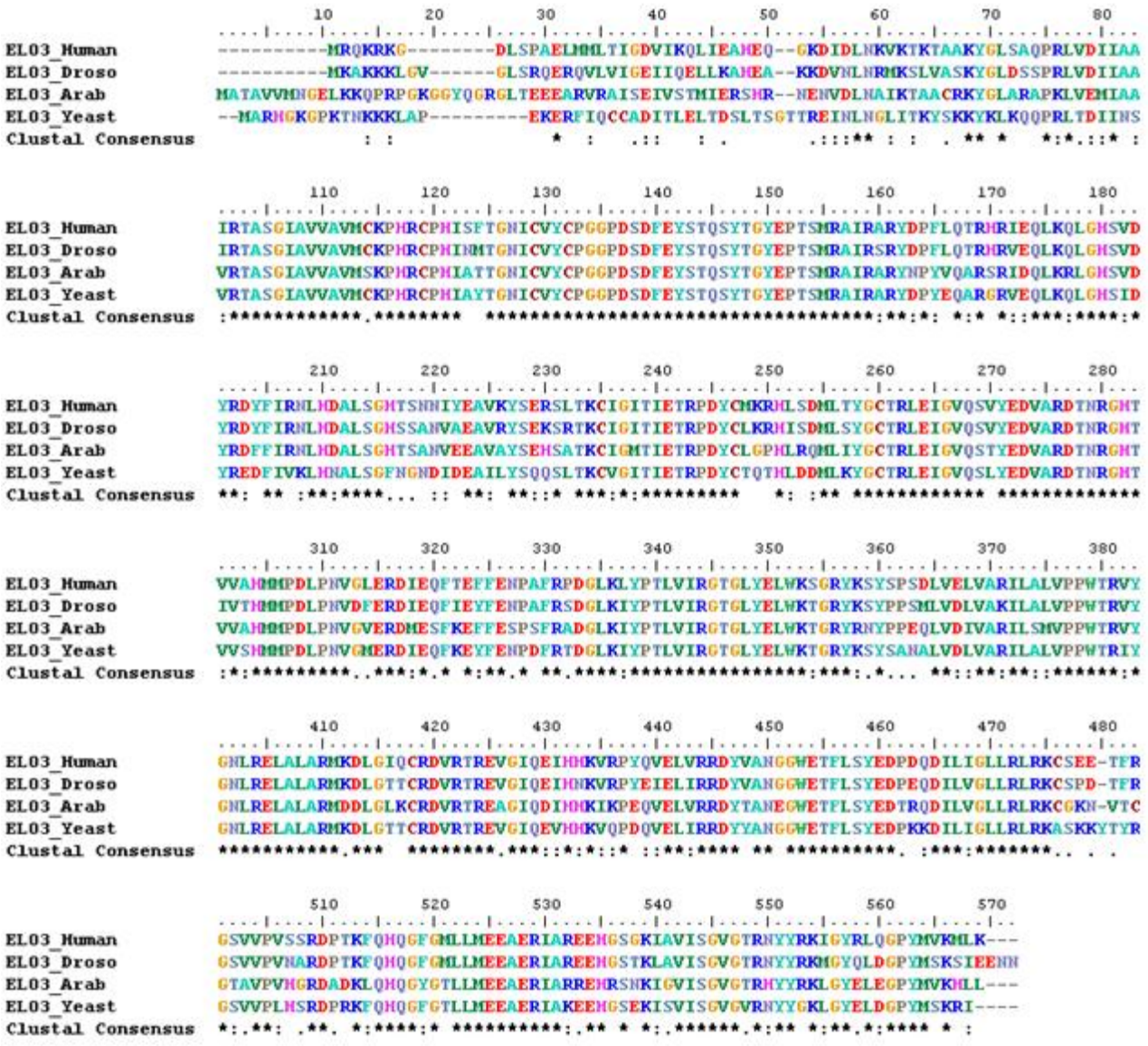

Fig. 10. Amino acid sequence alignment of ELP3 in Human, Drosophila, Arabidopsis and Yeast.

The p35S:ELO3:GFP constructs of the three species were introduced in the *elo3-6* (Col) and the *elo3-1*(Ler) Arabidopsis mutant. Subcellular localization studies were performed on the primary root of 5-day old transformants and showed nuclear localization for both the yeast and human ELP3 protein in Arabidopsis (Fig. 11). The GFP signal however was very weak compared to earlier studies (Chapter 4) with the endogenous Arabidopsis ELP3. The Drosophila ELP3 protein showed strong cytoplasmic localization with complete absence in the nucleus. In an earlier study we showed that the Arabidopsis ELP3 protein colocalizes with active euchromatin in the nucleus

(Chapter 4) and even though the ELP3 protein is highly conserved among the different species this data indicate that small amino acid changes have big effect on the localization of proteins.

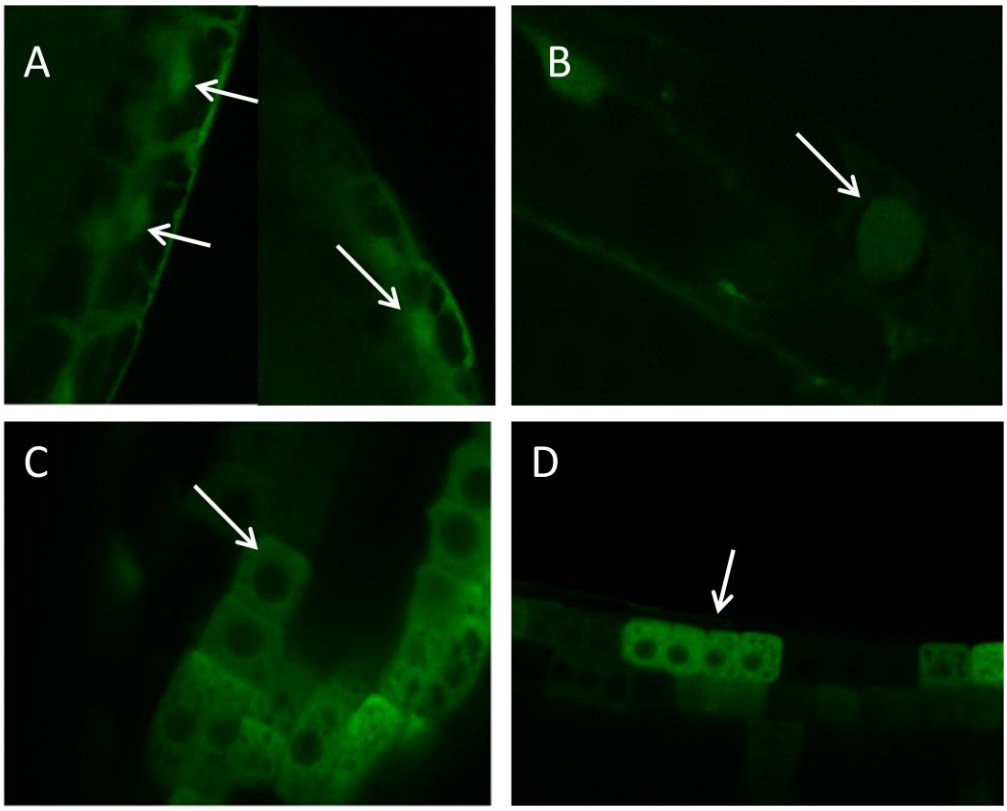

Figure 11. Subcellular localization of ELP3 subunits of Human (A), Yeast (B) and Drosophila (C and D) in primary root tissue of 5-day-old Arabidopsis transformants. Arrowheads indicate the nuclear (A and B) or cytoplasmic (C and D) GFP signal.

To verify whether the functionality of the Elongator complex could be restored by introducing the Human, Yeast or Drosophila ELP3 in the Arabidopsis *elo3-6* and *elo3-1* mutants , the mutants were transformed with the different p35S-ELP3-GFP constructs and phenotypically analyzed. None of the transformed seedlings showed reversion to the wild type phenotype.

III. Materials and Methods

Plant lines The mutants *elo1-1* and *elo3-1* were in L*er,* the *elo3-2* mutant in Ws (Nelissen *et al*., 2005), the *elo3-6* mutant in Col-0 (GABI-KAT collection code GABI555_H06). The growth chamber conditions were 16 h/8 h (day/night) with white light (neon tubes, cool white), 100 $\mu mol \cdot m^{-2} \cdot s^{-1}$ light intensity, and 20°C unless stated otherwise.

Hypocotyl assay Seeds were sown on 0.5x Murashige and Skoog (MS) medium, incubated at 4ºC for 48h, and then transferred to white light for 6 hours at 20ºC. Afterwards they were transferred to growth chambers for germination under white light (16h/d), continuous red ($10\mu mol.m^{-2}.s^{-1}$), far-red and blue light. Hypocotyl lengths were measured 7d after germination using ImageJ software. Student's t tests were performed to determine whether the difference between two sample means was significant at $\alpha = 0.05$.

Time course experiment Seeds were grown on medium containing 0.5x MS, 10g/l sucrose, 0.5g/l MES, pH5.7, plant agar 8g/l. Seeds were sown 2x20 seeds: mutant and wild type together in a round dish and placed in darkness at 4º for 24h. The seedlings were grown in SD (8hlight/16hdark) 12 days after germination while half of the seedlings were moved after 10 days to continuous light. Tissue was harvested every 4h for the next 48h: total of 13 time points. RNA was extracted using RNeasy (Qiagen, Germany) including DNase treatment (RQ1 RNase free DNase, Promega). First strand cDNA synthesis was performed (Superscript III , Invitrogen) and the Lightcycler 480 SYBR Green I (Roche) was used for Q-PCR with following primers: CCA1 fwd TCTCTATCACATCCTCCTTCAG rev TGAGCCACCACTAGAATCG ; LHY fwd CTCAGGTATGGTATCTCAAG rev AACGAACGGTAATCATCC ; TUB2 (housekeeping) fwd ACTCGTTGGGAGGAGGAACT rev ACACCAGACATAGTAGCAGAAATCAAG

Chromatin immunoprecipitation (ChIP) ChIP was done as described previously with minor modifications (Bowler *et al*., 2004). Seeds of Col-0 and the *elo3-6* mutant were sown on Murashige and Skoog medium and grown in vitro under short-day conditions. Seedlings were harvested after 3 weeks and fixed in 1% formaldehyde for 10 min in a vacuum and neutralized by 0.125 M glycine for 5 min. Samples were ground in liquid nitrogen and nuclei were isolated and lysed in the presence of protease inhibitors. The isolated chromatin was sonicated 5 times for 30 s in a Branson sonifier water bath. The antibodies for immunoprecipitation were purchased from Upstate Biotechnology: anti-histone H3K14Ac (07-353) and anti-histone H3 (05-499). Immunoprecipitated DNA was purified with the Roche PCR Purification Kit and dissolved in 50 µl supplemented with RNase A and analyzed by real-time PCR (Biorad iCycler) with primers in the promoter and coding regions of the *LHY* gene. A: fwd GCGTAAAAGTGAGGCCCATA rev TGGTGGTCCACAATTGCTTA B: fwd TTTGATTATTTCCGGGAACG rev

TCTCAGCAGCCAAACAGAGA C: fwd CCGAAAAATTCGGGTCAGTA rev GGCGGAATTTCTATGTCCAA D: fwd GCCATTGGCTCCTAATTTCA rev TCGAAGCCTTTTGCAGACTT

GFP localization and complementation of *elo3* mutants The Human ELP3 cDNA , Yeast ELP3 cDNA and Drosophila ELP3 cDNA was cloned inside the Gateway compatible vector pK7WGF2 (Karimi *et al*., 2002) and transformed to Arabidopsis wild type Columbia, *elo3-6* and *elo3-1* mutants.

Transformed plants were grown vertically *in vitro* for 5 days and primary roots analyzed with a confocal microscope 100M with software package LSM 510 version 3.2 (Zeiss). GFP fluorescence was imaged at 488 nm excitation. Emission fluorescence was captured in the frame-scanning mode, alternating GFP fluorescence via a 500- to 550-nm bandpass emission filter.

Chapter 6

RON3 is a novel component of auxin signaling

De Groeve S., Neyt, P., Sterck, L., Aesaert, S., Bruno, L., Van De Slijke, E., Van Minnebruggen, A., Ponce, M.R., Micol, J.L., Friml, J., De Jaeger, G. and Van Lijsebettens, M.

Steven De Groeve wrote this chapter and performed the cloning of the constructs (except TAP construct), subcellular localization, all auxin-related experiments, GUS staining, immuno-localization, Q-PCRs and morphological assays

The shaping of organs in plants is dependent of the intercellular flow of the phytohormone auxin, whose directional signaling depends on polar subcellular localization of PIN auxin transport proteins. The targeting of PINs depends on the activity of the PINOID kinase and PP2A phosphatase acting antagonistically to mediate apical-basal polar targeting. Here we report the identification of the *ROTUNDA3* (*RON3*) gene as a regulator of PP2A activity in plants. Map-based cloning of the *RON3* locus led to the identification of a plant specific protein (RON3) with no known functional domains. Morphological analysis of the *ron3* mutants showed phenotypes related to an aberrant auxin distribution and transcriptome profiling showed a significant downregulation of auxin-inducible genes. *RON3* is expressed at sites of meristematic activity and DR5::GUS staining in the *ron3* mutants showed high auxin accumulation at primary and lateral root primordia. Tandem affinity purification with RON3 as bait revealed different subunits of the PP2A complex interacting with RON3 and immunolocalization of PIN1 proteins showed a basal to lateral shift. These findings suggest that RON3 acts as a regulator of auxin distribution by modulating the activity of the PP2A complex.

I. Introduction

Despite the work of large initiatives aiming at the functional characterization of all Arabidopsis genes experimental data about the function is available for only a third of them (Ledford, 2010). Genes with unknown function have no detectable functional domains or homology to other genes over the kingdoms and functional analysis of such genes through mutational and transgene analysis is expected to reveal novel components of developmental, physiological or biochemical pathways. A number of computational initiatives such as CORNET and Aranet (De Bodt *et al*., 2010; Lee *et al*., 2010) combine available data sets on transcriptome, interactome and metabolome into networks that are searchable with a gene code and might reveal relationships with the gene of interest and help to assign function.

Plant growth is determined by cell number in the meristems and at organ initiation and by cell expansion in which the cell volume can increase significantly. Plant growth is affected by internal and external (environmental) factors. The external factors are a combination of nutrient supply, light-availability and temperature and put constraints on the extent to which the internal controls can permit the plant to grow and develop. The internal controls are all the products of the genetic instructions encoded in the plant genome. These influence the extent and timing of growth and are mediated by signals of various types transmitted within the cell, between cells, or all around the plant. Intercellular communication in plants may take place via hormones. There are several hormones each of which are produced at different location, that have a different target tissue and act in a different manner. The phytohormone auxin is a major regulator of cell division and expansion during plant growth and development. The detailed molecular mechanisms by which auxin controls these essential cellular responses are still poorly understood, despite recent progress in the identification of auxin receptors and components of auxin signaling pathways (Perrot-Rechenmann C, 2010). Auxin gradients in the cells are generated and maintained by auxin efflux carriers PIN proteins which contain transmembrane domains and continuously cycle between the plasma membrane and endosomes allowing rapid and dynamic changes in PIN localization. The sorting of PIN proteins into the apical or basal trafficking pathway depends on the phosphorylation status of PIN, which is controlled by the PINOID (PID) protein kinase and the PP2A phosphatase. The PP2A phosphatase is a heterotrimeric protein consisting of a C catalytic subunit together with A and B regulatory subunits. In Arabidopsis 5 loci encode C subunits, 17 loci were found to encode B subunits and 3 loci code for A subunits. RCN1 (ROOTS

CURL IN NAPHTHYLPHTHALAMIC ACID), one of the A subunit isoforms, acts as a key positive regulator of PP2A activity in seedlings and the *rcn1* mutant that lost PP2A activity displays abnormalities related to defective auxin transport such as altered gravity response and lateral root growth (Deruère *et al*., 1999; Rashotte *et al*., 2001; Kwak *et al*., 2002). In the nucleus, auxin binds the AUX/IAA repressors which activates ARF mediated transcription of auxine responsive genes, subsequently, the CUL1-TIR complex mediates the AUX/IAA repressor degradation by the proteasome (Weijers and Friml, 2009).

We study the genetic control of growth and focus on the Arabidopsis leaf as an experimental system. An EMS-induced collection of leaf mutants consisting of 94 loci (Berna *et al*., 1999) and in particular three phenotypic classes, i.e. elongata, angusta and rotunda with narrow and large leaves respectively, serves as the basis for gene identification. Mutants with narrow leaves identified the histone acetylation complex, Elongator, with auxin-biology related target genes (Nelissen *et al*., 2010), the histone monoubiquitination E3 ligase HUB1/ ANG4 that regulates G2 to M transition of the cell cycle (Fleury *et al*., 2007), and the ribosomal protein RPL5B/ ANG3 (Van Minnebruggen *et al*., 2010). It showed the importance of transcriptional activation and translation in the promotion of cell proliferation during lateral growth of the leaf lamina. The rotunda mutants with large leaf laminas identified the transcriptional repressor LEUNIG/ RON2 (Cnops *et al*., 2004) and the FIERY/ RON1/SAL1 (Robles *et al*., 2010) with a role in the restriction of cell expansion during lateral growth of the leaf lamina. Here we report on the map-based cloning of a plant-specific single copy gene, RON3, with no known functional domains. Morphological and molecular phenotyping of the *ron3* mutant together with RON3 protein localization and interactome data point to a nuclear role in auxin signaling and/or compartimentalization most likely by modulating the activity of the PP2A complex.

II. Results

A. RON3 is a unique plant-specific gene of unknown function

The ron3-1 mutant belongs to the rotunda class of leaf mutants and was obtained after ethyl methanesulfonate mutagenesis of the Ler ecotype. For the positional cloning of RON3, an F2 mapping population was derived from a ron3-1 (in a Ler background) x Col-0 cross. Fifty of these F_2 plants were used to low-resolution map the *ron3-1* mutation as described in Ponce *et al*. (2006), which allowed us to delimit a candidate interval flanked by the AtF7K2.1 (BAC F7K2) and AtM7J2.1 (BAC M7J2) markers, on chromosome 4 (Fig. S1). Further iterative assessment of linkage to molecular markers in 290 additional F_2 plants narrowed down the candidate interval to a genomic region of 68.7 kb, which encompassed 18 annotated genes.

To identify the RON3 gene in the candidate genetic interval containing the 18 genes, we assumed that EMS induced mutation in a gene would cause the loss of gene function and/or cause downregulation of this gene. The top 20 downregulated genes in the ron3 transcriptome were compared to the 18 genes in the genetic interval and showed that a severely downregulated gene, At4g24500, was also present in the candidate genetic interval. Subsequent sequencing of this gene in the ron3-1 mutant revealed a point mutation in the second exon whereby a cytosine nucleotide is replaced by a thymine nucleotide. At the amino acid level this mutation leads to the change of a glutamine coding codon to a stop codon (Fig. 1). The Gabi-Kat Line, GK374F12A, with a T-DNA insertion in the second exon of the At4g24500 gene showed similar phenotypes as the ron3-1 mutant. Twenty F1 plants derived from reciprocal crosses between homozygous GK374F12 (Col) and ron3-1 (Ler) mutants were verified with microsatellite markers as hybrids and displayed mutant phenotypes such as short petioles and reduced lateral root number which were similar to those in both parentals (Fig. 1). It showed that the mutations in both mutant lines were allelic and confirmed that the RON3 gene corresponded to At4g24500 (Fig 1). The GK374F12A was named ron3-2.

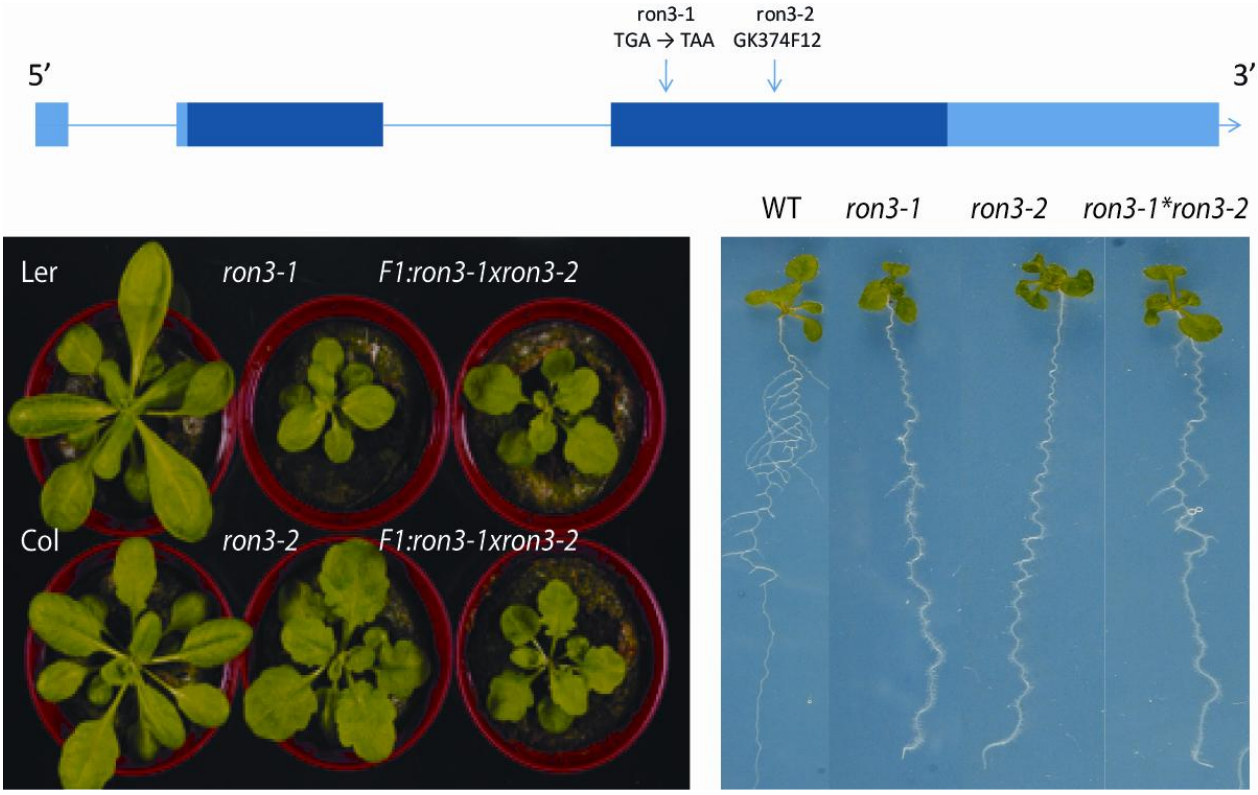

Fig 1. Top: schematic representation of the At4g24500 gene with light blue boxes and dark blue boxes indicating UTR's and exons respectively. Bottom: phenotypical respresentation of the ron3-1 and ron3-2 allele with the double mutant showing similar phenotype as the parentals.

The At4g24500 gene contains two exons, one intron and codes for a 319AA (35kDa) protein which is classified in TAIR (www.arabidopsis.org) as an hydroxy-proline rich glycoprotein (HRGP) with unknown function. HRGP's are a superfamily of plant cell wall proteins that function in diverse aspects of plant growth and development. The amino acid sequence of RON3 does indeed contain a high number of prolines (32/319) though they seem to be distributed in a manner non-specific to other HRGP's and a genome-wide search to classify all HRGP's did not identify RON3 as a HRGP (Showalter *et al*., 2010). Taking the amino acid sequence of At4g24500 as input we performed a BLASTp (Altschul *et al*, 1997) analysis against several protein databases, using an e value cut-off of e-5. Blasting against the Arabidopsis thaliana proteins did not return any hit indicating that it is a single copy gene in Arabidopsis thaliana. The blast search against the non-redundant protein databases yielded several hits from other higher plant species (Poplar(2), Ricinus(2), Zea(2), A.lyrata(1), Cucumis(1), Oryza(1), Sorghum(1), Vitis(1)), all of which lacked a functional description. Moreover not a single hit was returned from non plant species and not even from mosses or algae, suggesting that this gene is specific to

higher plants. Executing a more sensitive PSI-BLAST analysis (Altschul *et al*., 2009) did not result in more hits. These results are confirmed when quering At4g24500 in the PLAZA resource (Proost *et al*, 2009) which also showed that no protein domains or GO-labels are assigned to this protein. Secondary structure prediction of RON3 by I-TASSER (Roy *et al*.,2010) showed 3 helix regions with 2 of them at the amino- and carboxy-terminal end of the protein. I-TASSER predicts a structure for the RON3 protein similar to human HR23a (TM score = 0.94) which is a member of the RAD23 protein family involved in DNA repair and proteolysis (Zhang *et al*., 2005; Walters *et al*., 2003). With all the obtained blast hits and a representative set of true RAD23 proteins (Farmer *et al*., 2010) from A. thaliana we constructed a phylogentic tree. In the resulting tree RON3 was grouped together with it's Arabidopsis lyrata counterpart but clearly in a separate branch from the true RAD23 proteins (data not shown).

B. Expression and cellular localization of RON3

In order to investigate tissue or domain specific expression of the *RON3* gene mRNA *in situ* hybridization was performed on different organs of *Arabidopsis thaliana* young seedlings. As shown in Figure 2. *RON3* transcripts were localized in the whole meristematic dome of the shoot apical meristem, in the emerging leaf primordia as well as in the provascular strands of developing seedling. In the primary root tip, *RON3* expression was detected in the meristematic and elongation zone with a major accumulation of messengers in the epidermis and cortex compared to the stele. Gene expression was instead absent in the differentiated zone as well as in the root cap (Fig.2.B). In the lateral root primordium *RON3* mRNA was localized only in the differentiating procambial tissue (Fig.2.D). Interestingly, *RON3* hybridization signal was observed also in vesicles at the tip of the root hair (Fig..E,F). Signal was not observed in root tip processed with sense probe (Fig.2.C). Expression analysis of the RON3 gene using Genevestigator (Hruz *et al*., 2008) shows that the gene is expressed uniformly in all organs during all developmental stages (data not shown)**.** To confirm the in situ hybridization, the promoter of RON3 (1.5kb upstream region starting from the ATG start codon) was cloned into a vector containing the GUS marker gene and transformed into Arabidopsis plants. The GUS staining showed tissue specific activity of the RON3 promoter in the meristematic and elongation zone of the primary root tip, the shoot apical meristem, young leaves, vascular tissue of differentiated roots and accumulated at inititation sites of lateral roots confirming the in situ

hybridizations (Fig 2). No GUS activity was detected in the root cap, epidermis and cortex of differentiated zone of primary root and in expanded leaves.

To investigate the subcellular localization, the RON3 protein was fused to the Green Fluorescent Protein (GFP). The N- and C-terminal fusion did not abolish the function of the protein as the mutant phenotype was restored to the wild type upon transformation. Several independent T2 transgenic plants overexpressing the *GFP-RON3* fusion protein were analyzed by confocal microscopy of primary roots of 3 to 5 day old seedlings germinated on GM medium in vertical position. The GFP-RON3 fusion protein showed nuclear localization except for the nucleolus in all cells of the root apical meristem, meristematic, elongation and differentiation zone and colocalized with 4′,6-diamidino-2-phenylindole (DAPI) (Fig.S2). Interestingly, the brightly DAPI stained heterochromatic chromocenters do not overlap with the GFP signal (Fig 2). In mature cortical cells nuclear localization is also evident but membrane associations are also observed (Fig 2).

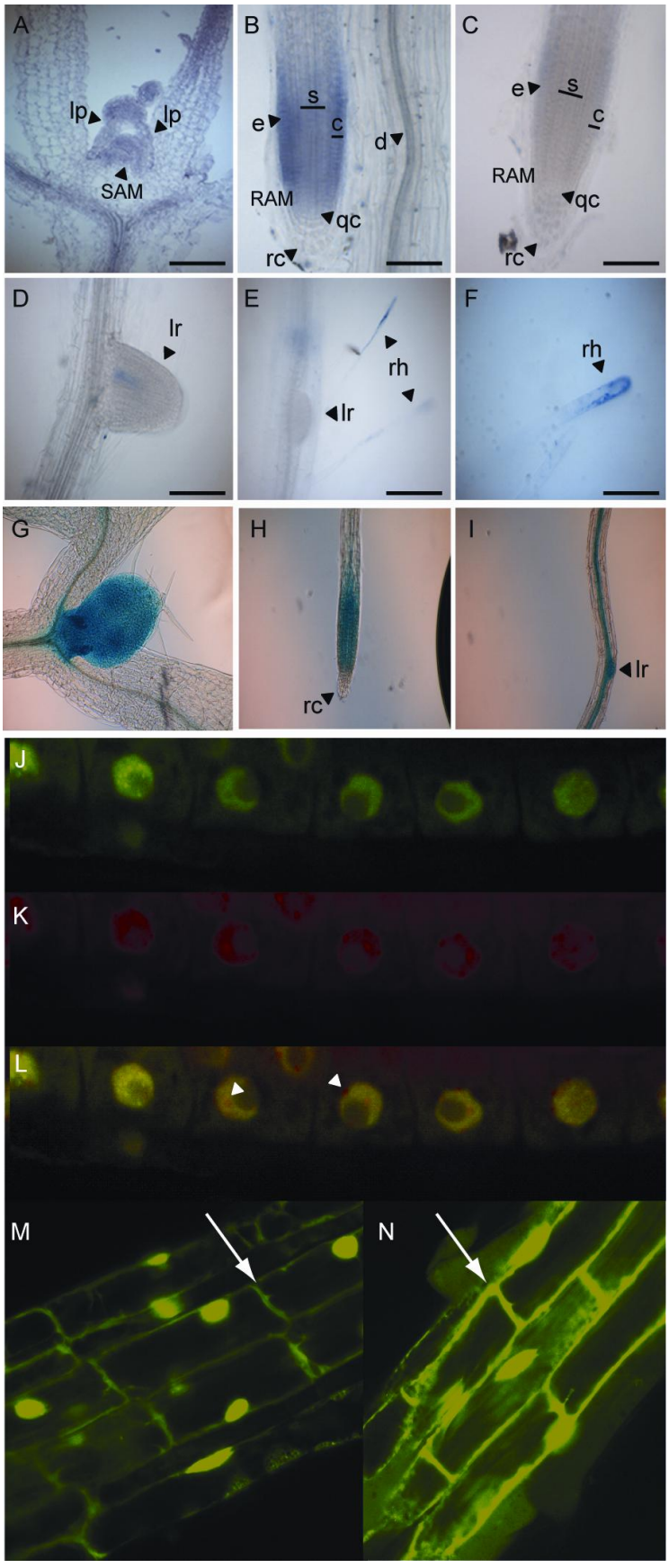

Fig 2. Expression, promoter activity and cellular localization of RON3. RON3 mRNA in situ hybridization on SAM (A), RAM (B), control (C), lateral root (D) and root hairs (E and F). GUS staining on seedlings transformed with the pRON3-GUS construct (G-I). Confocal microscopy on transgenic plants overexpressing the RON3-GFP construct (J), visualization of nuclei with DAPI (K) and colocalization of both signals (L). Arrowheads indicate heterochromatic regions. Membrane associations are found in mature cortical cells (M and N). Abbreviations: lp leaf primordium; SAM shoot apical meristem; e epidermis; c cortex; qc quiescent center; rc root cap; s stele; rh root hair; rc root cap; d differentiated tissue

C. Molecular phenotype of the *ron3-1* mutant

An Agilent microarray analysis was carried out on total RNA extracted from the green parts of stage 1.03 seedlings (Boyes *et al*., 2001) to compare the transcript profile between the ron3-1 mutant and Ler. After normalization of the hybridization signals, differentially expressed genes between Ler and ron3 were clustered according to their GO annotation using the BiNGO program (Maere *et al*., 2005). In total 1960 genes were upregulated in the ron3-1 mutant and 1122 genes were downregulated compared to the wild type. The upregulated genes clustered together in a variety of biological processes involved in stress and defense reactions. The downregulated genes however converged to only a couple of GO classes such as a very significant branch involded in reaction to auxin stimuli and a less significant branch involded in cytokinin mediated signal transduction and meiotic cell cycle (Figure 3). We were especially interested in the downregulated genes of the data set because ron3-1 is a recessive mutation and a loss-of-function mutation might cause downregulation of a number of molecular processes as primary effect. A high number of auxin response-related genes were downregulated in the mutant and are listed in Table 1.

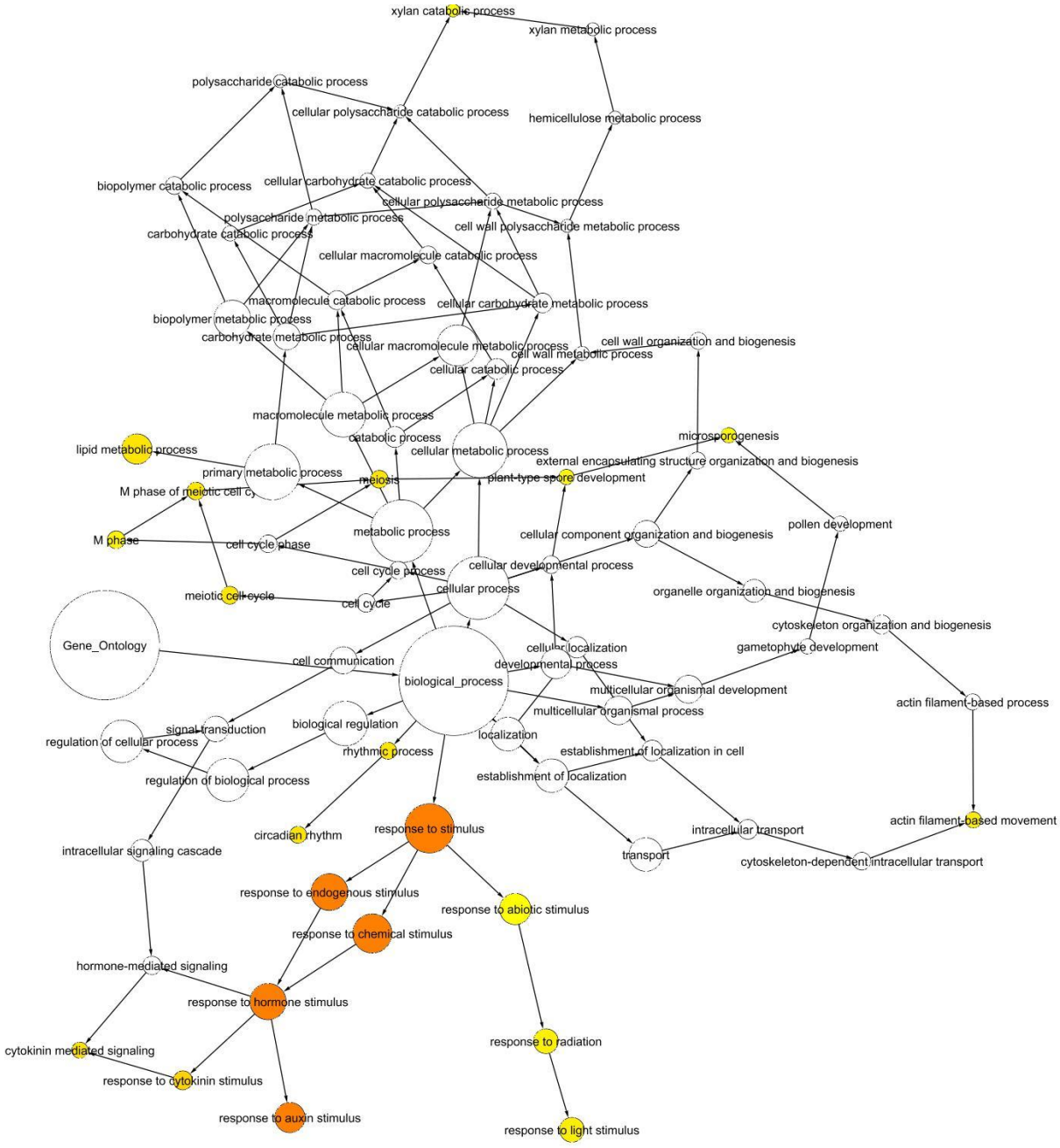

Figure 3. BiNGO analysis of the 1122 downregulated genes in the *ron3-1* mutant. The colour of the circles indicate the significance of overrepresentation in each GO-category (white = not significant , orange = highly significant). The size of the circles indicate the total number of genes in each GO-category.

Table 1. Auxin-related genes downregulated in the *ron3-1* mutant.

Gene	Description	fold change
At2g33830	dormancy/auxin associated family protein	0,0857
At1g29460	auxin-responsive protein, putative similar to auxin-induced protein 6B	0,1210
At4g32280	auxin-responsive AUX/IAA family protein	0,1392
At3g15450	expressed protein similar to auxin down-regulated protein ARG10	0,1566
At1g29450	auxin-responsive protein, putative similar to auxin-induced protein 6B	0,1679
At4g14560	auxin-responsive protein / indoleacetic acid-induced protein 1 (IAA1)	0,1978
At1g29500	auxin-responsive protein, putative similar to auxin-induced protein 6B	0,2050
At1g29420	auxin-responsive family protein, similar to auxin-induced protein TGSAUR12	0,2088
At4g27450	expressed protein similar to auxin down-regulated protein ARG10	0,2091
At5g18010	auxin-responsive protein, putative similar to auxin-inducible SAUR (Small Auxin Up RNAs)	0,2141
At1g52830	auxin-responsive protein / indoleacetic acid-induced protein 6 (IAA6)	0,2201
At1g29440	auxin-responsive family protein similar to auxin-induced protein 6B	0,2432
At3g03820	auxin-responsive protein, putative similar to auxin-inducible SAUR	0,2528
At5g18050	auxin-responsive protein, putative similar to auxin-inducible SAUR	0,2560
At3g03830	auxin-responsive protein, putative similar to auxin-inducible SAUR	0,2614
At2g22810	1-aminocyclopropane-1-carboxylate synthase 4 / ACC synthase 4 (ACS4)	0,2616
At5g18080	auxin-responsive protein, putative similar to SAUR	0,2637
At5g18060	auxin-responsive protein, putative similar to auxin-inducible SAUR	0,2721
At1g29430	auxin-responsive family protein similar to auxin-induced protein 10a 6B	0,2739
At1g29510	auxin-responsive protein, putative similar to auxin-induced protein 6B	0,2781
At5g18030	auxin-responsive protein, putative similar to auxin-inducible SAUR	0,2829
At4g38850	auxin-responsive protein/small auxin up RNA (SAUR-AC1); belongs to auxin-induced protein family	0,3056
At4g34790	auxin-responsive family protein similar to auxin-induced protein X10A	0,3118
At5g18020	auxin-responsive protein, putative similar to auxin-inducible SAUR	0,3575
At4g34770	auxin-responsive family protein similar to auxin-induced protein X10A; small auxin up-regulated RNA	0,3651
At2g06850	xyloglucan:xyloglucosyl transferase/xyloglucan endotransglycosylase/endo-xyloglucan transferase (EXT) (EXGT-A1)	0,3864
At3g15540	auxin-responsive protein / indoleacetic acid-induced protein 19 (IAA19)	0,3923
At2g01200	auxin-responsive AUX/IAA family protein	0,3930
At3g03850	auxin-responsive protein, putative similar to small auxin-up regulated protein SAUR	0,3954
At1g15050	auxin-responsive AUX/IAA family protein similar to auxin-responsive protein IAA12	0,4077
At5g63390	The function of this family of plant proteins is unknown	0,4082
At4g13260	flavin-containing monooxygenase / FMO (YUCCA2)	0,4095
NP454692	putative auxin-induced protein	0,4098
At5g27780	auxin-responsive family protein similar to Auxin-induced protein 10A5	0,4148
At1g28330	dormancy-associated protein, putative (DRM1)	0,4162
At1g56010	transcription activator NAC1; contains No apical meristem (NAM) domain	0,4295
At4g00880	auxin-responsive family protein similar to small auxin up RNA	0,4347
At4g14550	auxin-responsive AUX/IAA family protein identical to IAA14; similar to Auxin-responsive protein IAA7	0,4381
At2g46530	transcriptional factor B3 family protein / auxin-responsive factor AUX/IAA-related	0,4403
At1g15580	auxin-responsive protein/indoleacetic acid-induced protein 5 (IAA5)/auxin-induced protein (AUX2-27)	0,4476
At1g76190	auxin-responsive family protein similar to indole-3-acetic acid induced protein ARG7	0,4512
At1g28330	dormancy-associated protein, putative (DRM1) identical to dormancy-associated protein	0,4606
At2g18010	auxin-responsive family protein similar to auxin-induced protein TGSAUR22; similar to indole-3-acetic acid induced protein ARG7	0,4686
At4g38860	auxin-responsive protein, putative auxin-induced protein 10A	0,4698
At1g28330	dormancy-associated protein, putative (DRM1)	0,4734
At4g03190	F-box family protein (FBL18) almost identical to GRR1-like protein 1	0,4778
At4g12980	auxin-responsive protein, putative similar to auxin-induced protein AIR12	0,4900

D. Auxin-related morphological phenotypes in *ron3*

The *ron3* mutant belongs to the Rotunda class of leaf mutants with a round leaf lamina compared to the wild type (Berna *et al*., 1999). Leaf growth and development was examined by growing plants in vitro for 21 days and measuring different leaf parameters. Leaf series of all rosette leaves and cauline leaves of 10 seedlings were scanned, measured with the ImageJ program and mean values analyzed statistically by t-tests. Both lamina length and -width in the ron3-1 mutant are significantly reduced for all leaves compared to the wild type resulting in a smaller lamina area (Figure 4).

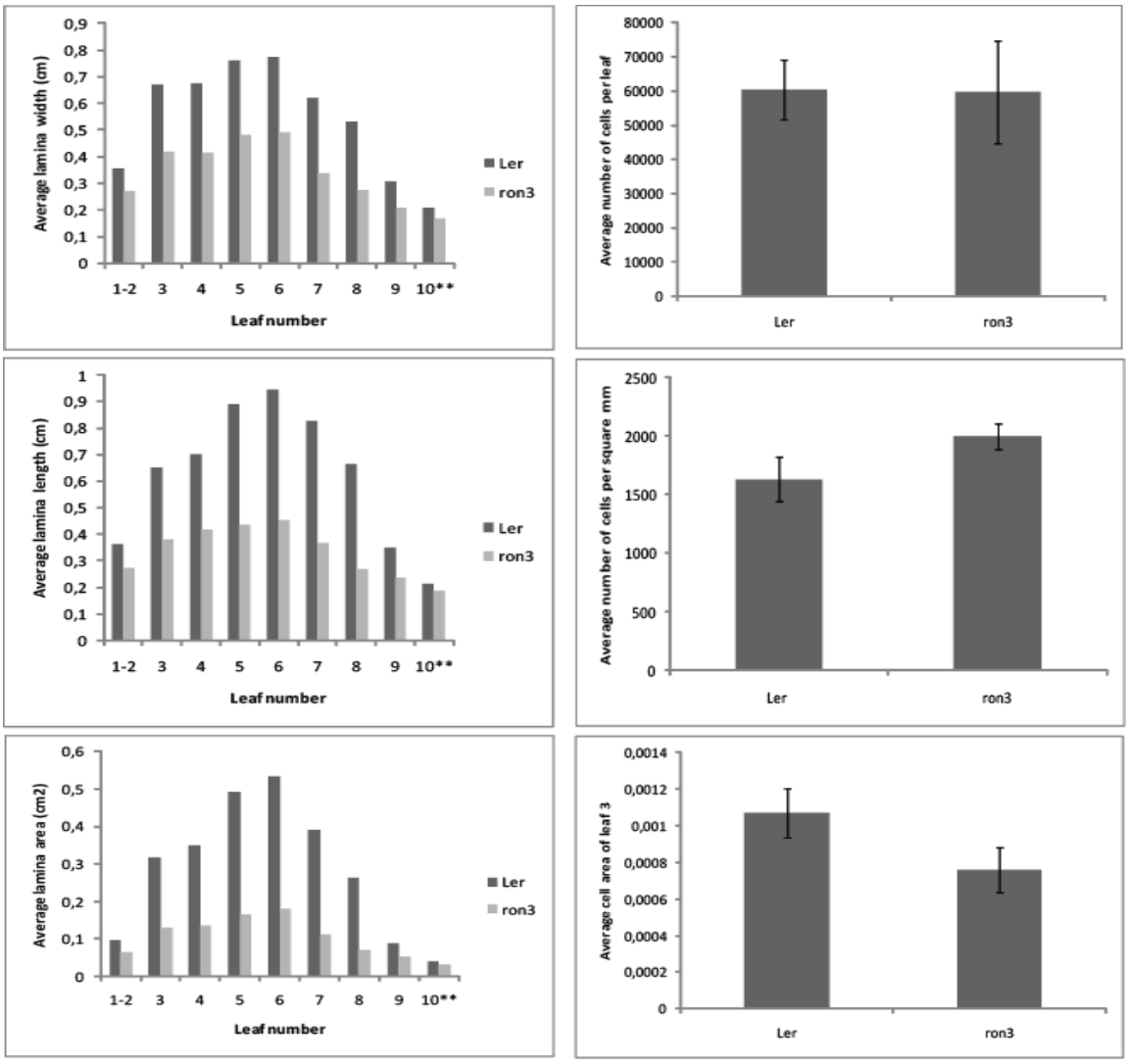

Fig 4. Leaf (left column) and cell (right column) measurements of Ler and *ron3-1* after growing for 21 days in long day (16hr light/8 hours dark) conditions.

To define the cellular basis of the smaller leaf area of the *ron3-1* mutant, we measured the area and number of cells in the abaxial epidermal cell layer in fully expanded leaf 3 of 21 day-old seedlings and calculated the average number of cells per mm^2 and per total leaf (Figure 4). The average number of cells per leaf was equal between *ron3-1* and Ler but the average number of cells per square mm was higher for the *ron3-1* mutant suggesting a smaller individual cell area in the *ron3-1* mutant. We measured the average cell area in leaf 3 and confirmed that the average cell area in the ron3 mutant ($0.76\times10^{-3}\pm0.122\times10^{-3}$) is significantly smaller compared to Ler ($1.07\times10^{-3}\pm0.132\times10^{-3}$) (P value < 0.05). The *ron3-1* mutants also display a late flowering phenotype (25.90±1.5 DAG) and higher leaf number (9.86±0.88) upon flowering compared to the wild type (respectively 24.22±1.4 DAG and 8.97±0.92).

We investigated whether the transcriptome data were confirmed by auxin-related phenotypes in the ron3 mutant. Plant growth regulators, such as auxin, control most of the characteristics of root systems and shoot architecture, including primary root growth, formation of lateral roots, root hair length, apical dominance and phylotaxis (Bohn-Courseau, 2010), these traits were analyzed in the ron3 mutant. Wild type Ler and ron3 plants were grown under constant light conditions and primary root growth and formation of lateral roots was followed for 15 days. Primary root growth was reduced and the number of lateral roots per cm was severely decreased in the ron3-1 mutant compared to WT throughout development and was respectively 0.6±0.4 and 3.6±0.9 after 21 days (Figure 5.A). The average length of root hairs in the ron3-1 mutant was significantly larger 0.7±0.2 cm compared to WT 0.2±0.1 cm (Figure 5.B) and is indicative of cell expansion defects (suggesting higher IAA levels in root hairs) (Strader *et al*., 2010; Strader and Bartel 2009). Root gravitropism was analyzed by measuring the gravitropical index (ratio of distance of hypocotyl to root tip and root length) on vertically grown seedlings after reorientation by 45º (Kleine-Vehn *et al*., 2010). The ron3-2 mutant showed a significant ($P<0.05$) hypergravitropic response with higher gravitropical index (0.88±0.04) compared to the wild type (0.74±0.07) (Figure 5.C and D). Auxin-related phenotypes were also observed in the shoot. Apical dominance is the phenomenon whereby the primary inflorescence of the plant is dominant over (grows more strongly) the secondary inflorescences and is controlled by auxin which diffuses downwards from the apical meristem and inhibits the development of axillary meristem growth (Taiz & Zeiger, 2006). The primary inflorescence was severely reduced in the *ron3-2* mutant 18.2 ± 3.16cm compared to the WT 33 ± 2.1. Secondary inflorescences in the ron3-2 mutant outgrew the primary inflorescence

(23.3 ±1.6cm) which is not the case for the WT (29.6 ± 2.9 cm) showing a reduced apical dominance in the ron3-2 mutant (Fig.5E); similar observations were made for the ron3-1 allele in Ler. Hypocotyl length was significantly reduced in the ron3-1 mutant under different light conditions (red, far red, blue, dark and white light) suggesting a non-photomorphogenic defect in hypocotyl elongation (Figure 5.F). The reduced lateral root number, enlarged root hairs, hyper-gravitropical response, reduced apical dominance and reduced hypocotyl elongation indicate a role for RON3 in auxin response-related processes and support the transcriptome data.

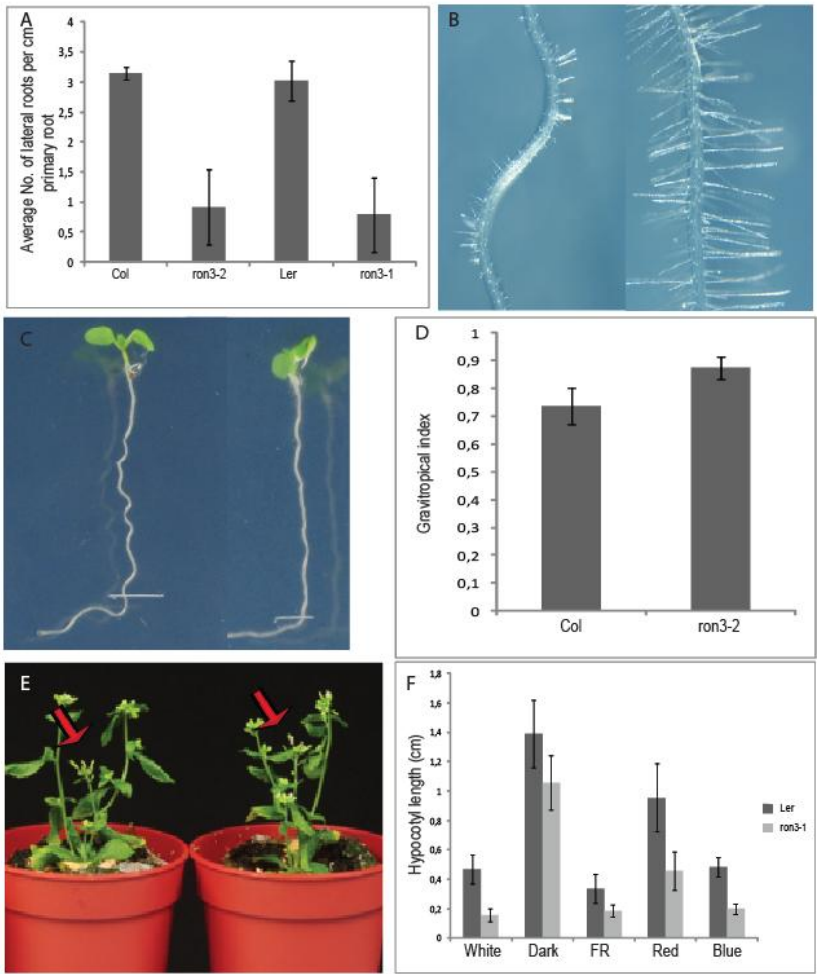

Fig 5. Auxin-related phenotypes in the ron3 mutant. A. Average number of lateral roots per cm primary root. B. Root hairs of Ler (left panel) and *ron3-1* mutant (right panel). C. Primary root growth of Col (left) and ron3-2 (right) on tilted plates (45º) and after reorientation of plates by 90º. D. Gravitropical index measured 10 DAG. Error bars represent standard deviation (n=10) E. Secondary inflorescences overgrowing the primary inflorescence (arrowheads) in the *ron3-2* mutant. F. Hypocotyl measurements of seedlings grown for 7 days under white, dark, far-red (FR), red and blue light conditions. Error bar represents standard deviation of at least 30 seedlings.

E. Auxin response and distribution is altered in *ron3-1* mutants

The plant hormone auxin transcriptionally activates early genes known as indolacetic acid (IAA) induced genes. In the ron3-1 transcriptome data genes of this family were downregulated (Table 1). We investigated whether the ron3 mutation has any altered effect on the respons of these genes to increased auxin level compared to the wild type (Abel *et al*., 1995) and if the transcription of RON3 itself is regulated by different auxin levels. Seedling were grown for 9 days under long day conditions and transferred to liquid medium with either 0 M NAA (mock controls), 20 μM NAA and 100μM NAA and incubated for 2 and 4 hours. All Aux/IAA genes tested were inducible after treatment with NAA in the RON3 mutant yet not as strongly as the wild type (Figure 6.A) and the expression of the RON3 gene remained unaffected after treatment with NAA.

High concentrations of auxin inhibit root elongation and instead enhance adventitious root formation and were used to assay auxin sensitivity in the ron3 mutant. Seedlings were grown vertically on growth medium containing 10nM IAA and root growth was measured every 2 days starting from day 5 (Figure 6.B). At day 5 both wild type and *ron3-1* showed a reduction in primary root growth of 30% compared to plants grown on medium without IAA. After day 7 the ron3-1 mutant showed a reduction in primary root growth of 28% compared to only 14% in wild type indicating an increased sensitivity to IAA in root growth inhibition (Fig 6.B).

To further investigate the auxin response in the ron3 mutants, we crossed the ron3-1 mutant with Arabidopsis lines carrying the promoter DR5-GUS construct which is an established marker for auxin response and indirectly for auxin accumulation. The expression of DR5::GUS in the *ron3-1* mutants showed stronger expression in the primary root tip and lateral root primordia compared to the DR5::GUS control line (Figure 6 C) suggesting auxin accumulation at these sites.

The hypergravitropical response and auxin accumulation in the *ron3* root tip suggests defects in auxin transport-related processes as an underlying cause. To test this hypothesis, we analyzed PIN1 and PIN2 distribution in the *ron3* background. The basal localization of PIN1 and PIN2 in respectively the vascular tissue and in the cortex and the apical localization of PIN2 in the epidermal cells did not seem to be affected by the *ron3* mutation (Fig 6.D).

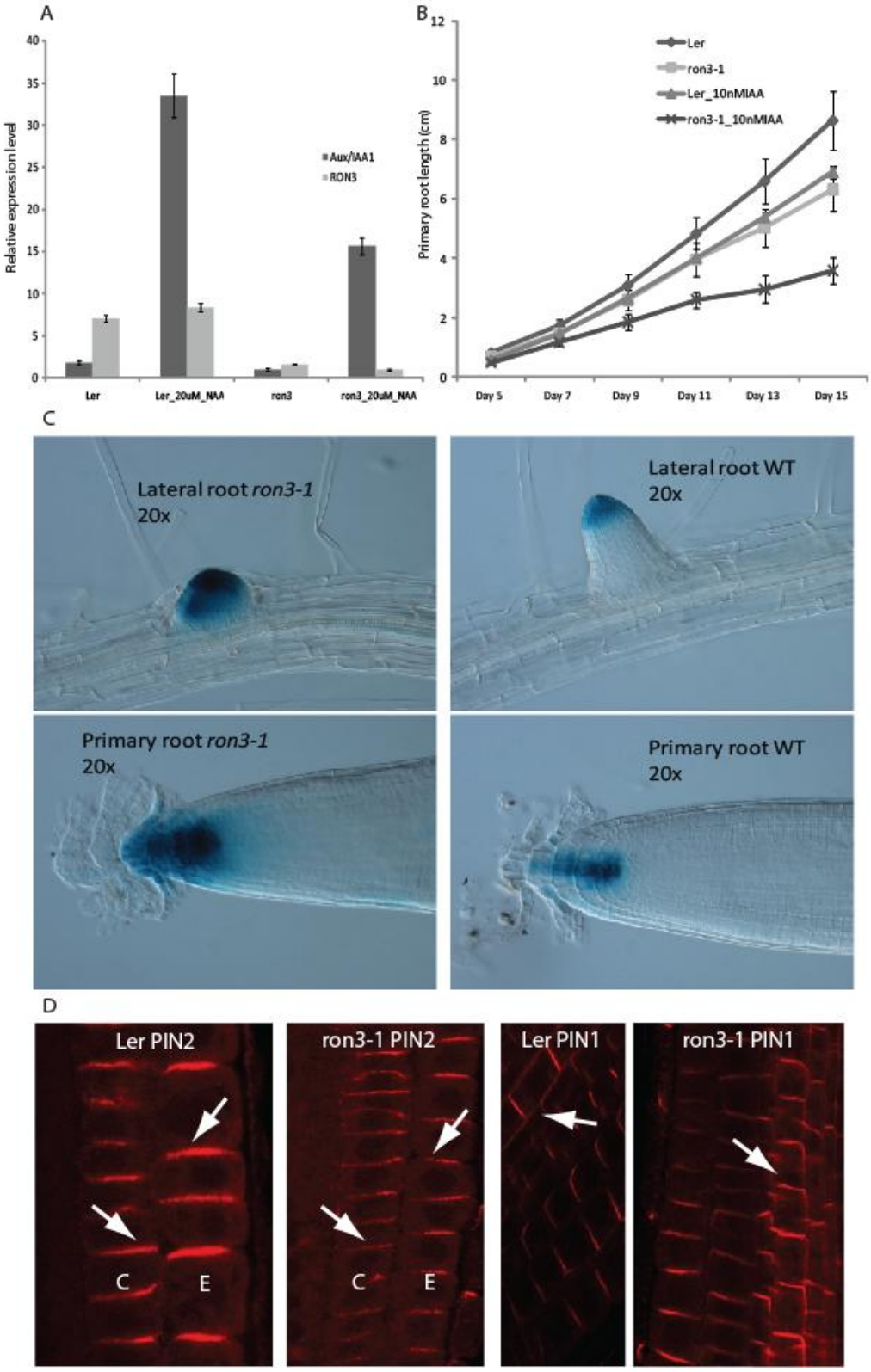

Fig 6. Auxin-response in the *ron3-1* mutant. A. Primary root growh of Ler and *ron3-1* on MS-media and MS-media containing 10 nM IAA. B. Expression level of RON3 and IAA1 in the Ler

WT and *ron3-1* mutant with and without induction of 20uM external NAA. C. DR5-GUS expression in lateral roots and primary roots of the *ron3-1* mutant and Ler WT. D. Immunolocalization of PIN1 and PIN2 in Ler and *ron3-1*.

F. RON3 interactome

To gain insight into the function of RON3, a tandem affinity purification (TAP) was performed on extracts of Arabidopsis cell suspension cultures, transformed with overexpression constructs for RON3 fused to IgG domains and the streptravidin-binding peptide (GS-TAP) of protein G. Two purifications with the GStag on the N-terminal and two purifications with the GStag on the C-terminal end of RON3 were separated on polyacrylamide gels and stained with Coomassie Brilliant Blue. Mass spectrometry revealed the presence of 32 proteins which are listed in Table 1 and 23 of these proteins were found in at least three experiments showing the reproducibility of the results. The majority of the proteins purified with RON3 as bait were not identified before amongst the 4430 proteins purified with different baits in the department and points to very specific interactions of the identified proteins with RON3. The high number of purified proteins might indicate that RON3 is involved in multiple cellular processes. Interestingly, three purified proteins, ECT2, ECT3 and TRN1 play a role in binding proteins with no classical nuclear import signal for transport to the nucleus and could thus explain the nuclear subcellular localization of RON3. In Table 2 the 32 proteins of the RON3 interactome are listed, their function and molecular process involved indicated that the RON3 protein interacts with nuclear proteins/complexes related to proteolysis and transcription. In Supplemental Table 2 the MS data for each protein and a corresponding value of expectance is listed.

Table 2. Copurified proteins identified by MS in TAP eluates of Arabidopsis cell cultures using RON3 as bait.

AT number	Protein Name	Total/4exp	Gene Ontology/Function/Involved in
AT5G28740	Tetratricopeptide repeat (TPR)-like superfamily protein	4	transcription-coupled DNA repair protein-related
AT2G38770	EMB2765	4	unknown
AT3G11910	UBP13	4	ubiquitin-dependent protein catabolic process
AT5G06600	UBP12	4	ubiquitin-dependent protein catabolic process
AT4G31770	DBR1	4	Encodes a RNA lariat debranching enzyme required for embryogenesis.
AT1G26460	pentatricopeptide (PPR) repeat-containing protein	4	RNA binding
AT5G53620	unknown protein	4	similar to protein which is phosphorylated during ABA treatment
AT3G06930	PRMT4B	4	histone methyltransferase
AT3G58500/AT2G42500	PP2A (PROTEIN PHOSPHATASE 2A)	4	subunit of the PP2A complex
AT1G51690	ATB ALPHA	4	subunit of the PP2A complex
AT3G47650	DnaJ/Hsp40	4	binding unfolded proteins
AT2G23350	PAB4	4	binds polyadenylated 3'end of mRNA
AT1G13690	ATE1	4	stimulates ATPase activity of DnaK/DnaJ
AT5G49020	PRMT4A	4	histone methyltransferase
AT3G13460	ECT2	3	nuclear import protein
AT5G01410/AT2G38230	PDX1	3	glutamine amidotransferase involved in pyridoxine/vitamin B6 biosynthesis
AT2G39700	ATEXPA4	3	putative expansin
AT5G61020	ECT3	3	nuclear import protein
AT1G17720	ATB BETA	3	subunit of the PP2A complex
AT4G29350	PFN2 (PROFILIN 2)	3	actin monomer-binding protein
AT3G25800	PDF1, PP2AA2	3	subunit of the PP2A complex
AT1G25490	RCN1	3	subunit of the PP2A complex
AT3G18790	unknown	2	unknown
AT1G42430	unknown	2	unknown
AT1G49760	PAB8	2	binds polyadenylated 3'end of mRNA
AT3G59890/AT2G44040	dihydrodipicolinate reductase family protein	2	amino acid metabolism
AT3G06810	IBR3 (IBA-RESPONSE 3)	2	enzyme involved in IBA metabolism
AT4G34110	PAB2	1	binds polyadenylated 3'end of mRNA
AT1G47128	RD21 (responsive to dehydration 21)	1	cysteine peptidase activity
AT1G06110	SKIP16 (SKP1/ASK-interacting protein 16)	1	SCF ubiquitin ligase complex
AT2G16950	TRN1 (TRANSPORTIN 1)	1	nuclear import protein

CORNET, a tool for the construction of protein-protein interaction networks (De Bodt *et al*., 2010), was used to identify pairwise protein interactions between the 32 purified proteins (Figure 7). For 20 out of 32 proteins predicted pairwise interactions were found. Six members of the cytoplasmic PP2A phosphatase complex were purified in at least three of the four purifications: ATB ALFA/PP2AA1 (At1g51690), PP2A-4/PP2A-3 (At3g58500/At2g42500), ATB BETA (At1g17720), PP2AA2 (At3g25800) and RCN1 (At1g25490). The ubiquitin-specific proteases UBP12 (At5g06600) and UBP13 (At3g11910) are predicted to interact with ATB BETA (Geisler-Lee *et al*., 2007) and were also purified in all TAP experiments. Besides the PP2A complex, a number of other purified proteins are nuclear and involved in mRNA processing such as the poly(A)binding proteins PAB4 (At2g23350), PAB8 (At1g49760) and PAB2 (At4g34110)

which are important translation initiation factors that bind to the polyadenylated 3'end of mRNA. Other proteins are involved in a variety of cellular processes such as histone modifications (PRMT4A/At5g49020 and PRMT4B/At3g06930), protein folding (DnaJ/Hsp40/At3g47650 and ATE1/At1g13690 which stimulates the ATPase activity of DnaK/DnaJ) and DNA damage repair (At5g28740).

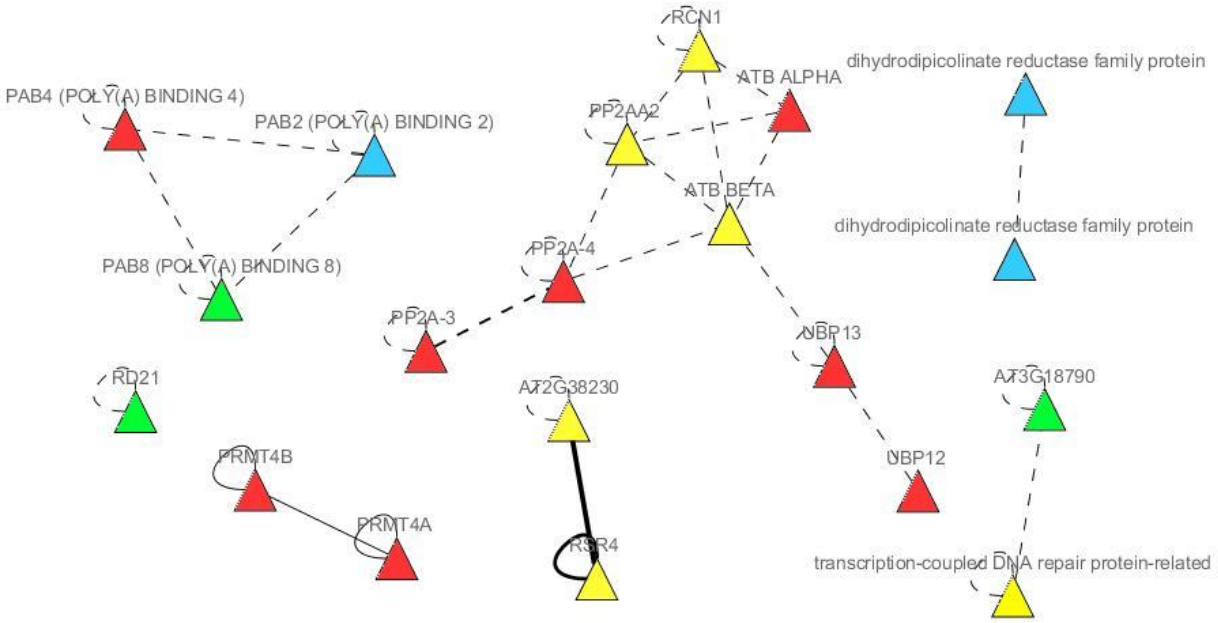

Figure 7. CORNET software showing pairwise interactions on copurified proteins after tandem affinity purification with RON3 protein as bait. The dashed lines show predicted interactions and full lines show experimentally confirmed interactions. The color of the node shows the number of times each protein was purified in the 4 TAP experiments (Red = 4 , Yellow = 3 , Green = 2 and Blue = 1)

III. Discussion

RON3 regulates its own expression

Identification of the *RON3* gene was performed by fine-mapping the *ron3* mutation to a candidate interval of 68.7kb, which encompassed 18 annotated genes. Remarkably one of those 18 genes, At4g24500, was also strongly downregulated in the *ron3* transcriptome and sequence analysis showed a point mutation in one of the first exons creating a stop codon, indicating it indeed corresponded to the *RON3* gene. Q-PCR analysis confirmed the severe downregulation of RON3 gene expression in the ron3 mutant. How can a point mutation which creates a stop codon and truncation of the respective protein be the cause of its downregulation at the mRNA level? The process of nonsense-mediated mRNA decay (NMD) is an mRNA surveillance pathway that ensures the rapid degradation of mRNAs containing premature translation termination codons (PTCs), thereby preventing the synthesis of truncated and potentially harmful proteins. The key players in the NMD pathway were initially identified in genetic screens in *Saccharomyces cerevisiae* and *Caenorhabditis elegans* (Hodgkin *et al*., 1989) but have also been found in plants (Reyes *et al*., 2006). The *aux1-21* allele of the AUX1 gene has been described as a candidate gene regulated by NMD (Marchant and Bennett, 1998). Our observations suggest that *ron3-1* allele is another allele regulated by NMD.

Putative function of RON3 in the regulation of auxin transport by interacting with the PP2A complex

The RON3 protein is assigned as a hydroxyrich glycoprotein (HRGP) by the TAIR database and HRGPs are well-known to be components of the plant extracellular matrix. Indeed, a high number of proline residues is present in the RON3 protein, however, these are dispersed and do not occur in the typical clusters as described for HRGPs. Moreover, the HRGP superfamily based on bioinformatics studies and described by Showalter *et al*., (2010) does not contain the RON3 gene. BLAST searches didn't find any homology with other cell wall proteins and no known functional domains in the RON3 protein are present. RON3 is a plant-specific gene present in Arabidopsis and other higher plants as a single copy and not present in moss or algae.

Auxin-dependent phenotypes were observed in both root and shoot organs in the ron3 mutant and the transcriptome analysis reveals a high number of downregulated auxin-related genes. The enlarged root hairs and hypergravitropical response could be attributed by an increase in

intracellular auxin levels in the root hairs and root tip (Ganguly *et al*., 2010). Indeed, DR5::GUS expression in the *ron3* mutants shows high auxin levels in the root tip and at lateral root initiation sites and suggests defects in auxin transport-related processes. This hypothesis is supported by the tandem affinity purification with a GStagged RON3 fusion protein in which the PP2A complex was purified. The PP2A complex directs auxin flux by dephosphorylating PIN proteins, thus reversing the phosphorylation of PINs by PINOID (Michniewicz *et al*., 2007). This antagonistic regulation of PIN phosphorylation by PP2A and PINOID mediates PIN apical-basal polar targeting (Fig. 8.A.).

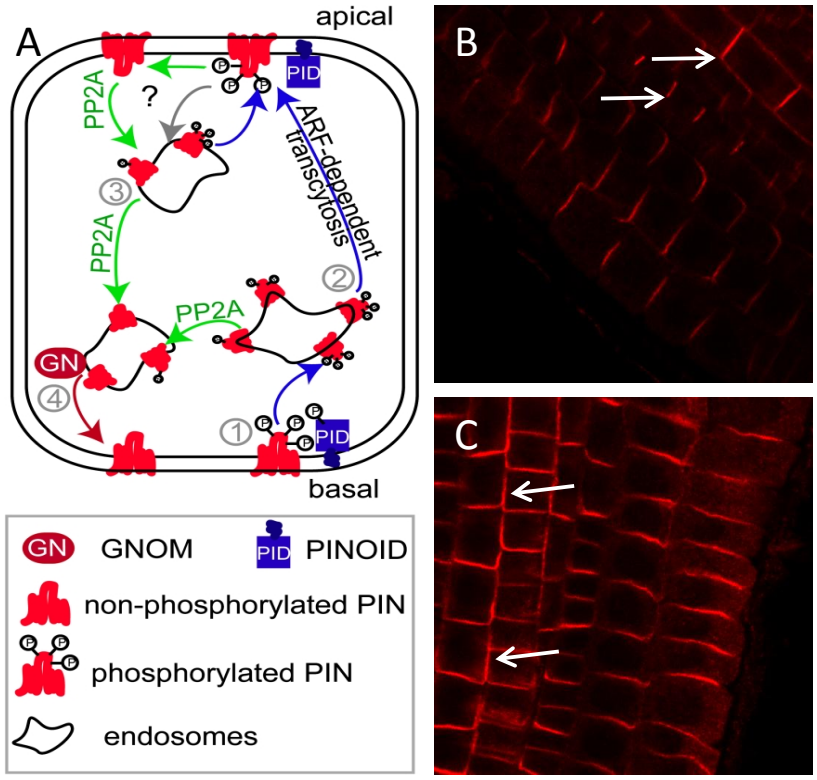

Fig. 8. Model of PID and GNOM-Dependent Intracellular PIN Sorting (A). PID might phosporylate PIN proteins preferentially at the plasma membrane (1). Phosporylated PIN proteins get internalized into endosomes but fail to get sorted to the ARF-GEF GNOM-dependent basal recycling pathway (4). Phosphorylated PIN proteins display an enhanced affinity for a GNOM-independent, but ARF-dependent, apical targeting pathway, eventually leading to basal-to-apical PIN transcytosis (2). PP2AA function can counteract (3) the PID-dependent PIN phosphorylation, leading to GNOM-dependent (GN) basal recycling of PIN proteins (4) (Kleine-Vhen *et al.*, 2009. Immunolocalization of PIN1 proteins in wild type and the *ron3-1* mutant (B and C respectively).

For example, the loss of PINOID causes an apical-to-basal shift in PIN polarity and the PINOID gain of function results in an opposite basal to apical PIN polarity shift, which leads to auxin depletion from the root meristem. Moreover, the localization of PINOID proteins in the primary root resembles strongly the in situ hybridization pattern of RON3 and suggests an antagonistic balance between both in the reverse fountain auxin flux in the primary root tip. Although we could not observe any major mislocalisation of PIN1 and PIN2 in the ron3 mutant, it might be

possible that small differences in apical-basal targeting of these proteins are only slightly influenced by the *ron3* mutation which explains the relatively weak phenotype of the *ron3* mutant compared to the *pid* mutant. Indeed, immunolocalization of PIN1 proteins in the *ron3* mutants shows basal and lateral localization in contrast to the strictly basal localization in the wild type (Fig. 8.B and 8.C). The confirmation of these findings is currently ongoing. The *ron3* mutant shares similar phenotypes with the knock-out mutant of the best studied subunit of the PP2A complex, ROOTS CURL IN NPA, RCN1 which was purified in the TAP with RON3. RCN1 was originally identified in a mutant screen looking for alteration in their responses to NPA, a well-known inhibitor of auxin-transport (Garbers *et al*., 1996). Subcellular localization studies show cytoplasmic and perinuclear RCN1 in cells of the root apical meristem but nuclear and membrane associated localization in mature cortical cells (Blakeslee *et al*., 2008). So RON3 does seem to at least partly colocalize with RCN1 and thus the PP2A complex. It is however still unclear how RON3 modulates the activity of the PP2A complex (inhibiting/activating) and double mutants between *ron3* and *rcn1* could give more information into the function of RON3. If RON3 modulates the activity of the PP2A complex in dephosphorylating PINs, it could explain the fact that RON3 is kept as a single copy gene during evolution since it might be under selection pressure because of a delicate gene dosage balance. Indeed, overexpression lines of RON3 seem to have a negative impact on growth (data not shown) just as overexpression lines of PINOID also show several growth defects (Benjamins *et al*., 2001).

Role in transcription

Our interactome data of RON3 reveals a high number of nuclear proteins involved in transcription and confirms the nuclear colocalization of RON3 with DAPI in euchromatic regions. For example, the protein arginine methyltransferases PRMT4A and PRMT4B are purified after TAP with RON3 as bait and are able to methylate histone H3 and nonhistone proteins (Niu *et al*., 2008) and play a role in transcriptional regulation. Moreover, the human homolog of PRMT4A and PRMT4B, CARM1 is able to methylate RNA-binding proteins such as PABP1 (Lee and Bedford, 2002) and fits with our interactome data of RON3 in which we pull down the poly-A binding proteins, PAB2, PAB4 and PAB8. So it appears that not only histones but also PABs are being methylated by PRMT4A and PRMT4B which is consistent with recent

findings in Arabidopsis subcellular localization experiments of PRMT4A/B where they are both nuclear and cytoplasmic localized (Niu *et al*.,2008). Lee and Bedford (2002) identified the region in PABP1 that is methylated by CARM1. This 100-amino-acid patch contains a propensity of proline and arginine residues with a specific RPAAPR motif. The RON3 protein also contains a high propensity of proline residues which are flanking arginine residues and might thus itself be a target for methylation by PRMT4A/B. *prmt4a/prmt4b* double mutants are late flowering and show no other growth defects, suggesting that they play a role in the proper regulation of Arabidopsis flowering time. The *ron3-1* mutants also display a late flowering phenotype and is another indication for its involvement in the PRMT4A/PRMT4B pathway.

We conclude that our data indicates that RON3 is not only involved in the PP2A-dependent trafficking of PIN proteins but might also play a role in the regulation of protein methylation and/or is itself regulated by methylation.

IV. Materials and Methods

Plant Material, Media and Culture Conditions The Arabidopsis thaliana (L.) Heyn. Ecotypes Landsberg erecta (Ler) and Columbia (Col) were obtained from the Nottingham Arabidopsis seed collection. The ron3-1 mutant is in the Ler background (Berna *et al*., 1999) and the ron3-2 allele, the Gabi-Kat_374F12 line, homozygous for the T-DNA insertion in At4g24500, is in Col background. Seeds were sterilized in 5 % bleach with 0.05 % Tween 20 for 10 minutes, washed and germinated on GM medium (Valvekens *et al*., 1988) and grown aseptically either horizontally on round Falcon 1013 petri dishes or vertically on square shape plates. Plants were germinated in rockwool and watered every two days with Hyponex solution and grown at 21 ºC, 100 μmol m^{-2} s^{-1} photosynthetically active radiation in a 16-h light regime, and 50% relative humidity.

Morphological analysis Leaf series were made of Ler and ron3 seedlings grown for 21 days in vitro, on large plates containing 1% plant tissue culture agar, and photographed. Lamina length , width and area were measured by the ImageJ program (rsbweb.nih.gov/ij/download.html). Primary root length of seedlings grown in vitro in vertical position was marked every 2 days for 15 days. The plates were scanned and the primary root length analyzed by ImageJ. Gravitropic response was measured using 7-day old seedlings. After 3 days of vertically growth, plates were

tilted for 45º and after 4 days root length and distance of root tip to hypocotyl was measured using ImageJ software.

Cellular analysis Leaves of L*er* and *ron3* seedlings grown for 21 days in vitro were cleared overnight in ethanol, transferred a few minutes in Hoyer medium (100 g chloral hydrate, 5 ml glycerol, 30 ml destilled water) to remove starch and kept in lactic acid. The lower epidermis of leaf one, two and three was visualized with differential interference contrast microscopy and drawn using a drawing tube, scanned and analysed by Image J and the cell area was measured (Cnops *et al*., 2004). The area of the drawings and the total leaf area were measured and together with the cell area measurements the total number of cells was calculated (De Veylder *et al*., 2001).

Map based cloning, sequence analysis of RON3 and F1 analysis For the positional cloning of *RON3*, an F_2 mapping population was derived from a *ron3-1/ron3-1* (in a L*er* background) x Col-0 cross. Fifty of these F_2 plants were used to low-resolution map the *ron3-1* mutation as described in Ponce *et al*. (2006), which allowed us to delimit a candidate interval flanked by the AtF7K2.1 (BAC F7K2) and AtM7J2.1 (BAC M7J2) markers, on chromosome 4. Further iterative assessment of linkage to molecular markers (Table S1) in 290 additional F_2 plants narrowed down the candidate interval to a genomic region of 68.7 kb, which encompassed 18 annotated genes. The At4g24500 gene was identified as a candidate gene in the genetic interval around RON3 and was amplified from the ron3 and Ler genomic DNA in several independent PCR amplifications. The DNA sequencing analysis was performed by the dideoxy chain termination method of Sanger *et al*. (1977).

F1 plants derived from reciprocal crosses between ron3 (Ler) and the Gabi-Kat Line, GK374F12A (Col), with a T-DNA insertion in the first exon of the At4g24500 were heterozygous for the microsatellite markers, nga8 and nga225, which confirmed their hybrid nature.

Transcriptome analysis ron3-1 and Ler seedlings were sown in vitro on half-strength Murashige and Skoog medium vernalized for 3 days and germinated at 21ºC under a 16h light regime. The green parts of stage 1.03 plants were harvested (Boyes *et al*., 2001), consisting of the SAM, the

first and second young leaves, the third leaf larger than 1mm, the fourth leaf smaller than 1mm and the cotyledons. Per genotype, four replicates were harvested and per replica three repetitions. Total RNA was extracted with RNeasy Plant Mini Kit (Qiagen, Hilden, Germany) and the samples analyzed at the VIB MicroArrays Facility with the Agilent microarray platform. The processed Cy3 and Cy5 intensities were normalized and statistically analyzed with the Feature Extraction Software (version 10.1.1.1; Agilent Technologies, Santa Clara,CA, USA). P values had to be lower than 0.05 and the absolute value of the log2 ratio had to be higher than one. To visualize over-represented Geno Ontology (GO) categories, upregulated and downregulated data sets were analyzed with BiNGO (Maere *et al*., 2005).

Auxin Treatment Intact seedlings of Ler and ron3 (eight to nine days old) were placed in liquid MS solution supplemented with NAA. The seedling were incubated at 21ºC with moderate shaking for two and four hours. Mock control incubations were supplemented with an equal amount of the solvent (2%NaOH) used to prepare the stock solution of NAA. After the indicated time, +/- 10 seedlings were removed, immediately frozen with liquid nitrogen and stored at -80ºC for quantitative PCR analysis.

Quantitative PCR analysis Total RNA from seedlings was extracted with the RNeasy Plant Mini Kit (Qiagen, Hilden, Germany) followed by first-strand cDNA synthesis (Invitrogen SuperscriptIII). cDNA was amplified in real-time quantitative polymerase chain reaction (PCR) with the Platinum SYBR Green qPCR Supermix-UDG (Invitrogen). The fluorescent dye was detected with the iCycler (BioRad, Hercules, CA, USA) and relative cDNA concentration was determined with the comparative Ct method (qBasePlus; Biogazelle, Zulte, Belgium). Samples were normalized using an endogenous actin housekeeping gene (At3g60830).

In situ hybridization and GFP localization Short and specific (GST) fragment of RON3 (At4g24500), gene was cloned in the pGEM-TEasy vector (Promega). Digoxigenin (DIG)-labeled RNA sense and antisense probes were synthesized by T7 and SP6 polymerase-driven in vitro transcription, respectively (DIG-RNA labeling kit protocol; Roche Diagnostics). Shoot apices and leaves, were excised from 12 old Ler seedlings, fixed, dehydrated, embedded in

paraffin, cut into 8-µm sections, and hybridized (55°C) to a DIG-labeled antisense RNA probe as described by (Cañas L.A. 1994).

Whole mount *in situ* hybridization was performed for the root tips 7 old Ler seedlings following the protocol of Hejátko J *et al*. (2006). Transcript accumulation was visualized as a violet-brown staining.

Localization of RON3 The 35S::GFP-RON3 construct was generated by cloning the cDNA of RON3 into the destination vector pK7WGF2 and pK7FWG2 (Karimi *et al*., 2002), which contained the CaMV 35S promoter sequence, the GFP open reading frame, the 35S terminator and the Gateway cassette. Wild-type Col and ron3 mutants were transformed with Agrobacterium strain C58C1(pMP90)(Koncz and Schell, 1986), containing the 35S::GFP-RON3 construct, using the floral dip method (Clough and Bent, 1998). T1 transformants were selected by high density plating on medium with Kanamycin (50mg/L). Transformants with 1 T-DNA copy were obtained by segregation analysis in the T2 generation. For confocal microscopy on the primary roots, plants were grown vertically for 4 days on MS medium. Fluorescence microscopy was done with a confocal microscope 100M with software package LSM 510 version 3.2 (Zeiss, Jena, Germany), equipped with a 63× water corrected objective (numerical aperture of 1.2). GFP fluorescence was imaged with 488 nm excitation. Emission fluorescence was captured in the frame-scanning mode alternating GFP fluorescence via a 500- to 550-nm bandpass emission filter.

Tandem Affinity Purification The RON3 cDNA was N and C-terminally fused to the GS- tag (Bürckstümmer *et al*, 2006), overexpressed by the constitutive cauliflower tobacco mosaic virus 35S promoter and transformed in Arabidopsis cell suspension cultures as previously described (Van Leene *et al*., 2007). Tandem affinity purification of protein complexes was done using the GS tag followed by protein precipitation and separation, according to Van Leene *et al*. (2008). For the protocols of proteolysis and peptide isolation, acquisition of mass spectra by a 4800 Proteomics Analyzer (Applied Biosystems), and MS-based protein homology identification based on the latest TAIR 9.0 genomic database, we refer to Van Leene *et al*. (2010). Experimental background proteins were subtracted based on approximately 40 TAP experiments on wild type cultures and cultures expressing TAP-tagged mock proteins GUS, RFP and GFP (Van Leene *et al*., 2010).

Localization analysis Histochemical stainings for GUS activity and whole-mount immunolocalization were performed as described (Friml *et al*., 2003; Sauer *et al*., 2006b). Antibodies were diluted as follows: anti-PIN1 (1:1000; Paciorek *et al*., 2005), anti-PIN2 (1:1000; Abas *et al*., 2006); CY3-conjugated anti-rabbit secondary antibodies were diluted 1:500. Signal was visualized with a confocal laser scanning microscopy (TCP SP2; Leica Microsystems; LSM 710; Carl Zeiss Microimaging).

V. Supplemental data

Table S1. Candidate interval for RON3

Locus	Gene product name
At4g24420	RNA recognition motif (RRM)-containing protein
At4g24430	expressed protein
At4g24440	transcription initiation factor IIA gamma chain / TFIIA-gamma (TFIIA-S)
At4g24450	starch excess protein-related
At4g24460	expressed protein
At4g24470	zinc finger (GATA type) protein ZIM (ZIM)
At4g24480	serine/threonine protein kinase, putative
At4g24490	geranylgeranyl transferase alpha subunit-related / RAB geranylgeranyltransferase alpha subunit-related
At4g24500	hydroxyproline-rich glycoprotein family protein
At4g24510	eceriferum protein (CER2)
At4g24520	NADPH-cytochrome p450 reductase, putative / NADPH-ferrihemoprotein reductase, putative
At4g24530	expressed protein
At4g24540	MADS-box family protein
At4g24550	clathrin adaptor complexes medium subunit family protein
At4g24560	ubiquitin-specific protease 16, putative (UBP16)
At4g24565	Pre-tRNA; tRNA-Ser
At4g24570	mitochondrial substrate carrier family protein
At4g24580	pleckstrin homology (PH) domain-containing protein-related / RhoGAP domain-containing protein

Table S2. Mass spectrometry of the identified proteins in four TAP eluates with GS-tag-RON3 as bait.

AT number	Protein MW	Peptide Count	Seq Coverage %	Protein Score	Expect	Best Ions Score	Expect
AT5G28740	107212	32	42	1190	3,30E-115	143	8,40E-14
AT2G38770	173996	28	27	1050	3,30E-101	109	1,30E-10
AT3G11910	131137	27	28	887	6,70E-85	110	1,70E-10
AT5G06600	115706	27	35	885	1,10E-84	108	2,40E-10
AT4G31770	48430	13	33	794	1,30E-75	106	7,00E-10
AT1G26460	70760	9	19	457	6,70E-42	102	5,00E-10
AT4G24500 (BAIT)	35200	5	16	553	1,70E-51	145	2,40E-14
AT5G53620	76442	12	24	354	1,30E-31	148	1,90E-14
AT3G06930	60275	14	44	434	1,30E-39	74	6,30E-07
AT3G58500/AT2G42500	36372	10	43	514	1,30E-47	123	8,40E-12
AT1G51690	57526	6	14	239	4,20E-20	64	8,90E-06
AT3G47650	15164	2	17	158	5,30E-12	102	1,50E-09
AT2G23350	72006	6	10	170	3,30E-13	63	9,90E-06
AT1G13690	19797	3	33	146	8,40E-11	89	3,60E-08
AT5G49020	59275	9	22	211	2,70E-17	64	4,60E-06
AT3G13460	72614	10	25	192	2,10E-15	54	2,60E-05
AT5G01410/AT2G38230	33480	7	23	206	8,40E-17	66	5,10E-06
AT2G39700	28286	3	18	112	2,10E-07	97	2,30E-09
AT5G61020	55476	3	8	107	6,70E-07	61	1,60E-05
AT1G17720	56696	4	8	116	8,40E-08	78	3,50E-07
AT4G29350	14103	3	43	93	1,80E-05	66	5,70E-06
AT3G25800	66183	5	12	/	/	43	1,40E-03
AT1G25490	66307	5	10	/	/	39	3,70E-03
AT3G18790	35412	12	45	387	6,70E-35	125	6,20E-12
AT1G42430	49115	9	27	144	1,30E-10	48	2,00E-04
AT1G49760	72961	8	17	94	1,30E-05	65	2,30E-06
AT3G59890/AT2G44040	37573	4	16	89	4,10E-05	37	4,60E-03
AT3G06810	92282	22	35	445	1,10E-40	111	1,30E-10
AT4G34110	68743	9	18	249	4,20E-21	72	3,00E-07
AT1G47128	52131	3	8	118	5,30E-08	95	5,00E-09
AT1G06110	49458	4	15	76	8,60E-04	59	1,90E-05
AT2G16950	100826	4	5	/	/	38	3,30E-03

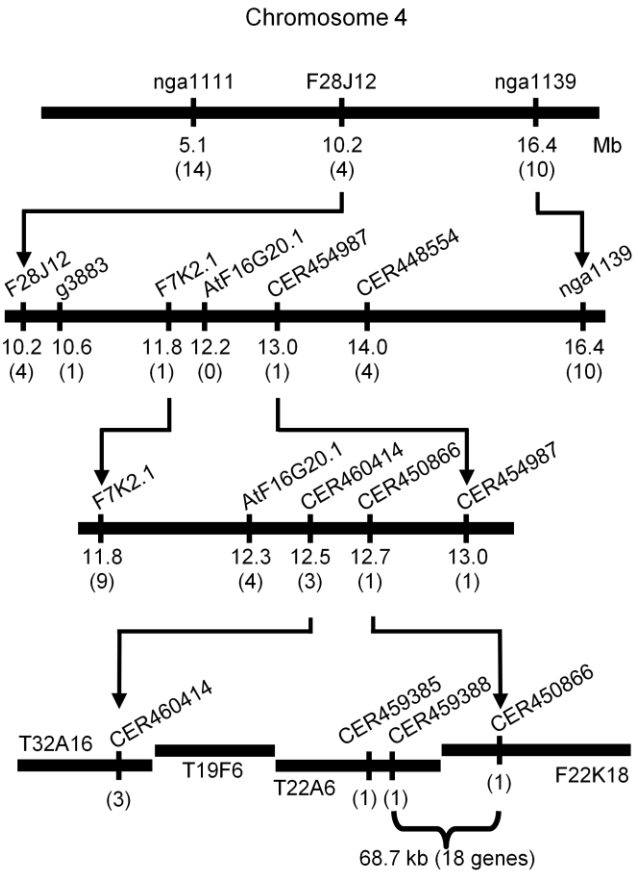

Fig. S1. **Map-based cloning of the *ron3-1* mutation.** The number of informative recombinants identified is indicated in brackets. A candidate interval of 68.7 kb was finally delimited, flanked by the CER459388 and CER450866 markers and encompassing the T22A6 and F22K18 BAC clones, which included 18 annotated genes (At4g24420-At4g24580).

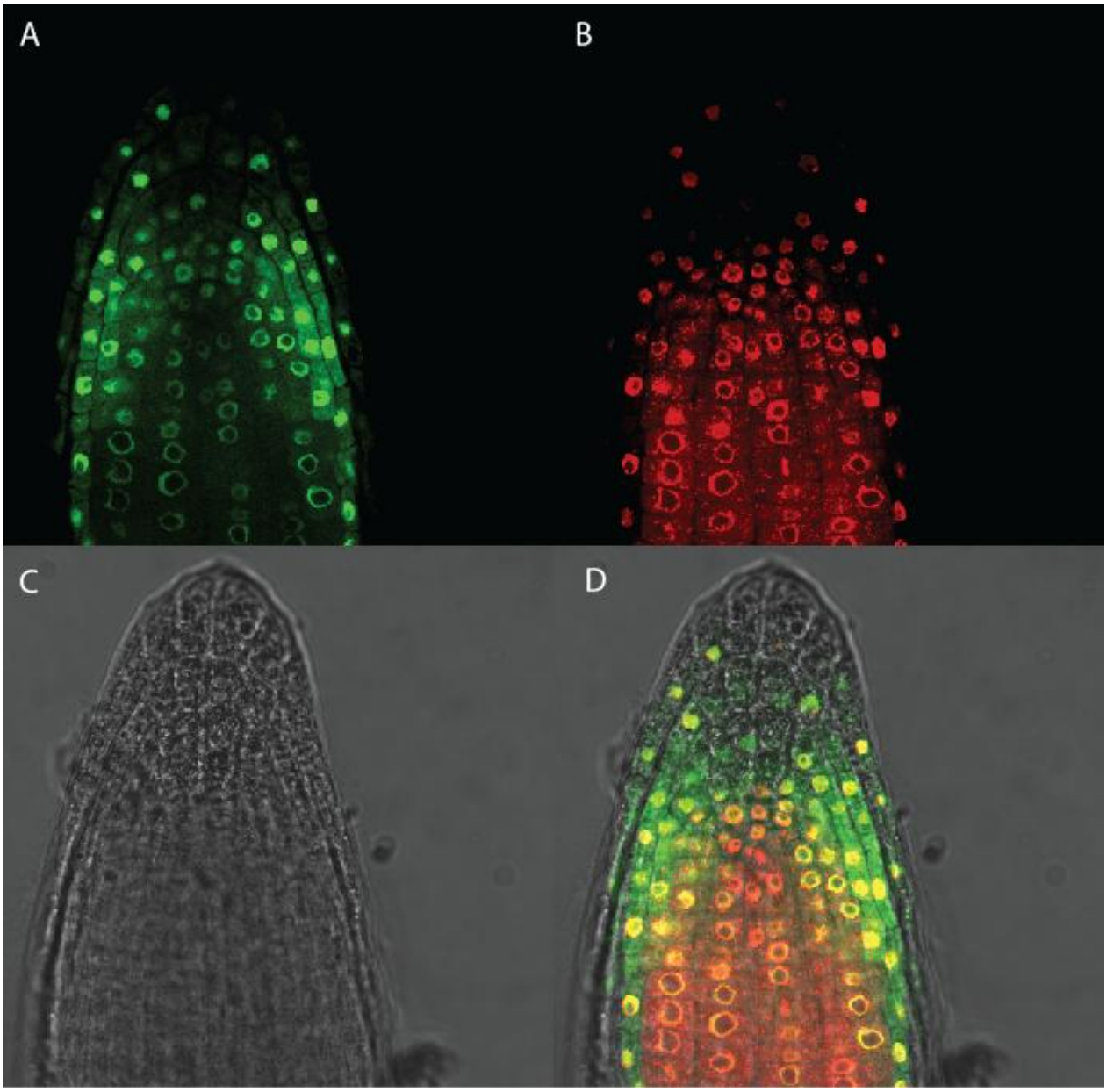

Fig S2. RON3-GFP colocalizes with DAPI. A. RON3-GFP localization in primary root tissue of 7 day old transformants. B. DAPI staining of the primary root and overlay (D).

Chapter 7

The *ang3* mutation identified the ribosomal protein gene *RPL5B* with a role in cell expansion during organ growth

Physiol Plant (2010) 138**:** 91-101

Annemie Van Minnebruggen, Pia Neyt, Steven De Groeve, Griet Coussens, María Rosa Ponce, José Luis Micol and Mieke Van Lijsebettens
Steven De Groeve performed sequence analysis including primer design and BiNGO analysis and the different Q-PCRs

The role of translation in the regulation of higher plant growth and development is not well understood. Mutational analysis is a powerful tool to identify and study the function of genes related to a biological process, such as growth. Here we analyzed functionally the *angusta3* (*ang3*) narrow leaf mutant. The *ANG3* gene was cloned by fine-mapping combined with candidate gene sequencing and it corresponded to the ribosomal protein gene *RPL5B*. Based on amino acid sequence homology, promoter DNA sequence homology and in silico gene expression analysis, *RPL5B* was found to be putatively functionally redundant with *RPL5A*. The morphological analysis of *ang3* mutants showed that the leaf lamina area was significantly reduced from the third rosette leaf on, mainly because of decreased width. Cellular analysis of the abaxial epidermal cell layer of the third leaf indicated that the cell number in the mutant was similar to that of the wild type, but the cell size was significantly reduced. We postulate that the reduced cell expansion in the epidermis contributes to the narrow shape of *ang3* leaves. Growth was also significantly impaired in hypocotyls and primary roots, hinting at a general role for *RPL5B* in organ growth, unrelated to axis formation. Comparison of the transcriptome of the shoot apices of the mutant and the wild type revealed a limited number of differentially expressed genes, such as *MYB23* and *MYB5*, of which the lower expression in the *ang3* mutant correlated with reduced trichome density. Our data suggest that translation is an important level of control of growth and development in plants.

I. Introduction

Organ size and shape are still an enigmatic research domain in higher plants. Organs grow along axes that are specified at initiation, i.e. roots grow and differentiate along an apical-basal and a radial axis; in contrast, leaves grow along a proximo-distal (length), a medio-lateral (width) and a dorsiventral (thickness) axis. As a result, leaves have a very typical sheath-like structure with a very restricted number of cell layers in the thickness direction and a pronounced growth in the length and width directions. Each plant species is characterized by its distinct leaf shape, which is used for classification and, hence, is genetically specified. In addition, it is plastic under different environmental conditions and, thus, regulated by a number of signaling pathways.

Leaves are formed from the peripheral zone of the shoot apical meristem (SAM) that consists of daughter cells derived from the stem cells in the SAM central zone. Local auxin accumulation determines the position of the leaf primordia. At the molecular level, there is a mutual repression between ARP (ASYMMETRIC LEAVES1 [AS1]/ ROUGH SHEATH2/ PHANTASTICA) MYB-domain transcription factors and class I KNOTTED1-like homeobox (KNOX) proteins. Meristem-promoting KNOX activity is confined to the SAM by ARP action and ARP proteins are restricted to leaves (for review, see Barkoulas *et al*. 2007). Subsequent steps in leaf growth are the acquisition of dorsiventral asymmetry, also referred to as polarity, lateral growth of the lamina along the medio-lateral axis and the restricted growth in the thickness direction by cell differentiation. All these processes are regulated by AS1 together with the KANADI and YABBY factors for dorsal and ventral domain identity, respectively. Finally, the petiole is formed by a restriction in growth, the lamina stops its meristematic activity and completes differentiation. Thus, size and shape of a leaf are determined by both cell proliferation and cell expansion. Indeed, local stimulation of cell division or cell expansion results in indentation or outgrowth of the leaf lamina, respectively (for review, see Fleming 2002). Perturbations in the cell cycle regulators modify leaf shape and size (De Veylder *et al*. 2001) as well as overexpression of expansin that plays a role in cell wall relaxation and cell expansion (Cho and Cosgrove 2000). Transcription factors have been identified that control leaf size, such as AINTEGUMENTA (Mizukami and Fischer 2000), but the translational machinery is also important as shown in mutants of the ribosomal protein genes (Van Lijsebettens *et al*. 1994; Ito *et al*. 2000; Yao *et al*. 2008).

The aim of our research is to study the genetic control of growth in the model plant *Arabidopsis thaliana*. As an experimental system, we used the leaf and our resource for gene

identification was a collection of leaf mutants consisting of 94 loci (Berná *et al*. 1999). The genes corresponding to the leaf mutants were cloned by fine-mapping combined with sequence analysis of candidate genes in the genetic interval around the locus of interest. Molecular analysis of the gene was combined with morphological and cellular analyses of the corresponding mutant to determine the cellular basis of the altered leaf size and shape and to gain deeper insight into the function of the gene (Cnops *et al*. 2004) and the molecular phenotypes were studied with microarray analysis to identify the molecular processes affected by the gene (Fleury *et al*. 2007). A number of loci had been cloned and functionally analyzed and provided a plethora of genes that gave insight into the molecular processes important in the control of leaf formation, such as chromatin-related factors (Nelissen *et al*. 2005; Barrero *et al*. 2007; Fleury *et al*. 2007), transcriptional regulators (Cnops *et al*. 2004) and signaling components (Pérez-Pérez *et al*. 2002, 2004). Here we report on the map-based gene cloning of the *ANG3* gene, identified by the *ang3* mutant in the collection, and show that it encodes the ribosomal protein gene *RPL5B*. The *ang3* mutation affects growth and development in several organs and the cellular basis of the narrow leaves is a defect in cell growth upon measuring the epidermal cell layer. A very restricted number of genes was downregulated in the *ang3* transcriptome and suggests that the RNA polymerase II (RNAPolII) transcriptional machinery for mRNA synthesis is rather independent of translation. These results provide novel insight into the function of the ribosomal protein RLP5.

II. Results

A. *ANG3* encodes *RPL5B*

The *ang3* mutant that belongs to the *ANG* class of leaf mutants was obtained after ethyl methanesulfonate mutagenesis of the L*er* ecotype (Berná *et al*. 1999). An F2 mapping population derived from a Col-0 x *ang3* cross was used to map the *ang3* mutation at low resolution between the MBK5 and AthPHYC markers of chromosome 5 (Robles and Micol 2001). The genotyping of four new polymorphic markers in 50 additional F2 plants allowed us to localize *ANG3* within a candidate genetic interval containing 11 genes (Supplemental Table 1). The genes in this interval were analyzed for their GO classification (TAIR website) and for their expression throughout plant development with Genevestigator (Hruz *et al*. 2008). From this analysis, three genes were retained as candidate *ANG3* genes, i.e. At5g39760, coding for the ATHB23 transcription factor with specific expression in the adaxial side of the leaf (Kim *et al*. 2007), and At5g39740 and

At5g39785, coding for the ribosomal proteins RPL5B and RPL34e, respectively. As it is well-known that mutation in ribosomal proteins cause leaf phenotypes (Van Lijsebettens *et al*. 1994; Micol 2009), the *RPL5B* gene was the first candidate gene of which the sequence of the promoter and the coding region of *ang3* and L*er* were amplified and compared. The alignment showed the presence of a point mutation in the third exon, namely a change from a guanine into an adenine nucleotide and a glycine (L*er*) into an aspartate (*ang3*) at the amino acid level (Fig. 1). Thus, sequencing of the first candidate gene revealed that the *ANG3* gene corresponded to *RPL5B*, which codes for the ribosomal protein RPL5. RPL5 binds the 5S rRNA to form a ribonucleoprotein particle, which participates in the formation of the large ribosomal subunit in the nucleolus and is subsequently exported to the cytoplasm (Mathieu *et al*. 2003). The sequence of RPL5 is conserved and its homolog in *Escherichia coli* is RPL18 (BLAST analysis). In yeast, RPL5 has a supporting role in the positioning of the peptidyl-tRNA at the P-site of the ribosome to maintain the reading frame during translation (Meskauskas and Dinman 2001). The RPL5 function in 5S rRNA binding and large ribosomal subunit assembly is conserved over the different kingdoms. In the *Arabidopsis* genome, there is one homolog, *RPL5A* (At3g25520) that is extremely conserved at the amino acid level (only five amino acid substitutions); its promoter sequence is also highly conserved and Genevestigator analysis of gene expression throughout development showed that both gene copies to have a very similar expression pattern. Hence, *RPL5B* and *RPL5A* were concluded to be duplicate genes with redundant function (Moore and Purugganan 2005). Mutations in the *RPL5A* gene, *asymmetric leaves1/2 enhancer 6* (*ae6*) and *piggyback 3* (*pgy3*), have narrow pointed leaves and interact genetically with the polarity genes *AS1*, *KANADI* and *REVOLUTA* (Pinon *et al*. 2008; Yao *et al*. 2008).

A

```
                ATGgtaag ccctagctaa gatctctctt tactccatag tttcttcttg
attttctcct caggcttcag attttgggtt tcgtttcatg tagaaatctt ctgcatttca
gtttgatagt tatggtaacg agaatttcat gaacatatgg ttctattcag cttcgtagat
gtttttcttc atgggttttg gttacgactt gcttgagaat cgaaagtagc atatttgtgt
ttttgttct tgggatttag aataaagttt aagactttag atcactgatg cgtttaaagt
ttgagacttt agctttttgt tctgtggttg aggtcactgg tgcgtttaaa tgtatgatct
ttcgttcgtt actttgaaaa aaatatggtt agatctttag atttattcct ttgtatatgt
tggtagGTGT TTGTGAAGTC CTCCAAATCG AATGCTTACT TCAAGAGGTA CCAAGTGAAG
TTCAGGAGAA GGAGAGgtat tgatctgttg ttactgtcaa gctagacttc gctttttggt
ctgttatata gagtttatat gggattaggt gttgtgacct gaaagttgtt gttcttataa
tctgtagATG GGAAGACTGA TTACAGGGCA AGGATCCGTC TTATCAATCA AGACAAGAAC
AAGTACAACA CCCCTAAGTA CCGTTTTGTT GTTCGATTTA CCAACAAAGA CATTGTGGCA
CAGATTGTAT CTGCAAGCAT AGCTGGTGAC ATTGTTAAAG CTTCGGCTTA CGCACATGAG
CTTCCTCAGT ATGGACTCAC TGTTGGTCTT ACCAACTATG CTGCAGgtat tgaatcagtt
ctatactttt gttttcccaa tatttgattc tgtgtgtatg gtttcttaaa gacttaatgt
ttttgtcatg ctagCTTACT GTACTGGCCT TCTTTTGGCT CGTCGTGTTC TGAAAATGCT
GGAAATGGAT GATGAGTACG AGGGAAACGT AGAGgtatgt tgtgatcttt tatttcatct
tgaaaataaa gaaacttgag agttttcatc ttttgattaa taactgaatc aaaattgatg
aatcagGCCA CTGGAGAGGA CTTTTCTGTG GAACCAACTG ATTCCAGAAG ACCTTTCCGT
GCTCTTCTTG ATGTTGGACT TATCAGGACT ACCACTGGAA ACCGTGTGTT TGGTGCACTC
AAGgtattgt gttttaatgt ggttgtctgt gttcttatct gttgtatagt gtgttcatga
tttgaagatg atgctagcaa tcctttaata ccctgttggt ttgcttcatg aaactatagG
GAGCTTTGGA CGGAGGTCTT GATATCCCTC ACAGTGACAA GAGATTTGCT GGTTTCCACA
AAGAGAACAA GCAACTTGAT GCTGAAATCC ACAGGAACTA CATCTACGGT GGCCACGTCT
CAAACTACAT GAAGCTGTTG GGGGAAGATG AGCCGGAGAA GTTGCAAACT CACTTCAGTG
CTTACATTAA GAAAGGAGTT GAAGCTGAGA GCATCGAGGA GATGTACAAG AAGGTTCACG
CAGCTATCCG AGCAGAACCC AACC↓ATAAGA AAACCGAGAA ATCTGCTCCC AAGGAACACA
AGAGgtaaaa acaaataaac attactgcct ttaatctttc ttgttgtgat tggtttgtct
cactgggttc ttgattgatt gtgtgatatt aaacaaaaca gGTACAACTT GAAGAAACTG
ACTTACGAAG AGAGGAAGAA CAAGTTGATC GAGAGAGTGA AGGCATTAAA CGGAGCAGGT
GGTGATGATG ATGATGAGGA TGATGAAGAG TAAatcacca atcaagcctt ctttgtctca
```

B

```
  1 MVFVKSSKSN AYFKRYQVKF RRRRDGKTDY RARIRLINQD KNKYNTPKYR FVVRFTNKDI
 61 VAQIVSASIA GDIVKASAYA HELPQYGLTV GLTNYAAAYC TGLLLARRVL KMLEMDDEYE
121 GNVEATGEDF SVEPTDSRRP FRALLDVGLI RTTTGNRVFG ALKGALDGGL DIPHSDKRFA
181 GFHKENKQLD AEIHRNYIYG GHVSNYMKLL GEDEPEKLQT HFSAYIKKGV EAESIEEMYK
241 KVHAAIRAEP NHKKTEKSAP KEHKRYNLKK LTYEERKNKL IERVKALNGA GGDDDDEDDE
301 E
```

Fig. 1. *ANG3* genomic and amino acid sequences and position of mutation.

(A) Genomic sequence of At5g39740 with position of mutation (bold and shaded) and place of T-DNA insertion (SALK 010121) (arrow) (ATGC, exon; atgc, intron). (B) Amino acid sequence of At5g39740 with position of mutation (bold, boxed and shaded).

Allelism tests between *ang3* and the mutant lines, Salk_016504 (At5g39785) and Salk_081531 (At5g39760), corresponding to two of three candidate genes in the genetic interval of *ANG3*, revealed a wild-type F1 progeny and showed that the *ANG3* locus differed from the tested loci. An allelism test between *ang3* (acceptor) and a homozygous line of SALK_010121 (pollen donor) with a T-DNA insertion near the splice acceptor site of the last intron of the third candidate gene At5g39740 (*RPL5B*) (Fig. 1) resulted in a kanamycin-resistant F1 progeny with a narrow and pointed leaf phenotype similar to that of the parental lines (Fig. 2). It showed that the mutant parental lines were two different alleles of the same gene, *ANG3*/At5g39740/*RPL5B.*

Fig. 2. Allelism test. From left to right, phenotype of 2-week-old plants of L*er*, Col-0, homozygous SALK_010121, *ang3* and F_1 cross of *ang3* with SALK_010121. Bar represents 10 mm.

B. *ang3* plant morphology

The rosette leaves of the *ang3* mutants grown in rockwool or in tissue culture were narrow and elongated when compared to those of the wild type (Fig. 3A). The midvein detached from one or a few rosette or cauline leaves of some individuals resulting in sometimes in an extremely narrow and short lamina, slightly curled upwards (Fig. 3B). It could be interpreted as a reversion of dorsiventral to radial symmetry or as a loss of polarity. The leaf phenotype in the *ang3* mutant (*RPL5B* gene) was similar to those described in *ae6* and *pgy3* (*RPL5A* gene) (Pinon *et al*. 2008; Yao *et al*. 2008), although no leaf parameters in the RPL5-defective plants had been measured. We

examined leaf growth and development in more detail by measuring lamina length, width and area for every rosette leaf of 21-day-old seedlings grown in vitro. Leaf series of all rosette and cauline leaves of 10 seedlings were scanned, measured with the ImageJ program and mean values analyzed statistically by *t*-tests. The lamina area was significantly reduced starting from leaf 3, because of a reduced lamina width, and lamina length also decreased in later leaves (Fig. 4).

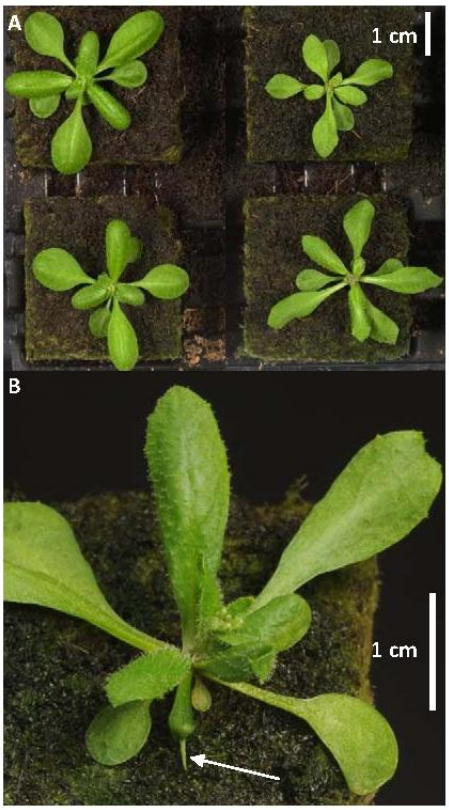

Fig. 3. *ang3* leaf phenotype.
(A) Ler (left) and *ang3* (right) plants grown for 25 days on rockwool. (B). Detached midvein at the tip of a rosette leaf lamina of an *ang3* plant. Bar represents 10 mm.

Flowering induction and leaf number were compared between *ang3* (n=58) and L*er* (n=63) plants germinated and grown on rockwool under long-day conditions. *ang3* plants flowered 1 day later than the wild type and formed an additional rosette leaf (Table 1). It is well-known that delay in flowering time is correlated with the formation of additional rosette leaves.

Table **1**. Flowering time (days) and number of leaves of L*er* and *ang3* grown on rockwool (mean ± standard deviation; *, *t*-test, P<0.05; ≠: significant different means)

Genotype	L*er*	*ang3*	*P**	Conclusion
Flowering time	24.22 ± 1.40	25.62±1.78	0	≠
Leaf number	8.97± 0.92	10.05 ± 1.02	0	≠

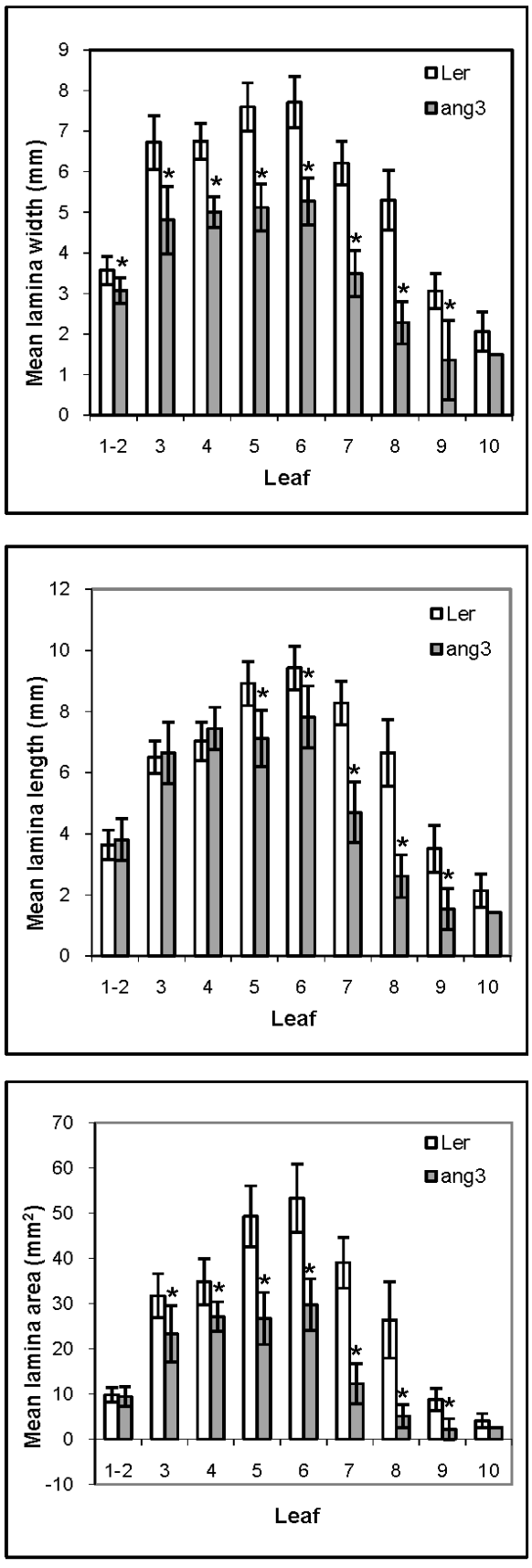

Fig. 4. Graphical representation of mean and standard deviation of lamina width (top), length (middle) and area (bottom) of the cotyledons and rosette leaves of 21-day-old L*er* and *ang3* plants grown in vitro. The asterisks indicate a statistically significant difference between mutant and wild type (*t*-test, $P<0.05$). There was only one measurement for the 10th leaf of *ang3*.

Primary root growth was monitored in *ang3* seedlings germinated in vitro on plates in vertical position, by marking the root tip every 2 days for 15 days. The primary root length was severely reduced in the *ang3* mutant (Fig. 5A) and was also apparent at every time point in the kinetics experiment (Fig. 5B). Finally, hypocotyl length was measured of seedlings germinated under long-day conditions: hypocotyl length was 0.31 ± 0.03 cm in the *ang3* mutants versus 0.37 ± 0.07 cm in the L*er* control and was significantly reduced in the *ang3* mutant.

In summary, the leaf area in *ang3* (*RPL5B*) was significantly reduced starting from leaf 3 on and in subsequent leaves predominantly because of a reduced lamina width. In addition, root and hypocotyl growth phenotypes were reported for the first time for RPL5-defective plants.

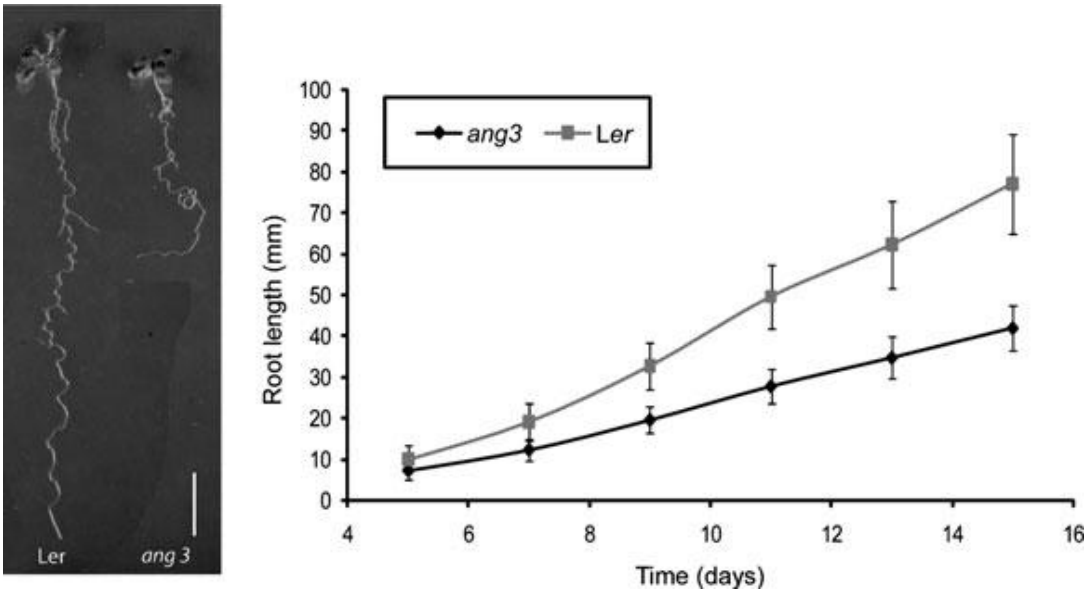

Fig. 5. Primary root growth in *ang3* mutant.
(A) Primary root length of L*er* and *ang3* 15 days after germination in vertical position. (B) Time course of primary root growth of L*er* and *ang3*. Bar represents 10 mm.

C. Cellular basis of the *ang3* leaf and root phenotype

As the cellular parameters in leaves of RPL5-defective plants had not been measured (Pinon *et al*. 2008; Yao *et al*. 2008) and only scanning electron micrographic pictures had been provided of adaxial and abaxial leaf epidermis, which were visually indistinguishable between *ae6* and wild-type plants (Yao *et al*., 2008), we analyzed the cellular basis of the narrow leaf phenotype. To this end, we measured the abaxial epidermal cell layer in fully expanded leaves 1, 2 and 3 of 21-day-old

seedlings grown in vitro as described (Cnops *et al*. 2004) and the leaf area with imageJ. The cell size between mutant and wild type for leaf 1 and 2 was similar, but was significantly reduced in leaf 3 in the *ang3* mutant (Table 2), corresponding with our previous measurements (Fig. 4) that revealed a significant difference only in lamina area from leaf 3 on and subsequent ones. Therefore, the cellular analysis was restricted to that of the third leaf. Leaves were cleared of chlorophyll, mounted on slides and their abaxial epidermal layer analyzed under differential interference contrast microscopy. Cells were drawn and subsequently measured by ImageJ. The total number of cells calculated in leaf 3 was 1892 in L*er* and 2123 in *ang3*. The cell area of all cell types in the abaxial epidermis was measured. The values were ln-transformed to obtain a normal distribution required for a *t*-test. The cell area did not differ in leaves 1 and 2 between the *ang3* mutant and L*er*, but was significantly reduced in leaf 3 in the *ang3* mutant (Table 3). The number of cells per mm^2 was calculated from the drawings and was significantly larger in leaf 3 of the mutant. However, the total number of cells per lamina did not differ significantly between *ang3* and wild type (Table 4). In summary, the lamina area was smaller in the *ang3* mutant because of the reduced cell area, whereas the total cell number remained the same as in the wild type.

Primary root tips of 4 day-old *ang3* and L*er* seedlings germinated in vitro in vertical position were stained with propidium iodide and the red fluorescent cell periphery was visualized with confocal microscopy. No obvious defects in the root apical meristem cellular structure were observed in the *ang3* mutant. The length of cortex cells in the mature zone of primary roots of 15 seedlings grown for 11 days in vertical position was significantly reduced in the *ang3* mutant (145 ± 45 µm, n=300) as compared to L*er* (157 ± 41 µm, n=273) ($p<0.001$). It showed that reduced primary root length was caused by reduced cell expansion.

Table **2**. Leaf area (mm²) of 21-day-old plants of L*er* and *ang3* grown in vitro (mean and standard deviation;*, *t*-test, P<0.05; =: equal means; ≠: significant different means)

Leaf	Genotype	Mean leaf area (mm²)	*P**	Conclusion
1 and 2	L*er*	17.47 ± 0.47		
	ang3	16.74 ±6.17	0.851	=
3	L*er*	37.10 ± 3.40		
	ang3	29.71 ±7.93	0.099	≠

Table **3**. Cell area (mm²) and of the logarithmic transformation of this cell area (ln(cell area)) for 21-day-old plants of L*er* and *ang3* grown in vitro. For leaf 1/2 of L*er* and *ang3*, the means were calculated from 1369 and 1503 cells; respectively, and for leaf 3 from 1892 and 2123 cells, respectively (mean and standard deviation; **t*-test, P<0.05 for ln(cell area); =: equal means; ≠: significant different means

Leaf	Genotype	Cell area (mm²)	ln(cell area)	P*	Conclusion
1/2	L*er*	5.97E-04 ± 8.50E-04	-8.14 ± 1.19		
	ang3	6.96E-04 ± 1.00E-03	-8.13 ± 1.22	0.831	=
3	L*er*	6.17E-04 ± 1.00E-03	-8.22 ± 1.25		
	ang3	4.27E-04 ± 7.10E-04	-8.50 ± 1.16	0	≠

Table **4**. Calculated number of cells per lamina for 21-day-old plants of L*er* and *ang3* grown in vitro (mean and standard deviation; *, t-test, P<0.05; =: equal means)

Leaf	Genotype	Mean number of cells per lamina	*P**	Conclusion
1/2	L*er*	28,706 ± 3206		
	ang3	22,727 ± 8642	0.314	=
3	L*er*	60,440 ± 8676		
	ang3	68,438 ± 13,303	0.310	=

D. Transcriptome analysis in *ang3* mutants

Total RNA was extracted from the green parts of stage 1.03 (Boyes *et al*. 2001) mutant and wild-type plants and an Agilent microarray analysis was carried out on four replicates. After normalization of the hybridization signals, differentially expressed genes between L*er* and *ang3* were analyzed with the BiNGO program (Maere *et al*. 2005) that visualizes the overrepresented GO categories within the gene set. The number of upregulated and downregulated genes between L*er* and *ang3* was 222 and only 63, respectively. The BiNGO analysis of the 222 upregulated genes at

significance level 0.05 for overrepresentation of GO categories revealed just a limited number of classes (Supplemental Table 2). We were especially interested in the downregulated genes of the dataset because *ang3* is a recessive mutation and a loss-of-function mutation might cause downregulation of a number of molecular processes as primary effect. BiNGO analysis of these 63 genes (Supplemental Table 3) at the significance level 0.05 did not show in any overrepresentation of GO classes, therefore the significance level was reduced to 0.16, with a few GO classes as a result, such as trichome differentiation and patterning and reaction to light (Supplemental Table 4). *MYB23* (At5g40330), which is partially redundant with *GLABRA1* (Kirik *et al*. 2005), and *MYB5* (At3g13540) (Li *et al*., 2009) encode transcription factors responsible for trichome differentiation and trichome patterning that were downregulated in the *ang3* mutant microarray data set. qPCR confirmed (Fig. 6A) that both genes are significantly (Student *t*-test, $p<0.1$ for *MYB23* and $p<0.01$ for *MYB5*) downregulated in the *ang3* mutant compared to the wild type in three biological repeats. Trichome density of leaves 1, 2, 3 and 4 of 21-day-old seedlings grown in vitro was measured in two independent experiments and was significantly reduced in *ang3*, when compared to L*er* (Table 5; Fig. 6B), indicating that the reduced expression level of *MYB23* and *MYB5* was biologically relevant.

Amongst the differentially expressed genes that were up- or downregulated in the microarray dataset, no polarity genes, such as *AS1*, *KANADI* or *REVOLUTA*, no KNOX-type meristem identity genes, no genes related to hormonal signaling or cell wall loosening (Supplemental Tables 2 and 4) were found that could explain the cell growth defect observed in the *ang3* mutant. Hence, the growth defects observed in RPL5-depleted plants were not the consequence of changes in transcript levels in relevant pathways.

Table 5. Trichome density in number of trichomes per mm² of L*er* and *ang3* and comparison with a *t*-test (mean and standard deviation;*, t-test, $P<0.05$; ≠: significant different means)

Leaf	Genotype	Trichome density per genotype	*P**	Conclusion
1-2	L*er*	0.4318 ± 0.1538	0	≠
	ang3	0.14386 ± 0.1251		
3	L*er*	0.6189 ± 0.2729	0	≠
	ang3	0.2394 ± 0.1375		
4	L*er*	0.6489 ± 0.1633	0.001	≠
	ang3	0.3287 ± 0.2412		

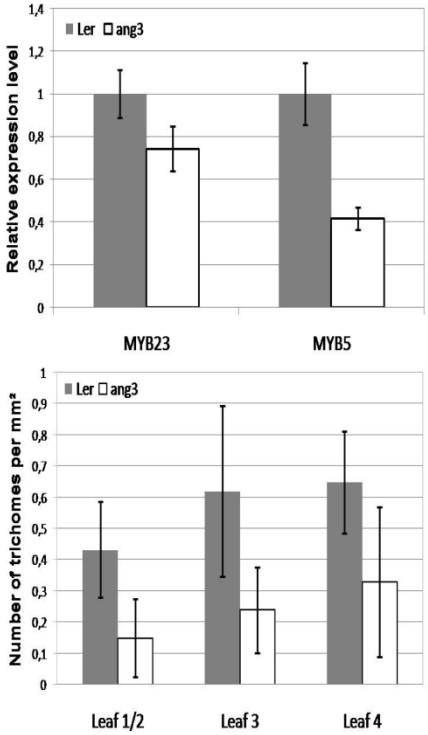

Fig. 6. Trichome density in ang3 mutants
(A) Relative expression level of *MYB23* and *MYB5* in green parts of *ang3* stage 1.03 seedlings compared to the wild type with qPCR. (B) Mean and standard deviation of the trichome density of L*er* and *ang3* per leaf type.

E. Discussion

Ribosomal proteins are usually encoded by several gene copies in the *Arabidopsis* genome, a number of reports exist on the differential expression patterns of the gene copies encoding a specific ribosomal protein (Ito *et al*. 2000; Micol 2009). *RPL5B*, identified by the *ang3* mutation, is a duplicate gene of *RPL5A* (Pinon *et al*. 2008; Yao *et al*. 2008) as shown by BLAST search and sequence alignment and are probably functionally redundant because of the high sequence

conservation at the promoter and coding sequences and similar expression pattern throughout development according to Genevestigator analysis. Indeed, the *ang3* mutation caused reduced lateral growth of the leaf lamina that was very similar to the narrow leaf phenotype seen in the *ae6* and *pgy3* mutations in the *RPL5A* gene copy (Pinon *et al*. 2008; Yao *et al*. 2008). These mutations interacted genetically with polarity genes that positioned the ribosomal protein RPL5 in the genetic pathway controlling dorsiventral asymmetry (Pinon *et al*. 2008; Yao *et al*. 2008). As no cellular measurements of the epidermal cell layer had been done on the *ae6* and *pgy3* mutants to understand the cellular basis of the narrow leaf phenotype, we investigated the lamina area in *ang3* and found that it was significantly reduced from leaf 3 on and in subsequent rosette leaves. The total number of cells in the epidermal layer of the third leaf in *ang3* was equal to that of the wild type, but the cell area was significantly smaller. Thus, the reduced leaf width and area were the consequence of decreased cell expansion rather than cell number. This reduced cell size might be explained by a shift towards the meristematic state and a retarded transition to the cell differentiation state, possibly provoking a prolongation of the cell proliferation as part of the so-called compensation mechanism described before (Ferjani *et al*. 2007). Indeed, reduced cell proliferation induced increased cell area in leaves of plants mutated for a cell cycle inhibitor (De Veylder *et al*. 2001) and was explained as a way to compensate for reduced leaf area. It is not clear whether a reduced cell area could provoke prolongation of cell division in leaves as part of the compensation mechanism. In either case, a reduced cell area in the epidermal cell layer might explain the narrow leaf size in the *ang3* mutants, because the L1 layer is an important determinant in leaf size and shape (Dolan and Poethig 1998).

Furthermore, the hypocotyl length was reduced as well in the *ang3* mutant probably due to decreased cell size, because hypocotyls grow mainly by cell expansion, while cell division is negligible (Gendreau *et al*. 1997). Primary root length was also severely reduced in *ang3* mutants because of reduced cell length, which was not described in *ae6* and *pgy3* mutants. In contrast to leaves that grow according to proximo-distal, medio-lateral and dorsiventral axes, roots and hypocotyls grow according to proximo-distal and radial axes. Therefore, besides its described effect on leaf polarity, reduced levels of RPL5 affect general growth processes in a number of organs that are not related to axis formation.

Decreased RPL5 levels in plants putatively lead to impaired translation because they are important for the recruitment of the 5S rRNA, the assembly of the large ribosomal subunit and the

maintenance of the reading frame during translation, possibly explaining the reduced cell size and coinciding with the lessened cell growth seen in mutants of the corresponding genes in *E. coli* and yeast (Korepanov *et al*. 2007; Moradi *et al*. 2008). Measurement of translational efficiency usually relies on reporter gene constructs and in vitro transcription-translation systems, such as wheat germ; hence it is not obvious to compare translational efficiencies between mutant and wild-type plant genotypes. Intriguingly, no important effect on the transcriptome was observed in the *ang3* mutants. Only a few GO classes were overrepresented at significance level 0.05 amongst the differentially expressed genes and no genes were present with a function in polarity, stem cell identity or maintenance, hormonal signaling, or cell wall loosening that could explain the growth phenotype. This result indicated that the organ and cell growth defects as well as the leaf polarity defect in RPL5 deficient plants were not due to an effect at the transcriptional level of expansins, *KANADI* or *YABBY* genes and that the phenotypes might rather result from a reduced general translation or, more specifically, from a shortage in polarity proteins and cell wall loosening enzymes. Indeed, reduced ribosome assembly or malfunctioning of the ribosome could become limiting for the translation of particular transcripts at specific stages of development or under stress conditions.

Our transcriptome data suggest that RNAPolII-mediated mRNA transcription is robust and quite independent of translation efficiency. However, a limited number of transcripts is significantly reduced, such as those of *MYB23* and *MYB5*, resulting even in reduced trichome density in the *ang3* mutant. The putatively limiting MYB23 and MYB5 proteins in the *ang3* mutant might have a regulatory effect on the transcription of their own open reading frame. In conclusion, our data are in support of translation representing another level of control of growth and developmental processes in plants.

III. Materials and Methods

Plant material and growth conditions The *Arabidopsis thaliana* (L.) Heyhn. ecotypes Landsberg *erecta (*L*er*) and Columbia (Col) were obtained from the Nottingham Arabidopsis Seed collection.The *ang3* mutants were in L*er* background (Berná *et al*. 1999) and Salk_010121 (Alonso *et al*. 2003), homozygous for the T-DNA insertion in At5g39740, in Col background. Seeds were sterilized in 5% bleach with 0.05% Tween20 for 10 min, washed and germinated on germination medium (Valvekens *et al*. 1988) and grown aseptically either horizontally on round Petri dishes

(Falcon 1013; BD Biosciences, Franklin Lakes, NJ, USA) or vertically on square plates. Plants were germinated in rockwool, watered every 2 days with 0.5 g/ L Hyponex solution (N:P:K = 7:6:19) (HYPONeX, Osaka, Japan) and grown at 21˚C, 100 $\mu EM^{-2}h^{-1}$ photosynthetically active radiation (cool white lamps; Radium, Wipperfürth, Germany) in a 16-h light regime, and 50% relative humidity.

Morphological analysis Leaf series were made of L*er* and *ang3* seedlings, grown for 21 days in vitro, on large plates containing 1% plant tissue culture agar, and photographed. Lamina length, width and area were measured by the ImageJ program (*rsbweb.nih.gov/ij/download.html)*. Primary root length of seedlings grown in vitro in vertical position was marked every 2 days for 15 days. The plates were scanned and the primary root length analyzed by ImageJ. Hypocotyls of these 15-day-old seedlings were dissected, transferred to agar plates, photographed and their length measured by ImageJ.

The trichomes on the adaxial side of leaf 1, 2, 3 and 4 of L*er* and *ang3* seedlings grown for 21 days in vitro were counted under a binocular microscope. The lamina area was measured by the Image J programme and the trichome density calculated as the number of trichomes per mm^2 lamina area. Two biological repeats were done.

t-tests were applied on the mean values of the normally distributed datasets of *ang3* and L*er* seedlings (ln transformation was done of the cell area measurement dataset to obtain normal distribution) with the Statistical Package for the Social Sciences program (SPSS Inc, Chicago, IL, USA) program.

Cellular analysis Leaves of L*er* and *ang3* seedlings grown for 21 days in vitro were cleared overnight in ethanol, transferred a few minutes in Hoyer medium (100 g chloral hydrate, 5 ml glycerol, and 30 ml distilled water) to remove starch and kept in 90% lactic acid. The lower epidermis of leaf 1, 2 and 3 was visualized with differential interference contrast microscopy and drawn with a drawing tube, scanned and analyzed by ImageJ. The cell area of the drawing and the total leaf area were measured (Cnops *et al*. 2004), while the total number of cells was calculated (De Veylder *et al*. 2001). Primary roots of 4 day-old seedlings germinated in vitro were stained with propidium iodide (10 µg/ml) for 15 min in order to visualize the cell walls and hence the cellular structure of the root tip with a confocal microscope 100M with software package LSM 510

version 3.2 (Zeiss, Jena, Germany) at 543 nm wave length using RFP laser. Seedlings, grown for 11 days on germination medium (Valvekens *et al*., 1988), were fixed in 70 % ethanol overnight, transferred to lactic acid and stored at room temperature in the dark. Primary roots were mounted on microscope slides, cortex cells in the mature zone were visualized with Normaski differential interference contrast optics and cell lengths measured with ImageJ (Fleury *et al*., 2007).

Transcriptome analysis *ang3* and L*er* seedlings were sown in vitro on half-strength Murashige and Skoog medium, vernalized for 3 days and germinated at 21°C and under a 16-h light regime. The green parts of stage 1.03 plants were harvested (Boyes *et al*. 2001), consisting of the SAM, the first and second young leaves, the third leaf larger than 1 mm, the fourth leaf smaller than 1 mm and the cotyledons. Per genotype, four replicates were harvested and per replica three repetitions. Total RNA was extracted with the RNeasy Plant Mini Kit (Qiagen, Hilden, Germany) and the samples analyzed In the VIB MicroArrays Facility with the Agilent microarray platform. The processed Cy3 and Cy5 intensities were normalized and statistically analyzed with the Feature Extraction Software (version 10.1.1.1; Agilent Technologies, Santa Clara, CA, USA). *P* values had to be lower than 0.05 and the absolute value of the log2 ratio had to be higher than one. To visualize overrepresented Gene Ontology (GO) categories, upregulated and downregulated data sets were analyzed with BiNGO (Maere *et al*. 2005; Fleury *et al*. 2007).

Quantitative PCR analysis Total RNA from the green parts of 1.03 stage seedlings, germinated in vitro was extracted with the RNeasy Plant Mini Kit (Qiagen, Hilden, Germany) followed by first-strand cDNA synthesis (Superscript III; Invitrogen, Carlsbad, CA, USA). cDNA was amplified in real-time quantitative PCR with the Platinum SYBR Green qPCR Supermix-UDG (Invitrogen). The fluorescent dye was detected with the iCycler (BioRad, Hercules, CA, USA) and relative cDNA concentration was determined with the comparative Ct method (qBasePlus; Biogazelle, Zulte, Belgium). Samples were normalized using an endogenous actin housekeeping gene (At3g60830).

Sequence analysis of *RPL5B* The *RPL5B* gene was identified as the first candidate gene in the genetic interval around *ANG3* and was amplified from the *ang3* and L*er* genomic DNA in several independent polymerase chain reaction amplifications. The sequences were compared and the point

mutation identified as being present in all independent amplifications. Primers for the RPL5B amplification were: At5g39740-1F, CGTGTCCGTTGATTAGAAGAG; At5g39740-1R, CCATACTGAGGAAGCTCATGT; At5g39740-2F, GAGCTTTGGACGGAGGTCTT; At5g39740-2R, TACATGTACTTTACGAAGATAATC; At5g39740-3F, CCGTGCTCTTCTTGATGTTGG; At5g39740-3R, AAGCTACTAGAGGCATGAGAC.

IV. Supplemental data

Table S1. Genetic interval of *ANG3* after fine-mapping (F: Foreward, R: Reverse)

Position in genome (bp)	Strand	Gene code	Description
15916874 - 15917881	F	At5g39720	Avirulence induced gene 2 like protein (AIG2L)
15918907 - 15920098	F	At5g39730	Avirulence-responsive protein-related/ avirulence induced gene 2 like protein
15920524 - 15922692	F	At5g39740	60S ribosomal protein L5-like (RPL5B)
15924103 - 15925170	F	At5g39750	Agamous-like 81 (AGL81), embryodefective 3008 (EMB3008), MADS-box
15928644 - 15930058	F	At5g39760	Arabidopsis thaliana homeobox protein 23 (ATHB23), contains a ZF-HD homeobox protein domain with Cys/His-rich dimerisation region
15936469 - 15944777	R	At5g39770	Repair endonuclease, MKM21.10, non-function pseudogene homologous to AtMSU81 (At4g30870)
15946416 - 15949504	F	At5g39785	Contains a Ribosomal Protein L34e domain and a domain with unknown function DUF1666
15949942 - 15952489	R	At5g39790	5'-AMP-activated protein kinase beta1 subunit related
15952692 - 15954360	F	At5g39800	60S ribosomal protein-related
15954506 - 15955572	R	At5g39810	AGL98, MADS box
15956528 - 15957719	R	At5g39820	Arabidopsis NAC domain containing protein 94 (ANAC094), contains a No apical meristem (NAM) protein domain

Table S2. Output of the BiNGO analysis of the 222 upregulated genes of *ang3* versus Ler at a significance of 0.05. The comparison is made with a total number of 20916 genes of Arabidopsis thaliana. (x: the number of genes in the test set annotated to a certain GO class, n: the number of genes in the reference set (Arabidopsis thaliana genome) annotated to a certain GO class, X: the total number of genes in the test set. This number is different from the number of upregulated genes (222) because the genes without any annotation are discarded.)

GO ID	Corrected *P* value	x	n	X	Description
9718	4.1699E-3	3	8	143	Anthocyanin biosynthetic process
46283	4.4231E-3	3	10	143	Anthocyanin metabolic process
46148	2.8429E-2	4	49	143	Pigment biosynthetic process
42440	3.3372E-2	4	58	143	Pigment metabolic process
42991	3.3372E-2	2	6	143	Transcription factor import into nucleus

Table S3. Significantly downregulated genes (63) in *ang3*

Gene code	Short description	log2-ratio *ang3*/L*er*
At5g55720	pectate lyase family protein similar to pectate lyase	-1.05108
At2g45135	expressed protein	-1.23501
At2g25780	hypothetical protein	-2.14837
At2g35310	transcriptional factor B3 family protein	-1.44243
At5g02170	amino acid transporter family protein	-1.13055
At5g56910	expressed protein	-1.48455
At4g34580	SEC14 cytosolic factor	-1.24299
At5g60780	high-affinity nitrate transporter	-1.76836
At3g16150	L-asparaginase. putative/L-asparagine amidohydrolase	-1.86537
At1g04660	glycine-rich protein	-1.27805
At1g11740	ankyrin repeat family protein	-2.39278
At5g02540	short-chain dehydrogenase/reductase (SDR) family protein	-1.30172
At2g25820	transcription factor. putative similar to TINY	-2.00419
At2g42120	DNA polymerase delta small subunit-related	-1.04913
At1g33340	epsin N-terminal homology (ENTH) domain-containing protein	-1.14432
At1g23110	hypothetical protein	-1.20985
At2g04032	metal transporter. putative (ZIP7)	-1.38187
At5g40330	myb family transcription factor: MYB23	-1.19218
At3g02125	hypothetical protein	-1.05856
TC267084	Q9LN00. T6D22.16. partial (81%)	-2.21093
At5g48700	ubiquitin-related contains similarity to SP-O1335	-1.79913
At1g59030	GDSL-motif lipase. putative similar to family II lipase EXL3	-1.38351
At1g58725	GDSL-motif lipase. putative similar to family II lipases EXL3. EXL1. EXL2	-1.57077
At4g13560	late embryogenesis abundant domain-containing protein	-1.00218
At1g29270	expressed protein	-1.18217
At1g01190	cytochrome P450	-1.80542
At2g26150	heat shock transcription factor family protein	-1.28281
At2g34060	peroxidase. putative similar to peroxidase ATP20a	-1.00835
At2g30670	tropinone reductase. putative/tropine dehydrogenase	-1.28873
At3g13540	myb family transcription factor: MYB5	-1.26877
At5g26200	mitochondrial substrate carrier family protein	-1.00743
At5g24420	glucosamine/galactosamine-6-phosphate isomerase-related	-1.08316
At5g09300	2-oxoisovalerate dehydrogenase	-1.17281
At1g74000	strictosidine synthase family protein	-1.21781
At5g44440	FAD-binding domain-containing protein	-3.30860
At1g11340	S-locus lectin protein kinase family protein	-1.01648
At3g36659	invertase/pectin methylesterase inhibitor family protein	-1.12505
At1g56680	glycoside hydrolase family 19 protein	-1.67336
At4g03610	phosphonate metabolism protein-related weak similarity to PhnP protein	-1.55196
At1g52830	auxin-responsive protein/indoleacetic acid-induced protein 6 (IAA6)	-1.18345
At1g19640	S-adenosyl-L-methionine:jasmonic acid carboxyl methyltransferase (JMT)	-1.76025
At3g03910	glutamate dehydrogenase	-1.17217
At3g20360	meprin and TRAF homology domain-containing protein	-1.90613
At1g70870	major latex protein-related	-1.11437
At1g69470	hypothetical protein	-1.06760
At3g54490	eukaryotic rpb5 RNA polymerase subunit family protein	-1.23277
At3g56220	expressed protein	-1.63158
At3g22830	heat shock transcription factor family protein	-1.17128
At1g60987	expressed protein	-1.20296
At5g59330	hypothetical protein	-1.24183
At5g50790	nodulin MtN3 family protein	-1.34545
At4g20140	leucine-rich repeat transmembrane protein kinase	-1.05502
At1g66460	protein kinase family protein	-1.26447
At3g47360	short-chain dehydrogenase/reductase (SDR) family protein	-1.96550
At1g65450	transferase family protein	-1.29919
At1g22120	hypothetical protein	-1.30730
At5g25880	malate oxidoreductase	-1.14989
At1g19510	myb family transcription factor	-1.41347
At1g50470	hypothetical protein	-1.06935
At2g02795	hypothetical protein	-1.14818
At5g15800	developmental protein SEPALLATA1/floral homeotic protein (AGL2) (SEP1)	-1.80534
At2g28210	carbonic anhydrase family protein similar to storage protein (dioscorin)	-2.49533
At3g01015	expressed protein	-1.44938

Table S4. Output of the BiNGO analysis of the 63 downregulated genes of *ang3* versus L*er* at a significance of 0.16. The comparison is made with a total number of 20916 genes of *Arabidopsis thaliana* (x: the number of genes in the test set annotated to a certain GO class. n: the number of genes in the reference set (*Arabidopsis thaliana* genome) annotated to a certain GO class. X: the total number of genes in the test set. This number is different from the number of downregulated genes (63) because the genes without any annotation are discarded.)

GO ID	Corrected *P* value	x	n	X	Description
9644	1.5759E-1	2	28	50	Response to high light intensity
35315	1.5759E-1	2	35	50	Hair cell differentiation
10026	1.5759E-1	2	35	50	Trichome differentiation
9642	1.5759E-1	2	38	50	Response to light intensity
10037	1.5759E-1	1	2	50	Response to carbon dioxide
48629	1.5759E-1	1	2	50	Trichome patterning

Table S5. Significantly upregulated genes (222) in *ang3*.

Gene code	Short description	log2-ratio *ang3*/L*er*
At1g73810	expressed protein	2.55653
At3g15310	expressed protein	2.60427
At5g52760	heavy-metal-associated domain-containing protein	2.56278
At5g60250	zinc finger (C3HC4-type RING finger) family protein	3.97740
At2g38340	AP2 domain-containing transcription factor. putative (DRE2B)	2.34028
At2g04050	MATE efflux family protein similar to ripening regulated protein DDTFR18	2.73347
CHR1:024129752-024129811		1.48546
At4g25330	expressed protein	2.67095
At5g57980	eukaryotic rpb5 RNA polymerase subunit family protein	1.58144
At5g14490	no apical meristem (NAM) family protein	3.54587
At1g36180	acetyl-CoA carboxylase 2 (ACC2) nearly identical to acetyl-CoA carboxylase 2 (ACC2)	3.16400
At5g03090	hypothetical protein	3.36197
At2g21450	SNF2 domain-containing protein/helicase domain-containing protein	1.58515
At5g53230	hypothetical protein	4.21601
At5g48850	male sterility MS5 family protein	2.09820
At1g71280	DEAD/DEAH box helicase	3.42245
At3g54730	hypothetical protein	4.77628
At2g29350	tropinone reductase. putative/tropine dehydrogenase	2.42492
At1g55030	F-box family protein	2.17354
At2g10440	hypothetical protein	1.66114
At1g49700	expressed protein	1.02951
At1g23410	ubiquitin extension protein. putative/40S ribosomal protein S27A (RPS27aA)	1.30735
At5g65850	F-box family protein	1.86782
At4g13680	hypothetical protein	4.38859
At4g01980	hypothetical protein	2.62203
At3g14700	expressed protein	1.63369
At3g26840	esterase/lipase/thioesterase family protein	1.11728
At5g59390	XH/XS domain-containing protein	4.94009
CHR3:007367507-007367566		1.69095
At2g16570	amidophosphoribosyltransferase/glutamine phosphoribosylpyrophosphate	2.19555
At3g62460	amidotransferase/phosphoribosyldiphosphate 5-amidotransferase expressed protein	1.12042

At5g19700	MATE efflux protein-related	2.18912
At1g09932	phosphoglycerate/bisphosphoglycerate mutase-related	1.27330
At2g05915	hypothetical protein	3.24335
At5g14010	zinc finger (C2H2 type) family protein	3.03468
At3g02810	protein kinase family protein	3.01888
At3g28500	60S acidic ribosomal protein P2 (RPP2C)	2.65841
At2g47780	rubber elongation factor (REF) protein-related	1.86749
CHR5:017326114-017326173		3.91040
At1g78190	expressed protein	1.05607
A_84_P22079		1.32869
At4g21990	5'-adenylylsulfate reductase (APR3)/PAPS reductase homolog (PRH26)	1.16584
At4g04830	methionine sulfoxide reductase domain-containing protein/SeIR domain-containing protein	1.10902
At2g47680	zinc finger (CCCH type) helicase family protein	1.07570
CHR1:015298370-015298429		1.65449
At5g52390	photoassimilate-responsive protein	1.69579
CHR4:007358551-007358610		1.65931
CHR1:010776117-010776176		1.50699
At2g14560	expressed protein	1.90215
At3g15357	expressed protein	1.51545
At4g09820	basic helix-loop-helix (bHLH) family protein	1.72068
At5g34838	hypothetical protein	1.24417
At1g26590	zinc finger (C2H2 type) family protein	1.01585
CHR3:016824027-016823968		1.98865
At2g02000	glutamate decarboxylase	1.85499
At4g08593	expressed protein	2.72783
At5g11410	protein kinase family protein	2.02678
At4g29200	hypothetical protein	3.89747
At1g60720	hypothetical protein	1.02782
NP454445	unknown protein	2.25945
At3g18610	nucleolin	2.59818
CHR1:007542907-007542848		4.07097
At2g21900	WRKY family transcription factor	1.20783
At1g69310	WRKY family transcription factor	1.58469
At1g56120	leucine-rich repeat family protein/protein kinase family protein	1.04737
At5g55270	hypothetical protein	3.21057
At3g25080	hypothetical protein	1.18251
At1g34315	expressed protein	1.35900
At5g33330	RNase H domain-containing protein	2.35274
At5g53240	expressed protei	3.82337
TC255286	Q9LR73 (Q9LR73) F21B7.12	1.58700
At1g35617	hypothetical protein	2.32996
NP301363	contains similarity to retroelement pol polyprotein gene_id:MSA6.7	2.54648
At4g22880	leucoanthocyanidin dioxygenase. putative/anthocyanidin synthase	1.48893
At3g24780	hypothetical protein	2.31518
At5g56810	F-box family protein	1.04817
At5g51330	meiosis protein-related (DYAD) (SWI1)	1.82845
At5g52740	heavy-metal-associated domain-containing protein	1.81273
CHR3:007355274-007355333		2.38453
At1g44830	AP2 domain-containing transcription factor TINY	1.04856
At5g35480	expressed protein	1.17340
At1g05710	ethylene-responsive protein	1.03158
At2g34655	expressed protein	2.54834
At3g58270	meprin and TRAF homology domain-containing protein/MATH domain-containing protein similar to ubiquitin-specific protease 12	2.11624

At4g28870	hypothetical protein	2.31226
At1g71770	polyadenylate-binding protein 5 (PABP5)	1.85327
At1g17960	threonyl-tRNA synthetase. putative/threonine--tRNA ligase	3.78351
At1g52905	expressed protein	3.03611
CHR2:011336004-011336063		2.40882
At3g42850	galactokinase	1.51200
At3g29590	transferase family protein	1.55963
At2g18720	eukaryotic translation initiation factor 2 subunit 3. putative/eIF2S3. putative/eIF-2-gamma. putative	2.33667
At2g42720	F-box family protein contains F-box domain	1.51748
At2g43590	chitinase	1.83110
At4g16215	expressed protein	6.26756
At2g36985	expressed protein	1.72924
At3g44040	expressed protein	1.72654
At4g39500	cytochrome P450	2.25553
At4g11350	fringe-related protein	1.44172
At1g05480	SNF2 domain-containing protein/helicase domain-containing protein	2.28554
At1g03710	expressed protein	2.03665
At4g12950	hypothetical protein	1.99442
At5g44570	hypothetical protein	2.05220
At5g27960	MADS-box protein (AGL90)	2.16404
At1g52000	jacalin lectin family protein	1.21748
At1g03420	expressed protein	1.79995
At5g58460	cation/hydrogen exchanger. putative (CHX25)	1.39534
At2g14560	expressed protein	1.95314
At3g27630	hypothetical protein	1.35740
At5g66150	glycosyl hydrolase family 38 protein	1.68662
At5g07990	flavonoid 3'-monooxygenase/flavonoid 3'-hydroxylase (F3'H)/cytochrome P450 75B1 (CYP75B1)/transparent testa 7 protein (TT7)	1.48602
At5g24910	cytochrome P450 family protein	2.15648
At5g01080	hypothetical protein	4.47590
At2g29350	tropinone reductase. putative/tropine dehydrogenase	2.73134
At2g14630	hypothetical protein	2.11013
At2g38250	DNA-binding protein-related	2.51063
At4g18330	eukaryotic translation initiation factor 2 subunit 3. putative/eIF2S3. putative/eIF-2-gamma	1.25184
At3g28330	F-box family protein-related	1.71197
CHR2:002326124-002326183		1.94699
At5g61740	ABC transporter family protein ABC family transporter	2.77925
At3g15720	glycoside hydrolase family 28 protein/polygalacturonase (pectinase) family protein	1.20047
At1g33860	hypothetical protein	2.64473
At3g24790	protein kinase family protein	1.02439
At1g29195	expressed protein	1.05746
CHR3:011485245-011485304		2.33150
CHR1:017326959-017327018		1.70491
At4g15910	drought-responsive protein/drought-induced protein (Di21)	1.24728
At1g73810	expressed protein	2.57152
At5g15690	hypothetical protein	2.58809
At5g49520	WRKY family transcription factor	1.66634
At4g14090	UDP-glucoronosyl/UDP-glucosyl transferase family protein	1.55229
At1g31580	expressed protein identical to ORF1	1.31390
At2g03130	ribosomal protein L12 family protein	4.48403
At2g30770	cytochrome P450 71A13	2.44091
At5g66052	expressed protein	2.38468
At4g07526	hypothetical protein	3.34255
At1g30170	hypothetical protein	3.78114

At5g24280	expressed protein	1.87847
NP454953	En/Spm-like transposon protein	1.44378
AA041063		3.43805
At1g62440	leucine-rich repeat family protein/extensin family protein	1.02861
At5g07610	F-box family protein	2.23419
At2g30250	WRKY family transcription factor	1.19960
At1g58025	DNA-binding bromodomain-containing protein	4.40923
At5g26690	heavy-metal-associated domain-containing protein	1.63452
At3g61630	AP2 domain-containing transcription factor	2.26079
At3g57240	beta-1.3-glucanase (BG3)	2.88509
At3g48770	hypothetical protein	1.44438
At1g27820	CCR4-NOT transcription complex protein	1.41497
At4g25200	23.6 kDa mitochondrial small heat shock protein (HSP23.6-M)	2.09327
TC259648	Q9LQF9 (Q9LQF9) F15O4.26. complete	4.00642
At3g28580	AAA-type ATPase family protein	2.79141
At2g38185	zinc finger (C3HC4-type RING finger) family protein	3.39227
At4g22870	leucoanthocyanidin dioxygenase. putative/anthocyanidin synthase	1.61004
TC256991		2.50540
At5g60900	lectin protein kinase family protein	1.79580
At3g30160	hypothetical protein	2.33320
At5g24780	vegetative storage protein 1 (VSP1)	1.36143
At4g01525	expressed protein	1.03595
CHR2:002264420-002264479		2.45368
At4g17470	palmitoyl protein thioesterase family protein	1.36676
At1g28480	glutaredoxin family protein	2.48480
At1g65370	meprin and TRAF homology domain-containing protein/MATH domain-containing protein	1.72090
At1g14880	expressed protein	1.94555
At3g22860	eukaryotic translation initiation factor 3 subunit 8	3.26975
CHR5:006663828-006663769		2.21974
At4g17710	homeobox-leucine zipper family protein/lipid-binding START domain-containing protein	1.92144
At5g22380	no apical meristem (NAM) family protein	1.93730
At5g18270	no apical meristem (NAM) family protein	1.58953
At2g41590	expressed protein	3.30277
TC273971	Q8WM48 (Q8WM48) MHC class II antigen alpha chain DAAg1 (Fragment). partial (7%)	2.82427
At1g52400	glycosyl hydrolase family 1 protein/beta-glucosidase. putative (BG1)	1.28358
At3g18320	F-box family protein contains Pfam PF00646: F-box domain	1.17172
At4g05380	AAA-type ATPase family protein	3.53784
At4g03320	chloroplast protein import component-related	1.52215
At4g02520	glutathione S-transferase. putative	1.27757
At3g25790	myb family transcription factor	1.72460
At3g27040	meprin and TRAF homology domain-containing protein/MATH domain-containing protein	2.05232
At4g05040	ankyrin repeat family protein	1.41154
At1g21520	expressed protein	1.55373
At1g35710	leucine-rich repeat transmembrane protein kinase	2.06262
TC256991		2.50540
At2g02520	hypothetical protein	1.25697
At4g35720	expressed protein	1.21453
At5g53290	AP2 domain-containing transcription factor	1.07053
At1g27030	expressed protein	1.01732
At4g14400	ankyrin repeat family protein	1.31390
At1g35730	pumilio/Puf RNA-binding domain-containing protein	1.15614
At5g54060	glycosyltransferase family protein	1.69094
At5g54610	ankyrin repeat family protein	2.15553
At4g39590	kelch repeat-containing F-box family protein	2.20325

CHR3:021340261-021340320		2.19024
At3g01600	no apical meristem (NAM) family protein	3.48240
At5g55790	expressed protein	3.06775
CHR3:021334717-021334776		2.72469
NP038997	Similar to gi|2443879 F11P17.5 jasmonate induced protein homolog from Arabidopsis thaliana BAC gb|AC002294	1.47799
TC267534	NOP5_YEAST (Q12499) Nucleolar protein NOP58 (Nucleolar protein NOP5). partial (7%)	1.36376
TC257202	RN12_HUMAN (Q9NVW2) RING finger protein 12 (LIM domain interacting RING finger protein)	3.79497
At3g20710	F-box protein-related	4.41937
At3g13080	ABC transporter family protein	1.08358
BP670915	BP670915 RAFL21 Arabidopsis thaliana cDNA clone RAFL21-37-B21 3'. mRNA sequence	1.96495
At3g46890	expressed protein hypothetical protein F2I9.20 - Arabidopsis thaliana.PID:g3785987	1.18941
At2g14610	pathogenesis-related protein 1 (PR-1)	3.03553
At5g05640	nucleoprotein-related	1.43147
At1g45100	polyadenylate-binding protein	2.95453
At4g22950	MADS-box protein (AGL19) MADS-box protein AGL14	2.75855
NP236773	mutator-like transposase-like	2.35725
At5g63230	glycosyl hydrolase family protein 17	2.66278
At5g45990	crooked neck protein. putative/cell cycle protein	2.02208
At5g42800	dihydroflavonol 4-reductase (dihydrokaempferol 4-reductase) (DFR)	1.59436
At5g13210	expressed protein	2.66591
At2g21640	expressed protein	1.09106
At5g58610	PHD finger transcription factor	1.75710
CHR3:015419665-015419724		3.30890
At3g30720	expressed protein	1.78754
At1g11070	hydroxyproline-rich glycoprotein family protein	1.35787
At1g75700	abscisic acid-responsive HVA22 family protein	1.44835
At1g31400	meprin and TRAF homology domain-containing protein/MATH domain-containing protein	4.75744
At1g01680	U-box domain-containing protein	3.48434
At1g70440	hypothetical protein	4.11743
At2g43960	SWAP (Suppressor-of-White-APricot)/surp domain-containing protein	1.44899

DISCUSSION

Chapter 8:
Elongator, a conserved multitasking complex?

Mol Microbiol (2010) 76: 1065-1069

Wim Versées, Steven De Groeve and Mieke Van Lijsebettens

This MicroCommentary was written in response to Nelissen and De Groeve *et al*. (2010) and Mehlgarten *et al*. (2010) to discuss the dual function of the Elongator complex in plants.

Posttranscriptional modifications on transferRNA (tRNA) molecules occur frequently, however, their implication on the translational regulation is only recently becoming fully appreciated. Several tRNA molecules in the eukaryotic cytoplasm carry a methoxycarbonylmethyl (mcm) or carbomoylmethyl (ncm) group on their wobble uridine to ensure the efficient and reliable decoding of A- or G-ending codons. Recent evidence suggests that the six subunits of the conserved Elongator complex are all required for an early step in the synthesis of the mcm and ncm groups in *Saccharomyces cerevisiae* as well as in *Caenorhabditis elegans*. Mehlgarten *et al*. (2010) convincingly shows that the tRNA modifying role of Elongator is also conserved in the plant *Arabidopsis thaliana*. Moreover, combinations of subunits of the *Arabidopsis* Elongator complex can structurally and functionally complement deletion mutants in yeast and substitute for the tRNA modification activity. The data suggest that Elongator might be a unique multitasking complex with at least two conserved roles in all eukaryotes, i.e. transcriptional activation via histone acetylation in the nucleus and translational control through tRNA modification in the cytoplasm.

Most cellular non-coding RNAs require the addition of posttranscriptional nucleoside modifications to be fully functional. To date, more than hundred different types of these modifications have been discovered, the majority occurring in transfer RNA (tRNA). Especially prevalent are those found in the anticodon loop of the tRNA molecules, particularly on position 37 (adjacent to the anticodon) and on the first position of the anticodon (position 34, called the wobble position) that is complementary to the third base of the mRNA codon. These wobble modifications play an important role in translation fidelity by stabilizing specific codon-anticodon interactions in the A site of the ribosome, preventing misreading of non-cognate codons and ensuring reading frame maintenance (Agris *et al*., 2007). The importance of tRNA modifications in translation efficiency and fidelity is underscored by the occurrence of some severe human diseases associated with malfunctioning of this process (Kirino *et al*., 2004). Recently, the awareness is growing that tRNA wobble modifications also provide cells with a powerful tool to regulate gene expression at the translational level (Gustilo *et al*., 2008). Indeed, clusters of genes have been identified that contain a statistic overrepresentation of a certain type of codon for a particular amino acid (Begley *et al*., 2007). As the expression efficiency of these genes will depend on the correct modification of the corresponding tRNA isoacceptor, regulation of the activity of one tRNA- modifying enzyme will enable up- or down-regulation of the translation of a specific subset of genes.

In the cytoplasm of eukaryotic cells, a methoxycarbonylmethyl (mcm) or carbamoylmethyl (ncm) group is added to the C5 of the wobble uridine of certain tRNA species (Johansson *et al*., 2008). These complex mcm^5U and ncm^5U modifications (and the mcm^5s^2U derivative) are required for the proper decoding of NNR codons (with N any nucleotide and R either A or G) in eukaryotes. Genes coding for the Elongator complex have been shown to be required for an early step in the synthesis of mcm^5U and ncm^5U in the yeast *Saccharomyces cerevisiae* (Huang *et al*., 2005) and also in the multicellular nematode *Caenorhabditis elegans* (Chen *et al*., 2009). Mehlgarten *et al.* (2010) demonstrates that the role of Elongator in tRNA modification also applies to the model plant *Arabidopsis thaliana*, suggesting a common function in all eukaryotes.

In yeast, the holo-Elongator complex consists of six proteins of which Elp1, Elp2 and Elp3 form the core and Elp4, Elp5, and Elp6 the accessory subcomplex (Winkler *et al*., 2001). Initially, the Elongator complex had been considered to be involved in transcription because it

co-immunoprecipitated with the elongating form of RNA polymerase II (RNAPII). Moreover, one of the Elongator subunits, Elp3, has motifs characteristic of the GCN5 family of histone acetyltransferases and is capable of acetylating the core histones *in vitro* (Wittschieben *et al*., 1999). The other components of the complex are also necessary for *in vivo* histone acetylation and confer specificity towards histone H3 and H4 (Winkler *et al*., 2002). Elp1 is the largest subunit that contains several WD40 repeats in its amino acid sequence and might serve as a platform for the assembly of the Elongator complex. Structural conservation of the Elongator complex has been demonstrated in human and plants (Hawkes *et al*., 2002; Nelissen *et al*., 2010). In plants, the *elo* mutations identified the Elp homologues (referred to in plants as ELO) and displayed growth and patterning defects that could be partially explained by reduced histone H3 acetylation at the coding region of auxin-related genes the expression of which was reduced. The plant Elp3/ELO3 colocalized with an euchromatic marker and the phosporylated subunit of RNAPII in the nucleus (Nelissen *et al*., 2005; 2010). Elongator also plays a role in the regulation of plant responses to ABA, oxidative stress resistance and anthocyanin biosynthesis (Zhou *et al*., 2009).

Mehlgarten *et al*. (2010) compared the *Arabidopsis* mutant *elo3*, defective for the Elp3/ELO3 component of the Elongator complex, with the control and showed that the tRNA was modified. tRNAs were prepared from total RNA, digested, hydrolysed, and analyzed by high-pressure liquid chromatography. Elution profiles were similar, except for the ncm^5U and mcm^5s^2U uridine nucleosides that were absent in the *elo3* mutant, indicating that the plant Elp3/ELO3 protein is responsible for the early steps of the ncm^5U and mcm^5s^2U uridine modification and that the Elongator complex might function in tRNA modification in plants.

In addition, Mehlgarten *et al*. (2010) combined yeast genetics and two functional assays to investigate whether the plant Elp3/ELO3 protein could substitute the tRNA-modifying activity of Elp3 in yeast. First, tagged plant *ELP3/ELO3* cDNA was expressed in the yeast Δ*elp3* mutant to investigate the structural conservation. Pull-down experiments showed that the plant Elp3/ELO3 promoted interactions between the yeast Elp2 and Elp5, and between Elp2 and Kti12 that had previously been demonstrated to occur with the yeast Elp3. Hence, the yeast Elp3 could be substituted structurally by the plant Elp3/ELO3. A similar strategy demonstrated that the plant Elp1/ELO2 could replace the yeast Elp1 in the Elongator complex. Second, the functional conservation of the plant Elp3/ELO3 in tRNA modification was assayed with a zymocin toxin

resistance assay. This assay is based on the sensitivity of yeast to the zymocin toxin secreted by *Kluyveromyces lactis* that cleaves a subset of tRNAs carrying the modified wobble uridine, mcm^5s^2U. Functional complementation of the tRNA- modifying function by the plant Elp3/ELO3 protein could be obtained only in the presence of the plant Elp1/ELO2 protein in the yeast *Δelp3 Δelp1* double mutant. A second assay in yeast, based on the *SUP4* suppressor tRNA gene showed that plant Elp3/ELO3 and Elp1/ELO2 could replace the corresponding yeast proteins in the Elongator complex to promote wobble uridine modification.

Thus, the phenotypes of the *elo* mutants in plant might be the consequence of a dual activity of the Elongator complex, one in tRNA modification (Mehlgarten *et al*., 2010) and one in RNAPII transcription elongation (Nelissen *et al*., 2010). In yeast, the overexpression of $tRNA^{Lys}$ and $tRNA^{Gln}$ bypass the requirement for the Elongator complex and were sufficient for suppression of the *elp* phenotypes (Esberg *et al*., 2006). Whether this would also be the case in *Arabidopsis* is not yet proven and would provide strong evidence that tRNA modification is the major function of Elongator in plants. However, in multicellular organisms, the Elongator complex is linked with kingdom-specific functions, such as auxin biology and neuronal development in plant and animals, respectively. How the kingdom- specific functions might be explained by an evolutionarily conserved tRNA-modifying function of Elongator is unclear. The Elongator complex might have originated early in evolution but acquired more functions in higher species. Indeed, Elp3 is highly conserved in Archaea, in contrast to the other Elongator subunits that have no counterparts in this kingdom, indicating an 'evolution' of the Elongator complex in higher species. Therefore, it would be interesting to investigate whether the yeast Elongator genes might complement specific phenotypes in the *elo* nutants of plants.

How can the dual activity of Elongator be explained? First, the catalytic subunit of the Elongator complex, Elp3, possibly shows an extreme form of substrate ambiguity. Accordingly, mutations in the C-terminal histone acetyl transferase (HAT) domain of Elp3, which is expected to be involved in histone acetylation, also affect the tRNA-modifying activity (Huang *et al*., 2005). Implication of a GNAT domain in tRNA modification would not be unprecedented, because also the protein TmcA uses a GNAT domain to transfer an acetyl group from acetyl-CoA to the N4 atom of a wobble cytidine in eubacterial $tRNA^{Met}$ (Chimnaronk *et al*., 2009). The N-terminal part of Elp3 consists of a radical S-adenosyl-methionine (SAM) domain. Enzymes belonging to this superfamily catalyze a range of chemically demanding reactions through a

radical mechanism, using a 4Fe-4S cluster and a SAM molecule. Although the role of this domain in neither of the Elongator functions has been investigated in detail, members of the radical SAM family have been implicated in at least five different RNA modifications (Atta *et al*., 2009), suggesting a role in the tRNA modification activity of Elp3. Alternatively, the dual substrate specificity of the Elp3 subunit might be modulated by the other subunits of the Elongator complex. The Elp1 and Elp2 subunits consist of a number of WD40 repeats, probably folding in one or more β-propeller structures. These domains could serve as docking stations for the binding of the substrate histone proteins to facilitate acetylation by Elp3, but might alternatively be used to bind a tRNA substrate. Indeed, recently the protein, Gemin5 has been reported to specifically bind to a small nuclear RNA through a WD40 repeat domain (Lau *et al*., 2008). Finally, the dual role of the Elongator complex in tRNA and protein modification raises a tantalizing analogy with the urmylation pathway in yeast (Leidel *et al*., 2009). Recently it was found that Urm1p (and the urmylation pathway), next to its role in protein modification, plays a second parallel function as sulphur carrier in the synthesis (2-thiolation) of mcm^5s^2U-modified tRNA. A genomic-scale genetic interaction map in *S. cerevisiae* revealed a synthetic lethal interaction between genes encoding the Elongator complex and those of the urmylation pathway, suggesting that the Elp complex and the Urm pathway collaborate in the modification of tRNA (Costanzo *et al*., 2010).

Elongator has been linked to two other cellular functions: exocytosis (Rahl *et al*., 2005) and tubulin acetylation (Creppe *et al*., 2009; Solinger *et al*., 2010). Mutation of Sec2, an essential Rab GTPase, caused defects in yeast exocytosis and this effect can be overcome by Elongator gene deletion. Rahl *et al*. (2005) showed a direct interaction between Elp1 and Sec2 and cytoplasmic localization of Elp1 was essential to complement the *elp1* phenotype. Whether the effect of *elp* mutation on exocytosis is directly linked to the Elongator function is not clear and might actually be a consequence of translational defects, such as tRNA modification (Esberg *et al*., 2006). Acetylation of α-tubulin is a posttranslational modification of microtubules that serves as a recognition signal for the anchoring of molecular motors and, as such, underlies the transport of various proteins or organelles in neurons. Recent studies have shown that Elp3, the catalytic subunit of the Elongator complex, promotes the acetylation of α-tubulin in microtubules and physically interacts with it (Creppe *et al*., 2009; Solinger *et al*., 2010). Although the mechanism

of tubulin acetylation and its biological consequences are not well understood, it provides insight into the importance of Elongator and tubulin acetylation in neuronal migration and development.

In conclusion, the activity of the Elongator Elp3 enzyme relates to acetylation of various substrates in different cellular compartments (Fig. 1). Major questions remain to be addressed about how and when Elp3 distinguishes these substrates – high resolution protein purification and chromatin immunoprecipitation analyses on sorted cell types in multicellular organisms might provide the answers.

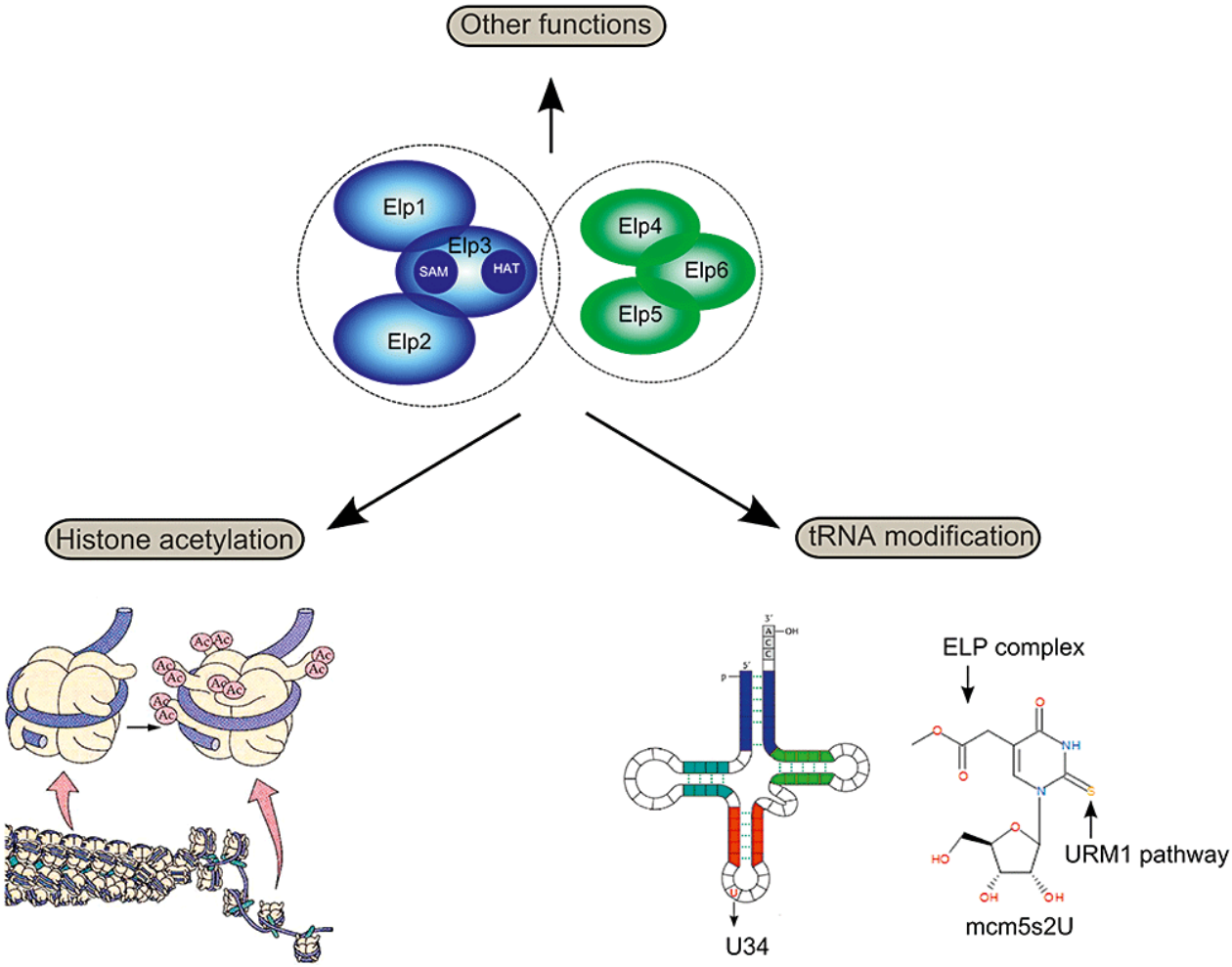

Fig. 1. Schematic representation of the different functions of the Elongator complex with the emphasis on histone acetylation (adapted from B.B. Buchanan, W. Gruissem, and R.L. Jones (2000) *Biochemistry & Molecular Biology of Plants* ©American Society of Plant Biologists) and tRNA modification. Elongator is composed of two subcomplexes consisting respectively of Elp1, Elp2, and Elp3, and Elp4, Elp5, and Elp6 components. Elp3 is the catalytic unit with a histone acetyl transferase (HAT) and radical *S*-adenosyl methionine domain (SAM).

Chapter 9:
Discussion, perspectives and conclusions

I. Elongator in transcription

All genes belonging to the *elongata* class (very narrow leaf lamina) appeared to code for subunits of the Elongator complex in Arabidopsis (Nelissen *et al*., 2005). The Elongator complex is conserved between different eukaryotic species ranging from yeast to human but the function of the complex is highly debated within and between the different species as discussed in the previous chapter. A role in transcription was supported in yeast and human by its association with an RNA polymerase II holoenzyme engaged in transcription elongation and evidence that the complex is involved in histone acetylation. Recent data support also a role in processes as diverse as exocytosis, tRNA modification and tubulin acetylation (Svejstrup., 2007; Creppe and Buschbeck., 2011).

In this thesis we provide evidence for Elongator to play a role in transcription elongation in plants by its intrinsic HAT activity (Chapter 4; Nelissen *et al*., 2010). The colocalisation of ELO3 with euchromatic markers and the decreased histone H3K14 acetylation levels in the coding region of downregulated genes in the *elo3* mutant point to a role in transcriptional regulation. This however did not seem to be a general effect of the *elongator* mutation since not all tested downregulated genes in the *elo3* mutant showed decreased histone H3K14 acetylation levels. Of the auxin-related genes (ATHB8, SHY2, ERF-AP2, BDL, LAX2 and PIN4) that were downregulated in *elo3* only SHY2 and LAX2 were targeted for histone acetylation by ELO3 as shown by ChIP.

So Elongator seems to show two kinds of specificity: (1) only specific down-regulated genes show decreased histone H3K14 acetylation and (2) only the coding region of target genes seems affected. This suggests specificity of the Elongator complex in target gene selection by an unknown mechanism. A possible explanation could be the interaction of Elongator with regulatory proteins providing specificity towards certain genes. RNA binding proteins could recruit the Elongator complex by recognizing RNA motives of nascent mRNA and as such contribute to facilitate further transcription of these nascent mRNA's. There is indeed increasing evidence that differential gene expression often depends on the regulation of transcription elongation via the release of stalled RNAPII (Levine, 2011). In our group RNA binding proteins were identified as interactors of HUB1 histone modifying complex (Boccardi, 2010) and recently an interactor of Elongator with RNA binding motif has been identified, MINIYO (IYO) (Sanmartin *et al.,* 2011). IYO interacts with RNAPII and the Elongator complex and is required

to sustain global levels of transcriptional elongation activity, specifically in differentiating tissues. Nonetheless, the TAP with Elongator subunits as bait did not provide us with any interactors besides the complex itself. However the current TAP results were performed on Arabidopsis cell suspension cultures grown in the dark while our data indicate a light-dependent function for Elongator. The circadian clock genes CCA1 and LHY are downregulated in the *elo3* mutant, hypocotyl elongation assay shows photomorphogenic effects in *elo3* and SHY2/IAA3, identified as a direct target of Elongator, is actually light-regulated (Chapter 5). So it is very possible that the initial TAPs did not pick up any light-dependent interactors as the cell suspension cultures are grown in the dark. In the future TAP experiments using Elongator protein baits will be performed on seedlings grown in the light to allow purification of putative light-dependent interactors. The fact that only the coding region of target genes shows decreased H3K14 acetylation is not surprising as Elongator in yeast only co-immunoprecipitates with the phosphorylated form of RNAPII involved in transcription elongation. Also in humans decreased Elongator levels affect histone H3 acetylation in the coding region of target genes and not at promoter regions (Close *et al*., 2006) which is consistent with our findings in Arabidopsis. However the data from both kingdoms (Animalia and plants) show that Elongator affects species-specific processes. While in plants auxin and light related genes are affected, in humans genes involved in cell motility such as gelsolin and beclin-1 are targeted by Elongator. So it seems that Elongator function in transcription is conserved between humans and plants but has evolved in different species to regulate species-specific processes. Arabidopsis *elo* mutants grown under continuous far-red light conditions show a hyposensitive photomorphogenic phenotype, while under continuous red light conditions a hypersensitive photomorphogenic phenotype is observed. Since PHYB predominates in responses to red light, whereas responses to continuous far-red light are exclusively mediated by PHYA (Fairchild *et al*., 2000), our data points to a light-dependent function of the Elongator complex in which both PHYA and PHYB signaling is affected. How Elongator fits into the phytochrome-dependent light signaling cascade is currently under investigation but a link with PHYA signaling seems to fit with our obtained data. The phenotype of the quadruple *phyAphyBphyDphyE* mutant resembles highly the *elo* mutants but less so in the triple *phyBphyDphyE* mutant (Franklin et al., 2003) and the hyposensitive photomorphogenic phenotype of the *elo* mutants during de-etiolation under far-red light conditions is shared by *phyA* mutants. PHYA is the major photoreceptor of de-etiolation, and

phyA expression is reversibly repressed by light. Recently it was shown that phyA activation in darkness was accompanied by a significant enrichment in histone H3K9 and H3K14 acetylation at the phyA transcription and translation start sites (Jang *et al*., 2011). Conversely, when phyA expression was repressed by light, an increase in deacetylation of histone H3K9 and H3K14 was seen. *PHYA* expression is thus under control of chromatin modifications. This is not the first report about chromatin control of light-regulated gene expression as it was shown that the expression of the SHY2/IAA3 gene is at least partly regulated by the HAT activity of GCN5 at the promoter region and mRNA abundance of genes coding for circadian clock components correlates with histone acetylation levels at their loci (Benhamed et al., 2006; Perales and Mas, 2007). In this thesis we showed that also the coding region of the SHY2/IAA3 is a target for the HAT activity of the Elongator complex and that the expression pattern of circadian clock genes is severely disrupted. It is possible that Elongator is at least partly responsible for establishing histone acetylation marks at the phyA locus and could explain the *phyA*-related phenotypes in the *elo* mutants. phyA however is not downregulated in the transcriptome data of the *elo3* mutants but this can be explained by the fact that the sampling of the plants for micro-array analysis happened during the day (lights are on) when phyA expression is completely repressed. The Elongator could also be involved in the transcription of genes downstream of PHYA and PHYB signaling (Fig. 1). Micro-array data show severe downregulation of PIF3 (phytochrome interacting factor 3) and HFR1 (long hypocotyl in far-red) in the *elo* mutants. The *hfr1* mutant exhibits a reduction in seedling responsiveness specifically to continuous far-red light (similar to *elo* and *phyA* mutants) and HFR1 forms a heterodimer with PIF3 which binds the Pfr form of both PHYA and PHYB phytochromes (Fairchild et al., 2000). Thus, HFR1 may function to modulate phyA signaling via heterodimerization with PIF3 and the observed photomorphogenic fenotypes in the *elo* mutants can be attributed to the downregulation of both HFR1 and PIF3. One of the main objectives in the future will be the identification of light-specific targets of Elongator. The transcriptome and proteome in *elo* mutants will be compared to wild type at the dark-light and light-shade transition points under different light qualities and specific target genes will be analyzed with chromatin immuno precipitation techniques such as ChIP-PCR and ChIP-on-chip or ChIP-Seq. So far we only identified two target genes of the Elongator complex, however hundreds of genes are expected to be directly regulated by the complex and a genome-wide setup

such as ChIP-Seq will allow us to identify these targets. This approach will result in a holistic view on all the processes regulated by Elongator upon different light stimuli.

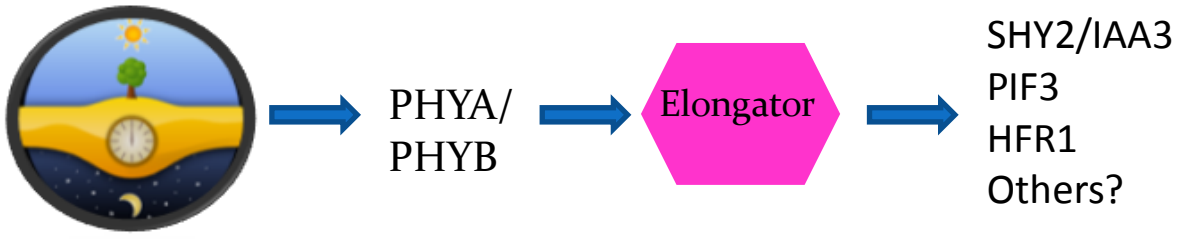

Figure 1. Light signals are perceived by the different phytochromes and influences their expression. Our working hypothesis is that the phytochromes regulate the activity of the Elongator complex which in turn regulates the expression of light-dependent genes through histone acetylation.

Another interesting observation is the fact that both upstream (fe. LHY) and downstream (fe. SHY2/IAA3) genes in the light signaling cascade are downregulated in our *elo3* mutants indicating that the chromatin interface is a fast and powerful interface between environmental stimuli and the RNAPII transcription elongation complex to regulate the expression of entire developmental pathways to adjust growth and morphology. By modifying the chromatin state of entire groups of genes involved in a specific process, very fast and strong responses could be accomplished.

II. RON3

In the *rotunda* class of leaf mutants (small round leaf lamina), we cloned the *ron3* allele and the functional analysis of the RON3 protein also points to multiple roles for this protein in cellular processes (Chapter 6; De Groeve *et al*., in preparation). On one hand we show the interaction of RON3 with the PP2A complex and its involvement in auxin signaling while at the same time providing evidence for a nuclear role likely involved in transcriptional regulation. The RON3 protein is classified as a hydroxyproline-rich glycoprotein (HRGP) most likely because of its high presence of proline residues in its amino acid composition. We could however not find any homology with other HRGP's and did not find evidence for any cell wall related function. The presence of a high number of proline residues could however support the hypothesis that certain arginine residues in RON3 are methylated by the co-purified PRTM4A/B complex which typically methylates arginine residues flanked by prolines (Niu et al., 2008). This is supported by the presence of poly-A binding proteins in our TAP data of RON3 which are known targets for

the human homolog of PRMT4A/B (Lee and Bedford, 2002). Moreover, bioinformatic studies show that RON3 is only present in higher plants and not in moss and algae which also lack the 3' RNA processing in which the PABs are involved (Proost et al., 2009).

In our study of RON3 we focused on the role of RON3 in auxin transport and the interaction with the PP2A complex. Since RON3 does not contain known functional domains or shows any significant homology with other proteins we could not attribute a specific function to RON3 but the interactome data combined with the molecular and biological phenotyping of the *ron3* mutant clearly show the relation to auxin transport. Genetic interaction between RCN1 (a subunit of the PP2A complex) and RON3 could provide additional evidence for its involvement in PIN targeting by PP2A and double mutants are being generated. If RON3 modulates the activity of the PP2A complex and as such influences the ratio of phosphorylated/unphosphorylated PIN proteins one could visualize the phosphorylated PIN fraction by immunolabeling and look for differences between the wild type and the *ron3* mutants. Our data also indicate high levels of auxines in the root which seems contradictory with the micro-array data in the *ron3* mutant where high numbers of Aux/IAA and SAUR genes are downregulated. The micro-array however was performed on shoot apexes without the root tissue and this discrepancy could just simply be the consequence of a defect in auxin transport from the shoot to the root where auxin depletes from the SAM and accumulates in the RAM. In the future RT-PCR of Aux/IAA's on the shoot and root of the *ron3* mutant will be performed to support this hypothesis and auxin transport measurements will be done. Although we looked into the auxin-related function of the RON3 protein by its association with the PP2A complex, a number of other roles have been attributed to the PP2A complex. The PP2A complex is a heterotrimeric complex consisting of a structural subunit A, a catalytic subunit C and a regulatory subunit B encoded in Arabidopsis by respectively 3, 5 and 18 genes. The loss of the structural subunits of the PP2A leads to basal-to-apical PIN polarity shift. The additional loss of PINOID reverses this effect and certain phenotypes observed in the PP2A mutants showing the antagonistic regulation of PIN phosphorylation by PP2A and PINOID (Michniewicz et al., 2007). The fact that not all phenotypes were restored in the *pp2a/pid* double mutant suggests additional roles for the PP2A. Indeed, PP2A also targets enzymes involved in ethylene biosynthesis (Skottke *et al*., 2011), the brassinosteroid receptor BRI1 (Di Rubbo *et al*., 2011), Phot2 phototropin (Tseng *et al*., 2010) and nitrate reductase (Heidari *et al*., 2011). The diverse substrates of the PP2A complex can be

explained by the fact that these studies use mutants in the structural subunits of the PP2A complex and thus impair the function of all the different PP2A complexes since differences in composition of the PP2A complex are assumed to regulate different processes. Indeed the B-type regulatory subunit functions as a targeting and substrate-specific factor and the holoenzyme assembly with the appropriate B-type subunit is crucial for PP2A specificity and regulation (Di Rubbo et al., 2011). The pleiotropic phenotype of the *ron3* mutants can thus be explained by a defect in the stability of the PP2A complex if RON3 stabilizes interactions involving the core structural subunits. Split-YFP experiments with RON3 and the different subunits of the PP2A complex would show which subunits interact directly with RON3 and provide insight whether RON3 plays a structural or regulatory role in the PP2A complex. Also reverse TAP experiments using PP2A subunits and PRMT4A/B as bait would verify the proposed dual function of RON3

III. ANG3

In the *angusta* class we cloned the ANG3 gene which corresponded to the ribosomal protein gene *RPL5B* (Chapter 7). Ribosomes are responsible for translating mRNA into protein and are generally perceived as housekeeping components of the cell with a presumed non-selective role in polypeptide synthesis. In plants, ribosomal proteins are encoded by small gene families and although there is no direct evidence to support the functional specialization of ribosomal proteins the existence of these small gene families could reflect a need to retain stoichiometric levels of ribosomal proteins that make up the ribosome (Blanc *et al*., 2004; Thomas *et al*., 2006). Alternatively, there could be heterogeneity in ribosome composition and as such functional specialization. This situation is different in animals where most ribosomal proteins are encoded by single-copy genes and loss-of-function mutations in those genes are generally homozygous lethal. In the Arabidopsis genome, there is one homolog for *RPL5B* that is extremely conserved: *RPL5A*. *RPL5B* and *RPL5A* are considered duplicate genes with redundant function (Moore and Purugganan 2005). Interestingly, mutation in either of the two homologues results in narrow pointed leaves suggesting that gene dosage of ribosomal proteins is important in plants. This was also observed in other species such as Drosophila, where reduction in expression of ribosomal mRNA's causes phenotypes (Sæbøe-Larssen et al., 1998). The *ang3* mutation is however caused by a change from a guanine into an adenine nucleotide and a glycine (Ler) into an aspartate

(*ang3)* at the amino acid level. So it is likely that a 'mutant' RPL5 protein is generated. This mutant protein might still be built into the ribosome but causes malfunctioning of the ribosome and competes with 'normal' ribosomes. This in turn would imply that the mutation is dominant while the *ang3* mutation is recessive. The amino acid change could also prevent the protein of forming a stable conformation resulting in rapid turnover and as such cause a decrease in the ribosomal RPL5 subunit which in a sense is the same effect as gene dosage effects. Besides the narrow leaf lamina of the *ang3* mutant caused by a reduced cell expansion in the epidermis, growth was also significantly impaired in hypocotyls and primary roots suggesting a general role for RPL5B in organ growth. Indeed, recent studies on ribosomal protein genes and ribosome assembly indicate that the basic translational machinery of the cell, the ribosome, has a regulatory role in plant development (Byrne, 2009). Our micro-array data of the *ang3* mutant suggests that this regulatory role in translation adds another level of complexity in plant development as the mutation had only a minor effect on transcription. The use of a proteomics approach such as tagged ribosomal proteins should help uncover the contribution of ribosomes and translation to eukaryote development (Mustroph et al., 2009).

IV. Plant growth

Plant growth consists of an increase in both cell number and cell size and is affected by internal and external factors. The internal controls are all the product of the genetic instructions carried in the plant. These influence the extent and timing of growth and are mediated by signals of various types transmitted within the cell, between cells, or all around the plant. The external environments of the root and shoot place constraints on the extent to which the internal controls can permit the plant to grow and develop. Prime among these are water and nutrient supplies, temperature and light. The past 25 years have seen an explosion of interest in the capacity of a given genotype to express different phenotypes in different environments, a phenomenon known as phenotypic plasticity. Plasticity is recognized now as a significant mode of phenotypic diversity and hence as an important aspect of how plants develop, function and evolve in their environments.

To better understand the developmental processes that are specific to plants, a genetic analysis of Arabidopsis was set up by performing a large-scale screening for EMS induced mutants with abnormal leaves (Berná et al., 1999). Mutants were divided in phenotypic classes according to

their leaf size and shape. In the "Chromatin and Growth Control" research group the leaf is taken as an experimental system to study the genetic control of growth. Three classes of the leaf mutant collection are being studied representing mutants with either narrower (*elongata* and *angusta*) or wider leaf lamina (*rotunda*). In this thesis one gene from each class and their respective proteins were studied: ELO3 coding for the HAT subunit of the Elongator complex, ANG3 coding for a ribosomal protein and RON3 coding for an unknown protein. The identification of the genes responsible for the mutant phenotype and the functional analysis of their encoded proteins led to diverse processes such as chromatin modification, translation and hormone signaling. Although the affected processes are very diverse they have the common feature of regulating key processes on a large scale. Elongator regulates transcription by modifiying histones and likely has hundreds of direct target genes. RON3 regulates the activity of the PP2A complex which has multiple roles and dephosphorylates different substrates involved in different pathways. ANG3 codes for the ribosomal subunit RPL5B involved in the major house-keeping process of translation. These findings show that plant growth is a complex trait regulated at different levels and that a mutational approach is of great potential for the genetic dissection of complex traits such as plant growth.

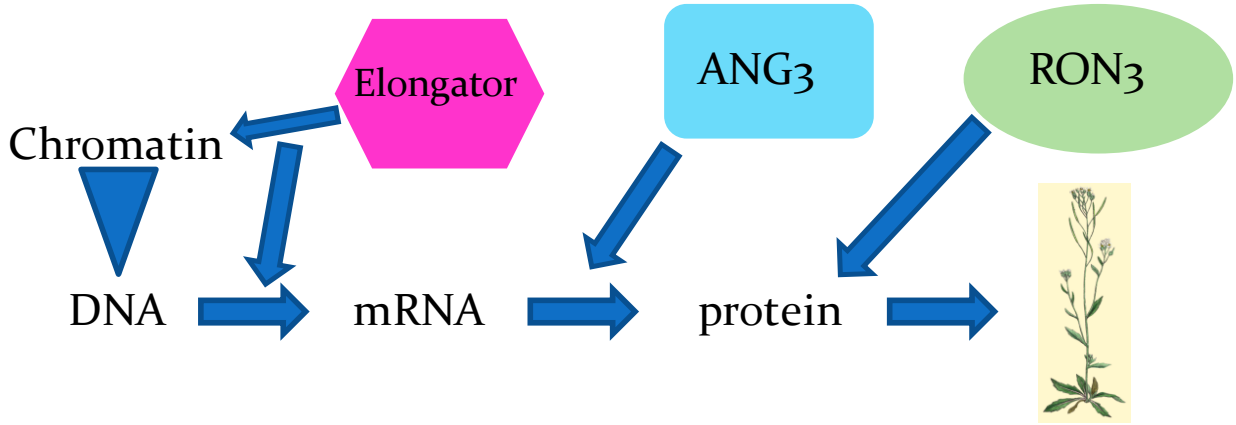

Figure 2. Functional analysis of 3 leaf mutants reveal that plant growth is regulated at different levels ranging from chromatin status to translation to protein activation.

SUMMARY

Summary

In the “Chromatin and Growth Control” research group the leaf is taken as an experimental system to study the genetic control of growth. Three classes of the leaf mutant collection are being studied representing mutants with either narrower (*elongata* and *angusta*) or wider leaf lamina (*rotunda*). In this thesis one gene from each class and their respective proteins were studied. The study of three leaf mutants and their involvement in different pathways shows that growth is a complex trait that involves the coordinate activation and repression of a number of pathways that differentially react to environmental and developmental stimuli. Our work demonstrates that cell proliferation is regulated at the chromatin level and also at the translational level.

The central dogma of molecular biology tells us that protein synthesis requires two steps: transcription with the synthesis of mRNA from a DNA template and translation where ribosomes synthesize proteins using the mRNA transcript produced during transcription. Transcription of protein-coding genes is a highly regulated process involving several protein complexes acting in a series of events (Chapter 1). Less then two decades ago many scientists working in the field of transcriptional gene regulation believed chromatin was not a central player. This view changed after observations showing the histone acetylation and deacetylation activity of promoter-associated coactivators and corepressors. One of those complexes with histone acetylation activity is associated with RNAPII during transcription and is called the Elongator complex. After its initial discovery in yeast it became clear that the genes coding for the subunits of this complex were conserved in a vast range of species. Despite the high conservance of the genes coding for this complex a lot of debate and discussion is going on about the actual function of the complex within and between the different species (Chapter 2 and Chapter 8).

In this thesis we provide evidence for a functional Elongator complex in plants which regulates transcription by its inherent histone acetyl transferase activity (Chapter 4). Interestingly, the complex does not seem to act in a general fashion to aid the transcription of all genes but shows specificity to certain genes and processes. How this regulation of the complex occurs is not known but experimental data show that specific genes in auxin- and light-related processes are affected. Light influences plant development and does so in part by modifying responses to the hormone auxin. Physiological studies have suggested correlations between light and regulation of

auxin transport and genetic studies indicate specific proteins that link light perception with auxin responses (Chapter 3). Also the Elongator mutants show photomorphogenic defects and supports the biological relevance of the obtained transcriptome and ChIP data (Chapter 5).

The work in this thesis also contains the cloning and functional analyis of two leaf mutants (*ang3* and *ron3*) with reduced lamina size. The RON3 genes codes for a protein that is assigned as a hydroxyproline-rich glycoprotein (HRGP) and HRGPs are well-known to be components of the plant extracellular matrix (TAIR). This assessment is made on the presence of a high number of proline residues in the RON3 protein. Our data however contradicts this cell wall related function and we provide evidence for RON3 as a component involved in auxin signaling (Chapter 6). The *ron3* mutant shows auxin dependent phenotypes in both root and shoot organs and the transcriptome data obtained by microarray analysis show a high number of downregulated auxin-related genes. BLAST searches didn't find any homology with other cell wall proteins and the RON3 protein does not localize to the cell wall but is predominantly located in the nucleus. Homology searches in other species don't give any significant hits and imply that this protein is specific to plants. The interactome data of RON3 indicates the involvement of the PP2A phosphatase complex in the observed *ron3* phenotypes. The PP2A complex acts as an antagonistic regulator of PIN phosphorylation by PINOID and as such directs auxin flux. How RON3 modulates the activity of the PP2A complex is currently under investigation. The ANG3 gene codes for the ribosomal protein RPL5B and phenotypical analysis shows the importance of the translation process in plant development (Chapter 7). How ribosomal proteins contribute to specific processes in plant development is a new field of research and many questions including the influence of ribosome dose on development and the extent and functional significance of ribosome heterogeneity remain to be resolved.

Samenvatting

In de onderzoeksgroep “Chromatin and Growth Control” wordt het blad als een experimenteel systeem gebruikt om de genetische controle van groei te bestuderen. Drie klassen van bladmutanten worden bestudeerd met enerzijds een smallere (*elongata* en *angusta*) en anderzijds bredere (*rotunda*) bladschijf. In deze thesis werd één gen van elke klasse en zijn overeenkomstig eiwit onderzocht. Deze studie van drie bladmutanten en hun betrokkenheid in verschillende processen toont dat groei een complex gegeven is welke de gecoördineerde activatie en repressie vraagt van een aantal processen welke verschillend reageren op omgevings- en ontwikkelings-stimuli. Ons werk toont aan dat celproliferatie gereguleerd wordt op het chromatine en het translationele niveau.

Het centrale dogma van de moleculaire biologie stelt dat eiwitsynthese twee stappen vereist: transcriptie waarbij mRNA gesynthetiseerd wordt op basis van een DNA template en translatie waarbij ribosomen eiwitten synthetiseren gebruik makend van het mRNA transcript geproduceerd tijdens transcriptie. De transcriptie van eiwit-coderende genen is een sterk gereguleerd proces waarbij verschillende eiwitcomplexen samenwerken in een serie van gebeurtenissen (Hoofdstuk 1). Minder dan twee decennia geleden geloofden vele wetenschappers dat chromatine geen hoofdrol speelde in de transcriptionele genregulatie. Deze opvatting veranderde na observaties dat promoter geassocieerde coactivators and repressors histon-acetylatie en –deacetylatie activiteit bezitten. Eén van deze complexen met histon-acetylatie activiteit is geassocieerd met het RNAPII tijdens transcriptie en wordt het Elongator complex genoemd. Kort na de ontdekking van dit complex in gist werd het duidelijk dat de genen welke coderen voor de eiwitten van dit complex geconserveerd waren in een variatie van speciës. Ondanks de hoge geconserveerdheid van deze genen is er grote onenigheid en discussie over de feitelijke rol van het complex binnen en tussen de verschillende speciës (Hoofdstuk 2 en Hoofdstuke 8).

In deze thesis tonen we aan dat het Elongator complex in planten transcriptie reguleert door zijn inherente histon-acetylatie activeit (Hoofdstuk 4). Bovendien blijkt het complex niet de transcriptie te sturen van alle genen maar vertoont specificiteit naar bepaalde genen en processen. Hoe deze regulatie van het complex gebeurt is niet geweten maar experimentele data tonen aan

dat specifieke genen betrokken in de auxine- en licht-gerelateerde processen gereguleerd worden door het Elongator complex. Licht beïnvloedt plantontwikkeling en doet dit deels door het modificeren van de respons door middel van het plantenhormoon auxine. Fysiologische studies suggereren een verband tussen licht en de regulatie van auxine transport en genetische studies indiceren een link tussen zekere eiwitten met een rol in lichtperceptie en de auxine respons. Ook de Elongator mutanten vertonen fotomorfogenetische defecten en ondersteunen de biologische relevantie van de bekomen transcriptoom en ChIP data (Hoofdstuk 5).

Het werk in deze thesis bevat ook het kloneren en functionele analyse van twee bladgroei mutanten (*ang3* en *ron3*) welke een verkleinde bladschijf vertonen. Het RON3 gen codeert voor een eiwit dat geännoteerd is als een hydroxyproline rijk glycoproteïne (HRGP) en HRGPs zijn gekende componenten van de plant extracellulaire matrix. Deze annotatie is gebaseerd op de aanwezigheid van een groot aantal proline aminozuren in het RON3 eiwit. Onze data echter weerlegt deze celwand gerelateerde functie en wij tonen aan dat RON3 betrokken is in auxine-gerelateerde processen (Hoofdstuk 6). De *ron3* mutant vertoont auxine-afhankelijke fenotypes in zowel de scheut als wortel en de transcriptoom data verkregen door micro-array analyse geeft een groot aantal van neergereguleerde auxine-gerelateerde genen. Bio-informatica studies tonen geen homologie tussen het RON3 eiwit en andere celwand proteïnen. Bovendien blijkt dat de subcellulaire localisatie van RON3 hoofdzakelijk nucleair is. De interactoom data van RON3 toont dat het PP2A fosfatase complex betrokken is in de geobserveerde fenotypes van de *ron3* mutant. Het PP2A complex werkt als een antagonistische regulator van PIN fosforylatie door PINOID en stuurt aldus auxine flux. Momenteel onderzoeken we hoe RON3 de activiteit van het PP2A complex beïnvloedt. Het ANG3 gen codeert voor het ribosomale eiwit RPL5B en fenotypische analyse toont het belang aan van het translatie-proces in plantontwikkeling (Hoofdstuk 7). Hoe ribosomale eiwitten bijdragen tot specifieke processen in plantontwikkeling is een nieuw onderzoeksveld en vele vragen over de invloed van ribosoom dosage op ontwikkeling en de functionele significantie van ribosoom samenstelling blijven voorlopig onbeantwoord.

REFERENCES

Abel S, Nguyen MD, Theologis A (1995) The PS-IAA4/5-like family of early auxin-inducible mRNAs in Arabidopsis thaliana. J Mol Biol 251: 533-549

Agris, P.F., Vendeix, F.A.P., and Graham, W.D. (2007) tRNA's wobble decoding of the genome: 40 years of modification. *J Mol Biol*, 366**:** 1-13.

Alonso JM, Stepanova AN, Leisse TJ, Kim CJ, Chen H, Shinn P, Stevenson DK, Zimmerman J, Barajas P, Cheuk R, Gadrinab C, Heller C, Jeske A, Koesema E, Meyers CC, Parker H, Prednis L, Ansari Y, Choy N, Deen H, Geralt M, Hazari N, Hom E, Karnes M, Mulholland C, Ndubaku R, Schmidt I, Guzman P, Aguilar-Henonin L, Schmid M, Weigel D, Carter DE, Marchand T, Risseeuw E, Brogden D, Zeko A, Crosby WL, Berry CC, Ecker JR (2003) Genome-wide insertional mutagenesis of *Arabidopsis thaliana*. Science 301: 653-657

Altschul SF, Madden TL, Schaffer AA, Zhang J, Zhang Z, Miller W, Lipman DJ (1997) Gapped BLAST and PSI-BLAST: a new generation of protein database search programs. Nucleic Acids Res 25: 3389-3402

Alvarez-Venegas R, Pien S, Sadder M, Witmer X, Grossniklaus U, Avramova Z (2003) ATX-1, an Arabidopsis homolog of trithorax, activates flower homeotic genes. Curr Biol 13: 627-637

Anderson J., Phan L., Cuesta R., Carlson B.A., Pak M., Asano K., Bjork G.R., Tamame M., Hinnebusch A.G. (1998) The essential Gcd10p-Gcd14p nuclear complex is required for 1-methyladenosine modification and maturation of initiator methionyl-tRNA. Genes Dev 12:3650-62.

Arents G, Burlingame RW, Wang BC, Love WE, Moudrianakis EN (1991) The nucleosomal core histone octamer at 3.1 A resolution: a tripartite protein assembly and a left-handed superhelix. Proc Natl Acad Sci U S A 88: 10148-10152

Astrom S.U., Nordlund M.E., Erickson F.L., Hannig E.M., Bystrom A.S. (1999) Genetic interactions between a null allele of the RIT1 gene encoding an initiator tRNA-specific modification enzyme and genes encoding translation factors in Saccharomyces cerevisiae. Mol Gen Genet 261:967-76.

Atta, M., Fontecave, M., and Mulliez, E. (2009) RNA-modifying mettaloenzymes. In DNA and RNA Modification Enzymes: Structure, Mechanism, Function and Evolution, (Molecular Biology Intelligence Unit), Grosjean, H. (ed). Austin: Landes Bioscience, pp. 347-361.

Backstrom S, Elfving N, Nilsson R, Wingsle G, Bjorklund S (2007) Purification of a plant mediator from Arabidopsis thaliana identifies PFT1 as the Med25 subunit. Mol Cell 26: 717-729

Bainbridge K, *et al*. (2008) Auxin influx carriers stabilize phyllotactic patterning. *Genes Dev* 22:810-823.

Barkoulas M, Galinha C, Grigg SP, Tsiantis M (2007) From genes to shape: regulatory interactions in leaf development. Curr Opin Plant Biol 10: 660-666

Barrero JM, González-Bayón R, del Pozo JC, Ponce MR, Micol JL (2007) *INCURVATA2* encodes the catalytic subunit of DNA polymerase α and interacts with genes involved in chromatin-mediated cellular memory in *Arabidopsis thaliana*. Plant Cell 19: 2822-2838

Bastow R, Mylne JS, Lister C, Lippman Z, Martienssen RA, Dean C (2004) Vernalization requires epigenetic silencing of FLC by histone methylation. Nature 427: 164-167

Bedford MT, Richard S (2005) Arginine methylation an emerging regulator of protein function. Mol Cell 18: 263-272

Begley, U., Dyavaiah, M., Patil, A., Rooney, J.P., DiRenzo, D., Young, C.M., *et al*. (2007) Trm9-catalyzed tRNA modifications link translation to the DNA damage response. *Mol Cell* 28**:** 860-870.

Benhamed M, Bertrand C, Servet C, Zhou DX (2006) Arabidopsis GCN5, HD1, and TAF1/HAF2 interact to regulate histone acetylation required for light-responsive gene expression. Plant Cell 18: 2893-2903

Benhamed M, *et al*. (2008). Genome-scale Arabidopsis promoter array identifies targets of the histone acetyltransferase GCN5. *Plant J* 56:493-504.

Benjamins R, Quint A, Weijers D, Hooykaas P, Offringa R (2001) The PINOID protein kinase regulates organ development in Arabidopsis by enhancing polar auxin transport. Development 128: 4057-4067

Benkova E, Michniewicz M, Sauer M, Teichmann T, Seifertova D, Jurgens G, Friml J (2003) Local, efflux-dependent auxin gradients as a common module for plant organ formation. Cell 115: 591-602

Bennett T, *et al*. (2006) The *Arabidopsis MAX* pathway controls shoot branching by regulating auxin transport. *Curr Biol* 16:553-563.

Berger SL (2007) The complex language of chromatin regulation during transcription. Nature 447: 407-412

Berná G, Robles P, Micol JL (1999) A mutational analysis of leaf morphogenesis in *Arabidopsis thaliana*. Genetics 152: 729-742

Bird A. (2002) DNA methylation patterns and epigenetic memory. Genes Dev 16:6-21

Blakeslee JJ, Bandyopadhyay A, Peer WA, Makam SN, Murphy AS (2004) Relocalization of the PIN1 auxin efflux facilitator plays a role in phototropic responses. Plant Physiol 134: 28-31

Blanc G, Wolfe KH (2004) Functional divergence of duplicated genes formed by polyploidy during Arabidopsis evolution. Plant Cell 16: 1679-1691

Blilou I, Xu J, Wildwater M, Willemsen V, Paponov I, Friml J, Heidstra R, Aida M, Palme K, Scheres B (2005) The PIN auxin efflux facilitator network controls growth and patterning in Arabidopsis roots. Nature 433: 39-44

Boccardi TM (2010) Interactome and transcriptome approaches to study HUB1 function in plant growth and development

Bohn-Courseau I (2010) Auxin: a major regulator of organogenesis. C R Biol 333: 290-296

Bowler C, *et al*. (2004) Chromatin techniques for plant cells. *Plant J* 39:776-789.

Boyes DC, Zayed AM, Ascenzi R, McCaskill AJ, Hoffman NE, Davis KR, Görlach J (2001) Growth stage-based phenotypic analysis of Arabidopsis: A model for high throughput functional genomics in plants. Plant Cell 13: 1499-1510

Byrne ME (2009) A role for the ribosome in development. Trends Plant Sci 14: 512-519

Canas BJ, Joe FL, Jr., Diachenko GW, Burns G (1994) Determination of ethyl carbamate in alcoholic beverages and soy sauce by gas chromatography with mass selective detection: collaborative study. J AOAC Int 77: 1530-1536

Cañas LA, Busscher M, Angenent GC, Beltrán J-P, van Tunen AJ (1994) Nuclear localization of the petunia MADS box protein FBP1. *Plant J* 6:597-604.

Cao Y, Dai Y, Cui S, Ma L (2008) Histone H2B monoubiquitination in the chromatin of FLOWERING LOCUS C regulates flowering time in Arabidopsis. Plant Cell 20: 2586-2602

Carrozza MJ, Li B, Florens L, Suganuma T, Swanson SK, Lee KK, Shia WJ, Anderson S, Yates J, Washburn MP, Workman JL (2005) Histone H3 methylation by Set2 directs deacetylation of coding regions by Rpd3S to suppress spurious intragenic transcription. Cell 123: 581-592

Cartagena JA, Matsunaga S, Seki M, Kurihara D, Yokoyama M, Shinozaki K, Fujimoto S, Azumi Y, Uchiyama S, Fukui K (2008) The Arabidopsis SDG4 contributes to the regulation of pollen tube growth by methylation of histone H3 lysines 4 and 36 in mature pollen. Dev Biol 315: 355-368

Castillon A, Shen H, Huq E (2007) Phytochrome Interacting Factors: central players in phytochrome-mediated light signaling networks. Trends Plant Sci 12: 514-521

Chen Y-T, *et al*. (2009) Loss of mouse *Ikbkap*, a subunit of Elongator, leads to transcriptional deficits and embryonic lethality that can be rescued by human *IKBKAP*. *Mol Cell Biol* 29:736-744.

Chen Z, *et al*. (2006) Mutation in ABO1/ELO2, a subunit of Holo-Elongator, increase abscisic acid sensitivity and drought tolerance in *Arabidopsis thaliana*. *Mol Cell Biol* 26:6902-6912.

Chen Z, Zhang H, Jablonowski D, Zhou X, Ren X, Hong X, Schaffrath R, Zhu JK, Gong Z (2006) Mutations in ABO1/ELO2, a subunit of holo-Elongator, increase abscisic acid sensitivity and drought tolerance in Arabidopsis thaliana. Mol Cell Biol 26: 6902-6912

Chen ZJ, Tian L (2007) Roles of dynamic and reversible histone acetylation in plant development and polyploidy. Biochim Biophys Acta 1769: 295-307

Chen, C.C., Tuck, S., and Byström, A.S. (2009) Defects in tRNA modification associated with neurological and developmental dysfunctions in *Caenorhabditis elegans* Elongator mutants. *PLoS Genet* 5**:** e1000561.

Chimnaronk, S., Suzuki, T., Manita, T., Ikeuchi, Y., Yao, M., Suzuki, T., and Tanaka, I. (2009) RNA helicase module in an acetyltransferase that modifies a specific tRNA anticodon. *EMBO J* 28**:** 1362-1373.

Chinenov Y (2002) A second catalytic domain in the Elp3 histone acetyltransferases: a candidate for histone demethylase activity? Trends Biochem Sci 27: 115-117

Cho H-T, Cosgrove DJ (2000) Altered expression of expansin modulates leaf growth and pedicel abscission in *Arabidopsis thaliana*. Proc Natl Acad Sci USA 97: 9783-9788

Chua YL, Brown AP, Gray JC (2001) Targeted histone acetylation and altered nuclease accessibility over short regions of the pea plastocyanin gene. Plant Cell 13: 599-612

Chua YL, Watson LA, Gray JC (2003) The transcriptional enhancer of the pea plastocyanin gene associates with the nuclear matrix and regulates gene expression through histone acetylation. Plant Cell 15: 1468-1479

Close P, Hawkes N, Cornez I, Creppe C, Lambert CA, Rogister B, Siebenlist U, Merville MP, Slaugenhaupt SA, Bours V, Svejstrup JQ, Chariot A (2006) Transcription impairment and cell migration defects in elongator-depleted cells: implication for familial dysautonomia. Mol Cell 22: 521-531

Clough SJ, Bent AF (1998) Floral dip: a simplified method for Agrobacterium-mediated transformation of Arabidopsis thaliana. Plant J 16: 735-743

Cnops G, Jover-Gil S, Peters JL, Neyt P, De Block S, Robles P, Ponce MR, Gerats T, Micol JL, Van Lijsebettens M (2004) The *rotunda2* mutants identify a role for the *LEUNIG* gene in vegetative leaf morphogenesis. J Exp Bot 55: 1529-1539

Costanzo, M., Baryshnikova, A., Bellay, J., Kim, Y., Spear, E.D., Sevier, C.S., *et al.* (2010) The genetic landscape of a cell. *Science* **327:** 425-431.

Courey AJ, Jia S (2001) Transcriptional repression: the long and the short of it. Genes Dev 15: 2786-2796

Cramer P (2002) Multisubunit RNA polymerases. Curr Opin Struct Biol 12: 89-97

Creppe C, Buschbeck M (2011) Elongator: an ancestral complex driving transcription and migration through protein acetylation. J Biomed Biotechnol 2011: 924898

Creppe C, Malinouskaya L, Volvert ML, Gillard M, Close P, Malaise O, Laguesse S, Cornez I, Rahmouni S, Ormenese S, Belachew S, Malgrange B, Chapelle JP, Siebenlist U, Moonen G, Chariot A, Nguyen L (2009) Elongator controls the migration and differentiation of cortical neurons through acetylation of alpha-tubulin. Cell 136: 551-564

De Bodt S, Carvajal D, Hollunder J, Van den Cruyce J, Movahedi S, Inze D (2010) CORNET: a user-friendly tool for data mining and integration. Plant Physiol 152: 1167-1179

De Smet I, Tetsumura T, De Rybel B, Frey NF, Laplaze L, Casimiro I, Swarup R, Naudts M, Vanneste S, Audenaert D, Inze D, Bennett MJ, Beeckman T (2007) Auxin-dependent regulation of lateral root positioning in the basal meristem of Arabidopsis. Development 134: 681-690

De Smet I, Vanneste S, Inze D, Beeckman T (2006) Lateral root initiation or the birth of a new meristem. Plant Mol Biol 60: 871-887

De Veylder L, Beeckman T, Beemster GTS, Krols L, Terras F, Landrieu I, Van Der Schueren E, Maes S, Naudts M, Inzé D (2001) Functional analysis of cyclin-dependent kinase inhibitors of Arabidopsis. Plant Cell 13: 1653-1667

De Veylder L, Beemster GT, Beeckman T, Inze D (2001) CKS1At overexpression in Arabidopsis thaliana inhibits growth by reducing meristem size and inhibiting cell-cycle progression. Plant J 25: 617-626

DeFraia CT, Zhang X, Mou Z (2010) Elongator subunit 2 is an accelerator of immune responses in Arabidopsis thaliana. Plant J 64: 511-523

Deruere J, Jackson K, Garbers C, Soll D, Delong A (1999) The RCN1-encoded A subunit of protein phosphatase 2A increases phosphatase activity in vivo. Plant J 20: 389-399

Dharmasiri N, Dharmasiri S, Estelle M (2005) The F-box protein TIR1 is an auxin receptor. *Nature* 435:441-445.

Di Rubbo S., Irani N.G., Russinova E. (2011) PP2A Phosphatases: The "On-Off" Regulatory Switches of Brassinosteroid Signaling. Sci Signal 4:pe25

Dolan L, Poethig RS (1998) The *Okra* leaf shape mutation in cotton is active in all cell layers of the leaf. Am J Bot 85: 322-327

Donner TJ, Sherr I, Scarpella E (2009) Regulation of preprocambial cell state acquisition by auxin signaling in *Arabidopsis* leaves. *Development* 136:3235-3246.

dos Santos Maraschin F, Memelink J, Offringa R (2009) Auxin-induced, SCF^{TIR1}-mediated poly-ubiquitination marks AUX/IAA proteins for degradation. *Plant J* 59:100-109.

Dover J, Schneider J, Tawiah-Boateng MA, Wood A, Dean K, Johnston M, Shilatifard A (2002) Methylation of histone H3 by COMPASS requires ubiquitination of histone H2B by Rad6. J Biol Chem 277: 28368-28371

Dubos C, Le Gourrierec J, Baudry A, Huep G, Lanet E, Debeaujon I, Routaboul JM, Alboresi A, Weisshaar B, Lepiniec L (2008) MYBL2 is a new regulator of flavonoid biosynthesis in Arabidopsis thaliana. Plant J 55: 940-953

Duroux M, Houben A, Ruzicka K, Friml J, Grasser KD (2004) The chromatin remodelling complex FACT associates with actively transcribed regions of the Arabidopsis genome. Plant J 40: 660-671

Earley KW, Shook MS, Brower-Toland B, Hicks L, Pikaard CS (2007) In vitro specificities of Arabidopsis co-activator histone acetyltransferases: implications for histone hyperacetylation in gene activation. Plant J 52: 615-626

Elgin SC (1996) Heterochromatin and gene regulation in Drosophila. Curr Opin Genet Dev 6: 193-202

Esberg A, Huang B, Johansson MJ, Bystrom AS (2006) Elevated levels of two tRNA species bypass the requirement for elongator complex in transcription and exocytosis. Mol Cell 24: 139-148

Estelle M (1998) Polar auxin transport. New support for an old model. Plant Cell 10: 1775-1778

Fairchild C.D., Schumaker M.A., Quail P.H. (2000) HFR1 encodes an atypical bHLH protein that acts in phytochrome A signal transduction. Genes Dev 14:2377-91.

Falcone A, Nelissen H, Fleury D, Van Lijsebettens M, Bitonti MB (2007) Cytological investigations of the Arabidopsis thaliana elo1 mutant give new insights into leaf lateral growth and Elongator function. Ann Bot 100: 261-270

Farmer LM, Book AJ, Lee KH, Lin YL, Fu H, Vierstra RD (2010) The RAD23 family provides an essential connection between the 26S proteasome and ubiquitylated proteins in Arabidopsis. Plant Cell 22: 124-142

Ferjani A, Horiguchi G, Yano S, Tsukaya H (2007) Analysis of leaf development in *fugu* mutants of Arabidopsis reveals three compensation modes that modulate cell expansion in determinate organs. Plant Physiol 144: 988-999

Fichtner L, Frohloff F, Jablonowski D, Stark MJ, Schaffrath R (2002) Protein interactions within Saccharomyces cerevisiae Elongator, a complex essential for Kluyveromyces lactis zymocicity. Mol Microbiol 45: 817-826

Fichtner L, Jablonowski D, Schierhorn A, Kitamoto HK, Stark MJ, Schaffrath R (2003) Elongator's toxin-target (TOT) function is nuclear localization sequence dependent and suppressed by post-translational modification. Mol Microbiol 49: 1297-1307

Finkemeier I, Laxa M, Miguet L, Howden A, Sweetlove L (2011) Proteins of diverse function and subcellular location are lysine-acetylated in Arabidopsis. Plant Physiol

Fleming AJ (2002) The mechanism of leaf morphogenesis. Planta 216: 17-22

Fleury D, Himanen K, Cnops G, Nelissen H, Boccardi TM, Maere S, Beemster GT, Neyt P, Anami S, Robles P, Micol JL, Inze D, Van Lijsebettens M (2007) The Arabidopsis thaliana homolog of yeast BRE1 has a function in cell cycle regulation during early leaf and root growth. Plant Cell 19: 417-432

Franklin KA (2008) Shade avoidance. New Phytol 179: 930-944

Franklin KA, Praekelt U, Stoddart WM, Billingham OE, Halliday KJ, Whitelam GC (2003) Phytochromes B, D, and E act redundantly to control multiple physiological responses in Arabidopsis. Plant Physiol 131: 1340-1346

Franklin KA, Whitelam GC (2007) Light-quality regulation of freezing tolerance in Arabidopsis thaliana. Nat Genet 39: 1410-1413

Friml J, Benkova E, Mayer U, Palme K, Muster G (2003) Automated whole mount localisation techniques for plant seedlings. Plant J 34: 115-124

Friml J, Jones AR (2010) Endoplasmic reticulum: the rising compartment in auxin biology. Plant Physiol 154: 458-462

Friml J, Wisniewska J, Benkova E, Mendgen K, Palme K (2002) Lateral relocation of auxin efflux regulator PIN3 mediates tropism in Arabidopsis. Nature 415: 806-809

Frohloff F, Fichtner L, Jablonowski D, Breunig KD, Schaffrath R (2001) Saccharomyces cerevisiae Elongator mutations confer resistance to the Kluyveromyces lactis zymocin. EMBO J 20: 1993-2003

Fujita T, Puiz I, Schlegel W (2009) Negative elongation factor NELF controls transcription of immediate early genes in a stimulus-specific manner. *Exp Cell Res* 315:274-284.

Fukaki H, Tasaka M (2009) Hormone interactions during lateral root formation. Plant Mol Biol 69: 437-449

Fuks F. (2005) DNA methylation and histone modifications: teaming up to silence genes.Curr Opin Genet Dev 15:490-5.
Fukuda H (2004) Signals that control plant vascular cell differentiation. Nat Rev Mol Cell Biol 5: 379-391
Ganguly A, Lee SH, Cho M, Lee OR, Yoo H, Cho HT (2010) Differential auxin-transporting activities of PIN-FORMED proteins in Arabidopsis root hair cells. Plant Physiol 153: 1046-1061
Garbers C, DeLong A, Deruere J, Bernasconi P, Soll D (1996) A mutation in protein phosphatase 2A regulatory subunit A affects auxin transport in Arabidopsis. EMBO J 15: 2115-2124
Gardiner J, Barton D, Marc J, Overall R (2007) Potential role of tubulin acetylation and microtubule-based protein trafficking in familial dysautonomia. Traffic 8: 1145-1149
Geisler-Lee J, O'Toole N, Ammar R, Provart NJ, Millar AH, Geisler M (2007) A predicted interactome for Arabidopsis. Plant Physiol 145: 317-329
Gendreau E, Traas J, Desnos T, Grandjean O, Caboche M, Höfte H (1997) Cellular basis of hypocotyl growth in *Arabidopsis thaliana*. Plant Physiol 114: 295-305
Gendrel A.V., Lippman Z., Yordan C., Colot V., Martienssen R.A. (2002) Dependence of heterochromatic histone H3 methylation patterns on the Arabidopsis gene DDM1. Science 297:1871-3.
Gendrel A-V, Lippman Z, Martienssen R, Colot V (2005) Profiling histone modification patterns in plants using genomic tiling microarrays. *Nat Methods* 2:213-218.
Gilbert C, Kristjuhan A, Winkler GS, Svejstrup JQ (2004) Elongator interactions with nascent mRNA revealed by RNA immunoprecipitation. Mol Cell 14: 457-464
Govind CK, Zhang F, Qiu H, Hofmeyer K, Hinnebusch AG (2007) Gcn5 promotes acetylation, eviction, and methylation of nucleosomes in transcribed coding regions. Mol Cell 25: 31-42
Greenwood C, Selth LA, Dirac-Svejstrup AB, Svejstrup JQ (2009) An iron-sulfur cluster domain in Elp3 important for the structural integrity of elongator. J Biol Chem 284: 141-149
Guo L, Zhou J, Elling AA, Charron JB, Deng XW (2008) Histone modifications and expression of light-regulated genes in Arabidopsis are cooperatively influenced by changing light conditions. Plant Physiol 147: 2070-2083
Gustilo, E.M., Vendeix, F.A.P., and Agris, P.F. (2008) tRNA's modifications bring order to gene expression. *Curr Opin Microbiol* **11:** 134-140.
Halliday KJ, Martinez-Garcia JF, Josse EM (2009) Integration of light and auxin signaling. Cold Spring Harb Perspect Biol 1: a001586
Hamann T, Benkova E, Bäurle I, Kientz M, Jürgens G (2002) The *Arabidopsis BODENLOS* gene encodes an auxin response protein inhibiting MONOPTEROS-mediated embryo patterning. *Genes Dev* 16:1610-1615.
Hawkes NA, Otero G, Winkler GS, Marshall N, Dahmus ME, Krappmann D, Scheidereit C, Thomas CL, Schiavo G, Erdjument-Bromage H, Tempst P, Svejstrup JQ (2002) Purification and characterization of the human elongator complex. J Biol Chem 277: 3047-3052
Hay A, Barkoulas M, Tsiantis M (2006) ASYMMETRIC LEAVES1 and auxin activities converge to repress BREVIPEDICELLUS expression and promote leaf development in Arabidopsis. Development 133: 3955-3961
Heidari B., Matre P., Nemie-Feyissa D., Meyer C., Rognli O.A., Moller S.G., Lillo C. (2011) Protein Phosphatase 2A B55 and A Regulatory Subunits Interact with Nitrate Reductase and Are Essential for Nitrate Reductase Activation. Plant Physiol 156:165-72

Heisler MG, Ohno C, Das P, Sieber P, Reddy GV, Long JA, Meyerowitz EM (2005) Patterns of auxin transport and gene expression during primordium development revealed by live imaging of the Arabidopsis inflorescence meristem. Curr Biol 15: 1899-1911

Hejatko J, Blilou I, Brewer PB, Friml J, Scheres B, Benkova E (2006) In situ hybridization technique for mRNA detection in whole mount Arabidopsis samples. Nat Protoc 1: 1939-1946

Herr AJ, Jensen MB, Dalmay T, Baulcombe DC (2005) RNA polymerase IV directs silencing of endogenous DNA. Science 308: 118-120

Hodgkin J, Papp A, Pulak R, Ambros V, Anderson P (1989) A new kind of informational suppression in the nematode Caenorhabditis elegans. Genetics 123: 301-313

Hruz T, Laule O, Szabo G, Wessendorp F, Bleuler S, Oertle L, Widmayer P, Gruissem W, Zimmermann P (2008) Genevestigator V3: a reference expression database for the meta-analysis of transcriptomes. Adv Bioinform 420747: 1-5

Hsieh TF, Fischer RL (2005) Biology of chromatin dynamics. Annu Rev Plant Biol 56: 327-351

Huang, B., Johansson, M.J.O., and Byström, A.S. (2005) An early step in wobble uridine tRNA modification requires the Elongator complex. *RNA* **11:** 424-436.

Hurtado L, Farrona S, Reyes JC (2006) The putative SWI/SNF complex subunit BRAHMA activates flower homeotic genes in Arabidopsis thaliana. Plant Mol Biol 62: 291-304

Hwang WW, Venkatasubrahmanyam S, Ianculescu AG, Tong A, Boone C, Madhani HD (2003) A conserved RING finger protein required for histone H2B monoubiquitination and cell size control. Mol Cell 11: 261-266

Ito T, Ikehara T, Nakagawa T, Kraus WL, Muramatsu M (2000) p300-mediated acetylation facilitates the transfer of histone H2A-H2B dimers from nucleosomes to a histone chaperone. Genes Dev 14: 1899-1907

Ito T, Kim G-T, Shinozaki K (2000) Disruption of an *Arabidopsis* cytoplasmic ribosomal protein S13-homologous gene by transposon-mediated mutagenesis causes aberrant growth and development. Plant J 22: 257-264

Jablonowski D., Frohloff F., Fichtner L., Stark M.J., Schaffrath R. (2001) Kluyveromyces lactis zymocin mode of action is linked to RNA polymerase II function via Elongator. Mol Microbiol 42:1095-105

Jang I.C., Chung P.J., Hemmes H., Jung C., Chua N.H. (2011) Rapid and reversible light-mediated chromatin modifications of Arabidopsis phytochrome A locus. Plant Cell 23:459-70

Jelinsky SA, Estep P, Church GM, Samson LD (2000) Regulatory networks revealed by transcriptional profiling of damaged Saccharomyces cerevisiae cells: Rpn4 links base excision repair with proteasomes. Mol Cell Biol 20: 8157-8167

Jensen PJ, Hangarter RP, Estelle M (1998) Auxin transport is required for hypocotyl elongation in light-grown but not dark-grown Arabidopsis. Plant Physiol 116: 455-462

Jerzmanowski A (2007) SWI/SNF chromatin remodeling and linker histones in plants. Biochim Biophys Acta 1769: 330-345

Johansson MJ, Bystrom AS (2002) Dual function of the tRNA(m(5)U54)methyltransferase in tRNA maturation. RNA 8: 324-335

Johansson, M.J.O., Esberg, A., Huang, B., Björk, G.R., and Byström, A.S. (2008) Eukaryotic wobble uridine modifications promote a functionally redundant decoding system. *Mol Cell Biol* 28**:** 3301-3312.

Joshi AA, Struhl K (2005) Eaf3 chromodomain interaction with methylated H3-K36 links histone deacetylation to Pol II elongation. Mol Cell 20: 971-978

Karam CS, Kellner WA, Takenaka N, Clemmons AW, Corces VG (2010) 14-3-3 mediates histone cross-talk during transcription elongation in Drosophila. PLoS Genet 6: e1000975

Karimi M, Inze D, Depicker A (2002) GATEWAY vectors for Agrobacterium-mediated plant transformation. Trends Plant Sci 7: 193-195

Keogh MC, Kurdistani SK, Morris SA, Ahn SH, Podolny V, Collins SR, Schuldiner M, Chin K, Punna T, Thompson NJ, Boone C, Emili A, Weissman JS, Hughes TR, Strahl BD, Grunstein M, Greenblatt JF, Buratowski S, Krogan NJ (2005) Cotranscriptional set2 methylation of histone H3 lysine 36 recruits a repressive Rpd3 complex. Cell 123: 593-605

Kepinski S, Leyser O (2005) The *Arabidopsis* F-box protein TIR1 is an auxin receptor. *Nature* 435:446-451.

Keuskamp DH, Pollmann S, Voesenek LA, Peeters AJ, Pierik R (2010) Auxin transport through PIN-FORMED 3 (PIN3) controls shade avoidance and fitness during competition. Proc Natl Acad Sci U S A 107: 22740-22744

Kim Y-K, Son O, Kim M-R, Nam K-H, Kim G-T, Lee M-S, Choi S-Y, Cheon C-I (2007) *ATHB23*, an *Arabidopsis* class I homeodomain-leucine zipper gene, is expressed in the adaxial region of young leaves. Plant Cell Rep. 26: 1179-1185

Kirik V, Lee MM, Wester K, Herrmann U, Zheng Z, Oppenheimer D, Schiefelbein J, Hülskamp M (2005) Functional diversification of *MYB23* and *GL1* genes in trichome morphogenesis and initiation. Development 132: 1477-1485

Kirino, Y., Yasukawa, T., Ohta, S., Akira, S., Ishihara, K., Watanabe, K., and Suzuki, T. (2004) Codon-specific translational defect caused by a wobble modification deficiency in mutant tRNA from a human mitochondrial disease. *Proc Natl Acad Sci USA* **101:** 15070-15075.

Kleine-Vehn J., Ding Z., Jones A.R., Tasaka M., Morita M.T., Friml J. (2010) Gravity-induced PIN transcytosis for polarization of auxin fluxes in gravity-sensing root cells. Proc Natl Acad Sci U S A 107:22344-9

Korepanov AP, Gongadze GM, Garber MB, Court DL, Bubunenko MG (2007) Importance of the 5 S rRNA-binding ribosomal proteins for cell viability and translation in *Escherichia coli*. J Mol Biol 366: 1199-1208

Kornberg RD (1974) Chromatin structure: a repeating unit of histones and DNA. Science 184: 868-871

Kornberg RD (2005) Mediator and the mechanism of transcriptional activation. Trends Biochem Sci 30: 235-239

Kouskouti A, Talianidis I (2005) Histone modifications defining active genes persist after transcriptional and mitotic inactivation. EMBO J 24: 347-357

Krogan NJ, Greenblatt JF (2001) Characterization of a six-subunit holo-elongator complex required for the regulated expression of a group of genes in Saccharomyces cerevisiae. Mol Cell Biol 21: 8203-8212

Kwak JM, Moon JH, Murata Y, Kuchitsu K, Leonhardt N, DeLong A, Schroeder JI (2002) Disruption of a guard cell-expressed protein phosphatase 2A regulatory subunit, RCN1, confers abscisic acid insensitivity in Arabidopsis. Plant Cell 14: 2849-2861

Lau, C.-k., Bachorik, J.L., and Dreyfuss, G. (2009) Gemin5-snRNA interaction reveals an RNA binding function for WD repeat domains. *Nat Struct Mol Biol* **16:** 486-491.

Ledford H (2010) Plant biologists fear for cress project. Nature 464: 154

Lee I, Ambaru B, Thakkar P, Marcotte EM, Rhee SY (2010) Rational association of genes with traits using a genome-scale gene network for Arabidopsis thaliana. Nat Biotechnol 28: 149-156

Lee J, Bedford MT (2002) PABP1 identified as an arginine methyltransferase substrate using high-density protein arrays. EMBO Rep 3: 268-273

Leidel, S., Pedrioli, P.G.A., Bucher, T., Brost, R., Costanzo, M., Schmidt, A., *et al*. (2009) Ubiquitin-related modifier Urm1 acts as a sulphur carrier in thiolation of eukaryotic transfer RNA. *Nature* 458**:** 228-232.

Levine M. (2011) Paused RNA Polymerase II as a Developmental Checkpoint. Cell 145:502-11.

Li B, Gogol M, Carey M, Lee D, Seidel C, Workman JL (2007) Combined action of PHD and chromo domains directs the Rpd3S HDAC to transcribed chromatin. Science 316: 1050-1054

Li H, Luan S (2010) AtFKBP53 is a histone chaperone required for repression of ribosomal RNA gene expression in Arabidopsis. Cell Res 20: 357-366

Li SF, Milliken ON, Pham H, Seyit R, Napoli R, Preston J, Koltunow AM, Parish RW (2009) The *Arabidopsis* MYB5 transcription factor regulates mucilage synthesis, seed coat development, and trichome morphogenesis. Plant Cell 21: 72-89

Lillycrop KA, Phillips ES, Jackson AA, Hanson MA, Burdge GC (2005) Dietary protein restriction of pregnant rats induces and folic acid supplementation prevents epigenetic modification of hepatic gene expression in the offspring. J Nutr 135: 1382-1386

Liu Y, Koornneef M, Soppe WJ (2007) The absence of histone H2B monoubiquitination in the Arabidopsis hub1 (rdo4) mutant reveals a role for chromatin remodeling in seed dormancy. Plant Cell 19: 433-444

Lolas IB, Himanen K, Gronlund JT, Lynggaard C, Houben A, Melzer M, Van Lijsebettens M, Grasser KD (2010) The transcript elongation factor FACT affects Arabidopsis vegetative and reproductive development and genetically interacts with HUB1/2. Plant J 61: 686-697

Lorenzo O, Solano R (2005) Molecular players regulating the jasmonate signalling network. *Curr Opin Plant Biol* 8:532-540.

Lu J, Huang B, Esberg A, Johansson MJ, Bystrom AS (2005) The Kluyveromyces lactis gamma-toxin targets tRNA anticodons. RNA 11: 1648-1654

Luger K, Mader AW, Richmond RK, Sargent DF, Richmond TJ (1997) Crystal structure of the nucleosome core particle at 2.8 A resolution. Nature 389: 251-260

Lusser A, Kadonaga JT (2003) Chromatin remodeling by ATP-dependent molecular machines. Bioessays 25: 1192-1200

Maere S, Heymans K, Kuiper M (2005) BiNGO: a Cytoscape plugin to assess overrepresentation of gene ontology categories in biological networks. Bioinformatics 21: 3448-3449

Malamy JE, Benfey PN (1997) Organization and cell differentiation in lateral roots of Arabidopsis thaliana. Development 124: 33-44

Maleck K, Levine A, Eulgem T, Morgan A, Schmid J, Lawton KA, Dangl JL, Dietrich RA (2000) The transcriptome of Arabidopsis thaliana during systemic acquired resistance. Nat Genet 26: 403-410

Marchant A, Bennett MJ (1998) The Arabidopsis AUX1 gene: a model system to study mRNA processing in plants. Plant Mol Biol 36: 463-471

Mathieu O, Yukawa Y, Prieto J-L, Vaillant I, Sugiura M, Tourmente S (2003) Identification and characterization of transcription factor IIIA and ribosomal protein L5 from *Arabidopsis thaliana*. Nucleic Acids Res 31: 2424-2433

Matsui K, Umemura Y, Ohme-Takagi M (2008) AtMYBL2, a protein with a single MYB domain, acts as a negative regulator of anthocyanin biosynthesis in Arabidopsis. Plant J 55: 954-967

Max T, Sogaard M, Svejstrup JQ (2007) Hyperphosphorylation of the C-terminal repeat domain of RNA polymerase II facilitates dissociation of its complex with mediator. J Biol Chem 282: 14113-14120

Mehlgarten C, Jablonowski D, Wrackmeyer U, Tschitschmann S, Sondermann D, Jager G, Gong Z, Bystrom AS, Schaffrath R, Breunig KD (2010) Elongator function in tRNA wobble uridine modification is conserved between yeast and plants. Mol Microbiol 76: 1082-1094

Meskauskas A, Dinman JD (2001) Ribosomal protein L5 helps anchor peptidyl-tRNA to the P-site in *Saccharomyces cerevisiae*. RNA 7: 1084-1096

Michniewicz M, Zago MK, Abas L, Weijers D, Schweighofer A, Meskiene I, Heisler MG, Ohno C, Zhang J, Huang F, Schwab R, Weigel D, Meyerowitz EM, Luschnig C, Offringa R, Friml J (2007) Antagonistic regulation of PIN phosphorylation by PP2A and PINOID directs auxin flux. Cell 130: 1044-1056

Micol JL (2009) Leaf development: time to turn over a leaf? Curr Opin Plant Biol 12: 9-16

Milgrom E, West RW, Jr., Gao C, Shen WC (2005) TFIID and Spt-Ada-Gcn5-acetyltransferase functions probed by genome-wide synthetic genetic array analysis using a Saccharomyces cerevisiae taf9-ts allele. Genetics 171: 959-973

Mizukami Y, Fischer RL (2000) Plant organ size control: *AINTEGUMENTA* regulates growth and cell numbers during organogenesis. Proc Natl Acad Sci USA 97: 942-947

Molinier J., Ries G., Zipfel C., Hohn B. (2006) Transgeneration memory of stress in plants. Nature 442:1046-9

Moore RC, Purugganan MD (2005) The evolutionary dynamics of plant duplicate genes. Curr Opin Plant Biol 8: 122-128

Moradi H, Simoff I, Bartish G, Nygård O (2008) Functional features of the C-terminal region of yeast ribosomal protein L5. Mol. Genet. Genomics 280: 337-350

Muse GW, *et al*. (2007) RNA polymerase is poised for activation across the genome. *Nat. Genet.* 39:1507-1511.

Mustroph A., Zanetti M.E., Jang C.J., Holtan H.E., Repetti P.P., Galbraith D.W., Girke T., Bailey-Serres J. (2009) Profiling translatomes of discrete cell populations resolves altered cellular priorities during hypoxia in Arabidopsis. Proc Natl Acad Sci U S A 106:18843-8

Nelissen H, Boccardi TM, Himanen K, Van Lijsebettens M (2007) Impact of core histone modifications on transcriptional regulation and plant growth. *Crit Rev Plant Sci* 26:243-263.

Nelissen H, Clarke JH, De Block M, De Block S, Vanderhaeghen R, Zielinski RE, Dyer T, Lust S, Inze D, Van Lijsebettens M (2003) DRL1, a homolog of the yeast TOT4/KTI12 protein, has a function in meristem activity and organ growth in plants. Plant Cell 15: 639-654

Nelissen H, De Groeve S, Fleury D, Neyt P, Bruno L, Bitonti MB, Vandenbussche F, Van der Straeten D, Yamaguchi T, Tsukaya H, Witters E, De Jaeger G, Houben A, Van Lijsebettens M (2010) Plant Elongator regulates auxin-related genes during RNA polymerase II transcription elongation. Proc Natl Acad Sci U S A 107: 1678-1683

Nelissen H, Fleury D, Bruno L, Robles P, De Veylder L, Traas J, Micol JL, Van Montagu M, Inze D, Van Lijsebettens M (2005) The elongata mutants identify a functional Elongator complex in plants with a role in cell proliferation during organ growth. Proc Natl Acad Sci U S A 102: 7754-7759

Niu L, Zhang Y, Pei Y, Liu C, Cao X (2008) Redundant requirement for a pair of PROTEIN ARGININE METHYLTRANSFERASE4 homologs for the proper regulation of Arabidopsis flowering time. Plant Physiol 148: 490-503

Ogas J, Kaufmann S, Henderson J, Somerville C (1999) PICKLE is a CHD3 chromatin-remodeling factor that regulates the transition from embryonic to vegetative development in Arabidopsis. Proc Natl Acad Sci U S A 96: 13839-13844

Okada K, Shimura Y (1994) Genetic analyses of signalling in flower development using Arabidopsis. Plant Mol Biol 26: 1357-1377

Orphanides G, LeRoy G, Chang CH, Luse DS, Reinberg D (1998) FACT, a factor that facilitates transcript elongation through nucleosomes. Cell 92: 105-116

Orphanides G, Wu WH, Lane WS, Hampsey M, Reinberg D (1999) The chromatin-specific transcription elongation factor FACT comprises human SPT16 and SSRP1 proteins. Nature 400: 284-288

Osley MA (2006) Regulation of histone H2A and H2B ubiquitylation. Brief Funct Genomic Proteomic 5: 179-189

Otero G, Fellows J, Li Y, de Bizemont T, Dirac AM, Gustafsson CM, Erdjument-Bromage H, Tempst P, Svejstrup JQ (1999) Elongator, a multisubunit component of a novel RNA polymerase II holoenzyme for transcriptional elongation. Mol Cell 3: 109-118

Owen-Hughes T (2003) Colworth memorial lecture. Pathways for remodelling chromatin. Biochem Soc Trans 31: 893-905

Paciorek T, Zazimalova E, Ruthardt N, Petrasek J, Stierhof YD, Kleine-Vehn J, Morris DA, Emans N, Jurgens G, Geldner N, Friml J (2005) Auxin inhibits endocytosis and promotes its own efflux from cells. Nature 435: 1251-1256

Pandey R, Muller A, Napoli CA, Selinger DA, Pikaard CS, Richards EJ, Bender J, Mount DW, Jorgensen RA (2002) Analysis of histone acetyltransferase and histone deacetylase families of Arabidopsis thaliana suggests functional diversification of chromatin modification among multicellular eukaryotes. Nucleic Acids Res 30: 5036-5055

Perales M, Mas P (2007) A functional link between rhythmic changes in chromatin structure and the Arabidopsis biological clock. Plant Cell 19: 2111-2123

Pérez-Pérez JM, Ponce MR, Micol JL (2002) The *UCU1 Arabidopsis* gene encodes a SHAGGY/GSK3-like kinase required for cell expansion along the proximodistal axis. Dev Biol 242: 161-173

Pérez-Pérez JM, Ponce MR, Micol JL (2004) The *ULTRACURVATA2* gene of Arabidopsis encodes an FK506-binding protein involved in auxin and brassinosteroid signaling. Plant Physiol 134: 101-117

Perrot-Rechenmann C (2010) Cellular responses to auxin: division versus expansion. Cold Spring Harb Perspect Biol 2: a001446

Pien S, Grossniklaus U (2007) Polycomb group and trithorax group proteins in Arabidopsis. Biochim Biophys Acta 1769: 375-382

Pinon V, Etchells JP, Rossignol P, Collier SA, Arroyo JM, Martienssen RA, Byrne ME (2008) Three *PIGGYBACK* genes that specifically influence leaf patterning encode ribosomal proteins. Development 135: 1315-1324

Pokholok DK, Hannett NM, Young RA (2002) Exchange of RNA polymerase II initiation and elongation factors during gene expression in vivo. Mol Cell 9: 799-809

Pokholok DK, Harbison CT, Levine S, Cole M, Hannett NM, Lee TI, Bell GW, Walker K, Rolfe PA, Herbolsheimer E, Zeitlinger J, Lewitter F, Gifford DK, Young RA (2005) Genome-wide map of nucleosome acetylation and methylation in yeast. Cell 122: 517-527

Polo SE, Almouzni G (2006) Chromatin assembly: a basic recipe with various flavours. Curr Opin Genet Dev 16: 104-111

Ponce MR, Robles P, Lozano FM, Brotons MA, Micol JL (2006) Low-resolution mapping of untagged mutations. Methods Mol Biol 323: 105-113

Prinsen E, Van Laer S, Öden S, Van Onckelen H (2000) in *Plant Hormone Protocols*, Methods in Molecular Biology, Vol 141, eds Tucker GA, Roberts JA (Humana Press, Totowa, NJ), pp 49-65.

Proost S, Van Bel M, Sterck L, Billiau K, Van Parys T, Van de Peer Y, Vandepoele K (2009) PLAZA: a comparative genomics resource to study gene and genome evolution in plants. Plant Cell 21: 3718-3731

Rahl, P.B., Chen, C.Z., and Collins, R.N. (2005) Elp1p, the yeast homolog of the FD disease syndrome protein, negatively regulates exocytosis independently of transcriptional elongation. *Mol Cell* **17:** 841-853.

Rahman A, Takahashi M, Shibasaki K, Wu S, Inaba T, Tsurumi S, Baskin TI (2010) Gravitropism of Arabidopsis thaliana roots requires the polarization of PIN2 toward the root tip in meristematic cortical cells. Plant Cell 22: 1762-1776

Rashotte AM, DeLong A, Muday GK (2001) Genetic and chemical reductions in protein phosphatase activity alter auxin transport, gravity response, and lateral root growth. Plant Cell 13: 1683-1697

Reik W (2007) Stability and flexibility of epigenetic gene regulation in mammalian development. Nature 447: 425-432

Reinberg D, Sims RJ, 3rd (2006) de FACTo nucleosome dynamics. J Biol Chem 281: 23297-23301

Reinhardt D (2003) Vascular patterning: more than just auxin? Curr Biol 13: R485-487

Reinhardt D, *et al*. (2003) Regulation of phyllotaxis by polar auxin transport. *Nature* 426:255-260.

Rizzini L., Favory J.J., Cloix C., Faggionato D., O'Hara A., Kaiserli E., Baumeister R., Schafer E., Nagy F., Jenkins G.I., Ulm R. (2011) Perception of UV-B by the Arabidopsis UVR8 protein. Science 332:103-6.

Robles P, Fleury D, Candela H, Cnops G, Alonso-Peral MM, Anami S, Falcone A, Caldana C, Willmitzer L, Ponce MR, Van Lijsebettens M, Micol JL (2010) The RON1/FRY1/SAL1 gene is required for leaf morphogenesis and venation patterning in Arabidopsis. Plant Physiol 152: 1357-1372

Robles P, Micol JL (2001) Genome-wide linkage analysis of *Arabidopsis* genes required for leaf development. Mol Genet Genomics 266: 12-19

Robzyk K, Recht J, Osley MA (2000) Rad6-dependent ubiquitination of histone H2B in yeast. Science 287: 501-504

Roh TY, Cuddapah S, Cui K, Zhao K (2006) The genomic landscape of histone modifications in human T cells. Proc Natl Acad Sci U S A 103: 15782-15787

Rolland-Lagan AG, Prusinkiewicz P (2005) Reviewing models of auxin canalization in the context of leaf vein pattern formation in Arabidopsis. Plant J 44: 854-865

Roth SY, Denu JM, Allis CD (2001) Histone acetyltransferases. Annu Rev Biochem 70: 81-120

Roy A, Kucukural A, Zhang Y (2010) I-TASSER: a unified platform for automated protein structure and function prediction. Nat Protoc 5: 725-738

Saeboe-Larssen S., Lyamouri M., Merriam J., Oksvold M.P., Lambertsson A. (1998) Ribosomal protein insufficiency and the minute syndrome in Drosophila: a dose-response relationship. Genetics 148:1215-24.

Sanger F, Nicklen S, Coulson AR (1977) DNA sequencing with chain-terminating inhibitors. Proc Natl Acad Sci U S A 74: 5463-5467

Sanmartin M., Sauer M., Munoz A., Zouhar J., Ordonez A., van de Ven W.T., Caro E., Sanchez M.D., Raikhel N.V., Gutierrez C., Sanchez-Serrano J.J., Rojo E. (2011) A Molecular Switch for Initiating Cell Differentiation in Arabidopsis. Curr Biol.

Sauer M, Balla J, Luschnig C, Wisniewska J, Reinohl V, Friml J, Benkova E (2006) Canalization of auxin flow by Aux/IAA-ARF-dependent feedback regulation of PIN polarity. Genes Dev 20: 2902-2911

Sauer M, Paciorek T, Benkova E, Friml J (2006) Immunocytochemical techniques for whole-mount in situ protein localization in plants. Nat Protoc 1: 98-103

Saunders A, Core LJ, Lis JT (2006) Breaking barriers to transcription elongation. Nat Rev Mol Cell Biol 7: 557-567

Scarpella E, Barkoulas M, Tsiantis M (2010) Control of leaf and vein development by auxin. Cold Spring Harb Perspect Biol 2: a001511

Schmitz RJ, Sung S, Amasino RM (2008) Histone arginine methylation is required for vernalization-induced epigenetic silencing of FLC in winter-annual Arabidopsis thaliana. Proc Natl Acad Sci U S A 105: 411-416

Servet C, Conde e Silva N, Zhou DX (2010) Histone acetyltransferase AtGCN5/HAG1 is a versatile regulator of developmental and inducible gene expression in Arabidopsis. Mol Plant 3: 670-677

Shilatifard A (2006) Chromatin modifications by methylation and ubiquitination: implications in the regulation of gene expression. Annu Rev Biochem 75: 243-269

Showalter AM, Keppler B, Lichtenberg J, Gu D, Welch LR (2010) A bioinformatics approach to the identification, classification, and analysis of hydroxyproline-rich glycoproteins. Plant Physiol 153: 485-513

Simpson CL, Lemmens R, Miskiewicz K, Broom WJ, Hansen VK, van Vught PW, Landers JE, Sapp P, Van Den Bosch L, Knight J, Neale BM, Turner MR, Veldink JH, Ophoff RA, Tripathi VB, Beleza A, Shah MN, Proitsi P, Van Hoecke A, Carmeliet P, Horvitz HR, Leigh PN, Shaw CE, van den Berg LH, Sham PC, Powell JF, Verstreken P, Brown RH, Jr., Robberecht W, Al-Chalabi A (2009) Variants of the elongator protein 3 (ELP3) gene are associated with motor neuron degeneration. Hum Mol Genet 18: 472-481

Singh N, Lorbeck MT, Zervos A, Zimmerman J, Elefant F (2010) The histone acetyltransferase Elp3 plays in active role in the control of synaptic bouton expansion and sleep in Drosophila. J Neurochem 115: 493-504

Skottke K.R., Yoon G.M., Kieber J.J., Delong A. (2011) Protein Phosphatase 2A Controls Ethylene Biosynthesis by Differentially Regulating the Turnover of ACC Synthase Isoforms. PLoS Genet 7:e1001370

Slaugenhaupt SA, Gusella JF (2002) Familial dysautonomia. Curr Opin Genet Dev 12: 307-311

Smalle J, Vierstra RD (2004) The ubiquitin 26S proteasome proteolytic pathway. Annu Rev Plant Biol 55: 555-590

Solinger JA, Paolinelli R, Kloss H, Scorza FB, Marchesi S, Sauder U, Mitsushima D, Capuani F, Sturzenbaum SR, Cassata G (2010) The Caenorhabditis elegans Elongator complex regulates neuronal alpha-tubulin acetylation. PLoS Genet 6: e1000820

Soppe WJJ, *et al*. (2002) DNA methylation controls histone H3 lysine 9 methylation and heterochromatin assembly in *Arabidopsis*. *EMBO J* 21:6549-6559.

Strader LC, Bartel B (2009) The Arabidopsis PLEIOTROPIC DRUG RESISTANCE8/ABCG36 ATP binding cassette transporter modulates sensitivity to the auxin precursor indole-3-butyric acid. Plant Cell 21: 1992-2007

Strader LC, Culler AH, Cohen JD, Bartel B (2010) Conversion of endogenous indole-3-butyric acid to indole-3-acetic acid drives cell expansion in Arabidopsis seedlings. Plant Physiol 153: 1577-1586

Strahl BD, Allis CD (2000) The language of covalent histone modifications. Nature 403: 41-45

Sukumar P, Edwards KS, Rahman A, Delong A, Muday GK (2009) PINOID kinase regulates root gravitropism through modulation of PIN2-dependent basipetal auxin transport in Arabidopsis. Plant Physiol 150: 722-735

Sung S, Amasino RM (2004) Vernalization in Arabidopsis thaliana is mediated by the PHD finger protein VIN3. Nature 427: 159-164

Sung S, Amasino RM (2006) Molecular genetic studies of the memory of winter. J Exp Bot 57: 3369-3377

Svejstrup JQ (2007) Elongator complex: how many roles does it play? *Curr. Opin Cell Biol* 19:331-336.

Svejstrup JQ (2007) Elongator complex: how many roles does it play? Curr Opin Cell Biol 19: 331-336

Svejstrup JQ (2010) The interface between transcription and mechanisms maintaining genome integrity. Trends Biochem Sci 35: 333-338

Swaminathan V, Kishore AH, Febitha KK, Kundu TK (2005) Human histone chaperone nucleophosmin enhances acetylation-dependent chromatin transcription. Mol Cell Biol 25: 7534-7545

Świątek A, Lenjou M, Van Bockstaele D, Inzé D, Van Onckelen H (2002) Differential effect of jasmonic acid and abscisic acid on cell cycle progression in tobacco BY-2 cells. *Plant Physiol* 128:201-211.

Tao Y, Ferrer JL, Ljung K, Pojer F, Hong F, Long JA, Li L, Moreno JE, Bowman ME, Ivans LJ, Cheng Y, Lim J, Zhao Y, Ballare CL, Sandberg G, Noel JP, Chory J (2008) Rapid synthesis of auxin via a new tryptophan-dependent pathway is required for shade avoidance in plants. Cell 133: 164-176

Tao Y, Xie Z, Chen W, Glazebrook J, Chang HS, Han B, Zhu T, Zou G, Katagiri F (2003) Quantitative nature of Arabidopsis responses during compatible and incompatible interactions with the bacterial pathogen Pseudomonas syringae. Plant Cell 15: 317-330

Tariq M., Paszkowski J. (2004) DNA and histone methylation in plants. Trends Genet 20:244-51.

Thain SC, *et al*. (2004) Circadian rhythms of ethylene emission in Arabidopsis. *Plant Physiol* 136:3751-3761.

Thomas B (2006) Light signals and flowering. J Exp Bot 57: 3387-3393

Thomas BC, Pedersen B, Freeling M (2006) Following tetraploidy in an Arabidopsis ancestor, genes were removed preferentially from one homeolog leaving clusters enriched in dose-sensitive genes. Genome Res 16: 934-946

Tian Q, Reed JW (1999) Control of auxin-regulated root development by the *Arabidopsis thaliana SHY2/IAA3* gene. *Development* 126:711-721.

Tse C, Sera T, Wolffe AP, Hansen JC (1998) Disruption of higher-order folding by core histone acetylation dramatically enhances transcription of nucleosomal arrays by RNA polymerase III. Mol Cell Biol 18: 4629-4638

Tseng T.S., Briggs W.R. (2010) The Arabidopsis rcn1-1 mutation impairs dephosphorylation of Phot2, resulting in enhanced blue light responses. Plant Cell 22:392-402

Vaillant I, Paszkowski J (2007) Role of histone and DNA methylation in gene regulation. Curr Opin Plant Biol 10: 528-533

Valvekens D, Montagu MV, Van Lijsebettens M (1988) Agrobacterium tumefaciens-mediated transformation of Arabidopsis thaliana root explants by using kanamycin selection. Proc Natl Acad Sci U S A 85: 5536-5540

Van Leene J, Hollunder J, Eeckhout D, Persiau G, Van De Slijke E, Stals H, Van Isterdael G, Verkest A, Neirynck S, Buffel Y, De Bodt S, Maere S, Laukens K, Pharazyn A, Ferreira PC, Eloy N, Renne C, Meyer C, Faure JD, Steinbrenner J, Beynon J, Larkin JC, Van de Peer Y, Hilson P, Kuiper M, De Veylder L, Van Onckelen H, Inze D, Witters E, De Jaeger G (2010) Targeted interactomics reveals a complex core cell cycle machinery in Arabidopsis thaliana. Mol Syst Biol 6: 397

Van Leene J, Stals H, Eeckhout D, Persiau G, Van De Slijke E, Van Isterdael G, De Clercq A, Bonnet E, Laukens K, Remmerie N, Henderickx K, De Vijlder T, Abdelkrim A, Pharazyn A, Van Onckelen H, Inze D, Witters E, De Jaeger G (2007) A tandem affinity purification-based technology platform to study the cell cycle interactome in Arabidopsis thaliana. Mol Cell Proteomics 6: 1226-1238

Van Leene J, Witters E, Inzé D, De Jaeger G (2008) Boosting tandem affinity purification of plant protein complexes. *Trends Plant Sci* 13:517-520.

Van Lijsebettens M, Vanderhaeghen R, De Block M, Bauw G, Villarroel R, Van Montagu M (1994) An S18 ribosomal protein gene copy, encoded at the *Arabidopsis PFL* locus, affects plant development by its specific expression in meristems. EMBO J 13: 3378-3388

Van Minnebruggen A, Neyt P, De Groeve S, Coussens G, Ponce MR, Micol JL, Van Lijsebettens M (2010) The ang3 mutation identified the ribosomal protein gene RPL5B with a role in cell expansion during organ growth. Physiol Plant 138: 91-101

Vanneste S, Friml J (2009) Auxin: A trigger for change in plant development. *Cell* 136:1005-1016.

Verbsky ML, Richards EJ (2001) Chromatin remodeling in plants. Curr Opin Plant Biol 4: 494-500

Versées W, De Groeve S, Van Lijsebettens M (2010) Elongator, a conserved multitasking complex? Mol Microbiol 76: 1065-1069

Wagner D, Meyerowitz EM (2002) SPLAYED, a novel SWI/SNF ATPase homolog, controls reproductive development in Arabidopsis. Curr Biol 12: 85-94

Walters KJ, Lech PJ, Goh AM, Wang Q, Howley PM (2003) DNA-repair protein hHR23a alters its protein structure upon binding proteasomal subunit S5a. Proc Natl Acad Sci U S A 100: 12694-12699

Wang D, Amornsiripanitch N, Dong X (2006) A genomic approach to identify regulatory nodes in the transcriptional network of systemic acquired resistance in plants. PLoS Pathog 2: e123

Weake VM, Workman JL (2008) Histone ubiquitination: triggering gene activity. Mol Cell 29: 653-663

Weijers D, Friml J (2009) SnapShot: Auxin signaling and transport. Cell 136: 1172, 1172 e1171

Welchman RL, Gordon C, Mayer RJ (2005) Ubiquitin and ubiquitin-like proteins as multifunctional signals. Nat Rev Mol Cell Biol 6: 599-609

Wery M, Shematorova E, Van Driessche B, Vandenhaute J, Thuriaux P, Van Mullem V (2004) Members of the SAGA and Mediator complexes are partners of the transcription elongation factor TFIIS. EMBO J 23: 4232-4242

Whitelam GC, Patel S, Devlin PF (1998) Phytochromes and photomorphogenesis in Arabidopsis. Philos Trans R Soc Lond B Biol Sci 353: 1445-1453

Winkler GS, Kristjuhan A, Erdjument-Bromage H, Tempst P, Svejstrup JQ (2002) Elongator is a histone H3 and H4 acetyltransferase important for normal histone acetylation levels *in vivo*. *Proc Natl Acad Sci USA* 99:3517-3522.

Winkler GS, Petrakis TG, Ethelberg S, Tokunaga M, Erdjument-Bromage H, Tempst P, Svejstrup JQ (2001) RNA polymerase II elongator holoenzyme is composed of two discrete subcomplexes. J Biol Chem 276: 32743-32749

Wittschieben, B.Ø., Otero, G., de Bizemont, T., Fellows, J., Erdjument-Bromage, H., Ohba, R., *et al*. (1999) A novel histone acetyltransferase is an integral subunit of elongating RNA polymerase II holoenzyme. *Mol Cell* **4:** 123-128.

Workman JL, Kingston RE (1998) Alteration of nucleosome structure as a mechanism of transcriptional regulation. Annu Rev Biochem 67: 545-579

Wu K, Tian L, Malik K, Brown D, Miki B (2000) Functional analysis of HD2 histone deacetylase homologues in Arabidopsis thaliana. Plant J 22: 19-27

Wynshaw-Boris A (2009) Elongator bridges tubulin acetylation and neuronal migration. Cell 136: 393-394

Xiao T, Kao CF, Krogan NJ, Sun ZW, Greenblatt JF, Osley MA, Strahl BD (2005) Histone H2B ubiquitylation is associated with elongating RNA polymerase II. Mol Cell Biol 25: 637-651

Xu L, Zhao Z, Dong A, Soubigou-Taconnat L, Renou JP, Steinmetz A, Shen WH (2008) Di- and tri- but not monomethylation on histone H3 lysine 36 marks active transcription of genes involved in flowering time regulation and other processes in Arabidopsis thaliana. Mol Cell Biol 28: 1348-1360

Yao Y, Ling Q, Wang H, Huang H (2008) Ribosomal proteins promote leaf adaxial identity. Development 135: 1325-1334

Yudkovsky N, Ranish JA, Hahn S (2000) A transcription reinitiation intermediate that is stabilized by activator. Nature 408: 225-229

Zaina S, Lindholm MW, Lund G (2005) Nutrition and aberrant DNA methylation patterns in atherosclerosis: more than just hyperhomocysteinemia? J Nutr 135: 5-8

Zgurski JM, Sharma R, Bolokoski DA, Schultz EA (2005) Asymmetric auxin response precedes asymmetric growth and differentiation of asymmetric leaf1 and asymmetric leaf2 Arabidopsis leaves. Plant Cell 17: 77-91

Zhang K, Sridhar VV, Zhu J, Kapoor A, Zhu JK (2007) Distinctive core histone post-translational modification patterns in Arabidopsis thaliana. PLoS One 2: e1210

Zhao J, Herrera-Diaz J, Gross DS (2005) Domain-wide displacement of histones by activated heat shock factor occurs independently of Swi/Snf and is not correlated with RNA polymerase II density. Mol Cell Biol 25: 8985-8999

Zhao N, Ferrer JL, Ross J, Guan J, Yang Y, Pichersky E, Noel JP, Chen F (2008) Structural, biochemical, and phylogenetic analyses suggest that indole-3-acetic acid methyltransferase is an evolutionarily ancient member of the SABATH family. Plant Physiol 146: 455-467

Zhou X, Hua D, Chen Z, Zhou Z, Gong Z (2009) Elongator mediates ABA responses, oxidative stress resistance and anthocyanin biosynthesis in Arabidopsis. Plant J 60: 79-90